Neurophysiological and neuroimaging markers of neurological outcome in Tuberous Sclerosis Complex

Jurriaan Michiel Peters

Layout and printing: Ridderprint BV, the Netherlands, www.ridderprint.nl
Cover art: © Copyright Pascal Lemaître, commissioned work, 2015
Support: Studies in this thesis have been supported by NIH P20 NS080199, R01 NS079788, and U01 NS082320 grants, and Harvard Catalyst | The Harvard Clinical and Translational Science Center (National Center for Research Resources and the National Center for Advancing Translational Sciences, NIH award UL1 TR001102). Financial support for the printing of this thesis was supported by the Department of Neurology, Boston Children's Hospital, Boston, MA, USA
ISBN: 978-94-6299-318-1

Neurophysiological and neuroimaging markers of neurological outcome in Tuberous Sclerosis Complex

Neurofysiologische en beeldvorming merkers van het neurologisch
ziektebeloop in Tubereuze Sclerose Complex
(met een samenvatting in het Nederlands)

Proefschrift

ter verkrijging van de graad van doctor aan de Universiteit Utrecht
op gezag van de rector magnificus, prof. dr. G.J. van der Zwaan,
ingevolge het besluit van het college voor promoties in het openbaar te verdedigen
op donderdag 28 april 2016 des ochtends te 10.30 uur

door

Jurriaan Michiel Peters
geboren op 16 december 1974 te Leiden

Promotoren:	Prof. dr. K.P.J. Braun
	Prof. dr. S.K. Warfield
Copromotoren:	Dr. F.E. Jansen
	Dr. M. Sahin

CONTENTS

For my wife, who helped,
and for Lina, Dounia and Simo, who did not

Chapter 1

Introduction and outline of the thesis

INTRODUCTION

Tuberous Sclerosis Complex

Tuberous sclerosis complex (TSC) is a rare genetic, multisystem disorder with a prevalence of 1 in 6,000, with over 50,000 patients in the USA and over 1 million patients worldwide[1]. Inactivation of *TSC1* or *TSC2* genes leads to an overactive mechanistic target of rapamycin (mTOR) pathway, and subsequent disinhibition of protein synthesis and cell growth. It is characterized by hamartoma formation in various organs, including the brain, where they are referred to as tubers. Cerebral cortical tubers are present in more than 80% of patients with TSC and arise due to abnormal cellular differentiation, migration, and proliferation[2].

Epilepsy occurs in up to 90% of patients with TSC, with a high occurrence rate in the first years of life, and is intractable in 60% of cases[3]. 40% of patients with TSC develop infantile spasms (IS), a severe infantile epilepsy syndrome[3,4]. In early childhood, the neurological symptoms are particularly devastating, as seizures interfere with neurodevelopment, and are strongly associated with autism spectrum disorder (ASD) and intellectual disability (ID)[5,6].

The diagnosis is made clinically, and recently the diagnostic criteria were updated (Table 1)[7]. The responsible genetic mutations are identified in approximately 85% of cases. For the remaining 15%, significant progress has been made in the discovery of mosaic mutations found in affected tissue such as hypopigmented skin lesions[8].

Variable Phenotype

While the diagnosis is not hard to make[9], and a genotype-phenotype correlation has been established[10], the spectrum of phenotypical neurologic presentation is wide and unpredictable.

Several implications of a highly variable and unpredictable neurologic phenotype are evident: First, young parents face a great deal of uncertainty when the diagnosis is made. The range of cognitive phenotype varies from the ability to graduate from college to severe ID. For example, in specialized TSC clinics, patients may present as paucisymptomatic adults with TSC as an incidental diagnosis.

Second, developmental monitoring and supportive therapies are applied often uniformly, in a one-size-fits-all manner; and adjustment towards more tailored interventions is done reactively rather than proactively. For example, once psychotherapeutic management of severe behavioral dysregulation fails, and supplemental psychopharmacological therapy is started, the behaviors may have led to failure in the school setting already. In a study of serial neuropsychological testing, several developmental "red flags" were identified in high-

risk patients with TSC[11]. The identification of such *early* clinical risk factors in a patient can guide *early* therapeutic decisions with the potential to improve outcome.

Third, the field is exploring the use of possible early *targeted* treatment to modify the neurological outcome, but patients at high risk for refractory seizures, ID or ASD need to be identified to justify the risk of such therapies[12,13].

Table 1. Revised diagnostic criteria for Tuberous Sclerosis Complex 2012

A. Genetic diagnostic criteria	
The identification of either a TSC1 or TSC2 pathogenic mutation in DNA from normal tissue is sufficient to make a definite diagnosis of tuberous sclerosis complex (TSC). A pathogenic mutation is defined as a mutation that clearly inactivates the function of the TSC1 or TSC2 proteins (e.g., out-of-frame indel or nonsense mutation), prevents protein synthesis (e.g., large genomic deletion), or is a missense mutation whose effect on protein function has been established by functional assessment (www.lovd.nl/TSC1, www.lovd/TSC2, and 8,9). Other TSC1 or TSC2 variants whose effect on function is less certain do not meet these criteria, and are not sufficient to make a definite diagnosis of TSC. Note that 10% to 25% of TSC patients have no mutation identified by conventional genetic testing, and a normal result does not exclude TSC, or have any effect on the use of clinical diagnostic criteria to diagnose TSC.	
B. Clinical diagnostic criteria	
Major features	
1.	Hypomelanotic macules (≥3, at least 5-mm diameter)
2.	Angiofibromas (≥3) or fibrous cephalic plaque
3.	Ungual fibromas (≥2)
4.	Shagreen patch
5.	Multiple retinal hamartomas
6.	Cortical dysplasias*
7.	Subependymal nodules
8.	Subependymal giant cell astrocytoma
9.	Cardiac rhabdomyoma
10.	Lymphangioleiomyomatosis (LAM)†
11.	Angiomyolipomas (≥2)†
Minor features	
1.	"Confetti" skin lesions
2.	Dental enamel pits (>3)
3.	Intraoral fibromas (≥2)
4.	Retinal achromic patch
5.	Multiple renal cysts
6.	Nonrenal hamartomas

Definite diagnosis: Two major features or one major feature with ≥2 minor features

Possible diagnosis: Either one major feature or ≥2 minor features

* Includes tubers and cerebral white matter radial migration lines.

† A combination of the two major clinical features (LAM and angiomyolipomas) without other features does not meet criteria for a definite diagnosis.

Markers of disease outcome

The criteria of a good marker include reliable reproducibility, an observable change in parallel with fluctuations in the clinical phenotype including in response to therapy[14], and the reflection of underlying neurobiology[15].

Neuroimaging may bare such promise, as it provides direct insight in the brain structure. Visualized easily with magnetic resonance imaging (MRI), traditionally, tubers were considered the hallmark of the disorder[15]. The association of focal brain abnormalities and neurodevelopmental morbidity suggested that these may underlie the cognitive deficits in TSC[16], perhaps through disruption of the local architecture. For examples, temporal lobe tubers were deemed necessary but insufficient to cause ASD[17,18], and cerebellar tubers may pose an increased risk[19,20]. Several studies demonstrated that the lesion load correlates with neurological severity[21,22], and recently it was shown that the disease burden corresponds to overall outcome even when radial migration lines (or other lesions) other than tubers were quantified[16]. A previously reported relationship, however, between tuber location and ASD could not be reproduced by others[23,24]. Currently, there may be consensus that overall tuber load reflects the disease burden, but the relationship is not strong enough to predict outcome individually and reliably. Also, epilepsy cannot be reliably predicted, diagnosed or localized from conventional (structural) MRI.

A neurophysiological approach is also possible. For epilepsy in TSC, the main tool for diagnosis and management is the electroencephalogram (EEG). EEG is a readily available, non-invasive, continuous biosignal reflecting cerebral function and has been used to study neurodevelopmental dysfunction in ASD. In the absence of a conventional EEG signature of ASD, computationally more advanced methods including cognitive event-related potentials, measures of spectral power or connectivity, and network analysis have been applied[25,26], but not specifically for TSC.

With conventional MRI failing, and EEG insufficiently explored, there are no objective imaging and neurophysiologic measures available to predict disease outcome in TSC. The lack of a widely available, non-invasive, and biologically relevant biomarker of outcome in TSC leaves patients, parents and providers with prognostic uncertainty, and prevents the rational design of a disease modification trial by pharmaceutical industry standards.

Advanced neuroimaging and neurophysiology

With the inception of diffusion-weighted imaging (DWI) and the quantification of diffusion by diffusion tensor imaging (DTI), novel tools became available. Diffusion-weighted imaging measures the diffusivity of water brain tissue water, based on Brownian motion of hydrogen atoms[27,28]. Unrestricted diffusion occurs when diffusion is equal in all directions,

and restricted diffusion reflects the presence of biological barriers. At times, water diffusion is *unrestricted* along one axis, e.g. inside the myelin sheath in axons, and *restricted* in the other two directions. This results in a preferential diffusion along the axis with the least restriction[15]. If brain regions show a consistent pattern of preferential diffusion and restriction, apparent patterns of consistent barriers to diffusion can be used to make assumptions about the microstructure of the brain tissue[29,30].

With DTI, diffusion properties can be quantified, and facilitate the modeling of microstructural tissue properties[31]. The average amount of diffusion in a volume (referred to as a voxel, imagine a 3D pixel) is called the mean diffusivity (MD) and the magnitude of preferential diffusion is expressed as the fractional anisotropy (FA). If several adjacent voxels in the white matter have a high preferential diffusion (high FA) in the same direction, a white matter pathway may be inferred[32]. In **Chapter 3**, the technique is graphically reviewed, and described in more detail.

In TSC, white matter that was previously deemed normal on conventional imaging, was found to have abnormal diffusion properties[33,34]. Whether and to what extent abnormal white matter diffusion relates to neurological phenotype is unknown. At Boston Children's Hospital, serial MRI monitoring for clinical and for research purposes in patients with TSC, has been done with standardized MRI acquisition schemes since approximately 2009. Early detection of the TSC diagnosis, and consistency in imaging has added longitudinal data and statistical power to the analysis, improving the possibility of outcome prediction.

With regards to neurophysiology, hypsarrhythmia has been reported to carry some prognostic utility in TSC[35], but otherwise EEG has undergone little investigation for use in the prediction or understanding of the neurological phenotype. For ASD in TSC, the frequent use of EEG studies for clinical management yields a rich dataset for exploration of network measures. For epilepsy in TSC, repeated recordings in the same patients provides an opportunity to assess longitudinal changes in the EEG and the relation to impending epilepsy.

OUTLINE

The main aim of this thesis is to develop advanced neuroimaging and neurophysiology markers of epilepsy and ASD in TSC. Essentially, this thesis reports the application of two tools to two major phenotypical outcomes in TSC (Table 2):

Table 2. Outline of thesis

	Autism Spectrum Disorder (Review in **Chapter 2**)	Epilepsy
Neuroimaging (structure) (Review in **Chapter 3**)	**Chapter 4** **Chapter 5**	**Chapter 6**
Neurophysiology (function)	**Chapter 8**	**Chapter 7**

In order to incorporate such markers in clinical practice or to become part of prospective trials, step-wise, several questions need to be addressed.

First, what is the current knowledge of ASD in TSC, and how do insights and novel therapeutic approaches apply to ASD and to disorders with early epilepsy in general? In **Chapter 2**, molecular mechanism underlying TSC are reviewed, and it is discussed how aberrant neural connectivity can lead to ASD symptoms. With advances in mechanism-based treatment of TSC, ASD symptoms may also improve after such targeted treatment. The potential of (early) treatment with vigabatrin and mTOR inhibitors, to control seizures and improve neurodevelopment is reviewed.

Second, how can the application of an advanced neuroimaging technique lead to disease insight and a potential marker of neurological outcome? In **Chapter 3**, applications of DTI are explained and illustrated for the non-radiologist, and we review how this has proven valuable to noninvasively characterize microstructural properties of the brain. Also, we review its potential in detecting the epileptogenic tuber, and its putative role as a neurological biomarker, specifically with respect to ASD. The limitations of the technique are highlighted, and novel diffusion models are introduced which partly overcome these shortcomings.

Third, how can DTI be applied in the early determination of the clinical phenotype in TSC? We investigate in **Chapter 4 and 5** whether the white matter DTI measures correlate cross-sectionally with overall neurological outcome in TSC, and with ASD in particular. One theory on the pathophysiology in autism is referred to as "developmental disconnection"[36]. This postulates that in ASD there is an impaired long-range corticocortical transfer of intrahemispheric and interhemispheric information, affecting higher order processing of complex information. Evidence of such processing difficulties have been found consistently deficient across multiple domains and across multiple modalities (fMRI, EEG, DTI, and others)[37,38].

The corpus callosum represents a major commissural white matter pathway, and structural abnormality may lead to impaired long-range connectivity,. Thus, in **Chapter 4**, DTI measures of the corpus callosum are investigated as markers for ASD in TSC. In **Chapter 5**, this work is extended by inclusion of more patients and a larger and younger cohort of control

subjects to establish normative data. Within the limits of statistical possibilities, we aimed to control for the confounding effects of refractory epilepsy and of cognitive function. In addition, patients with isolated ASD (no TSC) are included, to explore markers common to ASD, regardless of etiology.

With regards to DTI and epilepsy in TSC, in **Chapter 6** we lay the foundation for the study of the development of seizures ("epileptogenesis") by exploring the longitudinal evolution of DTI measures in various neuroanatomical areas in TSC. We investigate the continuum of neuropathology from tuber to perituber tissue, extending also to deeper white matter. In addition, we quantify and model the longitudinal diffusion changes of these tissue types. The findings are discussed in the context of apparent controversies in the literature on tuber vs. perituber onset of seizures[39-42].

Fourth, how can conventional and computational EEG be used in the prediction of neurological outcome in TSC? In **Chapter 7**, early results of the prospective observational Autism Centers of Excellence (ACE) study of early EEG markers for epilepsy in TSC are presented. The interim analysis will assess if with conventional EEG interpretation, epileptiform EEG abnormalities precede the onset of clinical seizures in TSC, to determine if serial routine clinical EEG is an accurate strategy for early detection of epilepsy in TSC.

After studying the aforementioned disconnection model of ASD in patients with TSC *structurally* with DTI in Chapter 4 and 5, in **Chapter 8** we study it *functionally*, through analysis of EEG coherence measures. Based on the literature, we anticipate decreased long-range connectivity and increased short-range connectivity in patients with ASD. Similar to the DTI work, we again aimed to distinguish patients with ASD but no TSC, to assess effects attributable to ASD. Important limitations of the interpretation of EEG connectivity measures in the context of the broad, non-converging literature on the neurobiology and neurophysiology of ASD are discussed[43].

Next, also in **Chapter 8**, more advanced measures are applied to study the neuronal network. Functional EEG connectivity, although averaged over time, reflects brief moments of time-dependent synchrony ("cross-talk") between various discrete regional collections of neurons[44]. These aggregates are transiently bound in functional units, forming a network[45] We apply graph theoretical network analysis to probe the design and performance of the functional network as a whole[46].

Chapter 9 provides a general discussion on the implications of the findings of this thesis, and covers directions for future research and clinical care.

REFERENCES

1. Curatolo P, Bombardieri R, Jozwiak S. Tuberous sclerosis. Lancet 2008;372:657-68.
2. Ess KC. The neurobiology of tuberous sclerosis complex. Semin Pediatr Neurol 2006;13:37-42.
3. Chu-Shore CJ, Major P, Camposano S, Muzykewicz D, Thiele EA. The natural history of epilepsy in tuberous sclerosis complex. Epilepsia 2010;51:1236-41.
4. Jeste SS, Sahin M, Bolton P, Ploubidis GB, Humphrey A. Characterization of autism in young children with tuberous sclerosis complex. J Child Neurol 2008;23:520-5.
5. Jansen FE, Vincken KL, Algra A, et al. Cognitive impairment in tuberous sclerosis complex is a multifactorial condition. Neurology 2008;70:916-23.
6. Numis AL, Major P, Montenegro MA, Muzykewicz DA, Pulsifer MB, Thiele EA. Identification of risk factors for autism spectrum disorders in tuberous sclerosis complex. Neurology 2011;76:981-7.
7. Northrup H, Krueger DA, International Tuberous Sclerosis Complex Consensus G. Tuberous sclerosis complex diagnostic criteria update: recommendations of the 2012 Iinternational Tuberous Sclerosis Complex Consensus Conference. Pediatr Neurol 2013;49:243-54.
8. Tyburczy ME, Dies KA, Glass J, et al. Mosaic and Intronic Mutations in TSC1/TSC2 Explain the Majority of TSC Patients with No Mutation Identified by Conventional Testing. PLoS Genet 2015;11:e1005637.
9. Datta AN, Hahn CD, Sahin M. Clinical presentation and diagnosis of tuberous sclerosis complex in infancy. J Child Neurol 2008;23:268-73.
10. van Eeghen AM, Black ME, Pulsifer MB, Kwiatkowski DJ, Thiele EA. Genotype and cognitive phenotype of patients with tuberous sclerosis complex. Eur J Hum Genet 2012;20:510-5.
11. Jeste SS, Wu JY, Senturk D, et al. Early developmental trajectories associated with ASD in infants with tuberous sclerosis complex. Neurology 2014;83:160-8.
12. Jülich K, Sahin M. Mechanism-based treatment in tuberous sclerosis complex. Pediatr Neurol 2014;50:290-6.
13. Sahin M. Targeted treatment trials for tuberous sclerosis and autism: no longer a dream. Current Opinion in Neurobiology 2012;22:895-901.
14. Tillema JM, Leach JL, Krueger DA, Franz DN. Everolimus alters white matter diffusion in tuberous sclerosis complex. Neurology 2012;78:526-31.
15. Peters JM, Taquet M, Prohl AK, et al. Diffusion tensor imaging and related techniques in tuberous sclerosis complex: review and future directions. Future neurology 2013;8:583-97.
16. van Eeghen AM, Ortiz-Teran L, Johnson J, Pulsifer MB, Thiele EA, Caruso P. The neuroanatomical phenotype of tuberous sclerosis complex: focus on radial migration lines. Neuroradiology 2013;55:1007-14.
17. Bolton PF, Griffiths PD. Association of tuberous sclerosis of temporal lobes with autism and atypical autism. Lancet 1997;349:392-5.
18. Bolton PF, Park RJ, Higgins JN, Griffiths PD, Pickles A. Neuro-epileptic determinants of autism spectrum disorders in tuberous sclerosis complex. Brain 2002;125:1247-55.
19. Eluvathingal TJ, Behen ME, Chugani HT, et al. Cerebellar lesions in tuberous sclerosis complex: neurobehavioral and neuroimaging correlates. J Child Neurol 2006;21:846-51.
20. Weber AM, Egelhoff JC, McKellop JM, Franz DN. Autism and the cerebellum: evidence from tuberous sclerosis. Journal of autism and developmental disorders 2000;30:511-7.
21. Chou IJ, Lin KL, Wong AM, et al. Neuroimaging correlation with neurological severity in tuberous sclerosis complex. Eur J Paediatr Neurol 2008;12:108-12.
22. Goodman M, Lamm SH, Engel A, Shepherd CW, Houser OW, Gomez MR. Cortical tuber count: a biomarker indicating neurologic severity of tuberous sclerosis complex. J Child Neurol 1997;12:85-90.

23. Walz NC, Byars AW, Egelhoff JC, Franz DN. Supratentorial tuber location and autism in tuberous sclerosis complex. J Child Neurol 2002;17:830-2.
24. Wong V, Khong PL. Tuberous sclerosis complex: correlation of magnetic resonance imaging (MRI) findings with comorbidities. J Child Neurol 2006;21:99-105.
25. Bosl W, Tierney A, Tager-Flusberg H, Nelson C. EEG complexity as a biomarker for autism spectrum disorder risk. BMC Med 2011;9:18.
26. Duffy FH, Als H. A stable pattern of EEG spectral coherence distinguishes children with autism from neurotypical controls - a large case control study. BMC Med 2012;10:64.
27. Bitar R, Leung G, Perng R, et al. MR pulse sequences: what every radiologist wants to know but is afraid to ask. Radiographics 2006;26:513-37.
28. Goldberg-Zimring D, Mewes AU, Maddah M, Warfield SK. Diffusion tensor magnetic resonance imaging in multiple sclerosis. J Neuroimaging 2005;15:68S-81S.
29. Le Bihan D, Breton E, Lallemand D, Grenier P, Cabanis E, Laval-Jeantet M. MR imaging of intravoxel incoherent motions: application to diffusion and perfusion in neurologic disorders. Radiology 1986;161:401-7.
30. Pierpaoli C, Jezzard P, Basser PJ, Barnett A, Di Chiro G. Diffusion tensor MR imaging of the human brain. Radiology 1996;201:637-48.
31. Basser PJ, Pajevic S, Pierpaoli C, Duda J, Aldroubi A. In vivo fiber tractography using DT-MRI data. Magn Reson Med 2000;44:625-32.
32. Mori S, Kaufmann WE, Pearlson GD, et al. In vivo visualization of human neural pathways by magnetic resonance imaging. Ann Neurol 2000;47:412-4.
33. Makki MI, Chugani DC, Janisse J, Chugani HT. Characteristics of abnormal diffusivity in normal-appearing white matter investigated with diffusion tensor MR imaging in tuberous sclerosis complex. AJNR Am J Neuroradiol 2007;28:1662-7.
34. Simao G, Raybaud C, Chuang S, Go C, Snead OC, Widjaja E. Diffusion tensor imaging of commissural and projection white matter in tuberous sclerosis complex and correlation with tuber load. AJNR Am J Neuroradiol 2010;31:1273-7.
35. Muzykewicz DA, Costello DJ, Halpern EF, Thiele EA. Infantile spasms in tuberous sclerosis complex: prognostic utility of EEG. Epilepsia 2009;50:290-6.
36. Geschwind DH, Levitt P. Autism spectrum disorders: developmental disconnection syndromes. Curr Opin Neurobiol 2007;17:103-11.
37. Courchesne E, Pierce K, Schumann CM, et al. Mapping early brain development in autism. Neuron 2007;56:399-413.
38. Minshew NJ, Williams DL. The new neurobiology of autism: cortex, connectivity, and neuronal organization. Arch Neurol 2007;64:945-50.
39. Koh S, Jayakar P, Dunoyer C, et al. Epilepsy surgery in children with tuberous sclerosis complex: presurgical evaluation and outcome. Epilepsia 2000;41:1206-13.
40. Ma TS, Elliott RE, Ruppe V, et al. Electrocorticographic evidence of perituberal cortex epileptogenicity in tuberous sclerosis complex. J Neurosurg Pediatr 2012;10:376-82.
41. Major P, Rakowski S, Simon MV, et al. Are cortical tubers epileptogenic? Evidence from electrocorticography. Epilepsia 2009;50:147-54.
42. Mohamed AR, Bailey CA, Freeman JL, Maixner W, Jackson GD, Harvey AS. Intrinsic epileptogenicity of cortical tubers revealed by intracranial EEG monitoring. Neurology 2012;79:2249-57.
43. Geschwind D. Autism: searching for coherence. Biol Psychiatry 2007;62:949-50.
44. Varela F, Lachaux JP, Rodriguez E, Martinerie J. The brainweb: phase synchronization and large-scale integration. Nat Rev Neurosci 2001;2:229-39.
45. van Putten MJ. Proposed link rates in the human brain. J Neurosci Methods 2003;127:1-10.

46. Rubinov M, Sporns O. Complex network measures of brain connectivity: uses and interpretations. Neuroimage 2010;52:1059-69.

Chapter 2

Tuberous Sclerosis: A New Frontier in Targeted Treatment of Autism

Peter E. Davis[1], Jurriaan M. Peters[1], Darcy A. Krueger[3], Mustafa Sahin[1,2]

1. Department of Neurology, Boston Children's Hospital, Harvard Medical School, 300 Longwood Avenue, Boston 02115, MA

2. F.M. Kirby Neurobiology Center, Boston Children's Hospital, Harvard Medical School, Boston, MA

3. Division of Neurology, Department of Pediatrics, Cincinnati Children's Hospital Medical Center, University of Cincinnati College of Medicine, Cincinnati, OH

ABSTRACT

Tuberous sclerosis complex (TSC) is a genetic disorder with a high prevalence of autism spectrum disorder (ASD). Tremendous progress in understanding the pathogenesis of TSC has been made in recent years, along with initial trials of medical treatment aimed specifically at the underlying mechanism of the disorder. At the cellular level, loss of TSC1 or TSC2 results in upregulation of the mechanistic target of rapamycin (mTOR) pathway. At the circuitry level, TSC and mTOR play crucial roles in axonal, dendritic, and synaptic development and function. In this review, we discuss the molecular mechanism underlying TSC, and how this disease results in aberrant neural connectivity at multiple levels in the central nervous system, leading to ASD symptoms. We then review recent advances in mechanism-based treatments of TSC, and the promise that these treatments provide for future mechanism-based treatment of ASD. Because of these recent advances, TSC represents an ideal model for how to make progress in understanding and treating the mechanisms that underlie ASD in general.

INTRODUCTION AND BACKGROUND

Prevalence of Tuberous Sclerosis Complex and Autism Spectrum Disorder

Tuberous sclerosis complex (TSC) is an autosomal dominant disorder due to mutations in either TSC1 or TSC2. Spontaneous genetic mutations occur in 2/3 cases. The incidence of TSC is about 1 in 6000 live births [1] and it presents with a wide range of manifestations caused by localized cellular overgrowth leading to benign tumors (hamartomas) in multiple organs, including the brain (cortical and subcortical tubers, subependymal nodules, and subependymal giant cell astrocytomas (SEGAs)), eye (retinal hamartomas), heart (rhabdomyomas), lungs (lymphangioleiomyomatosis), kidneys [angiomyolipomas], and skin (hypomelanotic macules, angiofibromas, and shagreen patches) [2-4].

Approximately 90 % of patients with TSC will have some level of tuberous sclerosis-associated neuropsychiatric disorder (TAND), including autism spectrum disorder (ASD), attention deficit hyperactivity disorder, depression and anxiety, intellectual disability, and specific learning disorders [5]. The prevalence of ASD in TSC varies depending on the sampled population, diagnosis definition, and testing methodologies used but ranges from 26 % to 50 % [6, 7]. TSC is one of the most frequently identified monogenic causes of ASD.

Advantages of TSC as a Disease Model to Study ASD

TSC provides a number of advantages as a model disorder in which to study early development and treatment of ASD. These include the possibility of pre- or neonatal identification of patients, the high prevalence of ASD among the TSC population, the phenotypic variability of TSC presentation, the current level of understanding and interest in the mechanisms underlying TSC, and the current progress in mechanism-based treatment for TSC [8]. Owing to the presence of cardiac rhabdomyomas being detected with ultrasound, many patients with TSC are now diagnosed prenatally or at birth [9]. Early diagnosis offers a chance to follow the development of ASD symptoms and biomarkers from the earliest possible time period, well before any neuropsychiatric symptoms become evident. The prevalence of ASD in patients with TSC is higher than in many other cohorts with the potential for presymptomatic identification, including siblings of children with ASD [6, 10].

The severity of ASD symptoms in patients with TSC varies from generally unaffected to severely affected, and ASD symptoms are accompanied by range of associated neuropsychological deficits. A recent study of ASD behavioral "signatures" found that out of a group of 6 genetic disorders associated with ASD, patients with TSC had the widest range of autistic features, and the most overlap with a sample of patients with idiopathic ASD [11]. This would indicate that findings related to ASD in TSC may have broad applicability to a range of patients with ASD of multiple causes. Some of the possible reasons underlying

this variability in ASD symptoms and severity in TSC will be explored in the section "The Pathophysiology of ASD in TSC."

One of the most compelling reasons to use TSC as a model in which to study ASD is that the cellular mechanisms at the root of the disorder have become increasingly well characterized over the last decade. The overactive mTOR pathway seen in TSC has been implicated in numerous other diseases, including cancer, obesity, type 2 diabetes, and neurodegenerative disorders, as well as other genetic disorders presenting with ASD, prompting intensive investigation into its normal function and pathological dysfunction [12–14]. Several mTOR-inhibiting drugs have been used and studied for some time in oncology and for immune suppression; more recently, these drugs have been approved for use in patients with TSC for the treatment of SEGAs and renal angiomyolipomas, and are being studied in the treatment of other manifestations of the disease, including neuropsychiatric symptoms [4, 7]. Understanding the cellular mechanisms of TSC and having a mechanism-based treatment opens a world of possibility for understanding and treating ASD "from the ground up".

Mechanism of TSC: The mTOR Pathway

The mTOR pathway is a common intracellular biochemical pathway responsible for regulating mRNA translation, autophagy, stress pathways, and other functions related to cellular growth and homeostasis [13, 15, 16]. mTOR is a serine– threonine kinase that is an essential component of two complexes, mTOR complex 1 and 2 (mTORC1 and mTORC2). mTORC1 is regulated by the products of TSC1 and TSC2, hamartin and tuberin, respectively. These bind together along with TBC1D7 to form a heteromeric complex that acts as a GTPase-activating protein, which inactivates Ras homolog enriched in brain (Rheb). When Rheb is inactivated, the function of the mTORC1 complex is inhibited.

The mTORC1 is a key regulatory complex that is controlled by extracellular signals that affect mRNA translation. In normally functioning cells, it is responsive to low energy levels (increased adenosine monophosphate/adenosine triphosphate ratio) via the adenosine monophosphate-dependent kinase, which then inhibits cell growth. mTORC1 is also activated by upstream activity of several growth factors on the TSC complex, including insulin and insulin-like growth factor 1, which stimulate the phosphoinositide 3-kinase and Ras pathways to trigger cell growth [12].

With loss of function of either TSC1 or TSC2 in TSC disease, mTORC1 becomes overactive, leading to phosphorylation of eIF4E-binding protein 1 and p70 S6 kinase 1, which activates mRNA translation. This leads to cellular overgrowth and metabolic overactivity, causing many of the multisystemic effects of TSC.

THE PATHOPHYSIOLOGY OF ASD IN TSC

The pathophysiology underlying ASD in patients with TSC is an area of intense interest and inquiry, and one in which attention to the mechanisms at play in TSC may shed some light. The core abnormality in TSC, dysregulation of the mTOR pathway, leads to abnormal brain development and functioning at all levels of neural function, from intracellular biochemistry to the brain as a whole. This includes abnormalities in intracellular signaling; cell growth and development; neuronal migration; and axon, dendrite, and synapse formation and maintenance. All of these mechanisms have been postulated to be part of the underlying pathophysiology leading to ASD. In TSC, these abnormalities lead to formation of dysplastic neurons, tubers, and aberrant neuronal connections, and presumably to the ASD, epilepsy, and other TAND symptoms seen in patients. This section will review recent findings related to TSC and autism due to these multilevel systemic defects.

Dysfunction of the mTOR Pathway Leading to Neuronal Intracellular Abnormalities

Loss of activity of either TSC1 or TSC2 leads to loss of inhibition of mTORC1 and increased downstream activity, including increased protein synthesis, without regard to upstream growth factors or energy availability (Fig. 1a). In neurons, this leads to dysregulation of a number of vital functions related to neuronal function and signaling, including axon specification and guidance, dendritic morphogenesis, and synapse formation and adaptation. Deficits in these fundamental processes can lead to abnormalities in neuronal circuit formation and activity-dependent plasticity. Additionally, dysfunction of the mTOR pathway leads to defects in autophagy and the cellular stress response [17–19], potentially increasing vulnerability to external stressors such as seizures, hypoxia, inflammation, and toxins. When the mTOR pathway is dysregulated in neuroglial progenitor cells, it results in abnormalities in brain development, including defects in cell growth, migration, lamination, and myelination [20]. Dysfunction of the mTOR pathway is also implicated in a number of other single-gene disorders with a high incidence of ASD, such as phosphatase and tensin homolog deleted in chromosome ten(PTEN)-associated disorders, neurofibromatosis type 1, and fragile X [14, 21, 22].

Abnormalities of Synaptic Function and Intercellular Signaling

The cellular abnormalities resulting from mTOR dysregulation have a cascading effect that leads to defects in synapse formation and function (Fig. 1b). Recent studies have pointed to abnormalities at the level of the synapse in a number of conditions associated with ASD [23–25]. Upregulation of the mTOR pathway leads to abnormal dendritic protein synthesis with reduced or dysmorphic dendritic spines and alterations in postsynaptic glutamate receptor-mediated long-term depression [26–28]. These synaptic abnormalities have been

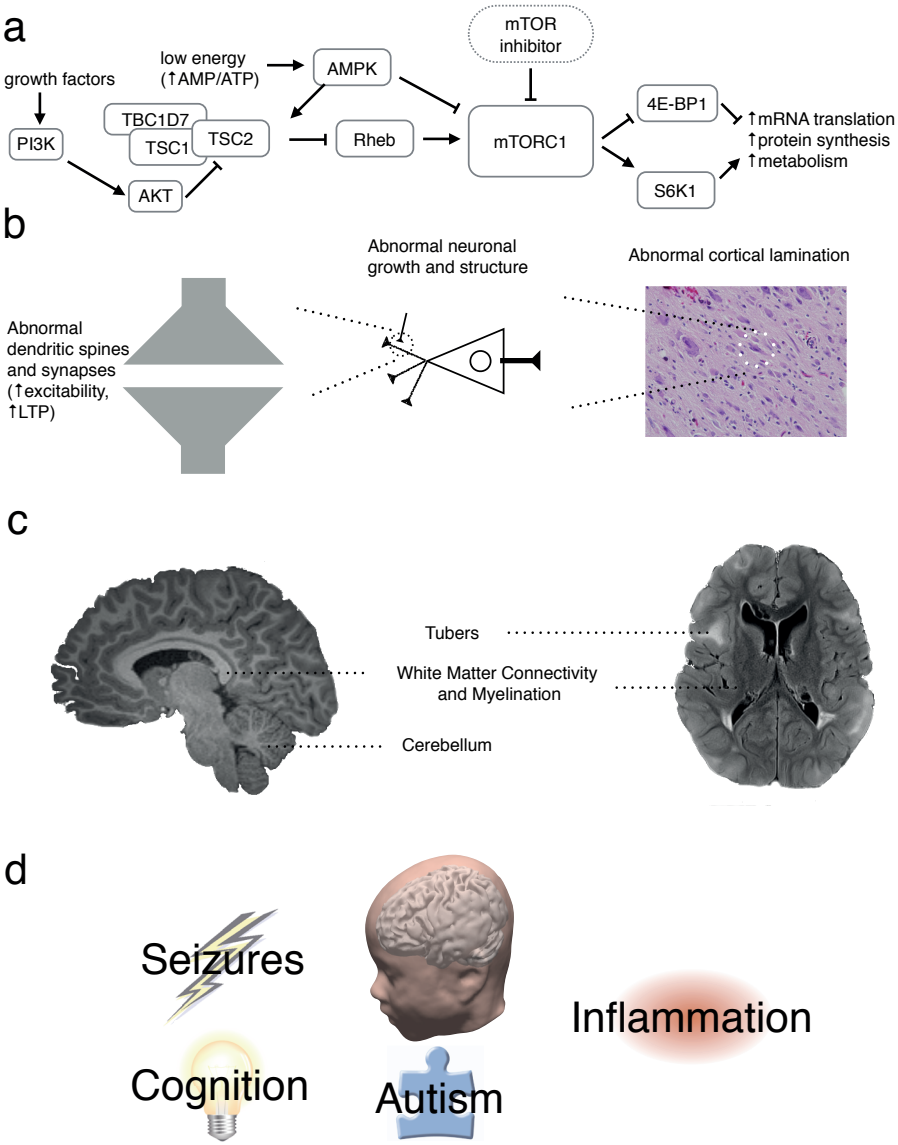

Figure 1: The multiple levels of neural structure and function affected in tuberous sclerosis complex (TSC).
(a) Biochemical: dysregulation of the mechanistic target of rapamycin (mTOR) pathway leads to unchecked cellular growth. (b) Neuronal: cellular overgrowth causes abnormal synaptic excitability and long-term potentiation (LTP), dendritic spine morphology, neuronal structure, and cortical lamination. (c) Brain: cellular overgrowth and abnormal migration results in formation of tubers, abnormal white matter myelination and connectivity, and cerebellar abnormalities. (d) Organism: multiple neural abnormalities result in seizures, abnormal cognition, inflammation, and autism spectrum disorder symptoms.
PI3K=phosphoinositide 3-kinase; AMP=adenosine monophosphate; ATP=adenosine triphosphate; AKT=protein kinase B; AMPK=AMP-activated protein kinase; mTORC1=mTOR complex 1; 4E-BP1=eIF4Ebinding protein 1; S6K1=p70 S6 kinase 1

postulated to contribute to deficits in learning, memory, and adaptation seen in ASD [15, 23, 29]. Changes at the synapse or electrical properties of the cells may then lead to abnormal neuronal excitability, which was decreased in cerebellar Purkinje cells and increased in hippocampal pyramidal neurons of TSC mutant mice [28, 30]. In addition, decreased gamma-aminobutyric acid (GABA)-ergic inhibition and increased glutamatergic excitation is implicated in the increased seizure susceptibility seen in TSC and likely also contributes to cognitive dysfunction [31–33].

Abnormalities of Brain Development and Neural Connectivity

The mTOR pathway is active during embryonic brain development and affects the initial growth and development of neurons and glia. In addition to causing abnormalities and overgrowth of individual cells, mTOR dysregulation leads to abnormalities in neuronal migration and formation of cortical lamination (Fig. 1b). These proliferation, differentiation and migration abnormalities appear to be responsible for the various structural brain malformations characteristic of TSC, including tubers, white matter heterotopias, radial migration lines, and subependymal nodules (Fig. 1c) [15]. Studies of postmortem brains of patients with TSC have also shown microscopic structural abnormalities in grossly normal-appearing regions, potentially indicating more widespread abnormalities in brain structure than would be suggested by neuroimaging [34]. The variety of phenotypes seen in TSC may be a result of variations in location of tubers and other macrostructural abnormalities, with tubers particularly in temporal and cerebellar locations being correlated with ASD symptoms in TSC [35–37].

In addition to abnormalities in glial and neuronal migration, the formation of myelin also appears to be affected in TSC [34, 38], thus contributing to the white matter abnormalities found using diffusion-weighted imaging of patients with TSC. These patients had decreased anisotropy in regions of radiographically normal-appearing white matter, indicating abnormal white matter microstructure. This decrease was more severe in patients with TSC with an autism phenotype throughout the white matter and specifically in language-related pathways [39, 40]. The abnormal neuronal formation, migration, and wiring in TSC may result in the deficits in functional neural connectivity that have been postulated to be at the root of ASD [41–43]. Local overconnection may result from clusters of cells that do not properly migrate and laminate and form excessive axonal and dendritic connections. Long-range underconnection may result from disorders of myelination, axonal pathfinding defects and abnormal larger-scale neuronal migration.

Epilepsy, Development, and Environment Effects on ASD in TSC

A number of systemic factors and comorbid conditions affect the ASD phenotype and severity in TSC, including epilepsy, cognitive impairment, and inflammation (Fig. 1d). Epilepsy

is the most prevalent neurologic comorbidity of TSC, present in about 85 % of patients, with the majority of patients developing seizures within the first year, and often within the first few months, of life. Infantile spasms are particularly common, although focal seizures also often occur before, after, or in conjunction with spasms [2, 3]. Studies have shown correlations with earlier onset of seizures and worse cognitive outcomes in rodents and humans [44, 45]. A study of early developmental trajectories in children with TSC and ASD found a trend towards more severe epilepsy in patients with TSC with ASD, as well as a decreased nonverbal intelligence quotient (IQ) in patients with longer seizure durations [10]. Early studies suggest treatment of epileptic abnormalities in TSC prior to the onset of seizures results in improved outcomes in intellectual ability and epilepsy control [46, 47]. This suggests that more severe or poorly controlled epilepsy may contribute to worse cognitive outcomes in TSC and ASD, and correlations to that effect have been shown, particularly with infantile spasms [48]. However, the correlative versus causal relationship between epilepsy and autism remains an area in need of further exploration [49, 50].

Patients with TSC have a high prevalence of cognitive impairment and intellectual disability, but there is a wide range of severity across patients. IQ scores in TSC appear to be roughly bimodally distributed, with one group of patients with severe intellectual disability and another group with intelligence in the normal range but with a downshifted mean [3]. The biological basis for this bimodal distribution remains unclear. Investigations of early developmental trajectories of children with TSC have shown correlations between cognitive impairment and autism, such that children with the most severe autism also have the most severe intellectual impairment. Even children with TSC but without an ASD diagnosis had impairment in their play behavior [6]. In addition, children with TSC and an ASD diagnosis had a decline in their nonverbal IQ, verbal IQ, and developmental quotient in the second to third year of life, evenwhen controlling for the duration of seizures, while their non-ASD counterparts had gains in these domains [10]. The relationship between cognition and autism in TSC may be a result of a common underlying neurodevelopmental dysfunction, increased difficulty with learning due impaired social interactions, or some combination thereof.

The relationship between inflammation and autism is an active area of research, as well as one of controversy. One area of particular relevance to autism in TSC is the relationship between mTOR pathway dysregulation and altered immune system activity in patients with ASD [51]. Other studies have focused on the interaction between prenatal inflammatory triggers and TSC genetics, including the finding that mice with *Tsc2* haploinsufficiency and intrauterine immune activation were more likely to show deficits in social behavior. This was paired with an observation that, when compared with children with TSC without ASD or children with idiopathic ASD, more children with both ASD and TSC had the third trimester

of their development occur during a time of peak seasonal influenza activity [8]. These findings suggest that the interaction of increased immune activation during late intrauterine development with the TSC genotype may contribute to the development of ASD.

PROMISING TREATMENTS

mTOR Inhibitors

The first mTOR inhibitor, rapamycin (sirolimus), was discovered in 1975 as an antifungal agent and was subsequently found to have antiproliferative and immunosuppressive properties, leading to its initial uses in preventing solid organ transplant rejection and restenosis of coronary arteries following angioplasty. Following the elucidation of the mTOR pathway and the role of TSC1 and TSC2, and with the development of derivative medications with improved pharmacokinetics and side effect profiles, over the last decade mTOR inhibitors have begun to be studied and used in treatment of the various manifestations of TSC, as well as in a number of malignancies (see [52] and [53] for reviews). Sirolimus and its derivatives ("rapalogs") such as everolimus work by binding FKBP12 and then interacting with the FKBP12–rapamycin-binding domain of mTORC1, inhibiting the serine–threonine kinase activity of mTORC1 and preventing mRNA translation. This effectively restores the mTORC1 inhibition that would normally be provided by the TSC1/2 complex that is dysfunctional in patients with TSC. A second generation of mTOR kinase domain inhibiting medications with activity against both mTORC1 and mTORC2 are now under development and in early clinical trials [53]. With the clinical availability of these medications, studies of their use in TSC have shown a number of promising results in animal and human studies.

Therapeutic Effects of mTOR Inhibitor Treatment in Animal Models of TSC

A number of animal models of TSC have been developed, with both spontaneous and conditional knockout of either TSC1 or TSC2 in neural stem cells, neurons, or glial cells (Table 1). These animals develop most of the pathologic features of TSC, including abnormal neuronal migration and lamination, increased cell size, and hypomyelination, as well as a number of neurocognitive features, including seizures, impairment in learning and memory, and deficits in social behavior. Trials using mTOR inhibitors in animal models of TSC have shown that blocking the action of mTOR can reverse a number of manifestations of TSC, both at the cellular level and in the behavior and survival of the animal. Zeng et al. [69] demonstrated in mice with conditional knockout of *Tsc1* in glial cells that early treatment with rapamycin prevented the development of epilepsy, and later treatment decreased seizures and prolonged survival. In another mouse model with neuron-specific conditional knockout of *Tsc1* in neuronal cells, treatment with rapamycin or everolimus normalized levels of mTOR pathway constituents with corresponding improvement in neurofilament abnormalities,

Table 1. Examples of Preclinical Mouse Models of TSC

Model	Cell Type	Phenotypes	Drug Treatment	Reference
CNPcre^{Cre}; Tsc1$^{fl/fl}$	oligodendrocytes	reduced myelination	rapamycin	[54]
Gbx2^{CreER}; Tsc1$^{fl/fl}$	thalamus relay neurons (mosaic)	seizures repetitive grooming	N/A	[55]
CamKIIalphaCre ; Tsc1fl/fl^{Cre}; Tsc1$^{fl/fl}$	forebrain excitatory neurons	kainate-seizures	N/A	[32]
hGFAP^{Cre}; Tsc1$^{fl/-}$ hGFAP^{Cre}; Tsc1$^{fl/-;}$ *Tsc2*$^{f/-}$	radial glial progenitor cells	seizures, reduced myelination, lethality	N/A	[56]
L7^{Cre}; Tsc1$^{fl/fl}$	cerebellar Purkinje cells	impaired sociability repetitive grooming	rapamycin	[30]
L7^{Cre}; Tsc2$^{fl/fl}$	cerebellar Purkinje cells	impaired sociability repetitive grooming	rapamycin	[57]
hGFAP2^{Cre}; Tsc1$^{fl/-}$ hGFAP2^{Cre}; Tsc2$^{fl/-}$	radial glial progenitor cells	seizures, reduced myelination, lethality	rapamycin	[58]
Dlx5/6^{Cre}; Tsc1$^{fl/fl}$	GABAergic interneurons	reduced seizure threshold, lethality	N/A	[59]
Emx^{Cre}; Tsc1$^{fl/fl}$	forebrain neural progenitor cells	seizures, reduced myelination, lethality	rapamycin	[60]
Syn^{Cre}; Tsc2$^{c\text{-}del3}$	neurons (hypomorphic allele)	impaired sociability and learning	N/A	[61]
Emx^{Cre}; Tsc1$^{fl/fl}$	forebrain neural progenitor cells	abnormal cortical lamination, expanded SVZ region	rapamycin	[62]
Nestin-CreER^{T2}; Tsc1$^{fl/fl}$	Neuronal progenitor cells (mosaic)	expanded SVZ region	N/A	[63]
Nestin-rtTA; TetOp-Cre; Tsc1$^{fl/fl}$	Neuronal progenitor cells (mosaic)	seizures, hyperactivity	rapamycin	[64]
hGFAP^{Cre}; Tsc2$^{fl/fl}$	astrocytes	seizures, lethality	rapamycin	[65]
Syn^{Cre}; Tsc1$^{fl/fl}$	neurons	tremor, seizures, reduced myelination, lethality	rapamycin RAD001	[38, 66]
Tsc2+/-	Constitutive heterozygous	deficits in hippocampal-dependent learning	rapamycin	[67]
hGFAP^{Cre}; Tsc2$^{fl/-}$	radial glial progenitor cells	abnormal cortical lamination, reduced myelination	N/A	[68]
hGFAP^{Cre}; Tsc1$^{fl/fl}$	astrocytes	seizures, lethality	rapamycin, vigabatrin	[65, 67-71]

reduction of enlarged cells, and restoration of myelination [66]. Treated animals showed significant improvement in seizures and overall survival, although these improvements were attenuated when treatment was discontinued. These improvements were seen despite no evidence in reversal of neuronal migration abnormalities and only minor improvement in dendritic spine density and length, indicating not all mTOR-related structural and functional abnormalities may be equally important for behavioral abnormalities or seizures, or that correction of some but not all abnormalities may be sufficient to improve outcome.

Ehninger et al. [67] showed that heterozygous *Tsc2* mice had abnormalities in hippocampal long-term potentiation, with induction of late long-term potentiation at a lower threshold. This led to deficits in spatial learning and contextual discrimination, even in the absence of frank neuropathology and seizures, and these deficits were abrogated with only 5 days of rapamycin treatment. Various approaches have been used to investigate the underlying mechanisms responsible for this hippocampal hyperexcitability [32], with at least 2 contributing pathways implicated to date. Tavazoie et al. [28] reported that loss of *Tsc2* is associated with increased α-amino-3-hydroxy-5-methyl-4-isoxazolepropionic acid(AMPA)-mediated excitatory currents, whereas Chevere-Torres et al. [26] found that metabotropic glutamate-induced long-term depression is impaired with functional disruption of *Tsc2* (in the DeltaRG mouse model of TSC) that is extracellular regulated kinase dependent and rapamycin sensitive [27]. This hyperexcitability is thought to contribute to the epilepsy and learning problems seen in TSC and demonstrates another mechanism in which mTOR inhibitors may prove beneficial for the treatment of ASD.

Several studies have specifically examined the underlying mechanisms of autism-like behaviors in animals with a TSC mutation. In contrast to hippocampal neurons, where loss of *Tsc1* or *Tsc2* results in hyperexcitability, loss of *Tsc1* in cerebellar Purkinje cells in mice results in decreased neuronal excitability [30]. These latter mice demonstrate an ASD-like phenotype, including abnormal social behavior and learning, repetitive behaviors, and vocalization. These changes were prevented by treatment with rapamycin. Similar results were obtained with Tsc2 knockout in the Purkinje neurons [57]. Talos et al. [72] reported that a rodent model of neonatal seizures results in mTORC1 overactivity, and seizures during a period of peak synaptogenesis contributed to deficits in a social novelty assay. Treatment with rapamycin in animals with neonatal hypoxic seizures was protective against the development of epilepsy and decreased the social novelty deficit. Another mouse model with conditional knockout of Tsc1 in forebrain neurons (under CaMKIIα-cre) further links mTOR hyperactivation with seizures and autism-like behaviors [73]. Decreased social behavior (in the 3-chamber social approach) and increased repetitive behaviors (marble burying) were observed in these mutantmice. As the recurrent seizure spread to the brainstem, the authors hypothesized that serotonergic neurons were specifically implicated in mediating

the autistic-like behaviors. Using a conditional knockout of Tsc1 in serotonergic neurons, they found that autism-like behaviors persisted, even though the mice did not develop spontaneous seizures. Treatment with rapamycin decreased mTOR hyperactivity and normalized measures of social preference and marble burying. Taken together, these studies show a complex relationship between early brain development, mTOR pathway overactivity in various brain regions, seizures, and the development of ASD-like behaviors, and also show that treatment with an mTOR inhibitor is a potentially promising method to normalize underlying mechanisms leading to the behavioral manifestations of ASD.

Preliminary Results of Neuropsychological Effects of mTOR Inhibitor Trials in Humans

The first human clinical trials using mTOR inhibitors in the treatment of TSC began in 2002, with the initial focus on reducing tumor burden and growth in the brain (SEGA), kidney (angiomyolipoma), and lung (lymphangioleiomyomatosis). These targets were selected based on significant diseaserelated morbidity and mortality, lack of effective noninvasive treatment options, and relative ease in objectively assessing treatment response. Rapamycin was shown to be effective and well tolerated for reducing SEGA tumor volume [74], renal angiomyolipoma volume [75–77], and pulmonary lung function [78], as long as treatment was maintained. However, in each case disease progression resumed upon discontinuation of treatment, similar to what had been observed in preclinical models. As a result, more recent studies have evaluated the sustained efficacy and long-term safety of continuous treatment. Krueger et al. [79, 80] treated 28 patients with SEGAs with everolimus for a median of 3 years without loss of SEGA tumor volume reduction and no newly encountered clinical toxicities. A placebo-controlled SEGA treatment study with everolimus involving 117 patients, with a median follow-up of 2 years, yielded similar results [81, 82]. Bissler et al. [83] reported safety and efficacy of everolimus treatment for angiomyolipoma but median treatment duration was much shorter (slightly over 6 months). Throughout these early clinical trials, unpublished anecdotal reports (Franz, NIH Curing Epilepsy 2007), case reports [84], and secondary end points [77, 79] suggested that rapalogs might have benefit for central nervous system (CNS)-related manifestations in TSC beyond reduction of tumors and tubers. For example, Krueger et al. [79] reported after 6 months of treatment with everolimus, seizure frequency was reduced in 56 % of participants. By 24 months, patients with daily seizures were reduced from 27 % to 13 %, while patients with no seizures increased from 39 % to 65 % during the same interval [80]. These improvements correlated with improvement in white matter integrity as measured with diffusion tensor imaging and were independent of SEGA treatment response [85]. Analysis of seizure control as a secondary end point in the placebo-controlled, blinded Phase III trial with everolimus to treat SEGA was unable to confirm these earlier results, largely owing to significant differences in baseline seizure frequency between the control and treatment groups, and the

fact that in both groups the majority of participants were seizure-free at time of treatment initiation [81]. Since then, smaller, mostly retrospective, studies have continued to report treatment benefit for epilepsy [86–89]. To date, the only clinical trial specifically to use mTOR inhibitors to treat epilepsy prospectively involved open-label treatment with everolimus for 4 months [90]. Eighteen of 20 participants reported a reduction in seizure frequency, with 12/20 (60 %) experiencing an improvement of 50 % or more. Furthermore, treatment response appeared to improve over time, with better response at 3–4 months compared with response at 1–2 months. This delayed or prolonged response time for optimal outcome supports involvement of mechanisms discussed in the previous sections that require weeks to months rather than hours to days to show effect, such as synapse remodeling, network connectivity, and neuronal plasticity. However, direct evidence that this is the case and the relative contributions each has on seizure susceptibility and treatment response remains to be determined. Longer-term treatment and placebo-controlled, double-blind clinical trials are already in progress to further investigate everolimus impact on seizures and epilepsy in TSC.

Evaluating the impact of mTOR inhibitors in patients with TSC with intellectual disability and other aspects of TAND, including ASD, has been more difficult. In the initial 28-patient SEGA study, a robust neurocognitive assessment battery was included but the majority of participants were developmentally and/or cognitively impaired such that relatively few were able to complete the assessments, and no conclusions could be drawn [79]. A similar attempt by Davies et al. [77] in adults treated with rapamycin for angiomyolipoma fared a little better, although the final size of the analysis cohort remained relatively small (n=8) and yielded mixed results. They reported improvements in recall memory (7/8) and executive function (5/8) but worsening in recognition memory (5/8) in adults with TSC following treatment with rapamycin for 4–12 months. In another study, Chung et al. [91] reported improvement in 3 patients with TSC with comorbid intermittent explosive disorder or adjustment disorder not otherwise specified who underwent formal psychiatric evaluations before and after initiating treatment with everolimus (n=2) or rapamycin (n=1). In the more recent open-label epilepsy trial by Krueger et al. [90], an indirect, more broad approach was utilized, sacrificing direct observational measures for indirect parental report using validated assessment tools with the goal of providing more universal assessment of TAND-related comorbidities and domains. Using the Nisonger Child Behavior Rating Form, adapted from the Child Behavioral Rating Form to allow assessment of both cognitively impaired and normal IQ children, they reported small but significant improvement in adaptive social behaviors, conduct problems, and insecurity/anxiety compared with baseline following treatment for 4 months. Quality of Life for Children with Epilepsy assessments done in parallel over the same time period identified similar improvements in multiple domains, including attention and concentration, behavior, social interactions and activity, and overall quality of life.

However, whether these changes were secondary to or independent of improvement in seizure control could not be determined.

Intense interest exists to confirm and expand these preliminary studies in order to determine if a longer treatment period results in sustained or further improvements, to verify results in a larger cohort using a placebo-controlled, double-blinded study design, and to incorporate direct observational assessment approaches to better determine the specific areas of neurocognitive and ASD-related subdomains affected by mTOR inhibitor treatment and further separate which effects are seizure control-dependent and which are seizure controlindependent. Ongoing trials include Everolimus (RAD001) Therapy for Epilepsy in Patients with TSC (clinicaltrials.gov: NCT01070316); Trial of RAD001 and Neurocognition in TSC (clinicaltrials.gov: NCT01289912); Efficacy of RAD001/Everolimus in Autism and NeuroPsychological Deficits in Children With Tuberous Sclerosis Complex (RAPIT) (clinicaltrials.gov: NCT01730209); A Placebo Controlled Study of Efficacy & Safety of 2 Trough-ranges of Everolimus as Adjunctive Therapy in Patients With TSC & Refractory Partial-onset Seizures (EXIST-3)(clinicaltrials.gov: NCT01713946); A Study of Everolimus in the Treatment of Neurocognitive Problems in Tuberous Sclerosis (TRON) (clinicaltrials.gov: NCT01954693); Rapalogues for Autism Phenotype in TSC: A Feasibility Study (RAPT) (clinicaltrials.gov: NCT01929642); and Long-term Follow-up for Growth and Development of Pediatric Patients From CRAD001M2301 (EXIST-LT) (clinicaltrials.gov: NCT02338609).

Early Vigabatrin Treatment Trials

Vigabatrin is a rationally designed drug that aims to increase the levels of GABA, the main inhibitory neurotransmitter in the CNS. The addition of a vinyl group to GABA (vi-GABAtrin) creates a substrate that irreversibly inhibits GABA-transaminase, the GABA-degrading enzyme, thus increasing GABA availability in the synaptic cleft. In humans, it has a specific and rapid mechanism of action and its antiepileptic properties are thought to be a direct result of increased inhibitory neurotransmission, although additional mechanisms are considered [92]. Side effects during initiation are those common to drugs affecting the CNS, and include irritability, drowsiness, and hypotonia, which typically resolve over time. One important side effect is irreversible peripheral visual field constriction, with a risk that increases cumulatively with higher doses and longer exposure [93]. In the USA, the manufacturer has implemented a vigorous monitoring program for this side effect. The clinically evident response of cessation of spasms within days to weeks provides an opportunity to try vigabatrin at a low risk. Other than as add-on for intractable complex partial seizures, vigabatrin is approved in the US as monotherapy for infantile spasms (IS). An early small controlled trial demonstrated efficacy compared with placebo but no patients with TSC were included [94]. In studies of high- versus low-dose vigabatrin and of vigabatrin versus steroid therapy for IS, patients with TSC had consistently higher response rates to vigabatrin [95, 96]. Indeed, an early

review of the literature suggested a response rate of 95 % to vigabatrin in IS due to TSC [97], an estimate that has not changed in subsequent literature [93].Within patients with TSC, in a head-to-head comparison with adrenocorticotropic hormone, vigabatrin showed clear superiority [98]. Based on these and other studies and reviews, the International TSC Consensus Conference recommends vigabatrin as first-line treatment for IS in TSC [4].Why IS in TSC in particular respond so dramatically to vigabatrin is not understood. Other drugs affecting GABAergic transmission (e.g., barbiturates and benzodiazepines) do not achieve comparable efficacy. Reported additional effects of vigabatrin such as decreased glial GABA uptake, enhanced GABA release, and reduction of glutamate have not been reproduced [92]. In a TSC mouse model, vigabatrin suppressed the mTOR pathway, which could be an additional explanation for the particular efficacy in TSC [70]. However, the rapid efficacy against IS is more likely based on GABAergic changes. Better long-term neurocognitive outcome has been reportedwith early, aggressive, and successful treatment of IS [99–101], and later cessation of IS is associated with poorer outcomes [102]. For partial seizures, however, efficacy is lower and the beneficial effects on outcome may not be present when compared with treatment of IS [100, 101]. When given even earlier, in a small open-label trial of vigabatrin initiation prior to onset of IS, good long-term outcomes were also seen [46]. If, indeed, mTOR pathway activity is modified by vigabatrin, it could contribute to these longerterm benefits. This raises the possibility that vigabatrin is not merely antiepileptic, but it may also be disease modifying. How to identify who would most benefit, with justifiable risk, from early or even pre-emptive intervention with vigabatrin, is a subject of active study. For example, epileptic spasms beyond infancy respond less well to vigabatrin, even though these seizures are similar to IS in their electroclinical presentation. Thus, there appears to be a therapeutic window in obtaining the longer-term neurodevelopmental benefits from early medical intervention. In the USA, a multicenter prospective observational study is currently underway to identify early developmental, neurophysiology, and neuroimaging markers for increased risk of epilepsy and ASD in TSC (clinicaltrials.gov: NCT01767779; NCT01780441). In a next phase, those markers will be used to stratify patients to either standard of care versus early aggressive, pre-emptive treatment with vigabatrin. In Europe, a similar effort is ongoing (clinicaltrials.gov: NCT02098759).

FUTURE DIRECTIONS OF TREATMENT FOR ASD IN TSC

We are on the cusp of a new era in targeted, disease-modifying treatment for TSC and other disorders associated with ASD. The initial results from a Phase II study looking specifically at effects on neurocognition in TSC after treatment with everolimus (clinicaltrials.gov: NCT01289912) are currently in the process of being analyzed. Open questions include the type of effects mTOR inhibitors will have on ASD symptoms in TSC and how the effects will

vary based on patient characteristics and disease manifestations. Another crucial question is what end points are quantifiable and dynamic in response to treatment within the duration of the trial. Finally, it is not yet clear whether there is a critical window during which treatments will be most effective. Once these questions are studied, we will be in a better position to determine which patients will most benefit from which treatment. Robust and early biomarkers of neurodevelopmental outcome in TSC are critical to best target treatments to patients who will most benefit from them, to avoid unnecessarily exposing patients to potentially harmful and irreversible treatment side effects, and to measure treatment effects. For ASD, behavioral and developmental signs may be recognized early in high-risk populations [10], and retrospective work has identified electroencephalography network properties and diffusion tensor imaging metrics as possible biomarkers [39, 103]. Diffusion imaging abnormalities may reflect changes in the underlying neurobiology [43], and these measures may even respond to intervention in parallel with clinical changes seen [85]. Further research on these and other biomarkers is needed to better characterize their utility for clinical use and future prospective studies. It is a rare but fortunate occurrence when our understanding of a disorder matches our ability to treat based on that understanding. We are approaching that point now for ASD in TSC. Our hope is that the recent advances described here in understanding and treating the mechanisms contributing to ASD in TSC will benefit our patients with TSC and provide a path towards better understanding and treatment for all people with ASD.

ACKNOWLEDGMENTS

P.E.D. is supported by a training grant from the National Institutes of Health (NIH) National Institute of Neurological Disorders and Stroke (NINDS; 3R25NS070682-04S1). J.M.P., D.A.K. and M.S. are supported by NIH (U01 NS082320, P20 NS080199, U54NS092090). The Developmental Synaptopathies Consortium (U54NS092090) is a part of the National Center for Advancing Translational Sciences (NCATS) Rare Diseases Clinical Research Network (RDCRN). RDCRN is an initiative of the Office of Rare Diseases Research (ORDR), NCATS, funded through collaboration between NCATS, National Institute of Mental Health, NINDS and National Institute of Child Health and Human Development. J.M.P. is also supported by Harvard Catalyst | The Harvard Clinical and Translational Science Center (National Center for Research Resources and the National Center for Advancing Translational Sciences, NIH Award UL1 TR001102). D.A.K. is also supported by Tuberous Sclerosis Alliance, Clack Foundation, Novartis, and Upsher-Smith. Research in the laboratory of M.S. is also supported by the NIH P30 HD018655, the Department of Defense, Tuberous Sclerosis Alliance, Autism Speaks, Nancy Lurie Marks Family Foundation, Simons Foundation, Boston Children's Hospital Translational Research Program, and Novartis, Shire and Roche. Full conflict of interest

disclosures are available in the electronic supplementary material for this article. Owing to limited space, we have not quoted all the literature in this field, and we apologize to those whose articles are not referenced. Finally, we are indebted to the children and families who participated in the studies reviewed in this article.

REFERENCES

1. Osborne JP, Fryer A, Webb D. Epidemiology of tuberous sclerosis. Ann N YAcad Sci 1991;615:125-127.
2. Curatolo P, Bombardieri R, Jóźwiak S. Tuberous sclerosis. Lancet 2008;372:657-668.
3. Curatolo P, Maria BL. Tuberous sclerosis. Handb Clin Neurol 2013;111:323-331.
4. Krueger DA, Northrup H, International Tuberous Sclerosis Complex Consensus Group. Tuberous sclerosis complex surveillance and management: recommendations of the 2012 International Tuberous Sclerosis Complex Consensus Conference. Pediatr Neurol 2013;49:255-265.
5. de Vries PJ,Whittemore VH, Leclezio L, et al., Tuberous sclerosis associated neuropsychiatric disorders (TAND) and the TAND Checklist. Pediatr Neurol 2015;52:25-35.
6. Jeste SS, Sahin M, Bolton P, Ploubidis GB, Humphrey A. Characterization of autism in young children with tuberous sclerosis complex. J Child Neurol 2008;23:520-525.
7. Leclezio L, de Vries PJ. Advances in the treatment of tuberous sclerosis complex. Curr Opin Psychiatry 2015;28:113-120.
8. Ehninger D, Sano Y, de Vries PJ, et al., Gestational immune activation and Tsc2 haploinsufficiency cooperate to disrupt fetal survival and may perturb social behavior in adult mice. Mol Psychiatry 2012;17:62-70.
9. Datta AN, HahnCD, Sahin M. Clinical presentation and diagnosis of tuberous sclerosis complex in infancy. J Child Neurol 2008;23:268-273.
10. Spurling Jeste S, Wu JY, Senturk D, et al. Early developmental trajectories associated with ASD in infants with tuberous sclerosis complex. Neurology 2014;83:160-168.
11. Bruining H, Eijkemans MJ, Kas MJ, et al. Behavioral signatures related to genetic disorders in autism. Mol Autism 2014;5:11.
12. LaplanteM, Sabatini DM. mTOR signaling in growth control and disease. Cell 2012;149:274-293.
13. Lipton JO, Sahin M. The neurology of mTOR. Neuron 2014;84: 275-291.
14. Ehninger D. From genes to cognition in tuberous sclerosis: implications for mTOR inhibitor-based treatment approaches.Neuropharmacology 2013;68: 97-105.
15. Feliciano DM, Lin TV, Hartman NW, et al., A circuitry and biochemical basis for tuberous sclerosis symptoms: from epilepsy to neurocognitive deficits. Int J Dev Neurosci 2013;31:667-678.
16. Chen J, Alberts I, Li X. Dysregulation of the IGF-I/PI3K/AKT/mTOR signaling pathway in autism spectrum disorders. Int J Dev Neurosci 2014;35:35-41.
17. Tang G, Gudsnuk K, Kuo SH, et al. Loss of mTOR-dependent macroautophagy causes autistic-like synaptic pruning deficits.Neuron 2014;83:1131-1143.
18. Di Nardo A, Wertz MH, Kwiatkowski E, et al. Neuronal Tsc1/2 complex controls autophagy through AMPK-dependent regulation of ULK1. Hum Mol Genet 2014;23:3865-3874.
19. Di Nardo A, Kramvis I, Cho N, et al. Tuberous sclerosis complex activity is required to control neuronal stress responses in an mTOR-dependent manner. J Neurosci 2009;29:5926-5937.
20. Lim K-C, Crino PB. Focalmalformations of cortical development: new vistas for molecular pathogenesis. Neuroscience 2013;252: 262-276.
21. Hoeffer CA, Klann E. mTOR signaling: At the crossroads of plasticity, memory and disease. Trends Neurosci 2010;33:67-75.
22. de Vries PJ. Targeted treatments for cognitive and neurodevelopmental disorders in tuberous sclerosis complex. Neurotherapeutics 2010;7:275-282.
23. Kelleher RJ, Bear MF. The autistic neuron: troubled translation? Cell 2008;13:401-406.
24. Auerbach BD, Osterweil EK, Bear MF. Mutations causing syndromic autism define an axis of synaptic pathophysiology. Nature 2011;480:63-68.

25. Won H, MahW, Kim E. Autism spectrum disorder causes, mechanisms, and treatments: focus on neuronal synapses. Front Mol Neurosci 2013;6:19.
26. Chevere-Torres I, Kaphzan H, Bhattacharya A, et al.Metabotropic glutamate receptor-dependent long-term depression is impaired due to elevated ERK signaling in the DeltaRG mouse model of tuberous sclerosis complex. Neurobiol Dis 2012;45:1101-1110.
27. Hou, L, Klann E. Activation of the phosphoinositide 3-kinase-Akt-mammalian target of rapamycin signaling pathway is required for metabotropic glutamate receptor-dependent long-term depression. J Neurosci 2004;24:6352-6361.
28. Tavazoie SF, Alvarez VA, Ridenour DA, Kwiatkowski DJ, Sabatini BL. Regulation of neuronal morphology and function by the tumor suppressors Tsc1 and Tsc2. Nat Neurosci 2005;8: 1727-1734.
29. Santini E, Klann E. Reciprocal signaling between translational control pathways and synaptic proteins in autism spectrum disorders. Sci Signal 2014;7:re10.
30. Tsai PT, Hull C, Chu Y, et al. Autistic-like behaviour and cerebellar dysfunction in Purkinje cell Tsc1 mutant mice. Nature 2012;488:647-651.
31. Zeng L-H, Ouyang Y, Gazit V, et al. Abnormal glutamate homeostasis and impaired synaptic plasticity and learning in a mouse model of tuberous sclerosis complex. Neurobiol Dis 2007;28: 184-196.
32. Bateup HS, Johnson CA, Denefrio CL, et al. Excitatory/inhibitory synaptic imbalance leads to hippocampal hyperexcitability in mouse models of tuberous sclerosis. Neuron 2013;78:510-522.
33. Curatolo P. Mechanistic target of rapamycin (mTOR) in tuberous sclerosis complex-associated epilepsy. Pediatr Neurol 2014;52:281-289.
34. Crino PB. Evolving neurobiology of tuberous sclerosis complex. Acta Neuropathol 2013;125:317-332.
35. Bolton P, Park RJ, Higgins J, Griffiths PD, Pickles A. Neuroepileptic determinants of autism spectrum disorders in tuberous sclerosis complex. Brain 2002;125:1247-1255.
36. Eluvathingal TJ, BehenME, Chugani HT, et al. Cerebellar lesions in tuberous sclerosis complex: neurobehavioral and neuroimaging correlates. J Child Neurol 2006;21:846-851.
37. Weber AM, Egelhoff JC, McKellop JM, Franz DN. Autism and the cerebellum: evidence from tuberous sclerosis. J Autism Dev Disord 2000;30:511-517.
38. Meikle L, Talos DM, Onda H, et al. A mouse model of tuberous sclerosis: neuronal loss of Tsc1 causes dysplastic and ectopic neurons, reduced myelination, seizure activity, and limited survival. J Neurosci 2007;27:5546-5558.
39. Peters JM, Sahin M, Vogel-Farley VK, et al. Loss of white matter microstructural integrity is associated with adverse neurological outcome in tuberous sclerosis complex. Acad Radiol 2012;19:17-25.
40. Lewis WW, Sahin M, Scherrer B, et al. Impaired language pathways in tuberous sclerosis complex patients with autism spectrum disorders. Cereb Cortex 2013;23:1526-1532.
41. Geschwind DH, Levitt P. Autism spectrum disorders: developmental disconnection syndromes. Curr Opin Neurobiol 2007;17:103-111.
42. Wass S. Distortions and disconnections: disrupted brain connectivity in autism. Brain Cogn 2011;75:18-28.
43. Peters JM, Taquet M, Prohl AK, et al. Diffusion tensor imaging and related techniques in tuberous sclerosis complex: review and future directions. Future Neurol 2013;8:583-597.
44. Waltereit R, Japs B, SchneiderM, deVries PJ, Bartsch D. Epilepsy and Tsc2 haploinsufficiency lead to autistic-like social deficit behaviors in rats. Behav Genet 2011;41:364-372.
45. Jansen FE, Vincken KL, Algra A, et al. Cognitive impairment in tuberous sclerosis complex is a multifactorial condition. Neurology 2008;70:916-923.
46. Jóźwiak S, Kotulska K, Domańska-Pakieła D, et al. Antiepileptic treatment before the onset of seizures reduces epilepsy severity and risk of mental retardation in infants with tuberous sclerosis complex. Eur J Paediatr Neurol 2011;15:424-431.

47. Domanska-Pakiela D, Kaczorowska M, Jurkiewicz E, et al. EEG abnormalities preceding the epilepsy onset in tuberous sclerosis complex patients—a prospective study of 5 patients. Eur J Paediatr Neurol 2014;18:458-468.
48. van Eeghen AM, Pulsifer MB, Merker VL, et al. Understanding relationships between autism, intelligence, and epilepsy: a crossdisorder approach. Dev Med Child Neurol 2013;55:146-153.
49. Berg AT, Plioplys S. Epilepsy and autism: is there a special relationship? Epilepsy Behav 2012;23:193-198.
50. El Achkar CM, Spence SJ. Clinical characteristics of children and young adults with co-occurring autism spectrum disorder and epilepsy.Epilepsy Behav 2015. doi:10.1016/j.yebeh.2014.12.022
51. Careaga M, Van de Water J, Ashwood P. Immune dysfunction in autism: a pathway to treatment. Neurotherapeutics 2010;7:283-292.
52. Gentzler RD, Altman JK, Platanias LC. An overview of the mTOR pathway as a target in cancer therapy. Expert Opin Ther Targets 2012;16:481-489.
53. Santulli G, Totary-Jain H. Tailoring mTOR-based therapy: molecular evidence and clinical challenges. Pharmacogenomics 2013;14:1517-1526.
54. Lebrun-Julien F, Bachmann L, Norrmen C, et al. Balanced mTORC1 activity in oligodendrocytes is required for accurate CNS myelination. J Neurosci 2014;34:8432-8448.
55. Normand EA, Crandall SR, Thorn CA, et al. Temporal and mosaic Tsc1 deletion in the developing thalamus disrupts thalamocortical circuitry, neural function, and behavior. Neuron 2013;78:895-909.
56. Mietzsch U,McKenna J, 3rd, Reith RM,Way SW, Gambello MJ. Comparative analysis of Tsc1 and Tsc2 single and double radial glial cell mutants. J Comp Neurol 2013;521:3817-3831.
57. Reith RM,McKenna J,Wu H, et al. Loss of Tsc2 in Purkinje cells is associated with autistic-like behavior in a mouse model of tuberous sclerosis complex. Neurobiol Dis 2013;51:93-103.
58. Magri L, Cominelli M, Cambiaghi M, et al. Timing of mTOR activation affects tuberous sclerosis complex neuropathology in mouse models. Dis Model Mech 2013;6:1185-1197.
59. Fu C, Cawthon B, Clinkscales W, et al. GABAergic interneuron development and function is modulated by the Tsc1 gene. Cereb Cortex 2012;22:2111-2119.
60. Carson RP, Van Nielen DL, Winzenburger PA, Ess KC. Neuronal and glia abnormalities in Tsc1-deficient forebrain and partial rescue by rapamycin. Neurobiol Dis 2012;45:369-380.
61. Yuan E, Tsai PT, Greene-Colozzi E, et al. Graded loss of tuberin in an allelic series of brain models of TSC correlates with survival, and biochemical, histological and behavioral features. Hum Mol Genet 2012;21:4286-4300.
62. Magri L, Cambiaghi M, Cominelli M, et al. Sustained activation of mTOR pathway in embryonic neural stem cells leads to development of tuberous sclerosis complex-associated lesions. Cell Stem Cell 2011;9:447-462.
63. Zhou J, Shrikhande G, Xu J, et al. Tsc1 mutant neural stem/progenitor cells exhibit migration deficits and give rise to subependymal lesions in the lateral ventricle. Genes Dev 2011;25:1595-1600.
64. Goto J, Talos DM, Klein P, et al. Regulable neural progenitorspecific Tsc1 loss yields giant cells with organellar dysfunction in a model of tuberous sclerosis complex. Proc Natl Acad Sci USA 2011;108:E1070-E1079.
65. Zeng LH, Rensing NR, Zhang B, et al. Tsc2 gene inactivation causes a more severe epilepsy phenotype than Tsc1 inactivation in a mouse model of tuberous sclerosis complex. HumMol Genet 2011;20:445-454.
66. Meikle L, Pollizzi K, Egnor A, et al. Response of a neuronal model of tuberous sclerosis to mammalian target of rapamycin (mTOR) inhibitors: effects on mTORC1 and Akt signaling lead to improved survival and function. J Neurosci 2008;28:5422-5432.
67. Ehninger D, Han S, Shilyansky C, et al. Reversal of learning deficits in a Tsc2+/- mouse model of tuberous sclerosis. Nat Med 2008;14:843-848.

68. WaySW,McKenna J, 3rd, Mietzsch U, et al. Loss of Tsc2 in radial glia models the brain pathology of tuberous sclerosis complex in the mouse. Hum Mol Genet 2009;18:1252-1265.
69. Zeng LH, Xu L, Gutmann DH, Wong M. Rapamycin prevents epilepsy in a mouse model of tuberous sclerosis complex. Ann Neurol 2008;63:444-453.
70. Zhang B, McDaniel SS, Rensing NR, Wong M. Vigabatrin inhibits seizures and mTOR pathway activation in a mouse model of tuberous sclerosis complex. PLoS ONE 2013;8:e57445.
71. Uhlmann EJ, Wong M, Baldwin RL, et al. Astrocyte-specific TSC1 conditional knockout mice exhibit abnormal neuronal organization and seizures. Ann Neurol 2002;52:285-296.
72. Talos DM, Sun H, Zhou X, et al. The interaction between early life epilepsy and autistic-like behavioral consequences: a role for the mammalian target of rapamycin (mTOR) pathway. PLoS ONE 2012;7:e35885.
73. McMahon JJ, Yu W, Yang J, et al. Seizure-dependent mTOR activation in 5-HT neurons promotes autism-like behaviors in mice. Neurobiol Dis 2015;73:296-306.
74. Franz DN, Leonard J, Tudor C, et al. Rapamycin causes regression of astrocytomas in tuberous sclerosis complex. Ann Neurol 2006;59:490-498.
75. Bissler JJ, McCormack FX, Young LR, et al. Sirolimus for angiomyolipoma in tuberous sclerosis complex or lymphangioleiomyomatosis. N Engl J Med 2008;358:140-151.
76. Dabora SL, Franz DN, Ashwal S, et al.Multicenter phase 2 trial of sirolimus for tuberous sclerosis: kidney angiomyolipomas and other tumors regress and VEGF-D levels decrease. PLoS ONE 2011;6:e23379.
77. Davies DM, de Vries PJ, Johnson SR, et al. Sirolimus therapy for angiomyolipoma in tuberous sclerosis and sporadic lymphangioleiomyomatosis: a phase 2 trial. Clin Cancer Res 2011;17:4071-4081.
78. McCormack FX, Inoue Y, Moss J, et al. Efficacy and safety of sirolimus in lymphangioleiomyomatosis. N Engl JMed 2011;364:1595-1606.
79. Krueger DA, Care MM, Holland K et al. Everolimus for subependymal giant-cell astrocytomas in tuberous sclerosis. N Engl J Med 2010;363:1801-1811.
80. Krueger DA, Care MM, Agricola K, et al. Everolimus long-term safety and efficacy in subependymal giant cell astrocytoma. Neurology 2013;80:574-580.
81. Franz, D.N., E. Belousova, S. Sparagana, et al. Efficacy and safety of everolimus for subependymal giant cell astrocytomas associated with tuberous sclerosis complex (EXIST-1): a multicentre, randomised, placebo-controlled phase 3 trial. Lancet 2013;381:125-132.
82. Franz DN, Belousova E, Sparagana S, et al. Everolimus for subependymal giant cell astrocytoma in patients with tuberous sclerosis complex: 2-year open-label extension of the randomized EXIST-1 study. Lancet Oncol 2014;15:1513-1520.
83. Bissler JJ, Kingswood JC, Radzikowska E, et al. Everolimus for angiomyolipoma associated with tuberous sclerosis complex or sporadic lymphangioleiomyomatosis (EXIST-2): a multicentre, randomised, double-blind, placebo-controlled trial. Lancet 2013;381:817-824.
84. Muncy J, Butler IJ, Koenig MK. Rapamycin reduces seizure frequency in tuberous sclerosis complex. J Child Neurol 2009;24:477.
85. Tillema J-M, Leach JL, Krueger DA, Franz DN. Everolimus alters white matter diffusion in tuberous sclerosis complex. Neurology 2012;78:526-531.
86. Kotulska K, Chmielewski D, Borkowska J, et al. Long-term effect of everolimus on epilepsy and growth in children under 3 years of age treated for subependymal giant cell astrocytoma associated with tuberous sclerosis complex. Eur J Paediatr Neurol 2013;17:479-485.
87. Wiegand G, May TW, Ostertag P, et al. Everolimus in tuberous sclerosis patients with intractable epilepsy: a treatment option? Eur J Paediatr Neurol 2013;17:631-638.
88. Canpolat M, Per H, Gumus H, et al. Rapamycin has a beneficial effect on controlling epilepsy in children with tuberous sclerosis complex: results of 7 children from a cohort of 86. Childs Nerv Syst 2014;30:227-240.

89. Cardamone M, Flanagan D, Mowat D, et al. Mammalian target of rapamycin inhibitors for intractable epilepsy and subependymal giant cell astrocytomas in tuberous sclerosis complex. J Pediatr 2014;164:1195-1200.
90. Krueger DA, Wilfong AA, Holland Bouley K, et al. Everolimus treatment of refractory epilepsy in tuberous sclerosis complex. Ann Neurol 2013;74:679-687.
91. Chung TK, Lynch ER, Fiser CJ, et al. Psychiatric comorbidity and treatment response in patients with tuberous sclerosis complex. Ann Clin Psychiatry 2011;23:263-269.
92. Ben-Menachem E. Mechanism of action of vigabatrin: correcting misperceptions. Acta Neurol Scand Suppl 2011:5-15.
93. Willmore LJ, AbelsonMB, Ben-Menachem E, Pellock JM, Shields WD. Vigabatrin: 2008 update. Epilepsia 2009;50:163-173.
94. Appleton RE, Peters AC, Mumford JP, Shaw DE. Randomised, placebo-controlled study of vigabatrin as first-line treatment of infantile spasms. Epilepsia 1999;40:1627-1633.
95. Elterman RD, Shields WD, Mansfield KA, Nakagawa J; US Infantile Spasms Vigabatrin Study Group, Randomized trial of vigabatrin in patients with infantile spasms. Neurology 2001;57:1416-1421.
96. Vigevano F, Cilio MR. Vigabatrin versus ACTH as first-line treatment for infantile spasms: a randomized, prospective study. Epilepsia 1997;38:1270-1274.
97. Hancock E, Osborne JP. Vigabatrin in the treatment of infantile spasms in tuberous sclerosis: literature review. J Child Neurol 1999;14:71-74.
98. Chiron C, Dumas C, Jambaque I, Mumford J, Dulac O. Randomized trial comparing vigabatrin and hydrocortisone in infantile spasms due to tuberous sclerosis. Epilepsy Res 1997;26: 389-395.
99. Bombardieri R, Pinci M, Moavero R, Cerminara C, Curatolo P. Early control of seizures improves long-term outcome in children with tuberous sclerosis complex. Eur J Paediatr Neurol 2010;14:146-149.
100. Jambaque I, Chiron C, Dumas C, Mumford J, Dulac O. Mental and behavioural outcome of infantile epilepsy treated by vigabatrin in tuberous sclerosis patients. Epilepsy Res 2000;38:151-160.
101. Yum MS, Lee EH, Ko TS. Vigabatrin and mental retardation in tuberous sclerosis: infantile spasms versus focal seizures. J Child Neurol 2013;28:308-313.
102. Muzykewicz DA, Costello DJ,. Halpern EF, Thiele EA. Infantile spasms in tuberous sclerosis complex: prognostic utility of EEG. Epilepsia 2009;50:290-296.
103. Peters JM, Taquet M, Vega C, et al. Brain functional networks in syndromic and non-syndromic autism: a graph theoretical study of EEG connectivity. BMC Med 2013;11:54.

Chapter 3

Diffusion Tensor Imaging in Tuberous Sclerosis Complex: Review and Future Directions

Jurriaan M. Peters[1,2,*], Maxime Taquet[2,4,*], Anna K. Prohl[1,2], Benoit Scherrer[2], Agnies M. van Eeghen[3], Sanjay P. Prabhu[2], Mustafa Sahin[1], Simon K. Warfield[2]

1. Department of Neurology and the Division of Epilepsy and Clinical Neurophysiology, Boston Children's Hospital, Boston, MA, USA
2. Department of Radiology and the Computational Radiology Laboratory, Boston Children's Hospital, Boston, MA, USA
3. Department of Neuroscience, ENCORE, Expertise Centre for Neurodevelopmental Disorders, Erasmus Medical Centre, Rotterdam, the Netherlands
4. ICTEAM Institute, Université catholique de Louvain, Louvain-La-Neuve, Belgium

* These authors contributed equally

ABSTRACT

In this article, the authors aim to introduce the nonradiologist to diffusion tensor imaging (DTI) and its applications to both clinical and research aspects of tuberous sclerosis complex. Tuberous sclerosis complex is a genetic neurocutaneous syndrome with variable and unpredictable neurological comorbidity that includes refractory epilepsy, intellectual disability, behavioral abnormalities and autism spectrum disorder. DTI is a method for modeling water diffusion in tissue and can noninvasively characterize microstructural properties of the brain. In tuberous sclerosis complex, DTI measures reflect well-known pathological changes. Clinically, DTI can assist with detecting the epileptogenic tuber. For research, DTI has a putative role in identifying potential disease biomarkers, as DTI abnormalities of the white matter are associated with neurocognitive morbidity including autism. If indeed DTI changes parallel phenotypical changes related to the investigational treatment of epilepsy, cognition and behavior with mTOR inhibitors, it will facilitate future clinical trials.

INTRODUCTION

Tuberous sclerosis complex (TSC) is a genetic neurocutaneous syndrome with an estimated incidence of one in 6000–10,000 [1,2]. Benign hamartomas, the hallmark of the disease, are found in multiple organ systems, including the brain, eyes, kidneys, lungs, skin and heart, and comprised nonmalignant and disorganized cells that often exhibit abnormal differentiation [3]. Inherited autosomal dominant mutations (<30%) and sporadic mutations (>70%) lead to inactivation of the tumor suppressor genes TSC1 (on chromosome band 9q34) and TSC2 (on chromosome band 16p13.3) and can be identified in 70–90% of patients who meet the clinical criteria of TSC [4,5]. TSC is diagnosed on the basis of major and minor clinical criteria, with three of the major criteria being based on neuroimaging findings [6]. In 2012, the International Tuberous Sclerosis Consensus updated the TSC diagnostic criteria from 1998; TSC can now be diagnosed via genetic testing if a pathogenic mutation is found [201].

Neurologically, TSC can manifest with developmental delay or intellectual disability, behavioral abnormalities, autism and seizures. Clinical presentation is highly variable and patients with a TSC2 mutation typically present with a more severe neurological phenotype [7,8]. Epilepsy occurs in 80–90% of all patients, is often medically refractory, and any seizure type can be seen [1]. Autism spectrum disorders (ASD) occur in up to 50% of patients by the age of 5 years [9]. Close to 45% of patients have varying degrees of intellectual disabilities [5]. Neurological sequelae are particularly devastating in children as they appear early in life and affect neurological development, with long-term effects on academic and socioeconomic outcome.

Conventional anatomical MRI is routinely used for the detection and monitoring of major CNS lesions in both the diagnosis and management of TSC. Neuroimaging in patients under the age of 1 year with a clinical suspicion of TSC results in a definite diagnosis in 95% of cases [7]. While conventional MRI is highly sensitive, it only gives an impression of the extent of CNS involvement, and it does not provide much information on the neurobehavioral phenotype nor on epilepsy.

First, no robust MRI biomarker that correlates consistently with the clinical phenotype or neurological outcome has been identified. For example, the presence of tubers in the temporal lobe has been linked to the risk of autism [10], but other critical regions including the cerebellum have also been proposed [11–14]. Although associations have been made between total tuber load, epilepsy and cognitive function [12,14,15], age at seizure onset is the only consistent and independent determinant of cognitive function [16]. A high tuber load or tubers in specific locations are, therefore, neither necessary nor sufficient to predict (early) seizures, cognitive impairment or autism (Figure 1A and 1B) [16,17]. Interand intra-observer variability in determination of tuber burden may be reduced by automated

tuber segmentation [16], but differences in magnet strengths, image acquisition specifics and quality form an additional challenge across institutions. Tuber-like pathology may be, in fact, more diffusely present below the conventional MRI resolution, with the visually discrete tubers just representing the 'tip of the iceberg'. The authors will discuss that large parts of normal-appearing white matter (NAWM), in fact, have an abnormal microstructure. In addition, there are other types of structural CNS abnormalities in TSC, as outlined below, which may need to be taken into account.

A second limitation of conventional MRI is the inability to identify epileptogenic tubers or perituber regions, a critical step in the presurgical evaluation of candidates for epilepsy surgery [18,19]. A third limitation is that microstructural CNS tissue characteristics of TSC, including abnormal differentiation, migration, organization, myelination and connectivity cannot be examined by conventional MRI [3,20–25].

Newer MRI techniques are used to investigate imaging correlates of neurobehavioral phenotype, epilepsy and microstructural CNS tissue properties in TSC. Diffusion-weighted MRI (DWI) probes natural barriers to the diffusion of water molecules in tissues, thereby providing information on their microstructural properties. To quantify this diffusion, multiple DWI images are used to generate a mathematical model of the diffusion. The most common model is called diffusion tensor imaging (DTI), which describes the 3D diffusion and strength with a tensor at each voxel. DTI models are consistent with known neuroanatomy and can demonstrate pathological microstructural changes of tissue in several neurological conditions, including multiple sclerosis [26], Alzheimer's disease [27] and epilepsy [28]. Using DTI, novel insights into the pathophysiology of TSC and the imaging determinants of clinical phenotype may lead to the identification of early prognostic indicators, and guide the development of targeted interventions. The authors review the literature on DTI and tuberous sclerosis, focusing on clinical implications, as well as its contribution to the understanding of the neuropathological processes in TSC. The imaging principles of DTI and several related techniques are introduced, and future directions are discussed.

STRUCTURAL CNS ABNORMALITIES IN TSC, CONVENTIONAL MRI

The intracranial lesions of TSC appear to result from abnormal expression of the genes within the germinal matrix stem cells, affecting differentiation and migration, resulting in dysplastic cells in the subependymal region, the cortex and along the cell migration pathways [29]. There are four common CNS lesions detected by conventional MRI, as described below.

Cortical tubers

Cortical tubers represent focal hamartomatous regions of disorganized cortical lamination. Histopathologic examination of tubers typically reveals prominent numbers of glia, neuronal appearing cells, and giant cells that express markers of both neuronal and glial lineages [3]. They are found in the brains of at least 80% of children with TSC [30]. On MRI, they are highly characteristic moderately well-circumscribed areas of increased signal intensity on T2-weighted (T2W) images and decreased signal intensity on T1-weighted (T1W) images. The overlying cortex may bulge and the gray–white matter differentiation is reduced. They are best appreciated on fluid attenuation inversion recovery images (Figure 1A and 1B) [31,32]. Based on conventional imaging, tubers can be classified following the scheme of Gallagher et al., which may have clinical implications [33]. The exact role of cerebellar lesions is still an active area of investigation [34], but recently a large series of 145 patients demonstrated that the MRI appearance of tubers is different in the cerebellum. Here, lesions are wedgeshaped, hyperintense on T2 and hypoor isointense on T1. Cerebellar tubers are more likely to enhance, and the enhancement may follow the underlying cerebellar neuroanatomy [35].

Subependymal nodules & subependymal giant astrococytomas Subependymal nodules (SENs) and subependymal giant astrocytomas (SEGAs) are found adjacent to the ventricles. SENs are small and can be found anywhere along the lining of the ventricles. SEGAs can cause obstructive hydrocephalus as they are larger than SENs and occur most commonly at the caudothalamic groove, near the foramen of Monro. They are noninvasive and nonmetastatic, and also histologically benign. However, SEGAs probably arise from SENs and the distinction is primarily made on the basis of size and location typically near the foramen of Monro [3]. As not all large lesions are astrocytomas, they are sometimes referred to as subependymal giant cell tumors. Other than glial-cell elements, they also contain dysplastic giant cells that express neuronal markers, similar to tubers [3,5]. On MRI, SENs and SEGAs are isoto hyper-intense on T1W images and variably hypointense on T2W images depending upon the extent of calcification. T2W images are optimal for showing susceptibility artifacts from calcification. Morphologically, they appear as discrete or roughly confluent areas of rounded hypertrophic tissue, bulging into the ventricle. Both can show contrast enhancement. The SENs over 5 mm in diameter which are incompletely calcified and enhanced after gadolinium administration may be at higher risk of growing into a SEGA (Figure 1C & D) [36,37].

White matter abnormalities

W hite matter abnormalities include radial migration lines (RMLs) that appear as linear abnormalities extending from the ventricular surface to the cortical tuber. Within the high signal of the RMLs, there are linear streaks of abnormalities that are isointense to cortex, best appreciated on T2W images and nonenhanced T1W images. These represent gliosis

and heterotopic glia and neurons along the course of abnormal cortical migration in the subcortical white matter. They are not always seen in relation to a tuber (Figure 1E) [36,38].

Discrete rounded cyst-like abnormalities

Discrete rounded cyst-like abnormalities are found subcortically or within the deep hemispheric white matter. They have cystic properties with signal intensities comparable to cerebrospinal fluid (CSF). Recently, a strong association of these lesions was found with TSC2 and a more severe seizure phenotype [39]. Originally thought to be static lesions derived from tuber degeneration or heterotopic tissue [38,40], their evolution over time has been clearly documented (Figure 1F) [41].

Microscopic abnormalities, such as micro-dysgenesis, heterotopic gray matter and lamination defects, are generally not visible at conventional MRI resolution. Rare associations with cortical malformations, such as hemimegalencephaly [42,43] and schizencephaly [44], are beyond the scope of this article. Finally, global cerebellar atrophy is reported in 4–17% of TSC patients and recently an association was shown with the presence of cerebellar tubers. Whether this is a destructive process (seizures, anti-epileptic medications, among others) or a primary developmental phenomenon is unknown [35,45].

DWI, DTI AND TRACTOGRAPHY

Diffusion-weighted imaging

DWI allows characterization and quantitative measurement of the diffusion of water molecules in tissues. It enables distinction between unrestricted and restricted diffusion of protons, based on the random (also known as Brownian) motion of water molecules in tissue [26,46]. The most well-known indication for DWI is detection of restricted diffusion in acute ischemic stroke.

In pure water, there is no barrier to the diffusion of water molecules and the diffusion is referred to as isotropic. By contrast, in the brain, local restriction of water diffusion such as that caused by the presence of densely organized white matter fascicles, gives rise to anisotropic diffusion. The degree of anisotropy is a measure of directional preference of diffusion and depends on the structure present in the voxel (3D pixel). In highly organized structures (e.g., white matter tracts), diffusion will be highly anisotropic, as molecules will diffuse preferably along the path of least resistance (e.g., along the axon within the myelin sheath) [26,46–48]. In less coherent structures (e.g., in a tuber consisting of poorly organized collection of cells), the diffusion will be almost isotropic.

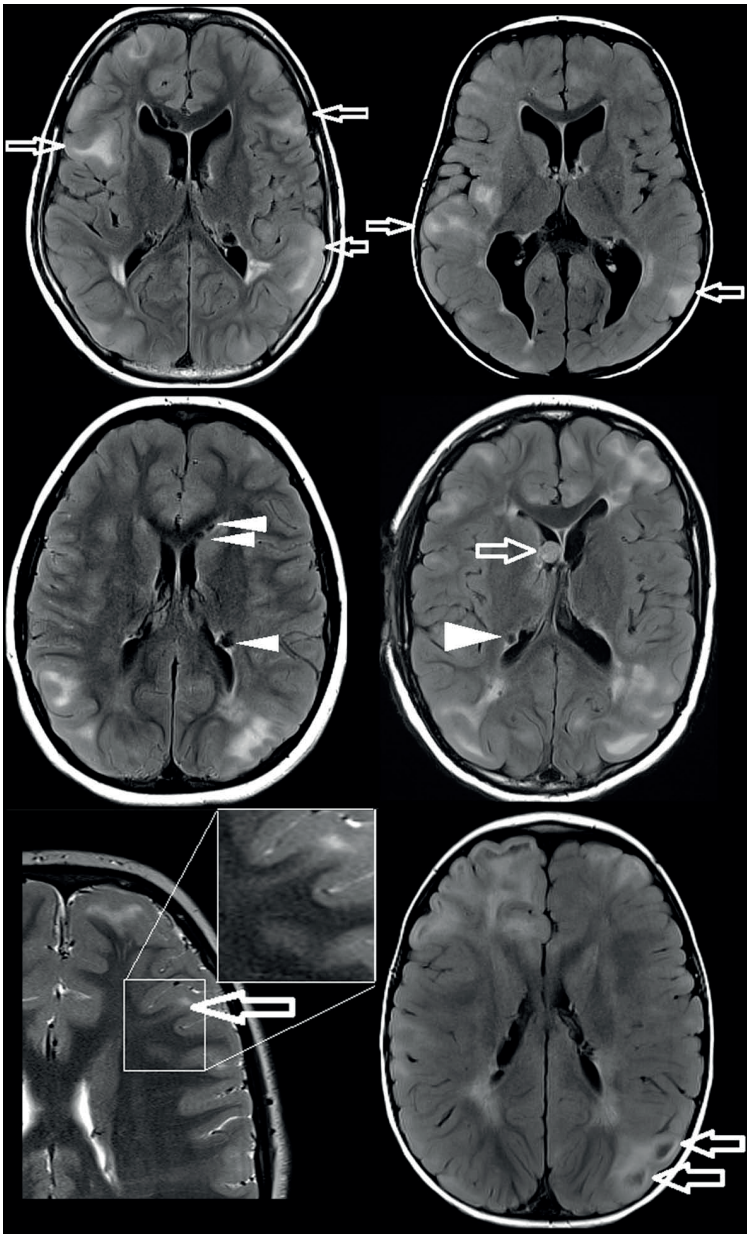

Figure 1: Conventional MRI findings in tuberous sclerosis complex.
(a) and (b) are axial FLAIR images. Both patients have subcortical tubers (arrows) of comparable size and distribution (not all tubers shown in current plane), but patient (a) has severe autism, no active seizure disorder and is non-verbal, while patient (b) has mild motor and language delays, no autism, and refractory seizures despite multiple antiepileptic drugs. (c) and (d): Axial FLAIR images. Subependymal nodules are seen lining the ependyma (arrowheads) and subependymal giant cell astrocytoma (SEGA) is seen in (d), at the level of the foramen of Monroe (arrow). (e) Axial T2-weighted image shows a radial migration line tracking from the tuber into the deep white matter (arrow, and zoom frame). (f) Axial FLAIR image. Cyst-like appearance of a tuber (arrows).

In an MRI scanner, protons' spins are initially aligned with the strong magnetic field produced by the magnet. Applying a short magnetic pulse changes this orientation and protons' spins start to precess (much like a spinning humming top deviates from its central a xis). This precession generates an electromagnetic signal detectable by an electric coil [46]. The rate of precession depends on the strength of the magnetic field. Applying a magnetic field that varies along a certain direction (adding a so-called field gradient pulse to the magnetic field), we can label the spins by different precession rates according to their position along the gradient direction. This variation in precession rates results in an interference between the precessing spins, leading to a signal loss. Applying the opposite field gradient pulse would refocus the spins and recover the signal loss, only if the protons did not move between the two pulses. However, due to motion, protons' spins are imperfectly refocused and the signal loss cannot be compensated for. The amount of remaining signal loss is related to the amount of motion that occurs in the gradient direction. Measuring the signal loss therefore measures the diffusion of protons (or water molecules that contain them). This is the physical basis of DWI.

Each DWI provides information about the diffusion along one particular direction (the gradient direction). Several DWI are thus needed to characterize the diffusion in all directions. Much like one only needs two points to characterize a linear relationship between two variables, one only needs a few DWI to estimate a diffusion model that characterizes the diffusion in all directions.

Diffusion tensor imaging

DTI is the most widely used model of the diffusion signal in tissues. DTI models the average diffusion direction and strength at each voxel with a tensor, which can be thought of as an ellipsoid (Figure 2). This ellipsoid is characterized by a principal direction along which diffusion is the strongest. In the two orthogonal directions, diffusion is more constrained and its magnitude is given by the width of the ellipsoid in those directions. A total of six parameters are required to fully define the ellipsoid: three parameters for the widths and length (these are also called diffusivities or eigenvalues), two parameters to define the direction of strongest diffusivity and one parameter to define the rotation of the ellipsoid around its principal axis. Mathematically, ellipsoids are represented as symmetric positive-definite matrices with three rows and three columns. Diffusivities can be obtained from those matrices through a mathematical method called eigen decomposition (hence their name 'eigenvalues').

Since six parameters define the diffusion tensor (the ellipsoid), six DWI acquired for different gradient directions would in theory be enough to estimate the values of the tensor parameters. However, owing to measurement errors, a larger number of DWI is usually acquired

(typically 30 directions). It is suggested to acquire as many images as time allows, and to strictly standardize acquisition details for research purposes.

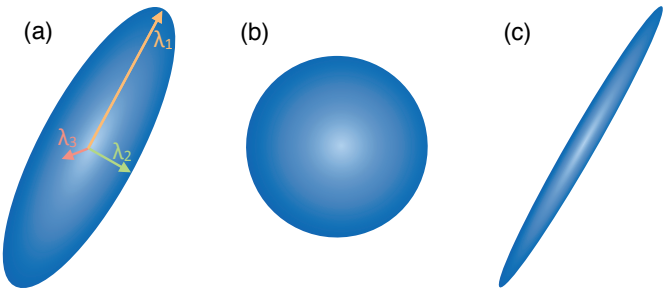

Figure 2: Diffusion tensor imaging is the most common model of the diffusion.
(a) DTI can be represented as an ellipsoid that consists of three axes of diffusion and the corresponding diffusivities (here λ1, λ2 and λ3). The shape of the ellipsoids provides information about the type of diffusion present in the voxel. (b) An isotropic diffusion leads to a spherical tensor. (c) Diffusion that are highly restricted in two directions and favored in one direction will present as an elongated tensor with very small second and third diffusivities.

The shape of the tensor provides information on the nature of the diffusion occurring in the corresponding voxel (Figure 2). Isotropic diffusion (which occurs in free water) gives rise to a spherical tensor, and its diffusivities are equal in all directions. Highly anisotropic diffusion gives rise to long and thin ellipsoids, indicating that the diffusion is highly favored along a principal direction and highly constrained in the other directions.

DTI-based measures

DTI-based measures quantify the shape of the ellipsoids and can be used as biomarkers for diseases. Two main measures are commonly used: the mean diffusivity (MD) and the fractional anisotropy (FA). The (bulk) MD is the average diffusion in all three directions. It was measured before the introduction of the diffusion tensor model by averaging the diffusion coefficient estimated in three orthogonal directions. In practice, this apparent diffusion coefficient is used interchangeably with MD. The MD is an intrinsic property of tissues. For example, the MD of demyelinated white matter is increased as there is more extracellular water and a weaker biological barrier to diffusion [26]. The FA reflects the degree of asymmetry of the diffusion in a particular location. If the diffusion is completely isotropic (Figure 2B), then FA is equal to zero. Conversely, if the diffusion is extremely anisotropic (water molecules can only diffuse in one direction and diffusivities are zero in the other two directions), then FA is equal to one. Diffusion within the white matter axons is restricted to the longitudinal axis by cell membranes and by the myelin sheath which forms a biological barrier, resulting in a high FA. When neurons or myelin sheaths are damaged, the FA decreases; there is less preferential directionality of diffusion because the fluid can

move freely along various axes [49]. MD and FA are nonspecific and can be altered by any pathological process that modifies tissue integrity and leads to a loss of structural barriers to water motion (Figure 3).

DTI tractography

DTI tractography is a technique based on relatively recently developed postprocessing algorithms for DTI, and allows for the study of the 3D configuration of major white matter tracts [50,51]. Orientation-based color-coding (also known as color maps) is a visualization approach in which the brightness of the image represents the magnitude of preferential diffusion (i.e., FA), and red (left–right axis), green (anterior–posterior axis) and blue (inferior–superior axis) indicate fascicle orientation. This color scheme assumes that the preferential diffusion axis coincides with the orientation of the fascicle, as explained above (Figure 4) [52]. To generate tracts, the main direction of the tensors (longest arrow in Figure 2) is followed from one voxel to another.

Based on the contiguity of adjacent voxels with a highly similar preferential diffusion axis, 3D tracts can be generated that represent the course of a major white matter pathway. The tract is formed by stepping along the line in both ortho and retro-grade directions according to the fascicle orientation (imagine a tract formed by a series of lined-up cucumbers) [26]. The tract starts at a seeding point, which is often defined manually by the examiner who delineates a certain region of interest. Regions of interest can be determined by (semi) automated techniques (e.g., functional MRI, or segmentation algorithms that isolate structures on conventional MRI).

Specifics of reconstructed tracts

The specifics of the reconstructed tracts are dependent on important modifiers that terminate the tract-generating algorithm when boundary conditions are met. Examples include the maximum angle a tract is allowed to make, the cutoff value of FA below which the next voxel is no longer considered to be part of the tract (stopping when the tensor is spherical and has an insufficient degree of anisotropy) and the FA-momentum, which permits the tractgenerating algorithm to go through an aberrant voxel with a poor FA if the previous few voxels in the tract had a high FA value, for instance carry momentum. This last modifier allows the tract generation not to stop prematurely. In both clinical and research applications of tractography, the exact parameters should always be scrutinized closely. Notably, the 3D tracts are not a (micro-)structural reality, but are traces of the major pathways representing white matter fascicles by means of connected diffusion tensors. The DTI tractography method has been validated with post-mortem anatomic and animal studies, showing good agreement [52,53].

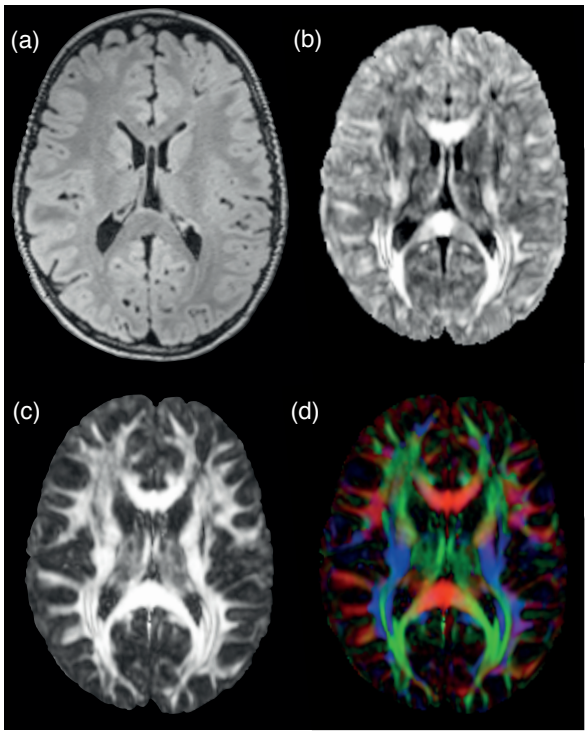

Figure 3: Diffusion tensor imaging and diffusion tensor imaging-based measures.
(a) FLAIR MRI structural image, axial plane. (b) Mean diffusivity (MD) image. Mean diffusivity is especially large in the corpus callosum and in corticospinal tracts. (c) Fractional anisotropy (FA) image shows where in the brain diffusion is more (white) or less (black) anisotropic. Because of the presence of highly structured white matter fascicles with aligned axons and myelin sheath, FA in the white matter is high. By contrast, grey matter presents axons with various directions, resulting in a lower FA. (d) FA can be colored based on the directions of the fascicle in each voxel: red means the fascicle is oriented left to right, green represents fascicles are oriented along the anterior-posterior axis and blue represents the superior-inferior axis.

Microstructural tissue properties

Microstructural tissue properties are reflected by FA and MD values of anatomical structures such as major white matter pathways (e.g., corpus callosum and language pathways) or specific regions of interest (e.g., neoplasm or tuber). A well-established relation between DTI parameters and tissue properties is not limited to only animal models, but is also present in humans. Changes in axonal integrity and diameter can affect axial diffusivity (the mean diffusion along the axial axis) [54]. Radial diffusivity (mean diffusion orthogonal to the longitudinal axis) values correlate with myelination in the normally developing mouse brain and in experimental dysmyelination [53,55,56]. FA relates to axonal packing, organization and myelination [57,58]. With tractography or with segmentation, an anatomically relevant collection of voxels can be selected for analysis. The investigation of local microstructural

information in a noninvasive manner is unique and has propelled the widespread use of DWI and DTI in the clinical and research setting over the past decade.

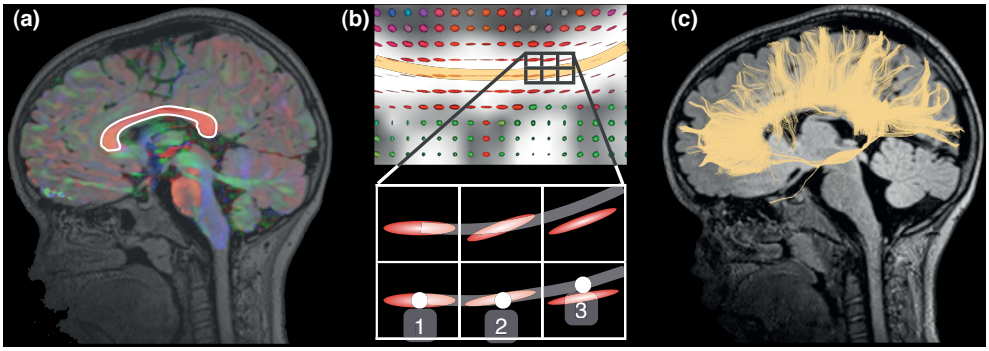

Figure 4: Tractography allows detection of white matter pathways in the brain.
A seeding region is first defined (here the corpus callosum) from where tracts will start growing (a). From each voxel of the seeding region, tracts grow in the direction of the tensor (b). Step by step, from voxel to voxel, tracts keep growing until they reach the grey matter where they stop. This yields three-dimensional maps of the fascicles in the brain, all connected to the seeding region (c).

LIMITATIONS OF THE DTI MODEL

Heterogeneous fascicle orientations

The DTI model assumes that at each voxel, the diffusion is Gaussian with at most one preferential direction. This assumption is reasonable only when all axons in the voxel are aligned in a specific orientation. However, owing to the presence of complex fascicle organization, heterogeneous fascicle orientations can be present in one voxel [59,60]. In the corona radiata, for example, corticospinal tracts cross fascicles of the corpus callosum (Figure 5). Another example are the pyramidal projections that give rise to fanning fascicles (i.e., fascicles that follow different directions from an original point at which they are aligned) [61]. Recent studies estimate the prevalence of those heterogeneities to range between 60 and 90% of voxels in the white matter [62]. When fascicles are crossing, kissing or fanning, interpretation of the DTI-based measures (MD and FA) may be misleading [63]. For instance, in the presence of two crossing fascicles, a single overly wide tensor would be estimated resulting in a decreased FA (Figure 5). This decreased FA is not related to a property of the fascicle and if interpreted this way may lead to the wrong assumption that the myelin integrity is altered for that fascicle.

Partial voluming effects

Voxels that are at the interface between different tissues (gray and white matter), between adjacent fiber bundles or between a tissue and CSF suffer another problem called partial

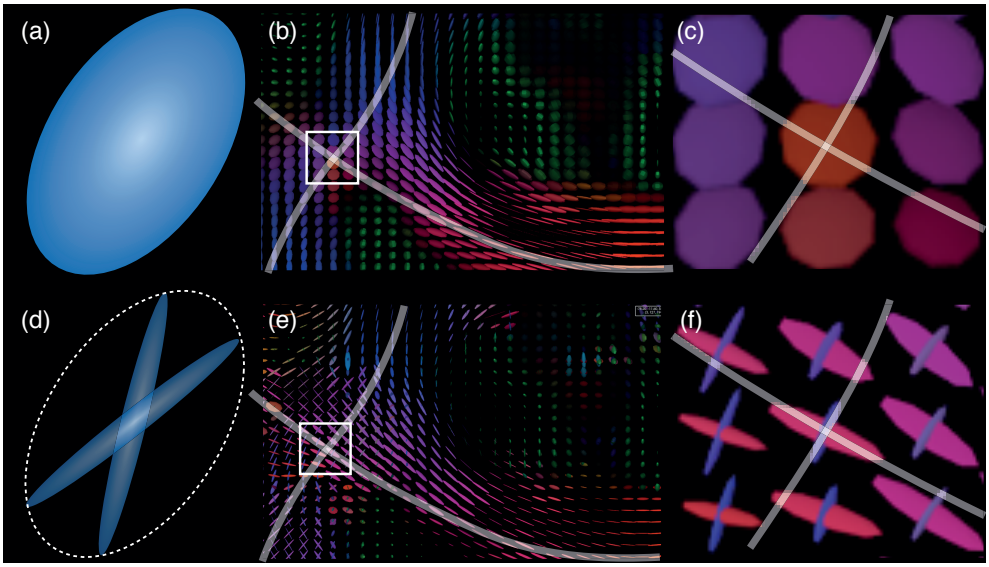

Figure 5: Single tensor and multifascicle models.
(a-c) Unlike assumptions of the diffusion tensor models, fascicles in the voxels may have more than one preferential direction . Diffusion tensor imaging model assumes that a single fascicle is present at each voxel. This assumption is violated in regions where fascicles cross, such as the corona radiata (b). In those regions, tensors are abnormally inflated to capture the signal arising from each fascicle (c), resulting in a lower FA that may be misleadingly interpreted. By contrast multi-fascicle models (d-f) represent each fascicle independently and are therefore able to characterize regions with crossing fascicles.

voluming. The diffusion signal arising from protons in the different compartments (CSF, gray or white matter) will be averaged into a single value that is observed in DWI. Because DTI assumes that a single fascicle is present in the voxel, influences of different compartments will conflate, resulting in an inflated tensor with a lower FA. As with heterogeneous fascicle orientations, this decreased FA may be misleadingly interpreted as altered myelin. Novel diffusion modeling methods that attempt to address these problems will be discussed in the future perspective section.

STRUCTURAL CNS ABNORMALITIES AND DTI

Cortical tubers

The first report on DWI and TSC stems from 2001 [64]. Tubers appear as structures with a decreased FA and increased MD, corresponding to tissue findings of poorly organized collections of dysplastic and large cells [3]. Although fluid attenuation inversion recovery imaging provides high-contrast images that allow for delineation of tubers, DTI imaging often reveals a larger area of perituberal diffusion abnormalities. This increased diffusivity

may better reflect the true extent of tuber pathology, at times demonstrating contiguity of tissue abnormalities between adjacent tubers, and a more gradual change to NAWM [65–67]. As tubers are prominent abnormalities, extensive research has been carried out on the relationship between tuber burden, location and clinical phenotype. Tuber burden has been quantified through counting numbers [10], calculation of total volume [68] or of relative volume as compared with white matter or total brain volume [16]. Although a relation has been established between tuber burden and the extent of white matter DTI abnormalities [68], the extent of SENs and R MLs also correlate with measures of tuber pathology, which is not surprising as histopathologically these lesions have common features too [69]. These relations suggest that widespread migration and differentiation abnormalities are present and the burden of any of these abnormalities is likely to be reflected in the broad neurophenotypical outcome.

SENs and SEGAs

There are no studies of the DTI properties of SENs and SEGAs available. Currently, a SEN that exceeds 1 cm in diameter, enhances with gadolinium contrast enhancement, and is not calcified is considered at high-risk for developing into a SEGA, although there is both a pathologic and a radiologic continuum between the two [70]. Early differentiation of SEGAs from SENs before the foramen of Monro is obstructed may provide opportunity to prevent hydrocephalus and associated morbidity and mortality [71,72]. SEGAs can grow fast, and once repeat imaging shows interval growth, resolution or stabilization have not been reported [73]. With serial DTI, it would be of interest to examine whether any microstructural differences between SENs and SEGAs could be established, and if such findings carry prognostic value.

White matter abnormalities & NAWM

A growing body of work, summarized in [23], has used DTI to describe abnormalities in white matter that appears normal on conventional imaging, referred to as NAWM [23–25,67,68,74,75]. DTI abnormalities are not limited to perituberal white matter [66,76,77], as myelination, migration and differentiation abnormalities extend beyond the discrete boundary of tubers described by conventional T2W (fluid attenuation inversion recovery) imaging. This has important implications as it is in concordance with findings of a global or diffuse microstructural white matter pathology found in neuropathological studies of TSC [78], in addition to multifocal tuber pathology [79]. Many regions have been implicated in DTI studies of the NAWM, but heterogeneity in the study population, image acquisition and processing, and statistical approach make synthesis of this work challenging. The presence of DTI abnormalities may be ubiquitous throughout the white matter [23].

In TSC, animal models provide a potential explanation for the abnormal diffusion characteristics. The diameter and integrity of the axon can affect axial diffusivity and the amount of diffusion according to the longitudinal axis. In the authors' laboratory, the Tsc1c/cSynI-Cre+ mouse model has an increased axonal diameter [Sahin M et al., Unpublished Data]. Radial diffusivity, the amount of diffusion perpendicular to the longitudinal axis, is dependent on myelination and the presence of extracellular changes such as glial and giant cells. In TSC, increased radial diffusivity may indicate poor myelination (thickness, integrity or permeability) or increased presence of extracellular material, impairing the biological barrier to diffusion in the radial direction. Indeed, hypomyelination [21] and aberrant neuronal organization [22] have been shown in animal models of TSC. A decreased FA may represent abnormal organization, packing or myelination of axons. In mouse models of TSC, loss of Tsc1 or Tsc2 is associated with abnormal neuronal connectivity – specifically neuronal polarity, axon formation and guidance [20–22].

Recently, the view of diffuse microstructural abnormality in the white matter was challenged. van Eeghen et al. found no differences in the NAWM of TSC patients compared with controls, once migrational abnormalities visible on conventional imaging were excluded from the analysis of white matter, and the R MLs accounted for the DTI abnormalities of the NAWM. This work should be reproduced as it would imply TSC is characterized by multifocal but not ubiquitous abnormalities in white matter connectivity [69]. Even with the view of TSC as a multifocal migrational disorder, DTI is supported as a putative biomarker for neurocognitive morbidity in TSC.

Finally, small animal imaging studies of TSC rodent models or imaging data of human pathological specimen are much needed to better establish the relation between DTI abnormalities and TSC pathology.

EPILEPSY, EPILEPSY SURGERY AND DTI

Epilepsy

Epilepsy, in particular, infantile spasms and early-onset refractory seizures have predictive value for poor cognitive outcome [16,80,81]. Early control may be associated with improved outcome [82,83]. However, this relation is inconsistent on an individual patient level. Moreover, heterozygous mouse models of TSC have failed to replicate typical neuroanatomical findings of human patients with TSC (SEGAs, tubers and SENs), and have neither neuropathological abnormalities nor seizures, yet demonstrate cognitive and behavioral abnormalities [34]. In these same animal models the presence of epilepsy is again detrimental,

worsening the neurophenotype. In short, early and complete seizure control is critical for neurodevelopmental outcome.

Abnormal diffusion can result from recurrent seizures and status epilepticus through various mechanisms including excitocytotoxic edema and neuronal cell-death, axonal damage and subsequent wallerian degeneration, systemic effects including vasoconstriction and hypoxia, antiepileptic drugs, secondary maladaptive developmental changes and plasticity-related reorganization of local and widespread connections [84]. In TSC, tubers have a relatively decreased FA and increased MD, and more so in epileptogenic compared with silent tubers [19,85]. The pathophysiology of these DTI changes is unclear; it could be a poorer microstructural integrity responsible for more severe epileptic properties, or conversely, local changes as a result from more epileptic discharges or both.

How varying levels of structural integrity of tubers relates to clinical manifestations of epilepsy is still subject to ongoing study. In 2010, a relationship was found between increased epilepsy severity and the predominance of poorly organized tubers on conventional imaging [33]. Apparent diffusion coefficient measures of the dominant tuber type confirmed quantitative differences in the subgroups. From the same researchers, again mainly based on conventional imaging, an association between cyst-like tubers (with by definition an exceptional low tissue integrity) and an aggressive seizure phenotype of infantile spasms and medically refractory seizures has been reported [39,41,86]. Thus, the evolution of DTI characteristics of (peri-)tuberal microstructure over time, and the relationship to epileptogenicity and epilepsy severity, are currently being studied in our laboratory.

Epilepsy surgery

Seizures arise in the vicinity of tubers, yet the specific origin of epileptiform activity is debated. Two studies have found seizures to originate from the tuber tissue itself [87,88] while others have indicated the perituberal tissue to be the source of epileptiform activity [89,90]. By contrast, many tubers are not epileptogenic at all, and anecdotally some patients have epilepsy in the absence of tubers on structural imaging.

For medically refractory seizures, resective epilepsy surgery typically consists of a tuberectomy. Clinical examination, seizure semiology, multiple imaging and neurophysiologic modalities are combined to identify epileptogenic tubers [87,91]. A recent report also suggests the potential use of magnetic resonance spectroscopy [92], a review of which is outside the scope of this paper. Using DTI, two studies with a total of 19 patients have independently reported a lower FA and higher MD in epileptogenic compared with nonepileptogenic tubers [19,85]. The main focus of epileptic activity remains stable in most patients [93]. With the routine availability of DTI as opposed to additional patient burden, high cost and

required expertise for other advanced auxiliary studies in the workup for epilepsy surgery, it is imperative that the predictive value of DTI in epileptogenic tuber identification in TSC be studied on a larger scale (Figure 6).

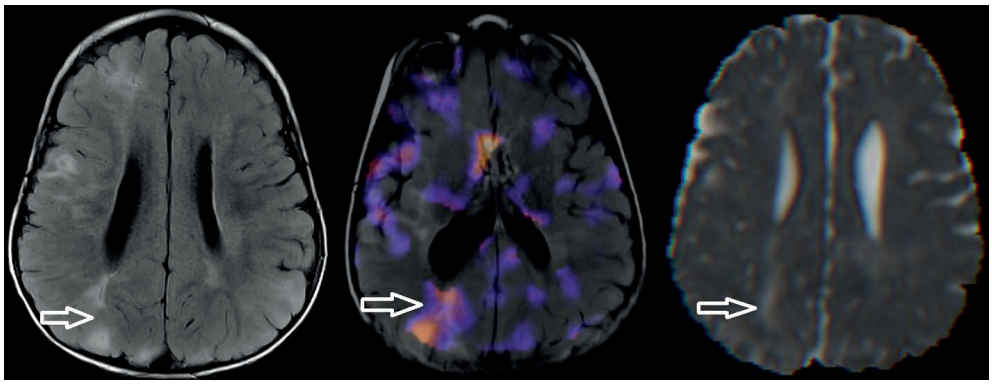

Figure 6: A 2-year-old patient with tuberous sclerosis complex with an epileptogenic right parietal tuber.
Visible on (a) axial fluid attenuation inversion recovery image, arrow indicates large right parietal tuber. (b) Single-photon emission CT scan with an injection shortly after onset of a seizure, demonstrating focal increased tracer uptake in the epileptogenic tuber (note the difference in angulation of the image). (c) Mean diffusivity image, revealing elevated mean diffusivity (0.0015 mm2/s) at the tuber compared with elsewhere in white matter (0.0008 mm2/s). The tuber was resected and the patient has been seizure-free for over 6 months.

AUTISM, COGNITION & DTI

Intellectual disability

Three lines of imaging research are explored as potential explanations for neurocognitive deficits in TSC. First, as outlined in the introduction, the number, location (frontal or occipital) and total volume of tubers have been associated with intellectual disability [15,16,94]. However, in clinical practice patients without tubers may have disabling symptoms while others with large tuber burden can have few neurologic symptoms. In 25 high-functioning adults with TSC and a normal intelligence, tuber burden was not correlated with cognitive measures [95]. Nontuber pathologies, including the frequency of SENs and R MLs, also appear to correlate with neurological phenotype [69].

Second, the cerebellum has been implicated, given its smaller size, in a morphometric study [45], which revealed the presence of lesions in more than a quarter of patients [11]. An association of ASD with PET abnormalities of the cerebellar white matter and of deep cerebellar nuclei has been made [96,97]. Recently, our group showed that loss of Tsc1 in mouse cerebellar Purkinje cells results in autistic-like behaviors [98].

Third, in various studies DTI has revealed widespread abnormalities in the NAWM, suggesting a role for aberrant microstructural connectivity in the pathophysiological mechanism of neurocognitive def icits. Typically study populations have not been sufficiently large to study detailed neuropsychological outcome data, other than presence of a diagnosis of autism [23,24]. A large, prospective, multicenter trial is underway to study neurocognitive effects of mTOR inhibitors (mTOR-is) but unfortunately, these subjects will not undergo imaging as part of this study.

Autism

In humans, TSC and decreased microstructural integrity of the corpus callosum and of the language pathways have been associated with ASD in two large DTI studies (Figure 7) [23,24]. While these were the first studies to correlate DTI with outcome, they were limited by the retrospective design, the binary nature of the diagnosis of autism and the potential confounders of intelligence measures and epilepsy severity. A prospective study is important because while classically ASD can be associated with normal or even superior intelligence, it appears in TSC that ASD and intellectual disabilities may co-occur [99]. On the other hand, there is a growing body of literature on idiopathic ASD and DTI abnormalities in the NAWM, including but not limited to the corpus callosum [100,101] and the arcuate fasciculus [102], reviewed elsewhere [103]. Aberrant long-range connectivity is central to the theory of autism as a developmental disconnection disorder, in which there is decreased integration of cognitive information from functionally separate and distant brain regions into a coherent, higher order concept [104]. In summary, abnormal microstructural connectivity is found in DTI studies of ASD, both with and without a concurrent diagnosis of TSC, which validates TSC as a natural model to study the development of autism. Indeed, in a recent electroencephalogram-based cross-disorder study of patients with TSC alone, TSC with ASD, and ASD without TSC, abnormal functional connectivity was associated with ASD regardless of the etiology [105]. An NIH-funded multicenter Autism Center of Excel-

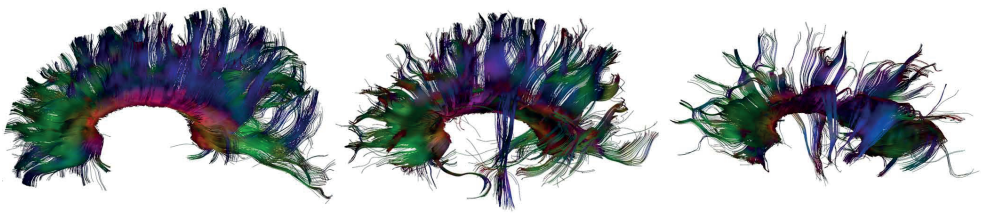

Figure 7: Diffusion tensor imaging of the corpus callosum in tuberous sclerosis complex.
(a–c) Tractography renderings of the corpus callosum of three subjects: (a) healthy control, mean fractional anisotropy (FA) is 0.46; (b) patient with tuberous sclerosis complex, no autism spectrum disorder, mean FA is 0.50; and (c) patient with tuberous sclerosis complex and autism spectrum disorder, mean FA is 0.34. The corpus callosum of (b) and (c) are more ragged owing to tubers interfering with streamlines, but only in the patient with autism spectrum disorder is the mean FA lower.

lence study has just been launched to prospectively study imaging and EEG predictors of neurophenotypical outcome, including autism, intellectual deficit and epilepsy.

CONCLUSION

TSC is a genetic, neurocutaneous, multiorgan disorder with potentially devastating sequelae including intractable epilepsy, intellectual impairment and ASD. There is a poor genotype–phenotype correlation and to date no conventional imaging biomarker reliably relates to neurophenotype. DTI is able to quantify microstructural tissue water diffusion properties, and reflects underlying pathology in TSC. With significant advances in the understanding of the molecular biology, the reversal of neurological comorbidity in mouse models, the clinical trials of mTOR-is for epilepsy and cognition, the potential of DTI as a biologically meaningful biomarker in TSC becomes even more important.

FUTURE PERSPECTIVE

Novel diffusion models allow for more biologically accurate qualification of microstructural properties. Over the next few years, these models will yield additional insights in human TSC in a noninvasive manner. Moreover, with the emergent use of mTOR-is, it will be important to establish a good biomarker that reliably corresponds to epilepsy and cognitive and behavioral outcome measures. DTI may prove to meet these requirements, and facilitate larger interventional trials.

Novel diffusion models

To overcome the aforementioned limitations of DTI, novel diffusion models have been proposed. One natural generalization of DTI is the development of multitensor models (also called multi-fiber and -fascicle models) [106]. Instead of assuming that a single fascicle is present in the voxel, multitensor models represent each fascicle present in the voxel with its own tensor (Figure 5D). With such a model, DTI-based measures (FA and MD) can be evaluated for each fascicle independently [107]. This solves the problem of artificially lower FA in areas with heterogeneous fascicle orientations. Furthermore, tissues with isotropic diffusion and CSF can be represented by an isotropic tensor (a sphere) and be included as one of the tensors in the multitensor model, thereby solving the partial voluming problem.

As these models are being defined by more parameters, they also require more DWI. However, recent developments have shown that we can estimate a multitensor model from 45 DWI [108] or even 30 DWI [109]. Imaging time with those novel techniques does not exceed 10 min and is therefore achievable in the clinical setting. Multitensor models also

require novel methods to estimate them. In particular, one challenge is to estimate how many fascicles are present in the voxel. Recent methods have been developed to solve this problem in an automatic fashion [110]. Besides overcoming the limitations of DTI, novel diffusion models open new opportunities to investigate the white matter microstructure. For instance, the amount of isotropic diffusion in the white matter has been related to the presence of neuroinflammation or edema [111]. Comprehensive studies of the white matter microstructure allow us to distinguish between axon and myelin

injury, cell infiltration and axonal loss [112].

The mTOR pathway, mTOR-is & DTI as a putative biomarker

TSC1 and TSC2 genes encode for hamartin and tuberin, respectively. These bind to form a protein complex that modulates the mTOR kinase, which plays a key role in the regulation of protein synthesis [113]. In the absence of a functional TSC protein complex, mTOR is overactive with subsequent disinhibited protein synthesis and cell growth [114]. Besides cell growth, mouse models have shown the TSC proteins play a critical role in axonal, dendritic and synaptic development and function, briefly reviewed here [115]. Loss of Tsc1 or Tsc2 function results in aberrant connectivity on a cellular level, and in mouse models is associated with seizures and neurobehavioral abnormalities. mTOR-i have a mechanism of action that virtually directly addresses the molecular defect in TSC, are safe and effective for treatment of SEGAs [73,116], and may also be safe in children under 3 years of age [117]. With DTI, microstructural changes of the white matter have been reported with the use of mTOR-i in patients with SEGA [79].

Epilepsy

In TSC mouse models, mTOR-i can prevent, improve and even stop seizures [118–120]. Accumulating evidence from small case-series and from larger SEGA treatment trials show that mTOR-is have anti-epileptic and potentially even anti-epileptogenic properties [120]. However, the neuroanatomic phenotype responds only partly, or not at all, to such intervention. A large multicenter trial is currently underway for everolimus (Afinitor®, Novartis, Inc., NJ, USA) as adjunct therapy for refractory partial complex seizures in TSC. DTI changes related to altered seizure control will be examined in a subset of the study population.

Cognition & autism

The defects in axonal, dendritic and synaptic development in TSC may well be related to neurobehavioral, cognitive and autistic symptoms in these patients. In mouse models, mTOR-i improve learning and prevent autistic features [98,121]. Given the first report of improvement of white matter microstructure with mTOR-is in humans [79], and the relation between autism and white matter microstructure [23], it will be exciting to investigate whether changes in DTI properties parallel the cognitive and neurobehavioral changes in

patients currently studied in the Autism Centers of Excellence network, and in subgroup analysis of the SEGA Phase III treatment trial. If so, DTI will become a biomarker for cognition in TSC, facilitating future therapeutic developments over the next few years, and allowing for exploration of mTOR-is in several genetic causes of autism.

EXECUTIVE SUMMARY

Table 1. Executive summary

Tuberous sclerosis complex is a multiorgan disorder with an unpredictable phenotype
* Neurologically, tuberous sclerosis complex (TSC) is associated with epilepsy, intellectual disability and autism spectrum disorder.
* Neither genotype nor any conventional imaging biomarker is a reliable and sufficient predictor for neurological outcome.
Diffusion tensor imaging is a modeling method of tissue water diffusion
* Water diffusion can be quantified by two main diffusion tensor imaging (DTI) measures: fractional anisotropy, which reflects degree of preferential directionality of diffusion, and mean diffusivity, which is an average of diffusion in all directions.
* Tractography is based on lining up diffusion tensors, prolate (cucumber) shapes, with the longest axis reflecting preferential diffusion. These tracts accurately reflect the anatomy of major white matter pathways in humans.
In TSC, DTI measures correlate with pathology and clinical phenotype
* Microstructural tissue properties, as measured by DTI, correspond to abnormalities in myelination, axonal organization, altered extracellular milieu and possibly to aberrations in axonal, dendritic and synaptic development and function. However, small-animal MRI with DTI of TSC mouse models is required to confirm these relationships.
* DTI can assist with localization of epileptogenic tubers, confirmed by neurophysiological and other imaging modalities, potentially affecting neurosurgical outcome of epilepsy surgery in TSC.
* DTI abnormalities of the normal-appearing white matter are associated with the presence of autism spectrum disorder in TSC.
mTOR inhibitors that target the molecular deficit in TSC are showing promise with regard to multiple neurological symptoms
* mTOR inhibitors (mTOR-is) reduce subependymal giant-cell astrocytoma in both adults and children with TSC.
* mTOR-is have shown anti-epileptic and, potentially, anti-epileptogenic effects in mouse models.
* mTOR-is may improve cognition and behavior, potentially opening avenues for early pharmacological treatment of autism in TSC.
* Whether DTI can become an industry-standard biomarker for mTOR-related treatment changes in TSC remains to be investigated.
Conclusion
* There is unprecedented and dramatic progress in the field of TSC, first with the emergent use of mTOR-is for seizures, cognition and potentially autism, and second with DTI as a candidate biomarker for cognitive and behavioral outcome.
* If DTI proves to be a reliable and biologically meaningful biomarker for patient stratification and treatment response, clinical trials will be much facilitated.

Financial & competing interests disclosure

This work was supported in part by the NIH (grant numbers R 01 R R 021885, R 01 L M010 033 , R03 EB008680 and UL1 RR025758 to SK Warfield; P20 RFA-NS-12-006 and 1U01NS082320-01 to M Sahin). In addition, JM Peters is supported by a Faculty Development Fellowship from the Eleanor and Miles Shore 50th Anniversary Fellowship Program for Scholars in Medicine, Boston Children's Hospital, Department of Neurology. M Taquet is supported by the Fonds de la Recherche Scientifique and the Belgian American Educational Foundation. M Sahin is supported by the Tuberous Sclerosis Alliance, Autism Speaks, John Merck Fund, Nancy Lurie Marks Family Foundation, Boston Children's Hospital, Translational Research Program and Boston Children's Hospital Intellectual and Developmental Disabilities Research Center (P30 HD18655). M Sahin is a consultant and site principal investigator for Novartis, Inc. and JM Peters is paid on a consultant basis for the Novartis EXIST-III trial: a three-arm, randomized, double-blind, placebocontrolled study of the efficacy and safety of two trough ranges of everolimus as adjunctive therapy in patients with tuberous sclerosis complex who have refractory partial-onset seizures. SK Warfield is a consultant for Siemens Medical Imaging, Inc. The authors have no other relevant affiliations or financial involvement with any organization or entity with a financial interest in or financial conflict with the subject matter or materials discussed in the manuscript apart from those disclosed. No writing assistance was utilized in the production of this manuscript.

REFERENCES

Papers of special note have been highlighted as: * of interest, ** of considerable interest

1. Crino PB, Nathanson KL, Henske EP. The tuberous sclerosis complex. N. Engl. J. Med. 355(13), 1345–1356 (2006).
2. Osborne JP, Fryer A, Webb D. Epidemiology of tuberous sclerosis. Ann. NY Acad. Sci. 615, 125–127 (1991).
3. Ess KC. The neurobiology of tuberous sclerosis complex. Semin. Pediatr. Neurol. 13(1), 37–42 (2006).
4. Jentarra G, Snyder SL, Narayanan V. Genetic aspects of neurocutaneous disorders. Semin. Pediatr. Neurol. 13(1), 43–47 (2006).
5. Curatolo P, Bombardieri R, Jozwiak S. Tuberous sclerosis. Lancet 372(9639), 657–668 (2008).
6. Roach ES, Gomez MR, Northrup H. Tuberous sclerosis complex consensus conference: revised clinical diagnostic criteria. J. Child Neurol. 13(12), 624–628 (1998).
7. Datta AN, Hahn CD, Sahin M. Clinical presentation and diagnosis of tuberous sclerosis complex in infancy. J. Child Neurol. 23(3), 268–273 (2008).
8. Dabora SL, Jozwiak S, Franz DN et al. Mutational analysis in a cohort of 224 tuberous sclerosis patients indicates increased severity of TSC2, compared with TSC1, disease in multiple organs. Am. J. Hum. Genet. 68(1), 64–80 (2001).
9. Jeste SS, Sahin M, Bolton P, Ploubidis GB, Humphrey A. Characterization of autism in young children with tuberous sclerosis complex. J. Child Neurol. 23(5), 520–525 (2008). 10. Bolton PF, Park RJ, Higgins JN, Griffiths PD, Pickles A. Neuro-epileptic determinants of autism spectrum disorders in tuberous sclerosis complex. Brain 125(Pt 6), 1247–1255 (2002).
11. Eluvathingal TJ, Behen ME, Chugani HT et al. Cerebellar lesions in tuberous sclerosis complex: neurobehavioral and neuroimaging correlates. J. Child Neurol. 21(10), 846–851 (2006).
12. Walz NC, Byars AW, Egelhoff JC, Franz DN. Supratentorial tuber location and autism in tuberous sclerosis complex. J. Child Neurol. 17(11), 830–832 (2002).
13. Weber AM, Egelhoff JC, McKellop JM, Franz DN. Autism and the cerebellum: evidence from tuberous sclerosis. J. Autism Dev. Disord. 30(6), 511–517 (2000).
14. Wong V. Study of the relationship between tuberous sclerosis complex and autistic disorder. J. Child Neurol. 21(3), 199–204 (2006).
15. Goodman M, Lamm SH, Engel A, Shepherd CW, Houser OW, Gomez MR. Cortical tuber count: a biomarker indicating neurologic severity of tuberous sclerosis complex. J. Child Neurol. 12(2), 85–90 (1997).
16. Jansen FE, Vincken KL, Algra A et al. Cognitive impairment in tuberous sclerosis complex is a multifactorial condition. Neurology 70(12), 916–923 (2008).

*** Studies the relationship between clinical (epilepsy), imaging and neuropsychological variables.**

17. Wong V, Khong PL. Tuberous sclerosis complex: correlation of magnetic resonance imaging (MRI) findings with comorbidities. J. Child Neurol. 21(2), 99–105 (2006).
18. Asano E, Chugani DC, Muzik O et al. Multimodality imaging for improved detection of epileptogenic foci in tuberous sclerosis complex. Neurology 54(10), 1976–1984 (2000).
19. Jansen FE, Braun KP, van Nieuwenhuizen O et al. Diffusion-weighted magnetic resonance imaging and identification of the epileptogenic tuber in patients with tuberous sclerosis. Arch. Neurol. 60(11), 1580 –1584 (2003).
20. Choi YJ, Di Nardo A, Kramvis I et al. Tuberous sclerosis complex proteins control axon formation. Genes Dev. 22(18), 2485–2495 (2008).
21. Meikle L, Talos DM, Onda H et al. A mouse model of tuberous sclerosis: neuronal loss of Tsc1 causes dysplastic and ectopic neurons, reduced myelination, seizure activity, and limited survival. J. Neurosci. 27(21), 5546–5558 (2007).

22. Nie D, Di Nardo A, Han JM et al. Tsc2–R heb signaling regulates Eph A-mediated axon guidance. Nat. Neurosci. 13(2), 163 –172 (2010).
23. Peters JM, Sahin M, Vogel-Farley VK et al. Loss of white matter microstructural integrity is associated with adverse neurological outcome in tuberous sclerosis complex. Acad. Radiol. 19(1), 17–25 (2012).

**** First report of sufficient power to suggest a relationship between diffusion tensor imaging of the white matter and neurocognitive phenotype in tuberous sclerosis complex.**

24. Lewis W W, Sahin M, Scherrer B et al. Impaired language pathways in tuberous sclerosis complex patients with autism spectrum disorders. Cereb. Cortex 23(7), 1526–1532 (2013).
25. Krishnan ML, Commowick O, Jeste SS et al. Diffusion features of white matter in tuberous sclerosis with tractography. Pediatr. Neurol. 42(2), 101–106 (2010).
26. Goldberg-Zimring D, Mewes AU, Maddah M, Warfield SK. Diffusion tensor magnetic resonance imaging in multiple sclerosis. J. Neuroimaging 15(Suppl. 4), S68–S81 (2005).
27. Bozzali M, Falini A, Franceschi M et al. White matter damage in Alzheimer's disease assessed in vivo using diffusion tensor magnetic resonance imaging. J. Neurol. Neurosurg. Psychiatry 72(6), 742–746 (2002).
28. Luat AF, Chugani HT. Molecular and diffusion tensor imaging of epileptic networks. Epilepsia 49(Suppl. 3), 15–22 (2008).
29. Curatolo P, Verdecchia M, Bombardieri R. Tuberous sclerosis complex: a review of neurological aspects. Eur. J. Paediatr. Neurol. 6(1), 15–23 (2002).
30. Crino PB, Henske EP. New developments in the neurobiology of the tuberous sclerosis complex. Neurology 53(7), 1384–1390 (1999).
31. Kato T, Yamanouchi H, Sugai K, Takashima S. Improved detection of cortical and subcortical tubers in tuberous sclerosis by fluid-attenuated inversion recovery MRI. Neuroradiology 39(5), 378–380 (1997).
32. Takanashi J, Sugita K, Fujii K, Niimi H. MR evaluation of tuberous sclerosis: increased sensitivity with fluid-attenuated inversion recovery and relation to severity of seizures and mental retardation. AJNR Am. J. Neuroradiol. 16(9), 1923–1928 (1995).
33. Gallagher A, Grant EP, Madan N, Jarrett DY, Lyczkowski DA, Thiele EA. MRI findings reveal three different types of tubers in patients with tuberous sclerosis complex. J. Neurol. 257(8), 1373–1381 (2010).
34. Tsai P, Sahin M. Mechanisms of neurocognitive dysfunction and therapeutic considerations in tuberous sclerosis complex. Curr. Opin. Neurol. 24(2), 106–113 (2011).
35. Vaughn J, Hagiwara M, Katz J et al. MRI characterization and longitudinal study of focal cerebellar lesions in a young tuberous sclerosis cohort. AJNR Am. J. Neuroradiol. 34(3), 655–659 (2013).
36. Kalantari BN, Salamon N. Neuroimaging of tuberous sclerosis: spectrum of pathologic findings and frontiers in imaging. AJR Am. J. Roentgenol. 190(5), W304–309 (2008).
37. Nabbout R, Santos M, Rolland Y, Delalande O, Dulac O, Chiron C. Early diagnosis of subependymal giant cell astrocytoma in children with tuberous sclerosis. J. Neurol. Neurosurg. Psychiatry 66(3), 370–375 (1999).
38. Griffiths PD, Bolton P, Verity C. White matter abnormalities in tuberous sclerosis complex. Acta Radiol. 39(5), 482–486 (1998).
39. Chu-Shore CJ, Major P, Montenegro M, Thiele E. Cyst-like tubers are associated with TSC2 and epilepsy in tuberous sclerosis complex. Neurology 72(13), 1165–1169 (2009).
40. Rott HD, Lemcke B, Zenker M, Huk W, Horst J, Mayer K. Cyst-like cerebral lesions in tuberous sclerosis. Am. J. Med. Genet. 111(4), 435–439 (2002).
41. Chu-Shore CJ, Frosch MP, Grant PE, Thiele EA. Progressive multifocal cystlike cortical tubers in tuberous sclerosis complex: clinical and neuropathologic findings. Epilepsia 50(12), 2648–2651 (2009).
42. Galluzzi P, Cerase A, Strambi M, Buoni S, Fois A, Venturi C. Hemimegalencephaly in tuberous sclerosis complex. J. Child Neurol. 17(9), 677–680 (2002).

43. Griffiths PD, Gardner SA, Smith M, Rittey C, Powell T. Hemimegalencephaly and focal megalencephaly in tuberous sclerosis complex. AJNR Am. J. Neuroradiol. 19(10), 1935–1938 (1998).
44. Huntsman RJ, Sinclair DB, Richer LP. Tuberous sclerosis with open lipped schizencephaly. Pediatr. Neurol. 34(3), 231–234 (2006).
45. Weisenfeld NI, Peters JM, Tsai PT et al. A magnetic resonance imaging study of cerebellar volume in tuberous sclerosis complex. Pediatr. Neurol. 48(2), 105–110 (2013).
46. Bitar R, Leung G, Perng R et al. MR pulse sequences: what every radiologist wants to know but is afraid to ask. Radiographics 26(2), 513–537 (2006).

**** Entry-level review regarding the physics of MRI and different acquisition schemes**.

47. Le Bihan D, Breton E, Lallemand D, Grenier P, Cabanis E, Laval-Jeantet M. MR imaging of intravoxel incoherent motions: application to diffusion and perfusion in neurologic disorders. Radiology 161(2), 401– 407 (1986).
48. Pierpaoli C, Jezzard P, Basser PJ, Barnett A, Di Chiro G. Diffusion tensor MR imaging of the human brain. Radiology 201(3), 637–648 (1996).
49. Piao C, Yu A, Li K, Wang Y, Qin W, Xue S. Cerebral diffusion tensor imaging in tuberous sclerosis. Eur. J. Radiol. 71(2), 249–252 (2009).
50. Basser PJ, Pajevic S, Pierpaoli C, Duda J, Aldroubi A. In vivo fiber tractography using DT-MRI data. Magn. Reson. Med. 44(4), 625–632 (2000).
51. Mori S, Kaufmann WE, Pearlson GD et al. In vivo visualization of human neural pathways by magnetic resonance imaging. Ann. Neurol. 47(3), 412–414 (2000).
52. Wakana S, Jiang H, Nagae-Poetscher LM, van Zijl PC, Mori S. Fiber tract-based atlas of human white matter anatomy. Radiology 230(1), 77–87 (2004).
53. Jiang Y, Johnson GA. Microscopic diffusion tensor imaging of the mouse brain. Neuroimage 50(2), 465–471 (2009).
54. Budde MD, Xie M, Cross AH, Song SK. Axial diffusivity is the primary correlate of axonal injury in the experimental autoimmune encephalomyelitis spinal cord: a quantitative pixelwise analysis. J. Neurosci. 29(9), 2805–2813 (2009).
55. Song SK, Yoshino J, Le TQ et al. Demyelination increases radial diffusivity in corpus callosum of mouse brain. Neuroimage 26(1), 132–140 (2005).
56. Sun SW, Liang HF, Trinkaus K, Cross AH, Armstrong RC, Song SK. Noninvasive detection of cuprizone induced axonal damage and demyelination in the mouse corpus callosum. Magn. Reson. Med. 55(2), 302–308 (2006).
57. Beaulieu C, Allen PS. Determinants of anisotropic water diffusion in nerves. Magn. Reson. Med. 31(4), 394–400 (1994).
58. Gulani V, Webb AG, Duncan ID, Lauterbur PC. Apparent diffusion tensor measurements in myelin-deficient rat spinal cords. Magn. Reson. Med. 45(2), 191–195 (2001).
59. Bandettini PA. What's new in neuroimaging methods? Ann. NY Acad. Sci. 1156, 260–293 (2009).
60. Mori S, van Zijl PC. Fiber tracking: principles and strategies – a technical review. NMR Biomed. 15(7–8), 468–480 (2002).
61. Tournier JD, Mori S, Leemans A. Diffusion tensor imaging and beyond. Magn. Reson. Med. 65(6), 1532–1556 (2011).
62. Jeurissen B, Leemans A, Tournier JD, Jones DK, Sijbers J. Investigating the prevalence of complex fiber configurations in white matter tissue with diffusion magnetic resonance imaging. Hum. Brain Mapp. doi:10.1002/ hbm.22099 (2012) (Epub ahead of print).
63. Vos SB, Jones DK, Jeurissen B, Viergever MA, Leemans A. The influence of complex white matter architecture on the mean diffusivity in diffusion tensor MRI of the human brain. Neuroimage 59(3), 2208–2216 (2011).

64. Sener RN. Tuberous sclerosis: diffusion MRI findings in the brain. Eur. Radiol. 12(1), 138–143 (2002).
65. Widjaja E, Simao G, Mahmoodabadi SZ et al. Diffusion tensor imaging identifies changes in normal-appearing white matter within the epileptogenic zone in tuberous sclerosis complex. Epilepsy Res. 89(2–3), 246–253 (2010).
66. Garaci FG, Floris R, BozzaoA et al. Increased brain apparent diffusion coefficient in tuberous sclerosis. Radiology 232(2), 461–465 (2004).
67. Makki MI, Chugani DC, Janisse J, Chugani HT. Characteristics of abnormal diffusivity in normal-appearing white matter investigated with diffusion tensor MR imaging in tuberous sclerosis complex. AJNR Am. J. Neuroradiol. 28(9), 1662–1667 (2007).
68. Simao G, Raybaud C, Chuang S, Go C, Snead OC, Widjaja E. Diffusion tensor imaging of commissural and projection white matter in tuberous sclerosis complex and correlation with tuber load. AJNR Am. J. Neuroradiol. 31(7), 1273–1277 (2010).
69. van Eeghen AM, Terán LO, Johnson J, Pulsifer MB, Thiele EA, Caruso P. The neuroanatomical phenotype of tuberous sclerosis complex: focus on radial migration lines. Neuroradiology 55(8), 1007–1014 (2013).
70. Clarke MJ, Foy AB, Wetjen N, Raffel C. Imaging characteristics and growth of subependymal giant cell astrocytomas. Neurosurg. Focus 20(1), E5 (2006).
71. Moavero R, Pinci M, Bombardieri R, Curatolo P. The management of subependymal giant cell tumors in tuberous sclerosis: a clinician's perspective. Childs Nerv. Syst. 27(8), 1203–1210 (2011).
72. Berhouma M. Management of subependymal giant cell tumors in tuberous sclerosis complex: the neurosurgeon's perspective. World J. Pediatr. 6(2), 103–110.
73. Krueger DA, Care MM, Holland K et al. Everolimus for subependymal giant-cell astrocytomas in tuberous sclerosis. N. Engl. J. Med. 363(19), 1801–1811 (2010).
74. Peng SS, Lee WT, Wang YH, Huang KM. Cerebral diffusion tensor images in children with tuberous sclerosis: a preliminary report. Pediatr. Radiol. 34(5), 387–392 (2004).
75. Arulrajah S, Ertan G, Jordan L et al. Magnetic resonance imaging and diffusion-weighted imaging of normal-appearing white matter in children and young adults with tuberous sclerosis complex. Neuroradiology 51(11), 781–786 (2009).
76. Karadag D, Mentzel HJ, Gullmar D et al. Diffusion tensor imaging in children and adolescents with tuberous sclerosis. Pediatr. Radiol. 35(10), 980–983 (2005).
77. Firat AK, Karakas HM, Erdem G, Yakinci C, Bicak U. Diffusion weighted MR findings of brain involvement in tuberous sclerosis. Diagn. Interv. Radiol. 12(2), 57–60 (2006).
78. Marcotte L, Aronica E, Baybis M, Crino PB. Cytoarchitectural alterations are widespread in cerebral cortex in tuberous sclerosis complex. Acta Neuropathol. 123(5), 685–693 (2012).

*** Demonstrates widespread microstructural pathology in tuberous sclerosis complex.**

79. Tillema JM, Leach JL, Krueger DA, Franz DN. Everolimus alters white matter diffusion in tuberous sclerosis complex. Neurology 78(8), 526–531 (2012).

**** Suggests that diffusion tensor imaging parameters of white matter may improve with the use of mTOR inhibitors, indicating microstructural alterations.**

80. Numis AL, Major P, Montenegro MA, Muzykewicz DA, Pulsifer MB, Thiele EA. Identification of risk factors for autism spectrum disorders in tuberous sclerosis complex. Neurology 76(11), 981–987 (2011).
81. Muzykewicz DA, Costello DJ, Halpern EF, Thiele EA. Infantile spasms in tuberous sclerosis complex: prognostic utility of EEG. Epilepsia 50(2), 290–296 (2009).
82. Jozwiak S, Kotulska K, Domanska-Pakiela D et al. Antiepileptic treatment before the onset of seizures reduces epilepsy severity and risk of mental retardation in infants with tuberous sclerosis complex. Eur J. Paediatr.Neurol. 15(5), 424–431 (2011).

*** Suggests that treatment of patients with tuberous sclerosis complex and certain EEG patterns before onset of infantile spasms improves neurological outcome.**

83. Bombardieri R, Pinci M, Moavero R, Cerminara C, Curatolo P. Early control of seizures improves long-term outcome in children with tuberous sclerosis complex. Eur. J. Paediatr. Neurol. 14(2), 146–149 (2010).
84. Otte WM, van Eijsden P, Sander JW, Duncan JS, Dijkhuizen RM, Braun KP. A meta-analysis of white matter changes in temporal lobe epilepsy as studied with diffusion tensor imaging. Epilepsia 53(4), 659–667 (2012).
85. Chandra PS, Salamon N, Huang J et al. FDG-PET/MRI coregistration and diffusion-tensor imaging distinguish epileptogenic tubers and cortex in patients with tuberous sclerosis complex: a preliminary report. Epilepsia 47(9), 1543–1549 (2006).
86. Gallagher A, Chu-Shore CJ, Montenegro MA et al. Associations between electroencephalographic and magnetic resonance imaging findings in tuberous sclerosis complex. Epilepsy Res. 87(2–3), 197–202 (2009).
87. Koh S, Jayakar P, Dunoyer C et al. Epilepsy surgery in children with tuberous sclerosis complex: presurgical evaluation and outcome. Epilepsia 41(9), 1206–1213 (2000).
88. Mohamed AR, Bailey CA, Freeman JL, Maixner W, Jackson GD, Harvey AS. Intrinsic epileptogenicity of cortical tubers revealed by intracranial EEG monitoring. Neurology 79(23), 2249–2257 (2012).
89. Major P, Rakowski S, Simon MV et al. Are cortical tubers epileptogenic? Evidence from electrocorticography. Epilepsia 50(1), 147–154 (2009).
90. Ma TS, Elliott RE, Ruppe V et al. Electrocorticographic evidence of perituberal cortex epileptogenicity in tuberous sclerosis complex. J. Neurosurg. Pediatr. 10(5), 376–382 (2012).
91. Jansen FE, van Huffelen AC, Algra A, van Nieuwenhuizen O. Epilepsy surgery in tuberous sclerosis: a systematic review. Epilepsia 48(8), 1477–1484 (2007).
92. Mori K, Mori T, Toda Y et al. Decreased benzodiazepine receptor and increased GABA level in cortical tubers in tuberous sclerosis complex. Brain Dev. 34(6), 478–486 (2012).
93. Jansen FE, van Huffelen AC, Bourez-Swart M, van Nieuwenhuizen O. Consistent localization of interictal epileptiform activity on EEGs of patients with tuberous sclerosis complex. Epilepsia 46(3), 415–419 (2005).
94. Jambaque I, Cusmai R, Curatolo P, Cortesi F, Perrot C, Dulac O. Neuropsychological aspects of tuberous sclerosis in relation to epilepsy and MRI findings. Dev. Med. Child Neurol. 33(8), 698–705 (1991).
95. Ridler K, Suckling J, Higgins N, Bolton P, Bullmore E. Standardized whole brain mapping of tubers and subependymal nodules in tuberous sclerosis complex. J. Child Neurol. 19(9), 658–665 (2004).
96. Ertan G, Arulrajah S, Tekes A, Jordan L, Huisman TA. Cerebellar abnormality in children and young adults with tuberous sclerosis complex: MR and diffusion weighted imaging findings. J. Neuroradiol. 37(4), 231–238 (2010).
97. Asano E, Chugani DC, Muzik O et al. Autism in tuberous sclerosis complex is related to both cortical and subcortical dysfunction. Neurology 57(7), 1269–1277 (2001).
98. Tsai PT, Hull C, Chu Y et al. Autistic-like behaviour and cerebellar dysfunction in Purkinje cell Tsc1 mutant mice. Nature 488(7413), 647–651 (2012).

**** Mouse model with cerebellar injury from Tsc1 mutations displays autistic behaviors.**

99. van Eeghen AM, Pulsifer MB, Merker VL et al. Understanding relationships between autism, intelligence, and epilepsy: a cross-disorder approach. Dev. Med. Child Neurol. 55(2), 146–153 (2013).
100. Keller TA, Kana RK, Just MA. A developmental study of the structural integrity of white matter in autism. Neuroreport 18(1), 23–27 (2007).
101. Alexander AL, Lee JE, Lazar M et al. Diffusion tensor imaging of the corpus callosum in autism. Neuroimage 34(1), 61–73 (2007).
102. Fletcher PT, Whitaker RT, Tao R et al. Microstructural connectivity of the arcuate fasciculus in adolescents with high-functioning autism. Neuroimage 51(3), 1117–1125 (2010).

103. Travers BG, Adluru N, Ennis C et al. Diffusion tensor imaging in autism spectrum disorder: a review. Autism Res. 5(5), 289–313 (2012).
104. Geschwind DH, Levitt P. Autism spectrum disorders: developmental disconnection syndromes. Curr. Opin. Neurobiol. 17(1),103–111 (2007).
105. Peters JM, Taquet M, Vega C et al. Brain functional networks in syndromic and non-syndromic autism: a graph theoretical study of EEG connectivity. BMC Med. 11(1), 54 (2013).

**** EEG study that found similar abnormalities in functional connectivity in nonsyndromic (idiopathic) and syndromic (tuberous sclerosis complex) autism, suggesting common biological mechanisms.**

106. Tuch DS, Reese TG, Wiegell MR, Makris N, Belliveau JW, Wedeen VJ. High angular resolution diffusion imaging reveals intravoxel white matter fiber heterogeneity. Magn. Reson. Med. 48(4), 577–582 (2002).
107. Taquet M, Scherrer B, Commowick O et al. Registration and analysis of white matter group differences with a multi-fiber model. Med. Image Comput. Comput. Assist. Interv.15(Pt 3), 313–320 (2012).
108. Scherrer B, Warfield SK. Parametric representation of multiple white matter fascicles from cube and sphere diffusion MRI. PLoS ONE 7(11), e48232 (2012).
109. Taquet M, Scherrer B, Boumal M, Macq B, Warfield SK. Estimation of a multi-fascicle model from single b-value data with a population-informed prior. Med. Image Comput. Comput. Assist. Interv. (2013) (In Press).

*** First study to demonstrate that estimation of multiple fascicles is possible with routine, short acquisition schemes and a single b-value.**

110. Scherrer B, Taquet M, Warfield SK. Reliable selection of the number of fascicles in diffusion images by estimation of the generalization error. Inf. Process. Med. Imaging 7917, 742–753 (2013).
111. Pasternak O, Westin CF, Bouix S et al. Excessive extracellular volume reveals a neurodegenerative pattern in schizophrenia onset. J. Neurosci. 32(48), 17365–17372 (2012).
112. Wang Y, Wang Q, Haldar JP et al. Quantification of increased cellularity during inflammatory demyelination. Brain 134(Pt 12), 3590–3601 (2011).
113. Kwiatkowski DJ, Manning BD. Tuberous sclerosis: a GAP at the crossroads of multiple signaling pathways. Hum. Mol. Genet. 14(Spec. No 2), R251–R258 (2005).
114. Wullschleger S, Loewith R, Hall MN. TOR signaling in growth and metabolism. Cell 124(3), 471–484 (2006).
115. Sahin M. Targeted treatment trials for tuberous sclerosis and autism: no longer a dream. Curr. Opin. Neurobiol. 22, 1–7 (2012).
116. Franz DN, Belousova E, Sparagana S et al. Efficacy and safety of everolimus for subependymal giant cell astrocytomas associated with tuberous sclerosis complex (EXIST-1): a multicentre, randomised, placebo-controlled Phase 3 trial. Lancet 381(9861), 125–132 (2012).
117. Kotulska K, Chmielewski D, Borkowska J et al. Long-term effect of everolimus on epilepsy and growth in children under 3 years of age treated for subependymal giant cell astrocytoma associated with tuberous sclerosis complex. Eur. J. Paediatr. Neurol. doi:10.1016/j. ejpn.2013.03.002 (2013) (Epub ahead of print).
118. Meikle L, Pollizzi K, EgnorA et al. Response of a neuronal model of tuberous sclerosis to mammalian target of rapamycin (mTOR) inhibitors: effects on mTORC1 and Akt signaling lead to improved survival and function. J. Neurosci. 28(21), 5422–5432 (2008).
119. Zeng LH, Xu L, Gutmann DH, Wong M. Rapamycin prevents epilepsy in a mouse model of tuberous sclerosis complex. Ann. Neurol. 63(4), 444–453 (2008).
120. Wong M. Mammalian target of rapamycin (mTOR) inhibition as a potential antiepileptogenic therapy: from tuberous sclerosis to common acquired epilepsies. Epilepsia 51(1), 27–36 (2010).
121. Ehninger D, Han S, Shilyansky C et al. Reversal of learning deficits in a Tsc2+/ mouse model of tuberous sclerosis. Nat. Med. 14(8), 843–848 (2008).
122. Wakana S, Caprihan A, Panzenboeck MM et al. Reproducibility of quantitative tractography methods applied to cerebral white matter. Neuroimage 36(3), 630–644 (2007).

Website

201. Roberds S. Diagnostic criteria.Tuberous Sclerosis Alliance. How is TSC diagnosed? (2013). www.tsalliance.org/pages.aspx?content=10 (Accessed 1 July 2013)

Chapter 4

Loss of white matter microstructural integrity is associated with adverse neurological outcome in Tuberous Sclerosis Complex

Jurriaan M. Peters[1,2], Mustafa Sahin[1], Vanessa K. Vogel-Farley[3], Shafali S. Jeste[4], Charles A. Nelson, III[3], Matthew C. Gregas[1,5], Sanjay P. Prabhu[2], Benoit Scherrer[2], Simon K. Warfield[2].

1. Department of Neurology, Boston Children's Hospital and Harvard Medical School, Boston, MA
2. Department of Radiology & Computational Radiology Laboratory, Boston Children's Hospital and Harvard Medical School, Boston, MA
3. Laboratories of Cognitive Neuroscience, Boston Children's Hospital and Harvard Medical School, Boston, MA
4. Clinical Research Program, Boston Children's Hospital, MA
5. Center for Autism Research and Treatment, Semel Institute, University of California, Los Angeles, CA

ABSTRACT

Rationale and Objectives: Tuberous sclerosis complex (TSC) is a genetic neurocutaneous syndrome in which cognitive and socialbehavioral outcomes for patients vary widely in an unpredictable manner. The cause of adverse neurologic outcome remains unclear. The aim of this study was to investigate the hypothesis that disordered white matter and abnormal neural connectivity are associated with adverse neurologic outcomes.

Materials and Methods: Structural and diffusion magnetic resonance imaging was carried out in 40 subjects with TSC (age range, 0.5–25 years; mean age, 7.2 years; median age, 5 years), 12 of whom had autism spectrum disorders (ASD), and in 29 age-matched controls. Tractography of the corpus callosum was used to define a three-dimensional volume of interest. Regional averages of four diffusion scalar parameters of the callosal projections were calculated for each subject. These were the average fractional anisotropy (AFA) and the average mean, radial, and axial diffusivity.

Results: Subjects with TSC had significantly lower AFA and higher average mean, radial, and axial diffusivity values compared to controls. Subjects with TSC and ASD had significantly lower AFA values compared to those without ASD and compared to controls. Subjects with TSC without ASD had similar AFA values compared to controls.

Conclusion: Diffusion tensor scalar parameters provided measures of properties of the three-dimensional callosal projections. In TSC, changes in these parameters may reflect microstructural changes in myelination, axonal integrity, or extracellular environment. Alterations in white matter microstructural properties were associated with TSC, and larger changes were associated with TSC and ASD, thus establishing a relationship between altered white matter microstructural integrity and brain function.

INTRODUCTION

Tuberous sclerosis complex (TSC) is a genetic neurocutaneous syndrome with an estimated incidence of one in 6000 to 10,000. Although some patients with TSC may never show neurologic symptoms affecting their quality of life, epilepsy occurs in 80% to 90% of all patients, close to 45% of patients have mild to profound intellectual disabilities, and autism spectrum disorders (ASD) occur in up to 50% of patients (1).

The cause of neurologic deficits in patients with TSC is a key unresolved question, and neurologic outcomes remains highly variable and unpredictable. It has been hypothesized that tubers disrupt local cerebral architecture, resulting in impaired brain function. However, no robust conventional magnetic resonance imaging (MRI) measure of tubers correlates consistently with the clinical phenotype or long-term neurologic outcomes (2), and neither a high tuber load nor tubers in specific locations are necessary or sufficient to predict seizures, cognitive impairment, or autism (3).

More recently, investigators have studied the hypothesis that disordered white matter and abnormal neural circuitry contribute to neurologic symptoms in patients with TSC. Such a neural mechanism would underlie both intellectual impairment and autism and may be responsible for comorbid autism in other disorders as well (4). Support for the existence of aberrant neural circuitry can be found in TSC mouse models. The Tsc1 and Tsc2 proteins appear to be crucial for proper axon specification, guidance, and myelination (5–7). Neuron-specific Tsc1 knockout mice display diffuse cortical and subcortical hypomyelination (6). In Tsc2 heterozygous mice, investigators have found abnormally exuberant and disordered axonal projections from the retina to the lateral geniculate nucleus, suggesting defects in axon guidance (7).

Similarly, in human subjects with TSC, diffusion tensor imaging (DTI) analysis of white matter that appears normal on conventional MRI has identified abnormalities suggesting abnormal myelination and astrogliosis (8–11). Moreover, in large studies of children with idiopathic autism (autism with no known cause), DTI abnormalities of the corpus callosum have been identified (12, 13).

We hypothesized that disruption of the normal development of brain function in patients with TSC is caused by alterations in the microstructural integrity of axons and myelination. Using DTI, we compared patients with TSC with healthy controls to further characterize abnormal white matter microstructure and aberrant connectivity in TSC. In addition, we hypothesized that an increase in loss of microstructural integrity in patients with TSC would lead to an increase in cognitive and social-behavioral deficits, specifically ASD. In this study,

we focused on the corpus callosum, a major commissural long-distance pathway that has been wellstudied in ASD as well as in TSC.

Finally, in this paper, we introduce a novel tractographic analysis method that considers all tractographic streamlines and adjusts for partial volume averaging in the calculation of DTI measures.

MATERIALS AND METHODS

Subjects

Forty patients (age range, 0.5–25 years) with established diagnoses of TSC and 29 age-matched control subjects were imaged using 3-T MRI. Control subjects underwent imaging as part of their routine care or as part of this research study. Each MRI study was reviewed by a pediatric neuroradiologist S.P.P., and all controls had normal MRI results and normal neurologic examination results. Controls did not undergo neuropsychological evaluation as part of this study. Recruitment of subjects and data acquisition were conducted using a protocol approved by the institutional review board of Children's Hospital Boston.

All patients fulfilled the clinical criteria for definite TSC, as defined by the Tuberous Sclerosis Consensus Conference (14). All patients with TSC were neurologically examined, and clinical data were obtained during office visits and from review of medical records. ASD diagnoses were based on clinical assessment by a board-certified pediatric neurologist (M.S.), using the Diagnostic and Statistical Manual of Mental Disorders, Fourth Edition, Text Revision (15), and in all but the three oldest subjects supported by additional testing with the Autism Diagnostic Observation Schedule (16) by experienced behavioral specialists (S.J., V.K.V.-F.).

Data acquisition and analysis

The MRI protocol was based on routine clinical imaging, extended with diffusion imaging. Sedation was used only in subjects undergoing clinical imaging if necessary to prevent significant motion. The imaging protocol included a T1weighted magnetization-prepared rapid-acquisition gradient-echo sequence and a T2-weighted turbo spin-echo sequence, with diffusion imaging (17) acquired in the axial plane, using 30 images with b = 1000 s/mm2 and five images with b = 0 s/mm2 (field of view, 22 cm; slice thickness, 2.0 mm; echo time, 88 ms; repetition time, 10 seconds; matrix size, 128 X 128; number of signals acquired, 1; iPAT = 2, modified as necessary to facilitate completion of the scan if the subject was unable to remain perfectly still).

A segmentation of the intracranial cavity was created from the structural magnetic resonance image (18,19). Compensation for residual distortion and patient motion was achieved by aligning the diffusion images to the T1-weighted magnetization-prepared rapid-acquisition gradient-echo scan, with appropriate reorientation of the gradient directions (20). Tensors were estimated using robust least squares and were displayed via color coding (21).

We used a stochastic streamline tractographic algorithm that combines the speed and efficacy of deterministic decision making at each voxel with probabilistic sampling from the space of all streamlines. Potential streamlines are stochastically initialized and evaluated, starting from a seeding region of interest (ROI), such as all the white matter in the brain. Streamlines are initialized at stochastically sampled locations inside the seeding ROI and are constructed by stepping with subvoxel resolution through the tensor field. For each potential streamline, we avoid loss of connectivity due to local aberrations by incorporating a low-pass filter along the estimated pathway for conventional stopping criteria, including streamline curvature and fractional anisotropy (FA) criteria. The range of potential streamlines examined is broad in comparison to conventional deterministic streamline tracing and is formed by log-Euclidean tensor interpolation (22) at each location, with stepping direction determined by a linear combination of tensor deflection (23) and primary eigenvector orientation, with stopping based on FA and angle criteria.

Specifically, from each stochastically selected subvoxel location p^k, a new point along the streamline is identified by stepping, with a fixed stepsize s, in the direction v^k , determined by the primary eigenvector of the tensor estimate at p^k:

$$p^{k+1} = p^k + v^k s$$

The new point p^{k+1} is tested to ensure it is inside the image boundary and inside the region to be considered for tractography. A mask can be used to ensure tractography does not step through regions with no white matter. Streamline generation is terminated if points are not validated. Streamline termination criteria related to the fractional anisotropy and angle changes are then checked.

The trajectory fractional anisotropy is assessed as a linear combination of the fractional anisotropy of the tensor estimate and the previous trajectory fractional anisotropy:

$$F^{k+1} = \alpha F^k + (1-\alpha)\mathrm{FA}(D^{K+1})$$

where $\mathrm{FA}(D^{k+1})$ is the FA of the tensor D^{k+1} . The primary eigenvector of the tensor is computed, providing e^{k+1}. The angle criterion is assessed by accumulating the cosine of trajectory angle changes, θ:

$$\theta^{k+1} = \beta\theta^{k} + (1-\beta)\left(\sum_{j=1}^{3} e_j^{k+1} v_k^j\right)$$

The new direction of the streamline is calculated using a combination of the primary eigenvector and tensor deflection, while accounting for the previous direction of the streamline:

$$v^{k+1} \propto \gamma v^{k} + (1-\gamma)\left[\delta\left(D^{k+1}\right)^{\varepsilon} v^{k} + (1-\delta)e^{k+1}\right]$$

Propagation of each streamline was terminated if the trajectory fractional anisotropy fell below 0.15, or if the tract trajectory angle exceeded 30 degrees. The trajectories were obtained using the step size parameter s=0.33mm, α=0.5, β =0.5, y=0.5, δ=0.5, and tensor deflection power ε=2.

Furthermore, as proposed by Wakana et al (24), ROIs may be specified to ensure potential streamlines meet requirements of known anatomy, by requiring streamlines to pass through certain ROIs (selection ROIs) or requiring that they do not pass through certain ROIs (exclusion ROIs). This process of stochastically sampling potential streamlines from the seeding ROI enables us to identify the streamlines that are most consistent with the diffusion tensor image, even in the presence of abnormal anatomy. Stochastic sampling is continued until a predetermined number of streamlines has been examined, and each streamline meeting all criteria is stored. A streamline density image is then constructed by counting the number of times each streamline entered a voxel and dividing by the total number of streamlines.

The streamlines identified by stochastic tractography can be used to delineate an ROI, in which the assessment of parameters of white matter microstructural integrity may be carried out. However, such an assessment can be confounded by partial volume effects, as described by Vos et al (25). When voxels associated with a fiber tract are identified, the proportion of the voxel associated with the fiber tract is important. A common strategy to select a tract-based ROI has been to threshold the streamline density to identify voxels associated with a particular white matter (26, 27). Average parameters, such as FA or mean diffusivity (MD), characteristic of the region are then assessed by computing the mean value of the parameter by summing the parameter over all the voxels above the threshold and dividing by the number of voxels in the region (26,27). Vos et al (25) demonstrated that the interaction between the geometry and curvature of a white matter fascicle and the voxel grid creates a partial volume effect that confounds the analysis. We propose to avoid the confounding due to the partial volume effect by avoiding the thresholding. Instead, we use the streamline density directly to enable an appropriate weighted average of diffusion tensor parameters. In our analysis, the diffusion tensor parameters of a region are calculated on the basis of equal weighting of each of the trajectories, rather than equal weighting of each

voxel. Given a streamline density image, *d*, and an image of a tensor scalar parameter, *p*, on the same discrete image lattice with voxels indexed by*i*, the streamline density–weighted mean, *m*, and variance, *v*, of the parameter are given by

$$m = \frac{\sum_i d_i p_i}{\sum_i d_i}, v = \frac{\sum_i d_i (p_i - m)^2}{\sum_i d_i^2}$$

The corpus callosum ROI was located by inspection of the structural MRI scans and a color-coded image of local tensor orientation and delineated interactively (Fig 1a) using previously established criteria (24). The stochastic tractography was used to identify streamlines consistent with the projections of the corpus callosum, which are illustrated in Figure 1b. Scalar measures of FA, MD, axial diffusivity, and radial diffusivity were derived from each tensor. These measures reflect properties of the underlying white matter but do not have high specificity for particular microstructural white matter changes (28). The streamlines passing through the corpus callosum ROI were used to construct a streamline density image, constructed by counting the number of times each trajectory entered a voxel and dividing by the total number of trajectories created, as illustrated in Figures 1c and 1d. To characterize the microstructural properties of the white matter of these trajectories, streamline density–weighted averages of these scalar parameter values were calculated.

This provided four scalar variables characterizing the projections of the corpus callosum in each subject, the average FA (AFA), average MD (AMD), average axial diffusivity (AAD), and average radial diffusivity (ARD). The weighted average and variance of the FA (and similarly for the other scalar parameters) in the projections of the corpus callosum were computed as

$$\mathrm{AFA} = \frac{\sum_i d_i \mathrm{FA}_i}{\sum_i d_i} \quad \mathrm{var}(\mathrm{AFA}) = \frac{\sum_i d_i (\mathrm{FA}_i - \mathrm{AFA})^2}{\sum_i d_i^2},$$

where *i* is the index of each voxel, d_i is the streamline density at voxel *i*, and FA_i is the FA.

Callosal volume was estimated by thresholding the streamline density image at 5% (29), counting the number of voxels, and multiplying by the size of each voxel.

Statistical analysis

The DTI measures were treated as response variables in a regression model with age, gender, and group status. Visual plots of the data suggest that age needed to be log transformed. This transformation was later confirmed by assessment of the value of the Akaike information criterion for the models with age log transformed and the model with age untransformed. Group status was initially defined as patients with TSC or controls. We then refined group status into three groups: controls and patients with TSC with and without

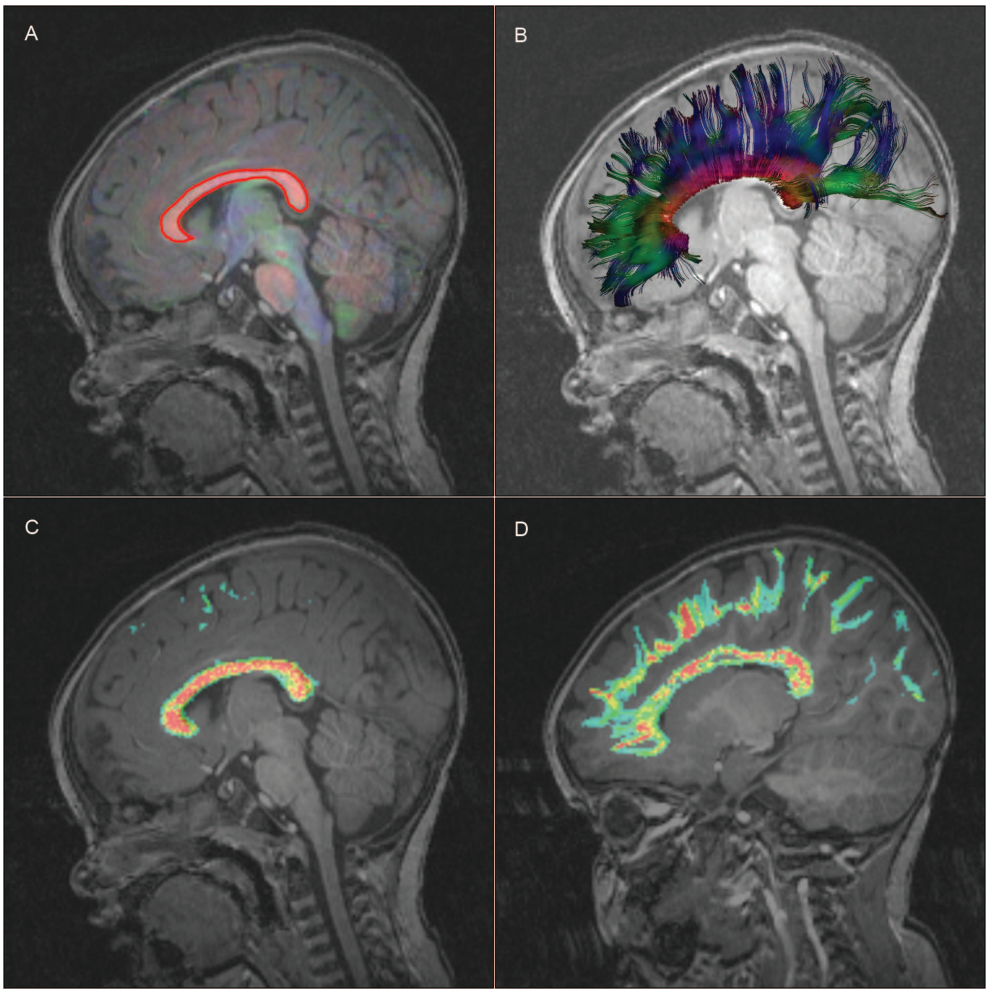

Figure 1: Tractography of the corpus callosum and density-weighted statistics.
(a) T1-weighted image, superimposed color coded representation of tensors, intensity proportional to the fractional anisotropy. Red for left-right, blue for superior-inferior, green for anterior-posterior. A manually drawn two-dimensional ROI delineates the corpus callosum (CC). (b) Visualization of the color-coded tractography of the CC. (c) Streamline Density weighted image of the CC. Red (high) and blue (low) colors represent streamline density at each voxel. (d) Out of the midsagittal plane, the streamline density weighted map follows the trajectories to the cortex.

ASD. All two-way and three-way interactions were considered. Interaction and main effect terms were dropped on the basis of likelihood ratio tests so that we achieved a model that accurately described the response without extraneous terms. Group and log (age) were identified as important terms. Gender was not significant after including age and group (TSC vs controls or ASD vs no ASD) in the model. The presence of group difference was determined by a likelihood ratio test. Significance tests were corrected for multiple comparisons (30), with a nominal a level of .05 and sequential model evaluation. Separate

models were fit for each DTI measure. Models were validated through residual plots, Q-Q plots, and added-variable plots.

RESULTS

Patients

Forty subjects (24 male, 16 female; mean age, 7.2 years; age range, 0.5–25 years; median age, 5.0 years) underwent MRI. Only one patient had normal results on MRI. Twenty-four had clinically significant developmental delays or intellectual disabilities, and 12 had ASD (note that six patients aged < 1.5 years were not considered for formal diagnosis of ASD). Thirty patients had genetic confirmation of their clinical diagnoses with abnormalities in the Tsc1 (n =8) and Tsc2 (n = 22) regions; in others, results were negative or testing was not performed (eg, in patients with family histories of TSC). Using Fisher's exact test, the prevalence of ASD was not significantly different in patients with Tsc1 compared to Tsc2 mutations (P = .4634), with or without global developmental delay or mental retardation (P =b.2919), and with or without family histories of TSC (P = .3891). Subjects with epilepsy (n = 25) and infantile spasms (n = 11 of those 25) were more likely to have ASD (P = .0132 and P = .0256, respectively). Twenty-nine age-matched controls (14 female, 15 male;bmean age, 7.7 years; age range, 0.9–25 years; median age, 6.48 years) with normal results on MRI were included.

Diffusion tensor properties of projections of the corpus callosum

Patients with TSC and controls

Patients with TSC and controls. Findings and P values are presented in Table 1. Significant group differences were found, with higher AMD, AAD, and ARD values in the patients with TSC compared to controls. AFA differences between the patients with TSC and controls were again significant (P = .035) but more complex: the model fit implied that the AFA increased less with age in the TSC group than in the control group.

Table 1. *p*-values using the linear regression model with the DTI measure as the response and group (control, TSC, TSC without ASD, TSC with ASD) and log(age) as the predictors

	Controls – TSC (all cases)	Controls – TSC without ASD	Controls – TSC with ASD	TSC with ASD – TSC without ASD
AMD	0.000652	0.022068	0.000807	0.128267 (NS)
ARD	0.00200	0.062096 (NS)	0.000764	0.060672 (NS)
AAD	0.000876	0.011224	0.005148	0.467143 (NS)
AFA	0.0350	0.8947 (NS)	0.0266	0.0421

AAD, average axial diffusivity; AFA, average fractional anisotropy; AMD, average mean diffusivity; ARD, average radial diffusivity; ASD, autism spectrum disorder; DTI, diffusion tensor imaging; TSC, tuberous sclerosis complex.
All four DTI measures differed significantly between controls and TSC patients. The AFA was significantly lower in the TSC subjects with ASD compared to those without ASD, but no difference was found between TSC patients without ASD and controls.

Patients with TSC with and without ASD and controls

Graphical displays of the linear regression model are shown in Figure 2. To summarize, significantly higher AMD, AAD, and ARD values were found in patients with TSC compared to control subjects, and a trend toward higher AMD, AAD, and ARD values was found in patients with TSC with autism compared to those without and compared to controls. Significantly lower AFA values were found in patients with TSC compared to controls (P = .035) and appeared to be nearly solely attributable to the ASD subgroup; subjects without ASD had similar AFA values as controls (P = .8947), but patients with TSC and ASD had lower AFA values than controls (P = .0266).

Callosal volume

Controls and patients with TSC without ASD were not different in estimated volume of the corpus callosum (mean, 69,717 vs 64,973 mm3; P = .2940), but controls did differ from patients with TSC with ASD (mean, 54,486 mm3; P = .00320). This difference reached significance too between patients with TSC with and without ASD (P = .0371). For all subjects and controls, the volume of the corpus callosum was inversely correlated with AMD, ARD, and AAD (Spearman's correlation = -0.80, -0.73, and -0.80, respectively, P < .000001) and correlated with AFA (Spearman's correlation = 0.40, P = .001).

DISCUSSION

Relation between white matter microstructure and development of brain function

Our study provides the first imaging data that identify an association between altered white matter microstructure and abnormal brain function in the TSC population. Moreover,

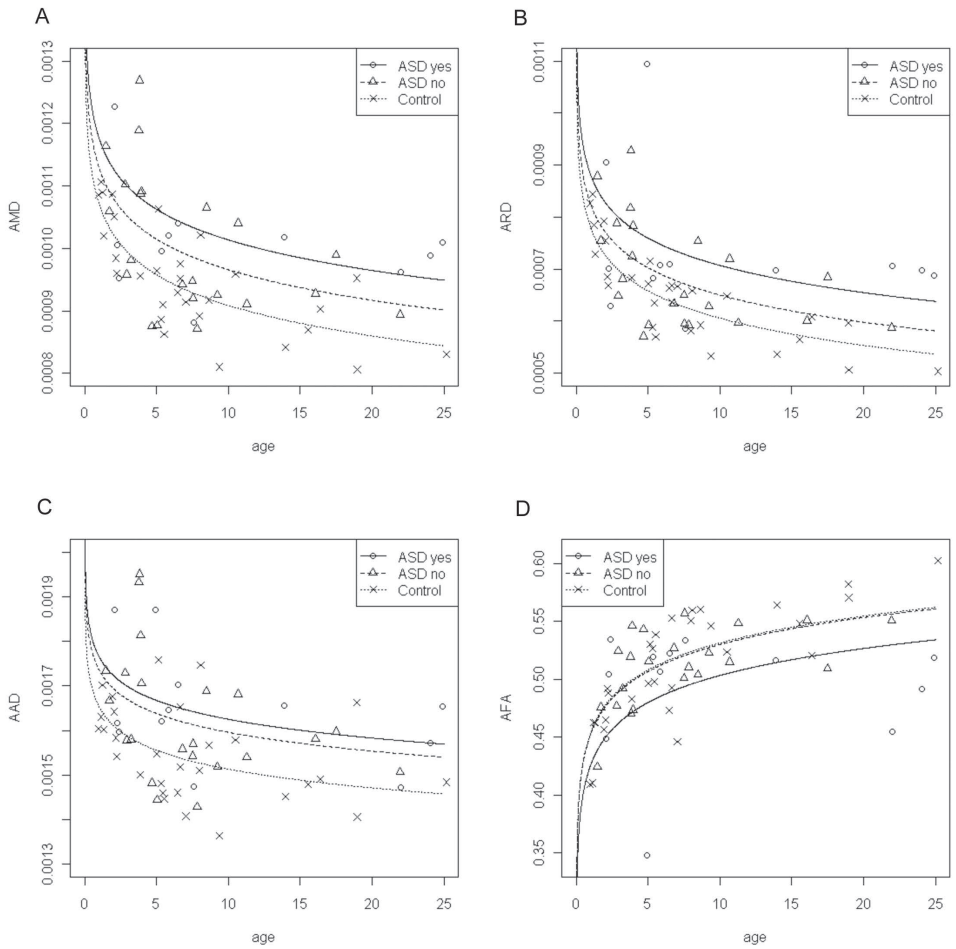

Figure 2: Linear regression models for various DTI measures.
(a-c) Graphical displays of the fit linear regression model for AMD (a), ARD (b) and AAD (c). Controls (dotted line) have lower AMD, ARD and AAD than TSC patients with ASD (solid line), but this difference only reaches significance for AMD and AAD when controls are compared to TSC patients without ASD (dashed line). For AFA (d), controls and TSC without ASD have highly similar values. AFA of the TSC patients with ASD are significantly lower than controls and TSC patients without ASD.

a reduction in white matter integrity is seen in patients with worse neurodevelopmental outcomes (ie, in those who have ASD; Fig 3).

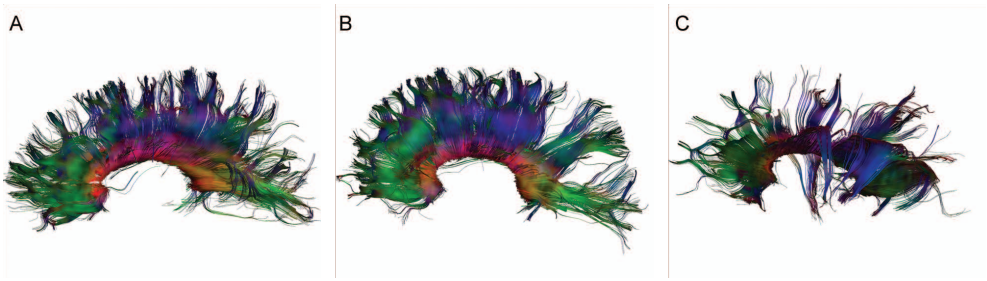

Figure 3: Illustration of projections of the corpus callosum and AFA values.
(a) 5.3 year-old healthy control, AFA = 0.53. (b) 4.7 year-old with TSC but no ASD, AFA = 0.54 and (c) 4.9 year old with TSC and autism, AFA = 0.34.

Several recent studies have reported DTI abnormalities in TSC of the normal-appearing white matter, indicating foci of microstructural abnormalities, depending on sample size and technique (8–11,31–34); summarized in Table 2. This body of data suggests that it is likely that microstructural changes are present throughout the cerebral white matter in TSC. Our study is consistent with previous literature and is the first to allow for phenotypical correlation because of its large sample size.

In TSC, several pathophysiologic substrates have been proposed for reduced FA and increased MD in the normal-appearing white matter. Changes in axonal integrity and diameter can affect axial diffusivity (35). RD values correlate with myelination in the normally developing mouse brain and in experimental dysmyelination (36). In our subjects, increased RD may represent disordered myelin sheaths but also axonal depletion or extracellular changes such as astrogliosis and giant cells (9,10). Such changes, including abnormal neuronal organization and hypomyelination, have been shown in animal models of TSC (6). Finally, lower FA may relate to disorganized (37) and poorly myelinated (38) axons. Our findings are again in accordance with animal studies, where loss of Tsc1 or Tsc2 function has detrimental effects on regulation of axonal growth, particularly neuronal polarity and axon formation (5–7).

In idiopathic autism, the white matter appears normal on conventional imaging, but the theory of "developmental disconnection" has driven research efforts in the direction of investigating connectivity on the functional and microstructural levels. In this model, disconnection relates to impaired corticocortical transfer of intrahemispheric and interhemispheric information, affecting the higher order processing of complex information. In patients with ASD, these processing difficulties have been found to be consistently deficient across multiple domains and across multiple modalities (12, 39–41).

Within the white matter, the corpus callosum has been implicated in ASD in several lines of research, including imaging studies of callosal volume, white matter density, functional imaging of information transfer or resting state functional connectivity, and postmortem studies (12,41,42). The corpus callosum represents a major interhemispheric tract of highly coherent white matter fibers, making it especially suited for DTI to study its microstructural connectivity as a model for disconnection in autism (12), and indeed, white matter microstructural abnormalities have been identified with diffusion imaging in patients with

Table 2. DTI studies involving NAWM in TSC.

Author, year	N	Age (y)	MRI	Directions	Key findings
Garaci 2004(32)	18	20, 12 - 30	1.5T	6	MD of perilesional NAWM higher than contralateral NAWM. NAWM of frontal, occipital and parietal and centrum semiovale higher MD than controls.
Peng 2004(33)	7	-, 0.5 - 15	1.5T	6	Lower FA of WM lesions associated with tubers vs. contralateral NAWM. Higher MD of corona radiata and sagittal striatum vs controls. Increased λ_3 of inferior longitudinal fasciculus and sagittal striatum vs controls.
Karadag 2005(40)	7	-, 2 - 20	1.5T	6	Higher MD of tubers vs cortex of controls. Increased MD and lower FA in WM lesions and perilesional WM vs controls. No difference in MD and FA of NAWM vs controls.
Firat, 2006(41)	6	9, 3 - 15	1.5T	6	MD of tubers higher than NAWM. MD of NAWM not different from controls.
Makki, 2007(9)	6	10, 6 - 15	1.5T	6	Higher MD, lower FA in combined NAWM of genu/splenium CC, IC/EC vs controls. Greatest increase was in $\lambda_{2,3}$, (i.e. RD).
Aruljajah 2009(8)	23	12, 1 - 25	1.5T	3-18	Increased MD of frontal and pontine NAWM (in subgroup 8-12 year), right parietal and occipital NAWM (in subgroup >12 year) vs controls.
Krishnan 2010(10)	10	-, 1.5 - 25	3T	35	Lower FA in splenium CC and GCT, lower AD in IC, STG and GCT, increased MD and RD in splenium CC of TSC vs controls.
Simao 2010(11)	12	9, 5 - 16	3T	15	Increased MD, decreased FA, increased RD in genu and splenium CC. Increased MD in IC. DTI measures of genu and splenium CC correlate with tuber volume (not number).
Peters, *this study*	40	7, 0.5 - 25	3T	35	Lower FA, higher MD, RD, AD of entire CC in TSC (all) vs controls and TSC (with ASD) vs controls. Lower FA of CC in TSC with ASD vs TSC without ASD. No difference in FA of CC in TSC without ASD vs controls.

AD, axial diffusivity; ASD, autism spectrum disorder; CC, corpus callosum; CR, corona radiata; CSO, centrum semiovale; DTI, diffusion tensor imaging; EC, external capsule; FA, fractional anisotropy; GCT, geniculocalcarine tract; IC, internal capsule; ILF, inferior longitudinal fasciculus;

MD, mean diffusivity; MRI, magnetic resonance imaging; NAWM, normal-appearing white matter; RD, radial diffusivity; SS, sagittal striatum; STG, superior temporal gyrus; TSC, tuberous sclerosis complex; WM, white matter.

*Age is expressed as mean (range) or as range.

Patients with TSC compared to controls unless otherwise stated.

idiopathic autism (43–45). Our DTI data confirm microstructural abnormalities of callosal white matter in patients with TSC and more prominently in the subjects with TSC with ASD, in support of the notion that abnormal white matter microstructure is related to impaired brain development and function.

Our volume estimation data are in concordance with findings of decreased callosal volume in autism in multiple imaging studies, summarized by Anderson et al (42). In TSC, cortical malformations including tubers and neuronal migration defects affect white matter as migrational failure results in impaired neocortical development, which is followed by a deficiency in corticocortical fibers destined to be part of the corpus callosum (46,47). In a recent study of 12 patients with TSC, DTI indices of major commissural white matter also correlated with tuber load (11), suggesting more extensive malformation leading to both more tubers and decreased microstructural quality of the corpus callosum. We found significant correlations between DTI parameters and volume estimates of projections of the corpus callosum. In this interhemispheric pathway, both macrostructural and microstructural characteristics were abnormal in patients with TSC with ASD.

Streamline Density Weighted Statistics

There are certain artifacts and pitfalls that must be taken into consideration with respect to diffusion imaging and tractography (52). Partial volume mixing and proximity of a pathway to other pathways containing many more tracts propagating in a different direction are some of the factors that introduce errors or even cause certain pathways to be missed completely. DTI tractography is consistent with known anatomy (24,49) and with the histologic appearance of fiber structure (50,51), but some fiber tracts are not identified, and spurious fiber tracts may be incorrectly detected.

Our use of streamline density weighting compensates for partial volume averaging of fiber tracts and treats each streamline in the same way. The alternative, of identifying a region on the basis of thresholding the streamline density and treating each voxel equally, fails to account for the different occupancy of voxels with many streamlines in comparison to voxels with few streamlines present. In this way, we compute the mean scalar parameter of each streamline of a structure rather than of each voxel. Thus, our use of streamline density–weighted statistics enables the analysis of the three-dimensional callosal projections while appropriately adjusting for changes in streamline density as well as spurious tracts. We propose that our calculation of streamline density–weighted averages of DTI scalar parameter values be used as a standard in the characterization of the microstructural properties of white matter fascicles.

CONCLUSIONS

Our novel method of streamline density–weighted calculation of mean DTI scalar parameters allows for the incorporation of all white matter projections while compensating for volume averaging, resulting in average DTI measures of a white matter structure defined by tractography rather than by its voxels. Using streamline density weighting, we found a relation between alterations in white matter microstructure and neurologic outcomes in TSC.

The finding of decreased AFA and increased AAD, AMD, and ARD of the corpus callosum in the TSC population compared to controls is a new finding consistent with the previous work that has identified alterations in the white matter of patients with TSC. These pathologic findings in the corpus callosum by DTI are likely typical of alterations throughout the cerebral white matter in TSC.

The significant difference of AFA between subjects with TSC with and without ASD lends further support to the current hypothesis of long-range functional and structural disconnection in autism. Our finding of AFA differences raises the possibility of using callosal AFA as an early biomarker to predict ASD in the TSC population. Future longitudinal studies of our younger patients will provide much-needed insights in pathologic developmental changes occurring at the critical periods in ASD (41).

ACKNOWLEDGEMENTS

M.S. is supported in part by the John Merck Fund and a Junior Investigator Award from the Children's Hospital Boston Translational Research Program. C.N. is supported by NIH grant R01 DC010290. This investigation was supported in part by NIH grant R01 RR021885, R01 LM010033, R03 EB008680 and NIH grant UL1 RR025758. Thanks go to Sarah Spence, MD, PhD for critical reading of the manuscript. We gratefully acknowledge the contribution of MRI scans from John Gilmore and Martin Styner, supported by grant P50 MH064065 from the National Institutes of Health. We are indebted to the children and families who have participated in this study.

REFERENCES

1. Curatolo P, Bombardieri R, Jozwiak S. Tuberous sclerosis. Lancet 2008; 372:657–668.
2. Wong V. Study of the relationship between tuberous sclerosis complex and autistic disorder. J Child Neurol 2006; 21:199–204.
3. Jansen FE, Vincken KL, Algra A, et al. Cognitive impairment in tuberous sclerosis complex is a multifactorial condition. Neurology 2008; 70: 916–923.
4. Clifford S, Dissanayake C, Bui QM, et al. Autism spectrum phenotype in males and females with fragile X full mutation and premutation. J Autism Dev Disord 2007; 37:738–747.
5. Choi YJ, Di Nardo A, Kramvis I, et al. Tuberous sclerosis complex proteins control axon formation. Genes Dev 2008; 22:2485–2495.
6. Meikle L, Talos DM, Onda H, et al. A mouse model of tuberous sclerosis: neuronal loss of Tsc1 causes dysplastic and ectopic neurons, reduced myelination, seizure activity, and limited survival. J Neurosci 2007; 27:5546–5558.
7. Nie D, Di Nardo A, Han JM, et al. Tsc2-Rheb signaling regulates EphAmediated axon guidance. Nat Neurosci 2010; 13:163–172.
8. Arulrajah S, Ertan G, Jordan L, et al. Magnetic resonance imaging and diffusion-weighted imaging of normal-appearing white matter in children and young adults with tuberous sclerosis complex. Neuroradiology 2009; 51:781–786.
9. Makki MI, Chugani DC, Janisse J, et al. Characteristics of abnormal diffusivity in normal-appearing white matter investigated with diffusion tensor MR imaging in tuberous sclerosis complex. AJNR Am J Neuroradiol 2007; 28:1662–1667.
10. Krishnan ML, Commowick O, Jeste SS, et al. Diffusion features of white matter in tuberous sclerosis with tractography. Pediatr Neurol 2010; 42:101–106.
11. Simao G, Raybaud C, Chuang S, et al. Diffusion tensor imaging of commissural and projection white matter in tuberous sclerosis complex and correlation with tuber load. AJNR Am J Neuroradiol 2010; 31:1273–1277.
12. Alexander AL, Lee JE, Lazar M, et al. Diffusion tensor imaging of the corpus callosum in Autism. Neuroimage 2007; 34:61–73.
13. Keller TA, Kana RK, Just MA. A developmental study of the structural integrity of white matter in autism. Neuroreport 2007; 18:23–27.
14. Roach ES, Gomez MR, Northrup H. Tuberous sclerosis complex consensus conference: revised clinical diagnostic criteria. J Child Neurol 1998; 13:624–628.
15. American Psychiatric Association. Diagnostic and statistical manual of mental disorders. 4th ed, text rev. Arlington, VA: American Psychiatric Association; 2000.
16. Lord C, Risi S, Lambrecht L, et al. The autism diagnostic observation schedule-generic: a standard measure of social and communication deficits associated with the spectrum of autism. J Autism Dev Disord 2000; 30:205–223.
17. Reese TG, Heid O, Weisskoff RM, et al. Reduction of eddy-currentinduced distortion in diffusion MRI using a twice-refocused spin echo. Magn Reson Med 2003; 49:177–182.
18. Grau V, Mewes AU, Alcaniz M, et al. Improved watershed transform for medical image segmentation using prior information. IEEE Trans Med Imaging 2004; 23:447–458.
19. Weisenfeld NI, Warfield SK. Automatic segmentation of newborn brain MRI. Neuroimage 2009; 47:564–572.
20. Ruiz-Alzola J, Westin CF, Warfield SK, et al. Nonrigid registration of 3D tensor medical data. Med Image Anal 2002; 6:143–161.
21. Douek P, Turner R, Pekar J, et al. MR color mapping of myelin fiber orientation. J Comput Assist Tomogr 1991; 15:923–929.

22. Arsigny V, Fillard P, Pennec X, et al. Log-Euclidean metrics for fast and simple calculus on diffusion tensors. Magn Reson Med 2006; 56:411–421.
23. Lazar M, Weinstein DM, Tsuruda JS, et al. White matter tractography using diffusion tensor deflection. Hum Brain Mapp 2003; 18:306–321.
24. Wakana S, Jiang H, Nagae-Poetscher LM, et al. Fiber tract-based atlas of human white matter anatomy. Radiology 2004; 230:77–87.
25. Vos SB, Jones DK, Viergever MA, et al. Partial volume effect as a hidden covariate in DTI analyses. Neuroimage 2011; 55:1566–1576.
26. Kubicki M, Alvarado JL, Westin CF, et al. Stochastic tractography study of Inferior Frontal Gyrus anatomical connectivity in schizophrenia. Neuroimage 2011; 55:1657–1664.
27. Powell HW, Parker GJ, Alexander DC, et al. Hemispheric asymmetries in language-related pathways: a combined functional MRI and tractography study. Neuroimage 2006; 32:388–399.
28. Basser PJ, Pierpaoli C. Microstructural and physiological features of tissues elucidated by quantitative-diffusion-tensor MRI. J Magn Reson B 1996; 111:209–219.
29. Chung HW, Chou MC, Chen CY. Principles and limitations of computational algorithms in clinical diffusion tensor MR tractography. AJNR Am J Neuroradiol 2011; 32:3–13.
30. Ge Y, Sealfon SC, Speed TP. Some step-down procedures controlling the false discovery rate under dependence. Stat Sin 2008; 18:881–904.
31. Widjaja E, Simao G, Mahmoodabadi SZ, et al. Diffusion tensor imaging identifies changes in normal-appearing white matter within the epileptogenic zone in tuberous sclerosis complex. Epilepsy Res 2010;89:246–253.
32. Garaci FG, Floris R, Bozzao A, et al. Increased brain apparent diffusion coefficient in tuberous sclerosis. Radiology 2004; 232:461–465.
33. Peng SS, Lee WT, Wang YH, et al. Cerebral diffusion tensor images in children with tuberous sclerosis: a preliminary report. Pediatr Radiol 2004; 34:387–392.
34. Luat AF, Makki M, Chugani HT. Neuroimaging in tuberous sclerosis complex. Curr Opin Neurol 2007; 20:142–150.
35. Budde MD, Xie M, Cross AH, et al. Axial diffusivity is the primary correlate of axonal injury in the experimental autoimmune encephalomyelitis spinal cord: a quantitative pixelwise analysis. J Neurosci 2009; 29:2805–2813.
36. Song SK, Yoshino J, Le TQ, et al. Demyelination increases radial diffusivity in corpus callosum of mouse brain. Neuroimage 2005; 26:132–140.
37. Beaulieu C, Allen PS. Determinants of anisotropic water diffusion in nerves. Magn Reson Med 1994; 31:394–400.
38. Gulani V, Webb AG, Duncan ID, et al. Apparent diffusion tensor measurements in myelin-deficient rat spinal cords. Magn Reson Med 2001; 45:191–195.
39. Geschwind DH, Levitt P. Autism spectrum disorders: developmental disconnection syndromes. Curr Opin Neurobiol 2007; 17:103–111.
40. Karadag D, Mentzel HJ, Gullmar D, et al. Diffusion tensor imaging in children and adolescents with tuberous sclerosis. Pediatr Radiol 2005; 35: 980–983.
41. Firat AK, Karakas HM, Erdem G, et al. Diffusion weighted MR findings of brain involvement in tuberous sclerosis. Diagn Interv Radiol 2006; 12:57–60.
42. Anderson JS, Druzgal TJ, Froehlich A, et al. Decreased interhemispheric functional connectivity in autism. Cereb Cortex 2011; 21:1134–1146.
43. Jou RJ, Jackowski AP, Papademetris X, et al. Diffusion tensor imaging in autism spectrum disorders: preliminary evidence of abnormal neural connectivity. Aust N Z J Psychiatry 2011; 45:153–162.

44. Lange N, Dubray MB, Lee JE, et al. Atypical diffusion tensor hemispheric asymmetry in autism. Autism Res 2010; 3:350–358.
45. Shukla DK, Keehn B, Lincoln AJ, et al. White matter compromise of callosal and subcortical fiber tracts in children with autism spectrum disorder: a diffusion tensor imaging study. J Am Acad Child Adolesc Psychiatry 2010; 49:1269–1278.
46. Volpe JJ. Neurology of the newborn. Philadelphia: Saunders, 2008.
47. Widjaja E, Blaser S, Miller E, et al. Evaluation of subcortical white matter and deep white matter tracts in malformations of cortical development. Epilepsia 2007; 48:1460–1469.
48. Le Bihan D, Poupon C, Amadon A, et al. Artifacts and pitfalls in diffusion MRI. J Magn Reson Imaging 2006; 24:478–488.
49. Zhang Y, Zhang J, Oishi K, et al. Atlas-guided tract reconstruction for automated and comprehensive examination of the white matter anatomy. Neuroimage 2010; 52:1289–1301.
50. Dauguet J, Peled S, Berezovskii V, et al. Comparison of fiber tracts derived from in-vivo DTI tractography with 3D histological neural tract tracer reconstruction on a macaque brain. Neuroimage 2007; 37:530–538.
51. Leergaard TB, White NS, de Crespigny A, et al. Quantitative histological validation of diffusion MRI fiber orientation distributions in the rat brain. PLoS One 2010; 5:e8595.

Chapter 5

Corpus callosum white matter diffusivity reflects cumulative neurological comorbidity in Tuberous Sclerosis Complex

Jurriaan M. Peters[*1,3,5], Fiona Baumer[*1,] Sean Clancy[3], Anna K. Prohl[3], Sanjay P. Prabhu[2], Benoit Scherrer[3], Floor E. Jansen[4], Kees P.J. Braun[4], Mustafa Sahin[1], Aymeric Stamm[3,5], Simon K. Warfield[#,2,3].

1-3. Departments of Neurology[1,] and Radiology[2], and the Computational Radiology Laboratory[3], Boston Children's Hospital & Harvard Medical School, Boston, MA, USA

4. Brain Center Rudolf Magnus, Department of Pediatric Neurology, University Medical Center Utrecht, the Netherlands

5. Laboratory for Modeling and Scientific Computing (MOX), Dipartimento di Matematica, Politecnico di Milano, Italy

[*]These authors contributed equally

ABSTRACT

Introduction: Neurological manifestations in Tuberous Sclerosis Complex (TSC) are highly variable and unpredictable. We investigated the use of diffusion tensor imaging (DTI) of callosal white matter as a marker for neurological burden in TSC, and distinguish effects attributable to autism spectrum disorder (ASD), intellectual disability (ID) and epilepsy.

Methods: 186 children underwent 3T MRI with 35 direction DTI: 51 with TSC (19 of whom also had ASD), 46 with non-syndromic ASD and 89 healthy controls (HC). Density-weighted DTI metrics were obtained from DTI tractography of the corpus callosum. Subgroups were based on presence of TSC, ASD, ID, and epilepsy. Logistic regressions of the age-adjusted FA and MD function were done, correcting for volume and volume-age interactions.

Results: TSC patients demonstrated significantly lower FA (higher MD) values than ASD, and ASD had a lower FA than HC. Intellectual disability, epilepsy and the presence of ASD were associated with lower FA values in both the TSC and ASD populations. Co-occurrence of ASD, ID or epilepsy in TSC, demonstrated additive effects, but some subgroups were too small for reliable data fitting.

Conclusions: Using a cross-disorder approach, this study demonstrates cumulative effects of TSC, ASD, ID and epilepsy-related variables on callosal white matter diffusion metrics. In TSC, ASD was inextricably linked to ID and epilepsy, and the DTI measures reflect the total neurological disease burden rather than ASD specifically.

INTRODUCTION

Tuberous sclerosis complex (TSC) is a genetic multisystem disorder, with formation of hamartomatous lesions in various organs, including the brain, where they are referred to as tubers. TSC is associated with severe neurological manifestations including epilepsy (90%), intellectual disability (ID, 40%), and autism spectrum disorder (ASD, 50%)[1]. With a prevalence of 1 in 6,000, it is the most common monogenic cause of epilepsy and ASD[2].

TSC is a model disease for studying both epilepsy and ASD, and their co-occurrence. Early onset epilepsy and early cognitive delays[3-5] are associated with ASD in TSC. Moreover, an improved cognitive outcome with early and aggressive treatment of infantile spasms has been reported[6, 7], suggesting an epileptic encephalopathy contributes to neurodevelopmental outcome. In addition, the autism phenotype in TSC is comparable to non-syndromic ASD[8], and understanding the mechanism of ASD in TSC may yield insight into the underlying biology of ASD in general.

While the identification of early clinical risk factors in a patient can guide therapeutic decisions, effects of even earlier, pre-emptive treatment on outcome should be studied[9]. Research, however, into the use of mTOR inhibitors or vigabatrin before early symptoms of epilepsy and ASD occur, could significantly benefit from a robust imaging biomarker. Such a marker should be reliably reproducible, change in parallel with fluctuations in the clinical phenotype, and reflect the underlying neurobiology.

Diffusion tensor imaging (DTI) bares such promise, as it non-invasively probes microstructural properties of the brain. DTI characteristics in TSC are abnormal even in structurally normal appearing white matter (NAWM), and were reported to change with exposure to mTOR inhibitors[10]. In TSC patients with ASD, a decreased fractional anisotropy (FA) and increased mean diffusivity (MD) have been reported in two large white matter tracts, the corpus callosum and the arcuate fasciculus[11, 12]. These studies, however, did not correct for the presence of intellectual disability and epilepsy. Diffusion abnormality of the callosal white matter has also been reported in non-syndromic ASD[13]. It remains unclear, therefore, if in TSC, if the altered diffusion is a biomarker specific for ASD.

The aim of this study was to examine the effects of both TSC and ASD on callosal white matter microstructural integrity, while accounting for concurrent neurological manifestations. To this end, we compared DTI values among three groups: TSC (with and without ASD), non-syndromic ASD, and healthy controls (HC), and assessed impact of co-morbid ID and epilepsy.

METHODS

Subjects

Fifty-one patients with TSC who had undergone 3T MRI were identified through the Boston Children's Hospital Multidisciplinary Tuberous Sclerosis Program. All patients were diagnosed with definite TSC based on clinical and/or genetic criteria[14], underwent neurological examination, and their medical records were reviewed. Forty-eight subjects with non-syndromic ASD (thus without TSC) who had undergone 3T MRI as part of their clinical care were identified via chart review of the Boston Children's Hospital clinic and neuroradiology records. In all patients, the ASD diagnoses were based on evaluation by a board-certified pediatric neurologist (JMP, MS) or developmental medicine specialist, using the Diagnostic and Statistical Manual (DSM-IV-TR, and DSM-V), supplemented in most with the Autism Diagnostic Observation Schedule (ADOS)[15].

Eighty-nine HC had a normal neurological exam and a normal MRI on review by a pediatric neuroradiologist (SPP), performed as part of routine clinical care (e.g. for soft indications like tension type headache, new onset simple tic disorder) or as part of this research project. Controls did not undergo formal neuropsychological evaluation as part of this study, but histories were negative for neurodevelopmental problems.

Medical Ethics Approval

Subject identification and data acquisition were conducted using a protocol approved by the institutional review board of Boston Children's Hospital.

Clinical Data

Electronic medical records including available neuropsychological testing, school performance, and clinic notes were reviewed to gather information about neurodevelopment and seizure history. Due to the retrospective nature of the study, a continuous measure of cognition was not feasible. Intelligence was evaluated based on formal neuropsychological assessment or estimated clinically based on development and level of education. To prevent undersampled subgroups, and subsequent underpowering of the study, intelligence was categorized as either no ID (which includes normal (IQ>85) and borderline intelligence (IQ >70) with learning disability, mild language delays, minor limitations in adaptive function), or as ID (IQ <70, severely impaired language, communication skills and judgment, ADL dependence).

The epilepsy variable was categorized as present or absent, as more sophisticated classification schemes based on the E-Chess[16] resulted in undersampling of subgroups.

Image Acquisition

On a 3T MRI, the protocol included a routine clinical imaging and a diffusion imaging addition. Procedural sedation (most often with propofol) was used for clinical imaging studies only, if necessary to prevent excessive motion. The imaging protocol included (1) a T1-weighted high-resolution magnetization-prepared rapid acquisition gradient-echo (MPRAGE) sequence, (2) a T2-weighted turbo spin-echo (TSE) sequence, (3) a sagittal 3D isotropic T2 fluid-attenuated inversion recovery (FLAIR), and (4) axial diffusion imaging using a single shell HARDI with 30 slices with b=1000 s/mm2 and 5 b=0 images. The intracranial cavity was segmented following the structural MRI. Diffusion images were aligned to the T1-weighted MPRAGE to compensate for distortion and patient motion. We estimated the tensor fit with robust least-squares, as previously described[17].

Tractography

We used a stochastic algorithm for tractography, combining the speed and accuracy of deterministic decision-making at each voxel with probabilistic sampling to better explore the space of all possible streamlines[11]. The corpus callosum tractography was created from automated generation of region of interest (ROI), based on a template and the STAPLE algorithm, as detailed prior[18]. After visual review for anatomical accuracy, streamline density-weighted corrected scalar measures of FA and MD were obtained to correct for partial voluming effects and spurious tracts[11].

Statistical Analysis

Statistical analysis was done using the R statistical software package[19]. Group differences in clinical variables (age, gender, epilepsy, ID) were calculated using chi-square and student-t tests.

The assessment of the impact of group status and clinical variable on DTI measures was done as follows. For each subject, the data is composed of categorical variables gender, group status (ASD, TSC, and HC), and continuous variables age, callosal volume at corresponding age, and DTI metrics at corresponding age. Since volume and DTI metrics are functions of age, these were represented as functions[20]. First, the irregular time-points of collected data informed these two functions. Next we performed regression analysis of the DTI metrics function against group status, while correcting for the volume function. Possible confounders on the impact of group status on DTI metrics included volume, age and gender. Early univariate analysis demonstrated gender not to be a confounder, and it was omitted from the model. Subgroup analyses were created to adjust for presence of ID, ASD and epilepsy.

First, to define the DTI measures and volume as functions of age, we chose a fitting approach. Given the sparse sampling of the time interval of interest (wide age range), and the different time points for each subject in each group and condition, a b-spline basis expansion with cubic splines passing through each data point, a least square fitting criterion and a penalty term to enable smoothing, could not be used. Specifically, choices including the number of basis functions used in the expansion, the time scale, or the weight of the smoothness penalty would all greatly affect the functional representation. Thus, we applied approximating functions, and prior knowledge based on models of growth with a minimal number of free parameters, depending on the assumed complexity of the developmental trajectory of the DTI metrics over time[11,12,17]. We explored both a single parameter (asymptotic model, or the Michaelis-Menten model) and the use of 2 parameters (both models concurrently), but the data lacked power to incorporate volume-age interactions and smaller subgroups for a stable estimation of the 2-parameter model. For the 1-parameter model we could not assume that at t=0 (i.e. at birth) both volume and FA were nil, so we used conception as a common starting point for all subjects (t=0.75).

Hence, we used the following models:

$$V(t) = Best\ Of \left[a_V \left(1 - e^{-e^{r_V}(t+0.75)}\right),\ \begin{matrix} a_{FA}(t+0.75) \\ k_{FA}(t+0.75) \end{matrix} \right] \quad (1)$$

$$FA(t) = Best\ Of \left[a_{FA} \left(1 - e^{-e^{r_V}(t+0.75)}\right),\ \begin{matrix} a_V(t+0.75) \\ k_V(t+0.75) \end{matrix} \right] \quad (2)$$

The parameter a is the horizontal asymptote reached by adulthood. Parameter r is the natural logarithm of the rate constant that defines the rate of convergence towards the asymptote, while k (the Michaelis parameter) represents the age at which half the asymptote is reached. For a given response variable (volume or FA) and group status, we estimated both models, and chose the one with maximal achieved likelihood. The estimation was performed by minimizing the non-linear least squares criterion[19].

Next, we assessed effects of group status and clinical variables on DTI measures. First, we performed random bootstrapping separations of the original dataset into a training dataset (80% of the original data) and a test dataset (the remaining 20% of the data), to assess the prediction error of the fitted functional representation of the data, and to produce a functional dataset composed of n=10,000 observed curves on a uniform grid of p=1,000 time points. Next, a regression analysis of FA(t) on the group status, while controlling for the effect of V(t) would typically require a *functional* regression analysis[20], but since observa-

tions of the functional curves are now made on a uniform grid of time interval and at the same time points, a *traditional* regression analysis for each fixed time point can be done[22]:

$$logit\,(FA_{ij}(t) = \beta_{0j}(t) + \beta_1(t)V_{ij}(t) + \varepsilon_{ij}(t) \quad (3)$$

where $i = 1, \ldots, n$ indices the observations, $j = 1, 2, 3$ indices the 3 pathologies considered in our study and $\varepsilon_{ij}(t)$ is a random error term. Since FA is a positive random variable, we assume that it is corrupted with a Gamma-distributed noise. The model fit of the predicted FA curves was only applied in the age range common to all subgroups, as there was no data available outside of this range. Multivariate regression analysis was done on to determine individual effects from ID, epilepsy, ASD across all sufficiently large subgroups.

RESULTS

Demographic data and clinical variables are presented in Table 1. Healthy controls were older than patients with TSC alone, TSC and ASD, and non-syndromic ASD. There were more males in the non-syndromic ASD group compared to HC, but no group differences in gender distribution otherwise.

By selection, all HC had normal intelligence and none had epilepsy. For patients with TSC alone, they had less frequent ID compared to TSC with ASD, and to non-syndromic ASD.

Prevalence of epilepsy was higher in patients with both TSC and ASD compared to TSC alone, and compared non-syndromic ASD. Patients without epilepsy were equally common in the TSC alone and non-syndromic ASD groups.

Fractional anisotropy (FA) values of callosal white matter are shown for each of the subgroups in Figures 1-3. MD parameters were complimentary, visualized in supplementary Figures e1-3.

Step-wise, three levels of analysis were done as follows:

(1) At the first level, the volume-corrected FA for age was predicted for the main groups (HC, TSC, ASD) (Figure 1). There were sufficient subjects to fit the FA prediction model using a 2-parameter fit. Not adjusted for neurodevelopmental and epilepsy variables, patients with TSC had significantly lower FA (higher MD) compared to those with ASD, and compared to the HC group. Patients with ASD also had a lower FA (higher MD) compared to the HC group (Figure 1).

(2) At the second level, the three categorical variables ID, epilepsy and ASD were used to divide the main groups into subgroups. For the presence of ID: TSC with and without ID, ASD with and without ID (Figure 2A). For the presence of epilepsy: TSC with and without epilepsy, ASD with and without epilepsy (Figure 2B). For the presence of ASD: TSC with and without ASD (Figure 2C). The subgroups from the second and third level had only sufficient numbers for a stable model fit with a 1-parameter model.

The effect of ID is shown in Figure 2A. The TSC with ID subgroup had lower FA values than the TSC without ID subgroup. Similarly, the ASD with ID subgroup had lower FA values than the ASD without ID subgroup.

The effect of epilepsy is shown in Figure 2B. TSC patients with recurrent seizures had lower callosal FA values than TSC patients without epilepsy. Again, this same finding was present in the ASD subgroups with and without epilepsy

The effect of ASD is shown in Figure 2C. Subjects with both TSC and ASD had significantly lower FA values than TSC alone.

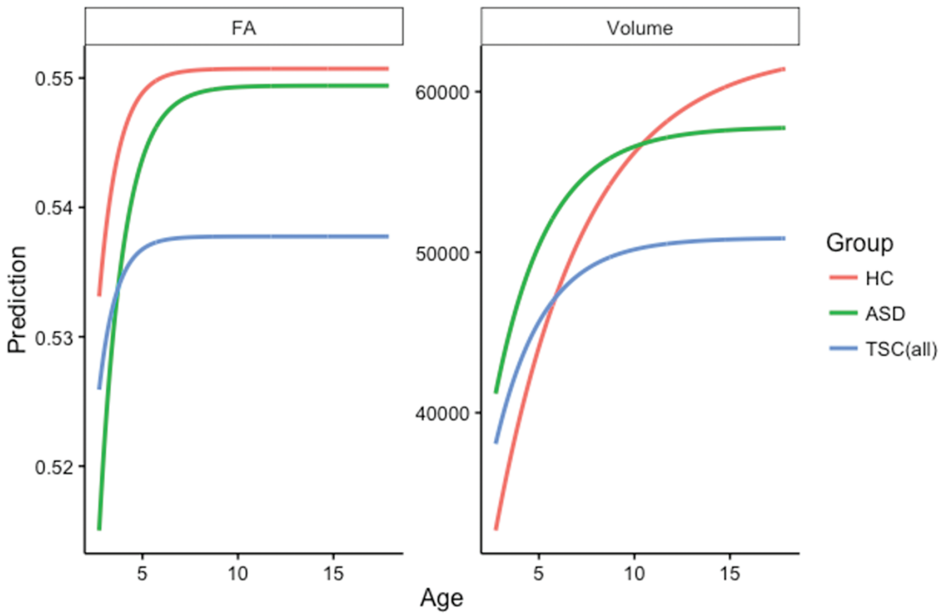

Figure 1: Predicted FA-values with age for the three main populations.
(A) Volume-adjusted predicted FA values of the model fit (line plots) are displayed for age, for each of the three main groups: Healthy controls (HC), Autism Spectrum Disorder (ASD), and Tuberous Sclerosis Complex (TSC). The developmental trajectory of white matter maturation has been described previously[11, 17], and was used as prior to inform the model.
(B) The volume of the corpus callosum is plotted by age, for each of the three groups HC, TSC, and ASD. Note the early overgrowth in the ASD group.

(3) At the third level, the possible iterations of the main groups (HC, TSC, ASD) with all three categorical variables (ID, epilepsy and ASD) were fitted (Figure 3). Small subgroups with less than 10 subjects (e.g. patients with TSC, no ID, no epilepsy but with ASD) were omitted as the model would not be stable.

Six subgroups (3 for TSC and 3 for ASD) were large enough for a stable model fit of FA prediction (Figure 3). Two subgroups could be made for TSC patients without ID: TSC_NO_ID with epilepsy, and TSC_NO_ID without epilepsy. The presence of epilepsy was again associated with lower FA values. A third subgroup of TSC patients had all 3 neurological co-morbidities (ASD, ID, and epilepsy), and demonstrated the lowest white matter FA values.

For ASD, a single subgroup could be made without ID, and without epilepsy, which displayed high FA values. The two other ASD subgroups both had ID: ASD_ID with epilepsy, and ASD_ID without epilepsy. In these ASD subgroups, again both the presence of ID and epilepsy were associated with a decreased callosal FA.

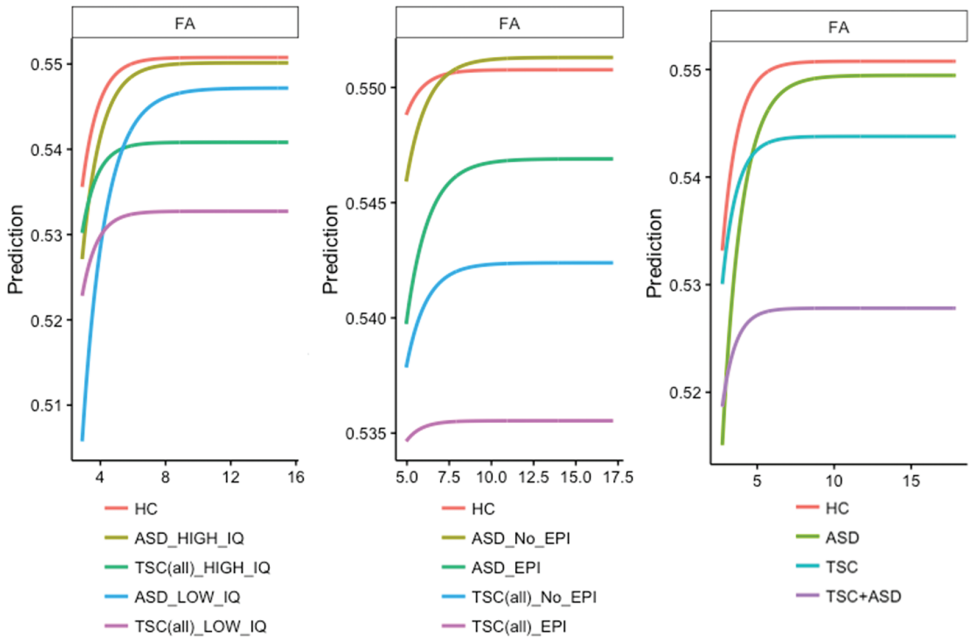

Figure 2: Predicted FA-values with age, corrected for cognition, epilepsy and ASD.
Volume-adjusted predicted FA values of the model fit (line plots) of the subgroups of TSC and ASD are shown. In (A), the effect of intellectual disability (ID) is shown on TSC, and on ASD. TSC with ID has lower FA values than TSC without ID, and the same applies to ASD with and without ID. In (B), a similar effect of epilepsy is shown on TSC and on ASD. In (C), the effect of ASD is demonstrated on TSC. TSC with ASD is associated with decreased FA values compared to TSC without ASD.

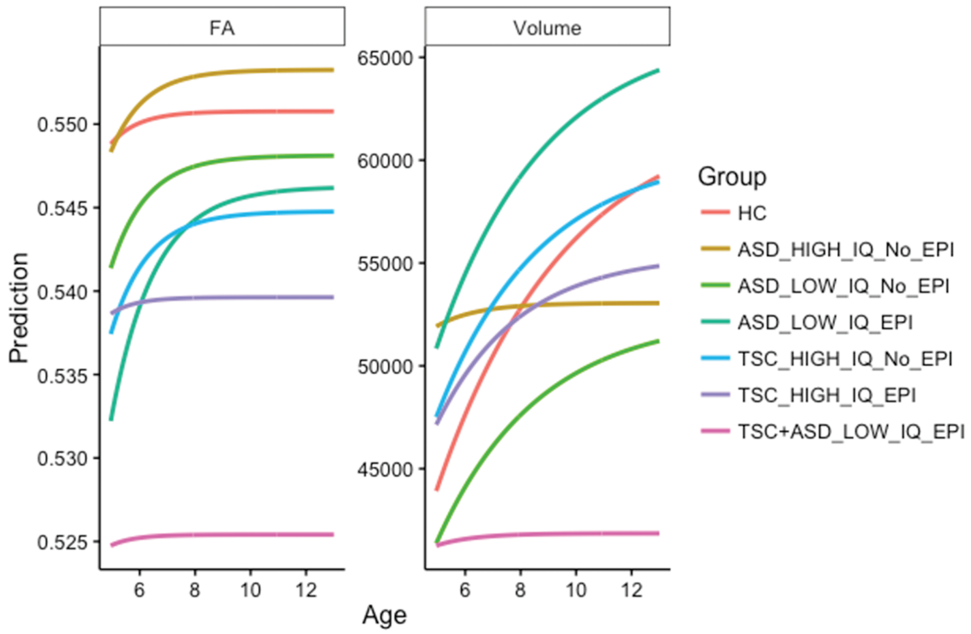

Figure 3: Predicted FA values with age for all possible subgroups.
Volume adjusted predicted FA values for the model fit (line plots) for all possible subgroups with ≥10 subjects are displayed. There were consistent cumulative effects from the co-occurrence of TSC, ID, epilepsy and ASD on FA trajectories.

DISCUSSION

This study demonstrates effects of both TSC and ASD on callosal white matter microstructural integrity, and cumulative effects of concurrent neurologic manifestations including ID and epilepsy. By the inclusion of patients with and without TSC, and with and without ASD, we attempted to isolate the effects of TSC from the effects of ASD.

The presence of ID had an effect on DTI measures of the white matter in both the TSC and ASD subgroups. In a previous DTI study of 20 patients with TSC, aberrant network connectivity was associated with ID[23], but in that study and in another, an effect of ASD was not found[24]. Another study in a non-syndromic ASD population reported a similar association between IQ and FA values of the corpus callosum[13]. Thus, given the relatively large sample size and the use of a binary measure of cognitive function in our study, it is not surprising to find an association between decreased microstructural integrity and ID in both TSC and ASD.

Similarly, the effect of recurrent seizures on diffusion of white matter tracts in TSC has been previously reported in a small study of 17 patients with TSC[24]. Abnormal local diffusion related to focal seizures could be both causative and a secondary effect to the seizures[25-27]. In our study, the average FA measure cannot separate regional differences in callosal white matter from diffuse effects involving the entire corpus callosum. Diffuse effects could suggest an overall more severe phenotype, associated with a higher prevalence of epilepsy.

In addition, in agreement with previous studies, we found aberrant callosal DTI metrics in subjects with ASD both with and without TSC[11-13, 28, 29]. In our work, the difference between HC group and non-syndromic ASD without ID was small but significant, suggesting our method is able to capture subtle abnormalities in patients with high-functioning non-syndromic ASD. In TSC, while the ASD phenotype is similar[8], the larger effect size (i.e., a more abnormal FA as compared to non-syndromic ASD) likely reflects a much less subtle widespread macro- and microscopic pathology beyond tubers[17]. The aberrant structural connectivity may affect functional connectivity as well. We previously reported decreased overall electroencephalogram (EEG) connectivity in TSC, and decreased long-range over short range connectivity in both TSC-related and non-syndromic ASD[30]. That study, however, did not separate out effects from the presence of ID.

The underlying neuropathology of aberrant diffusion of the NAWM in TSC is not yet elucidated. It may be due to the inclusion of microscopic pathology below MRI resolution, including changes in neuronal packing, increased heterotopic cells, and small satellite lesions referred to as "microtubers" beyond the tuber border identified on conventional imaging[17, 31, 32]. In animal models, abnormalities in myelination have been described[33]. The anatomopathological substrate of diffusion abnormality in TSC could also be studied through ex-vivo imaging of resection specimen obtained through epilepsy surgery. Secondary effects from recurrent seizures, including inflammatory and gliotic changes in the white matter adjacent to epileptogenic tissue, are likely to confound such an analysis[34, 35].

The scope of this study was limited to the examination of a single major white matter pathway, and other pathways are under investigation. While the corpus callosum structure has a role in the pathophysiology of ASD[28], it does not directly subserve the language or neurobehavioral functions affected in ASD. Examination of tracts involved in ASD-specific deficits in language, stimulus reward systems, and social cognition may yield more specific markers[36-38]. Finally, as diffusion tensor imaging techniques advance, novel acquisition schemes may enhance the ability for group-wise comparisons of white matter tracts and their role in ASD pathophysiology[39, 40].

Overall, this study demonstrates that DTI metrics of the corpus callosum are affected cumulatively by neurological symptoms in TSC and in non-syndromic ASD. These findings reflect

the complex relationship between biological disease burden, and subsequent ID, ASD and epilepsy in TSC[41]. The DTI changes, however, are neither sufficiently specific nor large early on, limiting its predictive value. Aside from more imaging samples at a young age, prospective and longitudinal data is needed to predict specific neurological comorbidity with DTI.

CONCLUSION

Using a cross-disorder approach, we report cumulative effects of neurological co-morbidity on callosal white matter diffusion in TSC and in ASD. The lack of specificity of callosal DTI metrics does not preclude its potential use as a marker for overall neurological outcome in TSC, although more early and longitudinal, prospective data are needed for validation.

ACKNOWLEDGEMENTS

J. Peters, S. Clancy, B. Scherrer, M. Sahin and S. Warfield are supported by NIH R01 NS079788 and U01 NS082320 grants. F. Baumer reports no disclosures relevant to the manuscript. A. Prohl is supported by Harvard Catalyst | The Harvard Clinical and Translational Science Center (National Center for Research Resources and the National Center for Advancing Translational Sciences, NIH award UL1 TR001102). M. Taquet is supported by WBI.World. S. Prabhu is supported by the Department of Defense W81XWH-11-1-0365 and NIH U01 NS082320 grants. F.Jansen is supported by the Framework Program FP7/2007-2013 under the project acronym EPISTOP (grant agreement no. 602391). K. Braun reports no disclosures relevant to the manuscript. M. Sahin is additionally supported by NIH P30 HD018655 and the Boston Children's Hospital Translational Research Program. The Developmental Synaptopathies Consortium (U54 NS092090) is part of the NCATS Rare Diseases Clinical Research Network (RDCRN). RDCRN is an initiative of the Office of Rare Diseases Research (ORDR), NCATS, funded through collaboration between NCATS, NIMH, NINDS, and NICHD. A. Stamm is supported by an NIH R01 EB013248 grant.

We are indebted to our patients and heathy controls for participation, and to Boston Children's Hospital MRI technical staff, for their diligent assistance with data acquisition.

NOTE

In Figures 2 and 3, the group with non-syndromic ASD (and no epilepsy) has higher FA values than the HC. This is an error. We are generating new plots where the bootstrapping is improved by fitting by weighted generalized non-linear least squares with weights that

account for a variance of the response variable proportional to the estimated power of the fitted response itself per group. The curves no longer show the erroneously high values for the non-syndromic ASD without epilepsy population. At the time of the thesis submission, these have not been formatted properly for clarity yet. Please consider the figures as "placeholders".

REFERENCES

1. Curatolo P, Bombardieri R, Jozwiak S. Tuberous sclerosis. Lancet 2008;372:657-668.
2. Davis PE, Peters JM, Krueger DA, Sahin M. Tuberous Sclerosis: A New Frontier in Targeted Treatment of Autism. Neurotherapeutics 2015;12:572-583.
3. Numis AL, Major P, Montenegro MA, Muzykewicz DA, Pulsifer MB, Thiele EA. Identification of risk factors for autism spectrum disorders in tuberous sclerosis complex. Neurology 2011;76:981-987.
4. Jansen FE, Vincken KL, Algra A, et al. Cognitive impairment in tuberous sclerosis complex is a multifactorial condition. Neurology 2008;70:916-923.
5. Jeste SS, Wu JY, Senturk D, et al. Early developmental trajectories associated with ASD in infants with tuberous sclerosis complex. Neurology 2014;83:160-168.
6. Bombardieri R, Pinci M, Moavero R, Cerminara C, Curatolo P. Early control of seizures improves long-term outcome in children with tuberous sclerosis complex. Eur J Paediatr Neurol 2010;14:146-149.
7. Jozwiak S, Kotulska K, Domanska-Pakiela D, et al. Antiepileptic treatment before the onset of seizures reduces epilepsy severity and risk of mental retardation in infants with tuberous sclerosis complex. Eur J Paediatr Neurol 2011;15:424-431.
8. Bruining H, Eijkemans MJ, Kas MJ, Curran SR, Vorstman JA, Bolton PF. Behavioral signatures related to genetic disorders in autism. Molecular autism 2014;5:11.
9. Julich K, Sahin M. Mechanism-based treatment in tuberous sclerosis complex. Pediatr Neurol 2014;50:290-296.
10. Tillema JM, Leach JL, Krueger DA, Franz DN. Everolimus alters white matter diffusion in tuberous sclerosis complex. Neurology 2012;78:526-531.
11. Peters JM, Sahin M, Vogel-Farley VK, et al. Loss of white matter microstructural integrity is associated with adverse neurological outcome in tuberous sclerosis complex. Acad Radiol 2012;19:17-25.
12. Lewis WW, Sahin M, Scherrer B, et al. Impaired language pathways in tuberous sclerosis complex patients with autism spectrum disorders. Cereb Cortex 2013;23:1526-1532.
13. Alexander AL, Lee JE, Lazar M, et al. Diffusion tensor imaging of the corpus callosum in Autism. Neuroimage 2007;34:61-73.
14. Northrup H, Krueger DA, Group ITSCC. Tuberous sclerosis complex diagnostic criteria update: recommendations of the 2012 Iinternational Tuberous Sclerosis Complex Consensus Conference. Pediatr Neurol 2013;49:243-254.
15. Lord C, Risi S, Lambrecht L, et al. The autism diagnostic observation schedule-generic: a standard measure of social and communication deficits associated with the spectrum of autism. J Autism Dev Disord 2000;30:205-223.
16. Humphrey A, Ploubidis GB, Yates JR, Steinberg T, Bolton PF. The Early Childhood Epilepsy Severity Scale (E-Chess). Epilepsy Res 2008;79:139-145.
17. Peters JM, Prohl AK, Tomas-Fernandez XK, et al. Tubers are neither static nor discrete: Evidence from serial diffusion tensor imaging. Neurology 2015;85:1536-1545.
18. Suarez RO, Commowick O, Prabhu SP, Warfield SK. Automated delineation of white matter fiber tracts with a multiple region-of-interest approach. Neuroimage 2012;59:3690-3700.
19. R: A language and environment for statistical computing [computer program]. Vienna, Australia: R Foundation for Statistical Computing, 2015.
20. Ramsay J, Silverman BW. Functional Data Analysis, 2 ed. New York: Springer-Verlag, 2005.
21. Peters JM, Tomas-Fernandez M, van Putten MJ, Loddenkemper T. Behavioral measures and EEG monitoring using the Brain Symmetry Index during the Wada test in children. Epilepsy Behav 2012;23:247-253.

22. Pini A, Vantini S. Interval-wise testing for functional data. Milan, Italy: Dipartimento di Matematica, Politecnico di Milano, 2015.
23. Im K, Ahtam B, Haehn D, et al. Altered Structural Brain Networks in Tuberous Sclerosis Complex. Cereb Cortex 2015.
24. Baumer FM, Song JW, Mitchell PD, et al. Longitudinal changes in diffusion properties in white matter pathways of children with tuberous sclerosis complex. Pediatr Neurol 2015;52:615-623.
25. Yogi A, Hirata Y, Karavaeva E, et al. DTI of tuber and perituberal tissue can predict epileptogenicity in tuberous sclerosis complex. Neurology 2015;85:2011-2015.
26. Jansen FE, Braun KP, van Nieuwenhuizen O, et al. Diffusion-weighted magnetic resonance imaging and identification of the epileptogenic tuber in patients with tuberous sclerosis. Arch Neurol 2003;60:1580-1584.
27. Otte WM, van Eijsden P, Sander JW, Duncan JS, Dijkhuizen RM, Braun KP. A meta-analysis of white matter changes in temporal lobe epilepsy as studied with diffusion tensor imaging. Epilepsia 2012;53:659-667.
28. Travers BG, Adluru N, Ennis C, et al. Diffusion Tensor Imaging in Autism Spectrum Disorder: A Review. Autism Res 2012.
29. Cheng Y, Chou KH, Chen IY, Fan YT, Decety J, Lin CP. Atypical development of white matter microstructure in adolescents with autism spectrum disorders. Neuroimage 2010;50:873-882.
30. Peters JM, Taquet M, Vega C, et al. Brain functional networks in syndromic and non-syndromic autism: a graph theoretical study of EEG connectivity. BMC Med 2013;11:54.
31. Marcotte L, Aronica E, Baybis M, Crino PB. Cytoarchitectural alterations are widespread in cerebral cortex in tuberous sclerosis complex. Acta Neuropathol 2012;123:685-693.
32. Ruppe V, Dilsiz P, Reiss CS, et al. Developmental brain abnormalities in tuberous sclerosis complex: a comparative tissue analysis of cortical tubers and perituberal cortex. Epilepsia 2014;55:539-550.
33. Meikle L, Talos DM, Onda H, et al. A mouse model of tuberous sclerosis: neuronal loss of Tsc1 causes dysplastic and ectopic neurons, reduced myelination, seizure activity, and limited survival. J Neurosci 2007;27:5546-5558.
34. Wong M. Mechanisms of epileptogenesis in tuberous sclerosis complex and related malformations of cortical development with abnormal glioneuronal proliferation. Epilepsia 2008;49:8-21.
35. Sosunov AA, McGovern RA, Mikell CB, et al. Epileptogenic but MRI-normal perituberal tissue in Tuberous Sclerosis Complex contains tuber-specific abnormalities. Acta neuropathologica communications 2015;3:17.
36. Fletcher PT, Whitaker RT, Tao R, et al. Microstructural connectivity of the arcuate fasciculus in adolescents with high-functioning autism. Neuroimage 2010;51:1117-1125.
37. Von Der Heide RJ, Skipper LM, Klobusicky E, Olson IR. Dissecting the uncinate fasciculus: disorders, controversies and a hypothesis. Brain 2013;136:1692-1707.
38. Abrams DA, Lynch CJ, Cheng KM, et al. Underconnectivity between voice-selective cortex and reward circuitry in children with autism. Proc Natl Acad Sci U S A 2013;110:12060-12065.
39. Scherrer B, Warfield SK. Parametric representation of multiple white matter fascicles from cube and sphere diffusion MRI. PLoS One 2012;7:e48232.
40. Taquet M, Scherrer B, Commowick O, et al. A mathematical framework for the registration and analysis of multi-fascicle models for population studies of the brain microstructure. IEEE Trans Med Imaging 2014;33:504-517.
41. van Eeghen AM, Pulsifer MB, Merker VL, et al. Understanding relationships between autism, intelligence, and epilepsy: a cross-disorder approach. Dev Med Child Neurol 2013;55:146-153.

Chapter 6

Tubers are neither static nor discrete: Evidence from serial diffusion tensor imaging

Jurriaan M. Peters[1, 2], Anna K. Prohl[2], Xavier Tomas-Fernandez[2], Maxime Taquet [2,3], Benoit Scherrer PhD[2], Sanjay P. Prabhu[2], Hart G. Lidov[4], Jolene S. Singh[2], Floor E. Jansen[5], Kees P. Braun, Mustafa Sahin[1], Simon K. Warfield[2,*], Aymeric Stamm[2].

1. Division of Epilepsy and Clinical Neurophysiology, Department of Neurology, Boston Children's Hospital and Harvard Medical School, Boston, MA, USA
2. Computational Radiology Laboratory, Department of Radiology, Boston Children's Hospital and Harvard Medical School, Boston, MA, USA
3. ICTEAM Institute, Université catholique de Louvain, Louvain-la-Neuve, Belgium
4. Department of Pathology, Boston Children's Hospital and Harvard Medical School, Boston, MA, USA
5. Brain Center Rudolf Magnus, Department of Pediatric Neurology, University Medical Center Utrecht, the Netherlands

ABSTRACT

Objective: To assess the extent and evolution of tissue abnormality of tubers, perituber tissue, and normal appearing white matter in patients with Tuberous Sclerosis Complex using serial diffusion tensor imaging (DTI).

Methods: We applied automatic segmentation based on a combined global-local intensity mixture model of 3T structural and 35 direction diffusion tensor magnetic resonance images (DTI) to define three regions: tuber tissue, an equal volume perituber rim, and the remaining normal appearing white matter (NAWM). For each patient, scan, lobe, and tissue type, we analyzed the averages of mean diffusivity (MD) and fractional anisotropy (FA) in a generalized additive mixed model (GAMM).

Results: 25 patients (mean age 5.9 year; range 0.5-24.5 years) underwent 2-6 scans each, totaling 70 scans. Average time between scans was 1.2 years (range 0.4-2.9). Patient scans were compared to those of 73 healthy controls. FA values were lowest, and MD values were highest in tubers, next in perituber tissue, then in NAWM. Longitudinal analysis showed a positive (FA) and negative (MD) correlation with age in tubers, perituber tissue and NAWM. All three tissue types followed a bi-exponential developmental trajectory, similar to the white matter of controls. An additional qualitative analysis showed a gradual transition of diffusion values across the tissue type boundaries.

Conclusions: Like normal appearing white matter, tuber and perituber tissue in Tuberous Sclerosis Complex undergo microstructural evolution with age. The extent of diffusion abnormality decreases with distance to the tuber, in line with known extension of histologic, immunohistochemical and molecular abnormalities beyond tuber pathology.

INTRODUCTION

TSC is a genetic, multisystem disorder characterized by hamartoma formation in various organs, including the brain, where they are referred to as tubers. Cerebral cortical tubers are present in more than 80% of TSC patients, and arise due to abnormal cellular differentiation, migration, and proliferation[1].

Although TSC traditionally has been considered a disorder of discrete, multifocal abnormalities, a growing body of evidence suggests that TSC neuropathology exists far beyond tuber borders visible on conventional magnetic resonance imaging (MRI). Tuber-like pathology has recently been identified in the direct vicinity of tubers, as well as diffusely throughout the white matter[2, 3]. Studies using diffusion tensor imaging (DTI) are in agreement and describe decreased fractional anisotropy (FA) or increased mean diffusivity in tubers[4], in perituber tissue[5], and in otherwise normal appearing white matter (NAWM)[6-8].

In addition, changes in tissue contrast, gadolinium enhancement, and cyst-like degeneration over time on conventional imaging have changed the view of tubers from static to dynamic[9-11]. While cross-sectional studies have linked DTI measures of tubers to epilepsy localization and severity[12], and DTI measures of NAWM to neurodevelopmental disorders[13, 14], the longitudinal evolution of tissue diffusion in TSC has not been investigated, to date.

In TSC, therefore, it is unclear when, and where such tissue abnormalities occur in the developmental trajectory. We sought to describe maturational changes of DTI measures in young patients with TSC, and assess the extent of diffusion abnormality across tuber, perituber and NAWM tissue types.

METHODS

Subjects

25 children and young adults followed in the Multidisciplinary TSC Program at Boston Children's Hospital with a definite diagnosis of TSC[15], underwent two to six MRI scans. Patients who underwent surgery for epilepsy or for resection of subependymal giant cell astrocytoma were excluded. There were no age cut-off criteria. Medical record review provided clinical and genetic data. Autism spectrum disorder was diagnosed clinically by DSM-IV criteria, and supplemented by ADOS[16] in most patients. Intractability was defined as ongoing seizures in the presence of 2 or more adequate anti-epileptic drugs (AEDs). 73 control subjects, not age matched, were recruited as part of this research study, and each underwent a single scan with normal MRI results per review by a pediatric neuroradiologist (SPP).

Standard protocol approvals, registrations, and patient consents.

Recruitment and data acquisition of subject and controls were conducted using a protocol approved by the institutional review board.

Image acquisition

Imaging was performed on a Siemens Trio 3T MRI. Acquisition parameters were unchanged with repeat imaging for each subject, and images acquired with a different protocol were excluded from the study. Sedation was used only in subjects undergoing clinical imaging if necessary to prevent significant motion.

The imaging protocol included (1) a T1-weighted high-resolution magnetization-prepared rapid-acquisition gradient-echo (MPRAGE) sequence (voxel size [mm] 0.5×0.5×1 to 1×1×1, field of view (FOV) 19.2-25.6 cm, echo time (TE) 1.66-3.39 ms, repetition time (TR) 1130-2530 ms, flip angle 7°-9°), (2), a T2-weighted turbo spin-echo (TSE) sequence, (3) sagittal 3D isotropic T2 fluid-attenuated inversion recovery (FLAIR) (voxel size [mm]=0.9x0.9x1, number of excitations (NEX) 1, TR 5000 ms, TE 390-400 ms, echo train length (ETL) 141, FOV 19-26 cm, flip angle 20°, acquisition matrix 256×256) and (4) diffusion imaging with single-shot spin echo acquisition in the axial plane, with twice refocused gradients to minimize Eddy currents, using 30 images with b=1000 s/mm2 and five images with b=0 s/mm2 (voxel size [mm] 1.72×1.72×2.2, FOV 22 cm, slice thickness 2.2 mm, TE 88 ms, TR 10 seconds, acquisition matrix 128×128, NEX 1, iPAT 2, TR 1000 ms, flip angle 90°, in-plane GRAPPA, modified as necessary to facilitate completion of the scan).

Compensation for residual distortion and patient motion was achieved by rigid registration of the diffusion images to the T1-weighted MPRAGE scan, with appropriate reorientation of the gradient directions[17]. Tensors were estimated using robust least squares[18].

Longitudinal alignment

For each subject, to ensure longitudinal analysis of the same structural regions, segmentation of the 3 tissue types (tuber, perituber, and NAWM) was only done once on a *reference scan* of highest quality structural imaging. Given maturational increases in tissue contrast, this was typically the latest image series acquired. For each scan the diffusion tensors were resampled and aligned to the T1 MPRAGE space. The other T1-weighted MRIs underwent rigid then non-rigid registration to the T1 reference scan, and this transform was applied to the diffusion images[19].

Tissue segmentation

Segmentation of three tissue types was based on a combined global-local intensity mixture model[20] on the FLAIR image. We used the Expectation-Maximization algorithm to estimate the parameters that maximize the tissue maximum a posteriori probabilities. Cortical tubers were modeled as outliers[21], and specifically validated for use in TSC[22] (Figure 1).

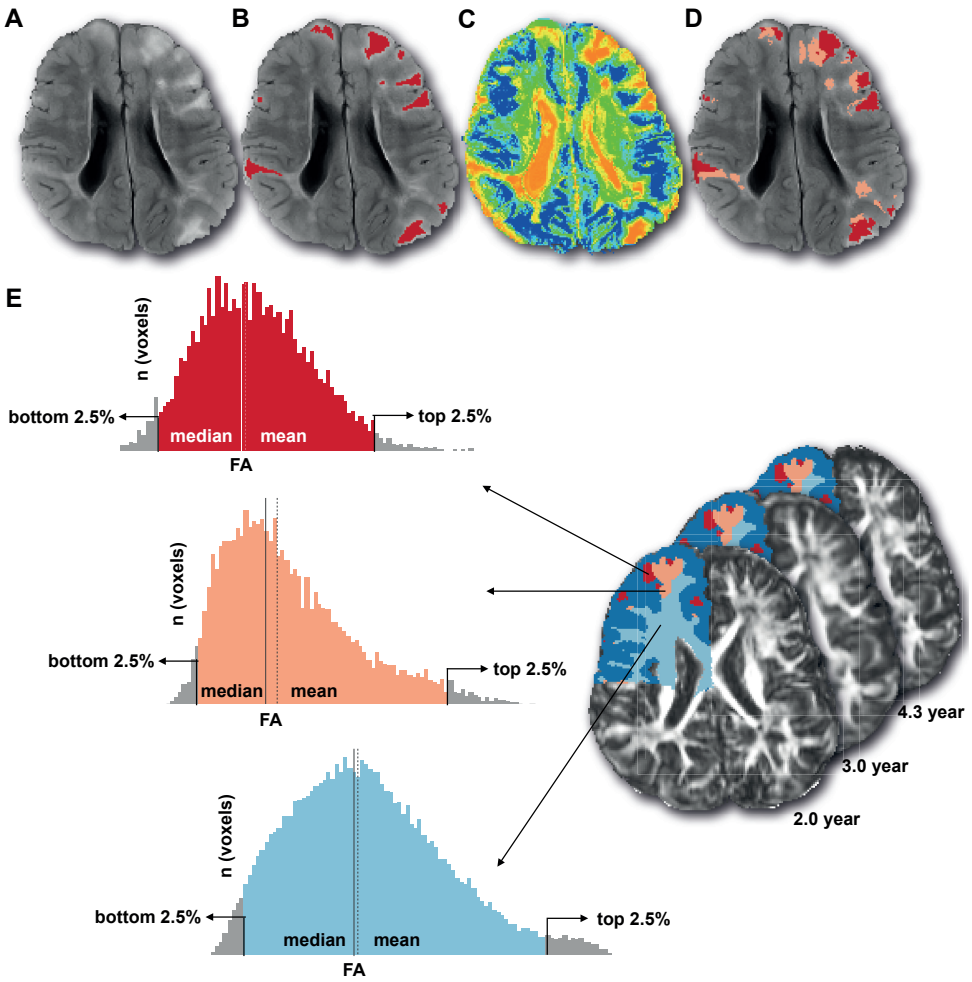

Figure 1: Segmentation algorithm and distribution histograms of FA-values of tuber, perituber, and NAWM tissues.
(A-D) Manual and automated tuber segmentation. (A) Axial Fluid Attenuation Inversion Recovery (FLAIR) image, with tubers appearing as bright areas of T2-prolongation. (B) Manual segmentation, areas indicating tuber tissue are marked red. (C) Intensity likelihood of outlier voxels with color spectrum from blue (least likely) to red (most likely), given the global-local intensity mixture model. (D) Automated tuber segmentation, tuber areas indicated in red, and perituber tissue in salmon, after removal of false positive areas (e.g. CSF pulsation artifacts).
(E) Example of distribution histograms of three tissue types in three scans of one patient.
On the right, three axial FA-maps are aligned, each acquired at a different time point. The superimposed automated segmentation reveals three different tissue types of the right frontal lobe (dark blue cortex not included): Red (tuber), salmon (perituber), light blue (normal appearing white matter).
On the left, the corresponding distribution histograms of FA values are displayed for each tissue type. For clarity, only the histograms of the right frontal lobe of the *first* acquired image are shown. The mean (dotted line) and median (vertical line) reflect the skew in each histogram.

The tuber segmentation was expanded in 3 dimensions to the adjacent perituber white matter, until a volume equal to the tuber was defined, and truncated in case of overlap with grey matter or other tubers. In patients, white matter that was neither tuber (T) nor perituber (PT) was designated as normal appearing white matter (NAWM). Radial migration lines were included in the tuber- and perituber tissues, depending on local density values. Parcellation of lobes was done using a local MAP PSTAPLE algorithm[23].

Empirically, small volumes of tissue classified as tuber with a volume of less than 500 voxels were excluded from analysis as the false detection rate approached zero at that cut-off, and so was the associated perituber rim in such cases. Calcified and cyst-like tubers were omitted as calcium deposits and free water, respectively, alter tensor estimates (Supplemental Figure 1).

Diffusion measures

For each subject, in each scan, in each lobe, the average mean diffusivity (MD), and average fractional isotropy (FA) of the tissue types were calculated. In each region, the median and skew were also calculated to assess distribution of MD and FA values.

As a qualitative analysis, the boundaries between different tissue types were examined by measuring neighboring voxels from one tissue type to the next in 6 random subjects. In the axial plane, the FA values were acquired with regular intervals along a trajectory from the periphery (tuber), via perituber tissue, to deep NAWM. The plots were smoothed with a moving average of 3 data points to correct for jitter.

Histopathology and immunohistochemistry

A left occipital lobe resection from a 6 year-old patient with TSC (consented for research, not part of the imaging cohort), as part of an epilepsy surgery, was studied histopathologically. Sections were stained with hematoxylin and eosin and Luxol fast blue (H&E/LFB), and immunohistochemical staining for glial fibrillary acidic protein (GFAP), neuronal nuclear antigen (NeuN), phosphorylated neurofilament (SMI 31), neurofilament protein (NFP), and synaptophysin. Each staining was performed using standard clinical laboratory protocols.

Statistical analysis

Normal distribution of variables was tested using Shapiro-Wilk, and when applicable, non-parametric testing was applied. Associations were tested by Kendall's tau rank correlation coefficient. Distributions were compared by non-parametric Wilcoxon rank-sum or Kruskal-Wallis testing, and the influence of tissue types (T, PT, NAWM, control WM), confounding for all other factors in the data set as a block variable, was tested by the non-parametric Friedman test. If distributions differed, Tukey or Dunnet multiple comparisons were made for further analysis.

The generalized additive mixed model (GAMM) was used for longitudinal analysis of the data. This extension of the linear model is suited whenever the outcome variable cannot be explanatory variables in a non-linear fashion (Supplemental Figure 2), with no known explicit parametrization[24].

In addition, the mixed component of the GAMM allows for the introduction of random effects that, in conjunction with repeated measure data, enables separation of inter- and intra-subject variability from the random error component, which ultimately yields greater statistical power to reveal the most important mechanisms impacting the outcome. The interested reader is invited to explore both the technical and layman introduction to GAMM (Appendix 1).

RESULTS

Patient characteristics

Patient were younger than controls (age at first scan 5.9, range 0.5-24.6 vs. 13.0, range 1.1-25.2, $p<0.0001$). Average time between 2 consecutive scans in patients was 1.2 years (range 0.4-2.9). Sex was not significantly different (17 (68%) patients vs. 37 (51%) controls were male). 17 (68%) patients had TSC2 mutations, 5 (20%) had TSC1 mutations, 3 had negative genetic testing. 11 (44%) had autism spectrum disorder. All patients had epilepsy (15 (60%) intractable), were on antiepileptic drugs, and 10 (40%) had a history of infantile spasms.

DTI evolution

The mean and median in each tissue type confirmed unimodal distribution of FA and MD values, and tail values of 2.5% on each end of the distribution histograms were omitted to ensure robust estimates of averages (Figure 1). Univariate analyses revealed that side and gender were poorly associated with both FA ($p=0.28$ and 0.44) and MD ($p=0.11$ and 0.41) and were thus discarded. The dependency of FA/MD with age in our regression model was described by 5 regressors (see detailed methods in Appendix), and after GAMM modeling, all regression coefficient estimates were statistically non-null (data not shown).

The selected GAMM model describes an evolution of FA and MD over time common to all lobes and tissue types, an evolution of these measures with a volume specific for each lobe and a different value of FA and MD at the intersect in each tissue type and in each lobe (Figure 2). The bi-exponential trajectory of FA and MD changes with age, are seen not only for the control subject and in the NAWM of patients, but also for tuber and peritube tissue. The tuber tissue type trajectory reaches a plateau at a lower FA and higher MD value, and the peritube tissue type displays characteristics intermediate to tuber and NAWM tissues.

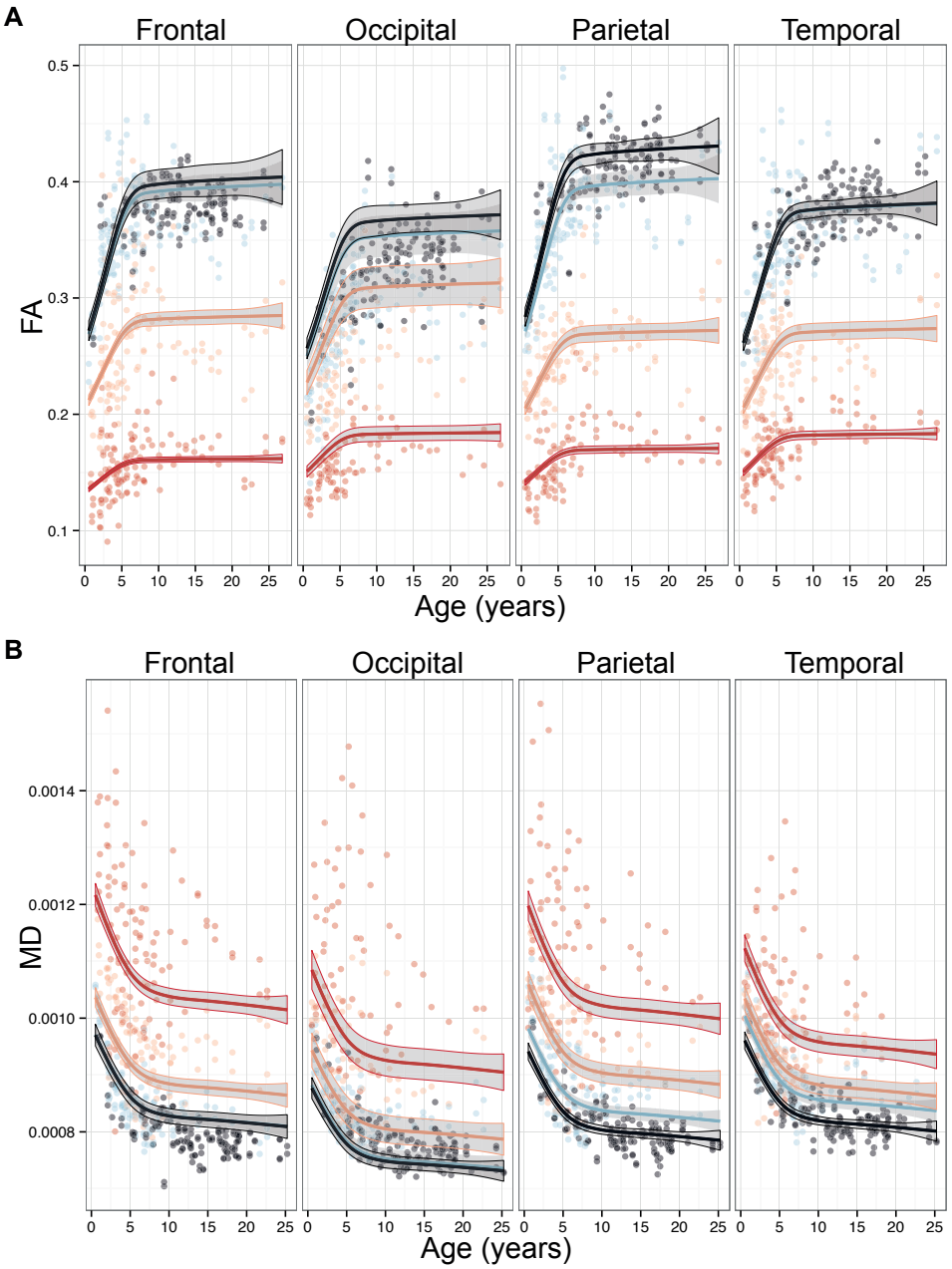

Figure 2: Diffusion measures over time in Tuberous Sclerosis Complex
Fractional Anisotropy (A) and Mean Diffusivity (B) measures are fitted with the GAMM, and evolution with age in years is shown for every lobe. Three different tissue types are color-colded: red (tuber), salmon (perituber), light blue (normal appearing white matter). White matter of controls is represented in black. Note the early, steep, linear increase before age 5-6 years and the slower increase thereafter.

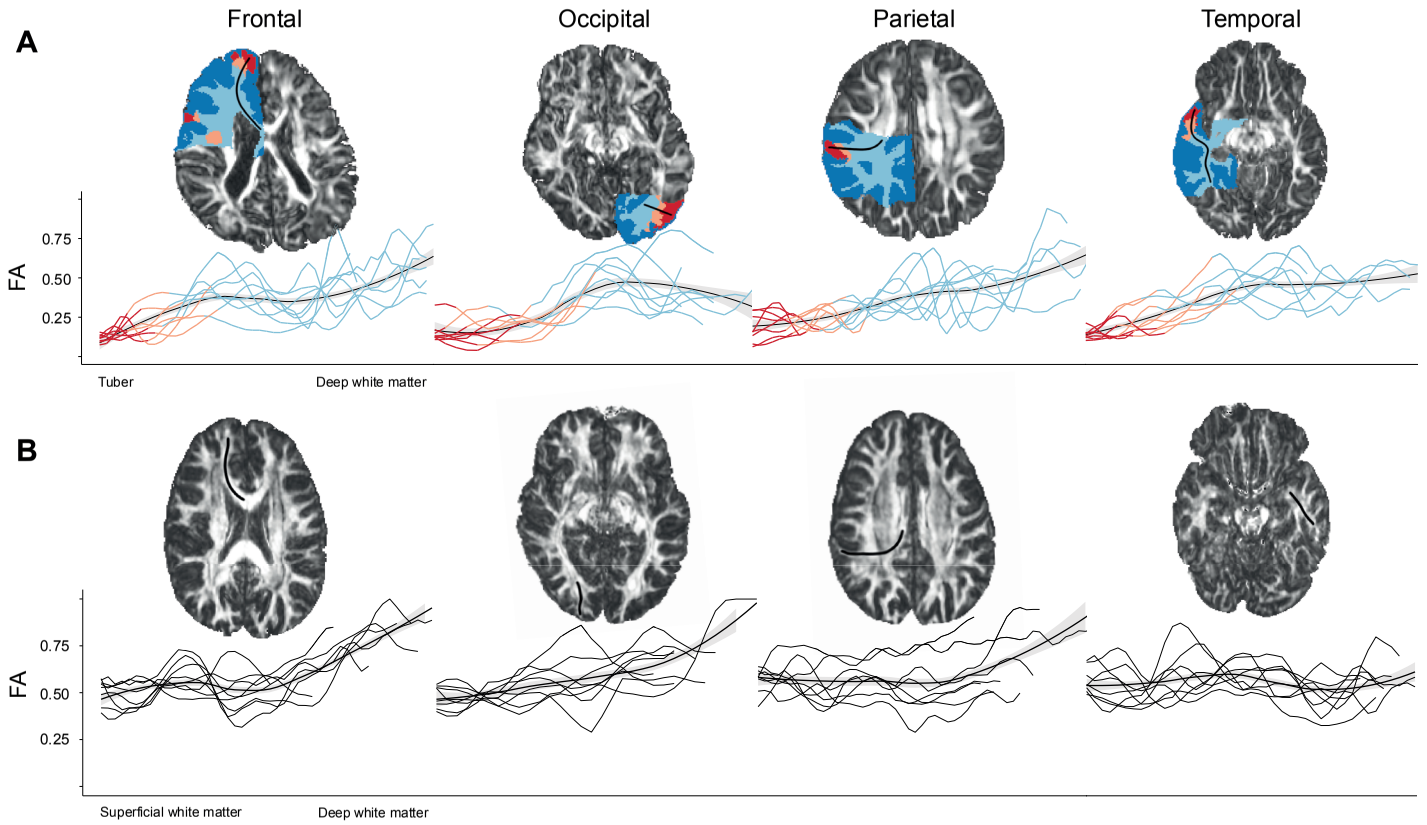

Figure 3: Gradual transition between tissue types from tuber to deep NAWM

In (A), changes in Fractional Anisotropy (FA) measured along trajectories from tuber to deep NAWM in each lobe of 5 patients reveal a gradual transition between tissue types (example trajectories in black above plots). The boundaries between the tuber (red), perituber (salmon) and NAWM (light blue) tissue types are not discrete, and thus segmentation is dependent on factors like imaging contrast, resolution and arbitrary thresholding. Note the deep "dips" in the curves of the NAWM, reflecting areas with more complex white matter[27], for example the crossing of pathways. In (B), the trajectories of 5 healthy controls, also with some increase of FA values in deeper white matter pathways.

Tuber and peritubertissue were different than the NAWM of controls, both globally and in each lobe. There was no consistent pattern of differences in the comparison of NAWM to control WM. For the FA only, and only in temporal and parietal regions, the NAWM tissue evolution differed significantly from the white matter of controls. Confidence intervals of these coefficients approached but did not cross zero, suggesting this may be a spurious finding. With the analysis of tissue types independently from lobes, the NAWM DTI trajectory with age did not differ significantly from controls (Supplemental Figure 3).

DTI across tissue boundaries

To qualitatively evaluate whether boundaries between the tissue types were discrete, we plotted DTI measures along a trajectory of adjacent voxels in the axial plane from tuber to deep white matter. For each of the 6 random examined patients, we found a gradual transition across tissue type boundaries, rather than abrupt changes. The change from tuber tissue to peritubertissue was smooth, and so was the change from peritubertissue to NAWM (Figure 3).

Neuropathological examination of illustrative case

Histopathology and immunohistochemistry of an occipital resection specimen of a 6 year old patient with TSC revealed a tuber characterized by a loss of lamination, abundant large dysplastic neurons, mixed with balloon cells of "ambiguous phenotype" and dense gliosis (GFAP). Surrounding this were a variety of pathological features including multiple small less compact tubers composed of balloon cells in both gray and white matter and abnormal neocortex with disorganized architecture and lamination, scattered large neurons in the superficial cortex, and extensive reactive gliosis. There were scattered focal disruptions of the myelination (LFB) by small clusters of balloon cells in the adjacent white matter, and more remotely in the NAWM, referred to as microtubers[2] (Figure 4).

DISCUSSION

This study presents a novel characterization of longitudinal diffusion changes of various tissue types in TSC, and establishes a natural evolution of maturing normal appearing white matter, peritubertissue and even tuber tissue. In addition, we show a gradient of abnormality between these tissue types, with a smooth transition across boundaries, confirming tuber-like pathology is widespread and decreases with distance to the tuber itself.

As tuber pathology is not discrete, the peritubertim is arbitrarily defined, and may microscopically include parts of both the NAWM and tuber tissue types. Thus, the finding of DTI measures of intermediate value between tuber and NAWM tissue types is not surprising.

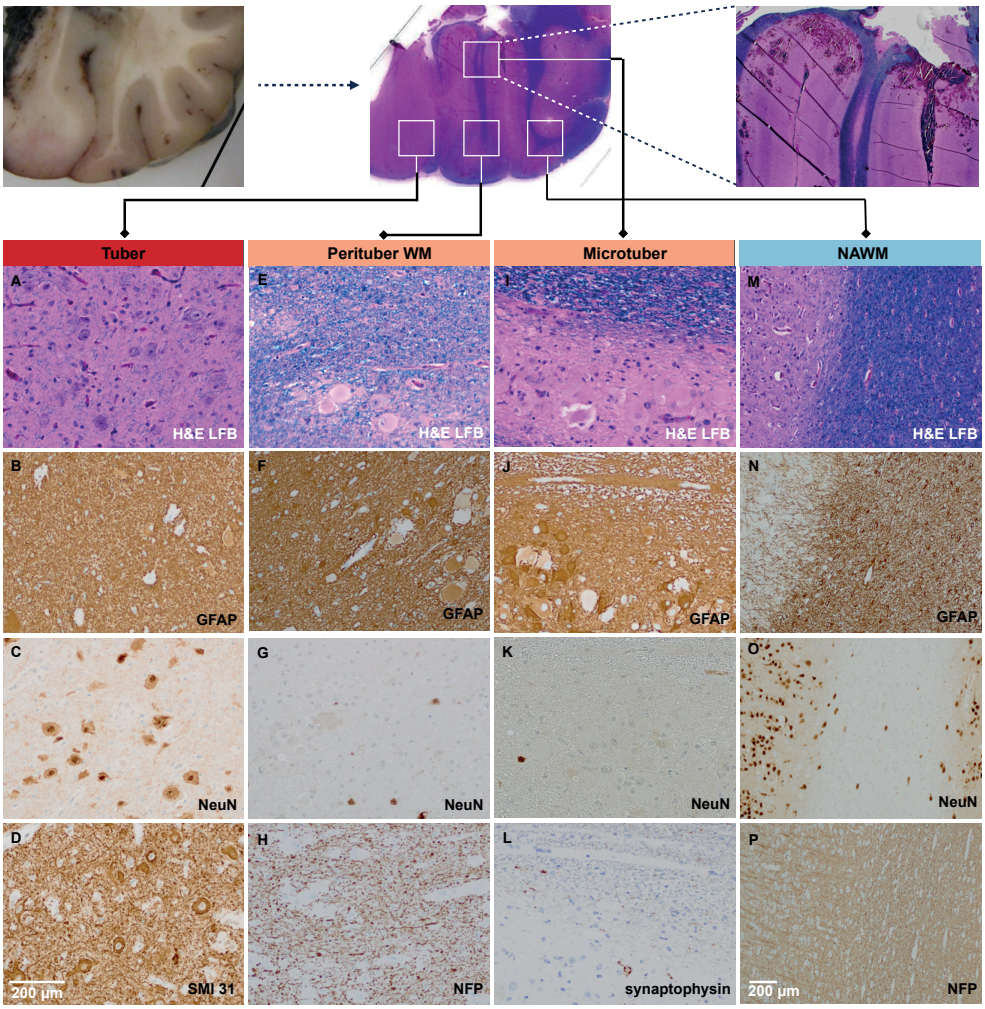

Figure 4: Histopathology and immunohistochemistry of tuber (A-D), perituber white matter (E-H), a microtuber area (I-L) and normal appearing white matter (M-P).

The gross specimen (top left), low magnification H&E/LFB (top middle) and pocket of tuber pathology (microtuber[2], top right) indicate the studied areas.

Tuber tissue (A) H&E/LFB demonstrates absence of cortical lamination, and presence of cells of "ambiguous phenotype" in tubers, variably positive for glial (B) and neuronal markers (C). SMI 31 (phosphorylated neurofilament) positivity in the perikarya is a feature of dysplastic neurons (D). In the white matter of perituber tissue (E), scattered balloon cells are also present, as well as occurring in small confluent clusters in the micro tuber (I). In more remote white matter (M), apparently normal myelination is seen. Reactive astrocytes, indicating gliosis likely related to seizure activity, are seen in tubers (B), as well as remote from the tuber, in (F) and (J), and in the NAWM (N). Scattered heterotopic neurons are seen in perituber tissue (G), in the micro tuber (K), and are easy to appreciate at lower magnification in the NAWM (O). NFP stain of perituber white matter marks some dysplastic neurons (H), as does the synaptophysin stain in the micro tuber area (L). In (P), a normal NFP stain shows white matter, with axons taking a radial turn into the cortex.

Likewise, small amounts of normal white matter were included in the tuber, and more so in perituber image segmentation, which may be responsible for the DTI changes resembling the NAWM developmental trajectory.

The smooth transition, however, between the three segmented tissue types, and the similar evolution, is consistent in every lobe, across all ages, and corrected for volumetric differences. Indeed, the perituber cortex contains similar but milder histologic, immunohistochemical and molecular abnormalities, suggesting dysplasia and aberrant mTOR signaling beyond tubers into perituber tissue[3]. Our neuropathological example illustrates that dysmorphic and heterotopic cells with a hybrid glial-neuronal differentiation and abnormal cell size are found far beyond tubers, throughout the white matter[2].

Several potential explanations exist for the differences between lobes. These differences, however, are minor and not consistent for FA and MD, and may simply reflect measurement variance. Regional differences in the timing and rate of myelination are insufficient as an explanation as myelination is largely completed by age 5[25]. Alternatively, the single tensor model falls short, as voxels containing crossing fiber pathways can be falsely low in FA as there is not a single preferential diffusion direction[26], and the model does not account for more intricate, complex, multi-fascicle pathways. Finally, if white matter is more normal as a function of distance from the tuber, smaller lobes will have more white matter in the proximity of a tuber – even if our model accounts for volume.

In both healthy subjects and in patients with TSC, DTI maturational changes of white matter, follow a biexponential time evolution, with the most dramatic DTI changes occurring in the first few years, and a slower rate in childhood and thereafter[27]. The steepest DTI maturational changes co-occur in time with the first clinical appearance of autism and epilepsy, reflecting the importance of medical and behavioral interventions during this critical period of development[28]. If indeed DTI changes are amenable to intervention with mTOR inhibitors[29], and parallel clinical outcome, then the greatest impact could be made in the first 5 years of maturational change.

In TSC epilepsy surgery, the apparently contradicting reports of intratuber[30, 31] vs. perituber[32, 33] epileptogenic activity may reflect a continuous spectrum of neuropathology. Multistage invasive monitoring approaches[34], and better outcomes with wide resection margin and even post-operative deficits[35], again suggest widespread pathology beyond the tuber. Our longitudinal imaging data confirms non-discrete borders of tuber pathology, which may in turn impact surgical planning and approach. Indeed, the various degrees of neuropathology beyond the tuber in the resection specimen (Figure 4) illustrates why a

depth electrode could potentially register activity from perituber and more remote sites with tuber-like pathology.

Images obtained through advances in high-resolution MRI suggest tubers and their ill-defined borders now represent the "tip of the iceberg" (Figure 5). Using structural imaging, both subtle increases and decreases in tuber volume have been reported[9, 10, 36]. The current view, however, suggests these volumetric differences may be attributed to inconsistent imaging acquisition schemes, operator dependence and maturational changes in contrast. Using diffusion imaging, one study sampled multiple small regions of interest in lobes without any structural white matter abnormalities, and found no difference of FA and MD between patients with TSC and controls[37]. We suggest that residual NAWM, remote from tubers or associated transmantle structural white matter abnormalities, has in fact subtle pathology below imaging resolution.

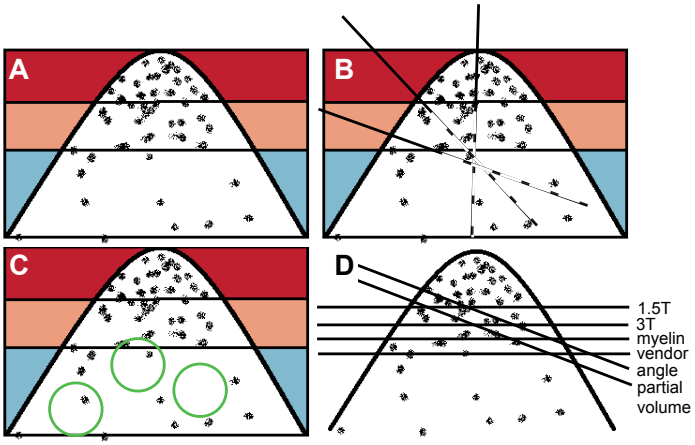

Figure 5: The changing view of TSC pathology

(A) Extent of neuropathology is indicated by the density of black dots. With a segmentation based on imaging density values, an arbitrary cut-off is established to obtain the borders of three tissue types: Tuber area in red, perituber in salmon, and remainder of NAWM in light blue. Tubers (and other macroscopic abnormalities) represent the "tip of the iceberg", and in the direct vicinity but also more remotely, areas of tuber-like pathology are found as well. With distance from the tuber, the extent of pathology diminishes. (B) Studies using depth electrodes (diagonal black lines) to elucidate whether seizures start in or next to a tuber[30-33], may be subject to measuring abnormal activity of microscopic collections of tuber-like pathology next to the tuber. (C) Reported pockets of normal white matter diffusion in patients with TSC compared to controls[37], may in fact describe regions (green circles) in which the pathological burden is below imaging resolution (D) Studies suggesting tuber volume changes over time[9] may be biased by different segmentation thresholds, as the border of tuber pathology is not discrete. From top to bottom, thresholding may be subject to subtle differences in acquisition (1.5T, 3T, MRI from different vendor), in maturation (myelin), and in partial voluming effects or angulation.

This study had a highly consistent imaging acquisition scheme, but its retrospective nature and insufficient power limited the assessment of correlations with clinical and neurobehavioral phenotype, which requires a dedicated study with prospective data collection. Patients who underwent surgery were excluded, which may bias the study towards patients with less severe seizures. In addition, controls were not age matched. Radial migration lines were not analyzed separately, and due to effects of free water and calcium on diffusion, calcified and cyst-like tubers were omitted.

Although inaccuracies in registration and segmentation may account for some of the observed DTI changes, all changes had consistently the same sign, which would not occur if extra-axial space, deep grey matter or CSF were included in the analysis. Tuber segmentation performed on an older subject, and projected onto a scan acquired at a younger age may lead to under- or over-estimation of the tuber volume if tissue contrast has improved over time. However, as outlined in the discussion, tuber boundaries are not discrete at any age and the arbitrary nature of the segmentation cutoff reflects the continuous spectrum of underlying neuropathological abnormality.

DTI and the single shell HARDI acquisition scheme are limited by the inability to solve for multiple fascicle orientations, do not account for isotropic diffusion, and are susceptible to partial voluming effects [26]. These limitations may lead to underestimation of anisotropy, and can hamper the detection of group differences. Novel acquisition schemes allow for the collection of multiple non-zero b-values while maintaining a good signal-to-noise ratio[38], which is critical to estimate a multi-fascicle model. High-resolution ex-vivo tissue imaging and correlation with histopathology will yield further insight into underlying neuropathology.

ACKNOWLEDGEMENTS

Jurriaan Peters is supported by National Institutes of Health (NIH) P20 NS080199, R01 NS079788 and U01 NS082320 grants. Anna Prohl reports no disclosures. Xavier Tomas-Fernandez reports no disclosures. Maxime Taquet is supported by WBI.World. Benoit Scherrer is supported by NIH R01 NS079788 and U01 NS082320 grants. Sanjay Prabhu Dr Prabhu is supported by the Department of Defense W81XWH-11-1-0365 and National Institute of Health U01 NS082320 grants. Hart Lidov reports no disclosures. Jolene Singh is supported by Harvard Catalyst | The Harvard Clinical and Translational Science Center (National Center for Research Resources and the National Center for Advancing Translational Sciences, NIH Award UL1 TR001102). Floor Jansen reports no disclosures. Kees Braun reports no disclosures. Mustafa Sahin is supported by NIH (U01 NS082320, P20 NS080199, P30 HD018655), Boston Children's Hospital Translational Research Program. The Developmental Synaptopathies

Consortium (U54NS092090) is a part of the NCATS Rare Diseases Clinical Research Network (RDCRN). RDCRN is an initiative of the Office of Rare Diseases Research (ORDR), NCATS, funded through collaboration between NCATS, NIMH, NINDS and NICHD. Simon Warfield is supported by NIH U01 NS082320, R01 NS079788 grants. Aymeric Stamm is supported by NIH R01 EB013248. The authors would like to thank Benjamin Ferland for his technical assistance.

REFERENCES

1. Curatolo P, Bombardieri R, Jozwiak S. Tuberous sclerosis. Lancet 2008;372:657-668.
2. Marcotte L, Aronica E, Baybis M, Crino PB. Cytoarchitectural alterations are widespread in cerebral cortex in tuberous sclerosis complex. Acta Neuropathol 2012;123:685-693.
3. Ruppe V, Dilsiz P, Reiss CS, et al. Developmental brain abnormalities in tuberous sclerosis complex: a comparative tissue analysis of cortical tubers and perituberal cortex. Epilepsia 2014;55:539-550.
4. Luat AF, Chugani HT. Molecular and diffusion tensor imaging of epileptic networks. Epilepsia 2008;49 Suppl 3:15-22.
5. Karadag D, Mentzel HJ, Gullmar D, et al. Diffusion tensor imaging in children and adolescents with tuberous sclerosis. Pediatr Radiol 2005;35:980-983.
6. Arulrajah S, Ertan G, Jordan L, et al. Magnetic resonance imaging and diffusion-weighted imaging of normal-appearing white matter in children and young adults with tuberous sclerosis complex. Neuroradiology 2009;51:781-786.
7. Makki MI, Chugani DC, Janisse J, Chugani HT. Characteristics of abnormal diffusivity in normal-appearing white matter investigated with diffusion tensor MR imaging in tuberous sclerosis complex. AJNR Am J Neuroradiol 2007;28:1662-1667.
8. Simao G, Raybaud C, Chuang S, Go C, Snead OC, Widjaja E. Diffusion tensor imaging of commissural and projection white matter in tuberous sclerosis complex and correlation with tuber load. AJNR Am J Neuroradiol 2010;31:1273-1277.
9. Hersh DS, Chun J, Weiner HL, et al. Longitudinal quantitative analysis of the tuber-to-brain proportion in patients with tuberous sclerosis. J Neurosurg Pediatr 2013;12:71-76.
10. Vaughn J, Hagiwara M, Katz J, et al. MRI characterization and longitudinal study of focal cerebellar lesions in a young tuberous sclerosis cohort. AJNR Am J Neuroradiol 2013;34:655-659.
11. Chu-Shore CJ, Major P, Montenegro M, Thiele E. Cyst-like tubers are associated with TSC2 and epilepsy in tuberous sclerosis complex. Neurology 2009;72:1165-1169.
12. Gallagher A, Grant EP, Madan N, Jarrett DY, Lyczkowski DA, Thiele EA. MRI findings reveal three different types of tubers in patients with tuberous sclerosis complex. J Neurol 2010;257:1373-1381.
13. Lewis WW, Sahin M, Scherrer B, et al. Impaired language pathways in tuberous sclerosis complex patients with autism spectrum disorders. Cereb Cortex 2013;23:1526-1532.
14. Peters JM, Sahin M, Vogel-Farley VK, et al. Loss of white matter microstructural integrity is associated with adverse neurological outcome in tuberous sclerosis complex. Acad Radiol 2012;19:17-25.
15. Northrup H, Krueger DA, International Tuberous Sclerosis Complex Consensus G. Tuberous sclerosis complex diagnostic criteria update: recommendations of the 2012 Iinternational Tuberous Sclerosis Complex Consensus Conference. Pediatr Neurol 2013;49:243-254.
16. Lord C, Risi S, Lambrecht L, et al. The autism diagnostic observation schedule-generic: a standard measure of social and communication deficits associated with the spectrum of autism. J Autism Dev Disord 2000;30:205-223.
17. Taquet M, Scherrer B, Commowick O, et al. A mathematical framework for the registration and analysis of multi-fascicle models for population studies of the brain microstructure. IEEE Trans Med Imaging 2014;33:504-517.
18. Fillard P, Pennec X, Arsigny V, Ayache N. Clinical DT-MRI estimation, smoothing, and fiber tracking with log-Euclidean metrics. IEEE Trans Med Imaging 2007;26:1472-1482.
19. Commowick O, Wiest-Daesslé N, Prima S. Block-matching strategies for rigid registration of multimodal medical images. 9th IEEE International Symposium on Biomedical Imaging (ISBI 2012). Barcelona, Spain2012: 700-703.

20. Tomas-Fernandez X, Warfield SK. A Model of Population and Subject (MOPS) Intensities with Application to Multiple Sclerosis Lesion Segmentation. IEEE Trans Med Imaging 2015.
21. Tomas-Fernandez X, Warfield SK. Population intensity outliers or a new model for brain WM abnormalities. 2012 IEEE 9th International Symposium on Biomedical Imaging (ISBI 2012). Barcelona, Spain2012: 1543-1546.
22. Tomas-Fernandez X, Prabhu S, Peters J, Sahin M, Warfield S. Automatic cortical tuber segmentation based on a combined global-local intensity mixture model. MICCAI Challenge Workshop on Segmentation Algorithms, Theory and Applications (SATA) MICCAI 2013 Nagoya, Japan2013.
23. Akhondi-Asl A, Hoyte L, Lockhart ME, Warfield SK. A logarithmic opinion pool based STAPLE algorithm for the fusion of segmentations with associated reliability weights. IEEE Trans Med Imaging 2014;33:1997-2009.
24. Wood SN. Generalized Additive Models (Chapman & Hall/CRC Texts in Statistical Science). Kindle edition: Chapman and Hall/CRC, 2011.
25. Schmithorst VJ, Wilke M, Dardzinski BJ, Holland SK. Correlation of white matter diffusivity and anisotropy with age during childhood and adolescence: a cross-sectional diffusion-tensor MR imaging study. Radiology 2002;222:212-218.
26. Peters JM, Taquet M, Prohl AK, et al. Diffusion tensor imaging and related techniques in tuberous sclerosis complex: review and future directions. Future neurology 2013;8:583-597.
27. Mukherjee P, McKinstry RC. Diffusion tensor imaging and tractography of human brain development. Neuroimaging clinics of North America 2006;16:19-43, vii.
28. Jeste SS, Wu JY, Senturk D, et al. Early developmental trajectories associated with ASD in infants with tuberous sclerosis complex. Neurology 2014;83:160-168.
29. Tillema JM, Leach JL, Krueger DA, Franz DN. Everolimus alters white matter diffusion in tuberous sclerosis complex. Neurology 2012;78:526-531.
30. Koh S, Jayakar P, Dunoyer C, et al. Epilepsy surgery in children with tuberous sclerosis complex: presurgical evaluation and outcome. Epilepsia 2000;41:1206-1213.
31. Mohamed AR, Bailey CA, Freeman JL, Maixner W, Jackson GD, Harvey AS. Intrinsic epileptogenicity of cortical tubers revealed by intracranial EEG monitoring. Neurology 2012;79:2249-2257.
32. Ma TS, Elliott RE, Ruppe V, et al. Electrocorticographic evidence of perituberal cortex epileptogenicity in tuberous sclerosis complex. J Neurosurg Pediatr 2012;10:376-382.
33. Major P, Rakowski S, Simon MV, et al. Are cortical tubers epileptogenic? Evidence from electrocorticography. Epilepsia 2009;50:147-154.
34. Madhavan D, Weiner HL, Carlson C, Devinsky O, Kuzniecky R. Local epileptogenic networks in tuberous sclerosis complex: a case review. Epilepsy Behav 2007;11:140-146.
35. Krsek P, Jahodova A, Kyncl M, et al. Predictors of seizure-free outcome after epilepsy surgery for pediatric tuberous sclerosis complex. Epilepsia 2013;54:1913-1921.
36. Daghistani R, Rutka J, Widjaja E. MRI characteristics of cerebellar tubers and their longitudinal changes in children with tuberous sclerosis complex. Childs Nerv Syst 2014.
37. van Eeghen AM, Ortiz-Teran L, Johnson J, Pulsifer MB, Thiele EA, Caruso P. The neuroanatomical phenotype of tuberous sclerosis complex: focus on radial migration lines. Neuroradiology 2013;55:1007-1014.
38. Scherrer B, Warfield SK. Parametric representation of multiple white matter fascicles from cube and sphere diffusion MRI. PLoS One 2012;7:e48232.

APPENDIX

Part A. Statistical rationale for application of the GAMM

We quantitatively determined and compared the variations of FA and MD over age in the four tissue types. The modeling strategy that we adopted is known as Generalized Additive Mixed Modeling (GAMM). We refer the reader to the Appendix part B for a quick introductory overview on GAMMs and to [1]. The different steps involved are summarized below:

1. Choice of statistical distribution and link function for generalized linear modeling

The theory of GLMs provides the opportunity to express non-linear functions (link functions) of the outcome as a linear model in the regression coefficients and extends the range of outcome distributions from the homoscedastic Gaussian distribution to the Poisson, binomial, gamma and inverse Gaussian distributions. In our case, outcome is either FA or MD. The former is a positive variable bounded in [0,1] while the latter is an unbounded positive variable. Theoretical considerations favor the use of an inverse link function for FA (see why in appendix) and a logarithmic link function turns the positive outcome MD into a variable with infinite support. Furthermore, given the positive supports of both FA and MD, candidate distributions that lie within the GLM theory reduce to the gamma and inverse Gaussian distributions. The former is characterized by a variance proportional to its squared mean while the latter has a variance proportional to the cubic mean. Supplemental Figure 3 shows that FA variance varies more linearly with the squared mean than with the cubic mean. Similar observations were made for MD. Hence, we opted for gamma-distributed outcomes.

2. Selection of relevant independent variables

Given the low number of patients (25), we could not apply the traditional backward stepwise strategy that consists in starting with a full multivariate model including all the independent variables in the dataset (and their interactions) and then sequentially discarding regressors that are less supported by the data. Instead, we conducted a series of univariate analyses to test for a possible association between the outcome variable (FA or MD) and all the independent variables. Decision of variable elimination was made based upon null hypothesis statistical testing with a type I error rate of 10%. This means that 10 times out of 100 we will retain as potential predictor a variable that in fact has very little effect on the outcome. This is slightly higher than the usual 5% because we deliberately wanted to be conservative in these univariate procedures that do not account for confounding effects. Since the outcome variables are continuous, association with a categorical variable was assessed with Wilcoxon rank sum test while association with a continuous variable was assessed with Kendall's test of association based on Kendall's tau measure of association. Despite the greater power obtained by using parametric tests, our data strongly supported

the claim that outcomes are not Gaussian-distributed, which complicates the conclusions of such tests.

3. Estimation of the non-linear variations with age

Our data suggests that FA and MD evolve non-linearly over time, which is well recognized in the literature. Previous work accounted for this non-linear dependency by replacing the regressor *age* with log(age)[2]. However, the large resulting fitting error suggests that micro-structural changes as depicted by FA or MD are far more intricate. In this paper, we are interested in modeling the variations of FA and MD over the whole relevant time domain (~0-21 year-old). Modeling maturational changes with a cubic spline is particularly well suited for this purpose[1]. The idea is to decompose the time domain into q - 1 segments of equal length during which we assume that maturational changes can be described by cubic polynomials. The q - 1 polynomials are then joint continuously up to the second derivative to form a cubic spline of order q. It is of common practice to select the order of the cubic spline a little larger than what one would expect to be well suited for describing the underlying functional relationship[1]. We hypothesize that decomposing the time domain [0-21] into 3 sub-domains ([0-7], [7-14] and [14-21]) should be sufficient to accurately describe maturational changes: data indeed seem to suggest a steep increase (resp., decrease) of FA (resp., MD) over [0-7] y.o., followed by a transition period over [7-14] y.o. and a stabilization period over [14-21] y.o. We thus set the order of the cubic spline to q = 5 to model 4 (thus 1 extra with respect to what we would expect to be sufficient) age sub-domains. We turn the problem of fitting a cubic spline into linear regressors by decomposing the cubic spline of order 5 linearly along the 5 corresponding cubic spline basis functions. The dependency of FA/MD with *age* in our regression model is thus described by 5 regressors corresponding to the 5 cubic spline basis functions evaluated in *age*.

4. Determination of the appropriate degree of smoothness

A cubic spline can over-smooth or, on the contrary, under-smooth the underlying true dependency between two continuous variables. A way to address this model selection problem consists in fitting the cubic spline that minimizes the classic least squares regression problem augmented with a penalty term that controls the degree of smoothness of the spline. In the present work, we penalized the least squares criterion with the integral of the second derivative of the cubic spline over the whole time domain and we determine its optimal degree of smoothness (determined by the penalty weight) by minimizing the generalized cross validation (GCV) score[1].

5. Relevant interaction terms

The final list of potential predictors of FA/MD included 2 continuous variables (age and tissue volume) and 2 categorical variables (tissue type and lobe). In constructing the regres-

sion model to predict FA/MD from these variables, an important question to be addressed is whether variations of FA/MD with the continuous predictors need to be modeled differently within each level of the categorical variables. For instance, FA might evolve at different rates over time in the different lobes or in the tuber compared to the NAWM. This problem can be assessed by including interaction regressors in the regression model. Which interaction terms are to be included is another model selection problem. We address this by fitting many models with all possible combinations of interaction terms and by selecting the model selection with smallest unbiased Akaike information criterion (AICu)[3].

(Note: The AICu suggested that the evolution of FA and MD over time might be lobe- and tissue type-specific but our data is insufficient to validate this hypothesis. The presented model has the lowest AICu given the data. With a large multicenter prospective dataset, we can solve dependencies better and allow for true estimation of the developmental trajectory of each tissue type).

6. Intra- and inter-subject variability

One subtlety of the modeling described in the 5 previous steps is that we are constructing a fitting curve of the evolution of FA/MD over time from different patients followed over a brief period of time. As a result, each patient only contributes to a small portion of the whole [0-21] range of age. It is thus important to account for this in the analysis by explicitly modeling intra- and inter-subject variabilities. This can be handled by including two random effects in the model: the scan ID and the patient ID. Inclusion of these random effects tags each measurement to the corresponding pair (Patient, Imaging Session) and allows us to separate the intra- and inter-subject variabilities from the variability induced by pure noise. This ultimately improves all null hypothesis statistical testing procedures based on the noise variance estimate.

7. Significance of individual regression coefficients

We tested the significance of the individual regression coefficients using the unified framework for simultaneous inference in general parametric models with generally correlated coefficients proposed in[4].

8. Comparison of FA/MD evolution over time in patients to normal evolution of WM

We compared the evolution of FA/MD over time in the different tissue types to the normal evolution in the WM of controls. Specifically, we used Dunnett's many-to-one multiple comparison procedure. We performed this comparison globally on average over all lobes and, subsequently, per lobe (Supplemental Figure 3A and 3B).

Part B. GAMM: Introduction to Generalized Additive Mixed Modeling

Through this example, we will step-wise explain why commonly applied models fall short, and extensions of the linear model are needed. We will use the feeding habits of wolves, with the assumption that their rather restrictive diet consists of captured rabbits only.

1. Linear Model

1.1 Linear model

The capture rate is our outcome variable and we want to examine the effect of rabbit density on the capture rate. We can first hypothesize that rabbit population (χ_1) density has a fixed linear effect on the capture rate (y), that is:

$$y = a_0 + a_1\chi_1 \quad (1)$$

where a_0 and a_1 are referred to as the *linear coefficients*, with a_0 being the capture rate in absence of any rabbits, and a_1 describing the magnitude (value) of the linear effect of rabbit density on capture rate. For example, if we were to actually carry out the experiment and determined that $y = 0 + 0.04\chi_1$, we could conclude that the capture rate increases with rabbit density by a factor of 0.04.

This model is a simplification of what the capture rate is in reality. As such, it is likely that there will be a discrepancy between observed and predicted capture rates for any given rabbit density. The most common way to account for that random variability is to complete the model by adding a *random error component* which, on average, amounts to zero but randomly varies around 0. To insert this into the model, the random error component needs to be characterized. In linear regression modeling, the error component is assumed to follow a Gaussian distribution (bell curve) with constant variance.

1.2 Multivariate linear regression

Now, we might want to study the effect of additional variables on the capture rate, and we will need a *multivariate linear regression model*. For example, it is likely that the wolves' hunting experience might influence the capture rate as well (though it is not our primary concern to understand the precise relationship between experience and capture rate). A simple way to account for experience is to include the wolf's age as an additional explanatory variable χ_2 and specify the model as $y = 0.3 + 1.2\chi_1 + 0.5\chi_2$. In this particular example, we can deduce that a wolf's age has a positive effect on the capture rate, meaning that the older the wolf, the more experienced it becomes and thus the more rabbits it captures. Note also that the coefficient associated with rabbit density changed, now showing a much more pronounced effect because we adjusted the model to monitor the effect of age.

1.3 Non-linearity in a linear model

One could argue that it is flawed to assume a linear effect for age. Indeed, wolf pups will learn very quickly, but the learning curve will slow down as it grows up, and eventually plateau (you can't teach an old wolf new tricks!). Thus, the effect of age might be regarded as exponential. It is possible to include non-linearity in a linear regression model through *explicit parametrization* of the explanatory variables. Indeed, if we define χ_2 as the exponential age instead of the age itself, then we still have:

$$y = a_0 + a_1\chi_1 + a_2\chi_2 \quad (2)$$

and thus the model is still linear, even though we just introduced a non-linearity.

1.4 Limits of the model

However, while wolves may get smarter with age, they are not able to run faster than when in their prime. With that in mind, it seems that the effect of wolf age on their capture rate might be more complex than an exponential variation. Likewise, the capture rate is a *bounded variable* by definition (positive, between 0 and 1) but the linear regression model implies that, as the rabbit density increases, the capture rate will at some point exceed 1 (or 100%). So what can we do to ensure a better modeling?

Also, back to the *random error component* of the model, the Gaussian distribution of this error term is the key assumption which allows statistical testing on whether explanatory variables (rabbit density, age) significantly affect the outcome variable (rabbit capture rate). In fact, the wolf capture rate being a positive variable, the use of the Gaussian distribution implies that negative observed values could occur, which is not plausible (wolves spitting out live rabbits!).

2. Generalized Linear Model

2.1 Link functions

It is possible to model some *functions of the outcome variable* rather than the outcome variable itself. It may turn out, for example, that the rabbit density explains the logarithm of the capture rate better than the capture rate itself. These functions are known as link functions, denoted by (g). While theoretically any function could be attempted to model, in practice there are only four of them that are statistically sufficiently understood to use: identity ($g(y) = y$), logarithm ($g(y) = \log(y)$), reciprocal ($g(y) = 1/y$) and squared reciprocal ($g(y) = 1/y^2$).

For instance, it seems to be more plausible to model the effect of rabbit density on wolf capture rate as:

$$y = \frac{a\chi_1}{h + \chi_1} (3)$$

This way, as the rabbit density increases, the predicted capture rate remains bounded by the maximum capture rate of alpha (which is equal to or smaller than 1).

2.2 Improved error terms

Additionally, *the random error component* that models the variability of the outcome variable is not restricted to the Gaussian distribution for subsequent statistical testing on which explanatory variables significantly impact the outcome. Now other distributions can also be used, such as the binomial and Poisson distributions for discrete outcome variables, and Gamma and inverse Gaussian distributions for continuous variables. For or example, a Gamma distribution is better than Gaussian, as it ensures that the outcome capture stays positive as it should be. Hence, our *generalized* linear model now will not predict negative capture rates or capture rates greater than 100% anymore.

2.3 Limits of the model

It is very unlikely that the capture rate (CR) will depend on the rabbit population density (PD) through a relationship as simple as the one described by equation (3). With severe under population (very low PD), the starving wolves may move out of the region or switch food source, in which case, CR should be close to zero. Similarly, with rabbit overpopulation (very high PD), wolves will be less interested as they are not as hungry and will get slower as they are overweight. However, they may spend more time reproducing as they need to spend less time hunting, and baby wolves too will need food. So it is unclear whether the WCR should increase, decrease or tend to a positive constant as the RPD increases.

In general, one could try further explicit parametrization strategies (see 1.3, but these are not recommended because they do not reflect reality well and introduce strong biases.

3. Generalized Additive Model

*3.1 Linking the link function **g** with another function ƒ*

With generalized *additive* models (GAM)[5], the idea is to admit that we have no clue about the way PD affects CR. So, we write that the appropriate link function of the CR depends upon the PD via *an unknown mechanism described by a function :*

$$g\,(CR) = f\,(PD)\ (4)$$

and the goal of finding the relationship between WCR and RPD simply comes down to estimating f This is not a trivial task because (i) it might seem we are looking for a needle in a haystack and (ii) the sample size actually limits the arbitrariness of f. In practice, GAM

theory is well understood and there is a sound statistical framework for its estimation that guarantees an appropriate optimally smoothed solution that limits overfitting.

3.2 Smoothing and overfitting

These functions can be smoothed (if plotted, they look smoother), for a better fit to the real observed data, but the smoothing process is arbitrary. That can lead to data overfitting, and bear risk that conclusions drawn from such a model are not properly supported by the data.

Cross-validation or generalization error metrics, applied to make the GAM as generalizable as possible, can be used to determine the amount of smoothness and thus minimize overfitting[6]. The only limitation to this approach is the sample size. Too small samples indeed limit the number of functions f that can be "explored" (as candidate functions) for the real relationship between CR and PD.

3.3 Limits

Generalized additive models cannot account for small but important systematic variations in the data, explained below.

4. Generalized Additive Mixed Model

4.1 Random effects, systematic variation

Other factors, not explained by the models above, might have influence and introduce a *systematic bias* if not appropriately accounted for. For example, the landscape which hunt takes place on can either augment or limit the wolf capture rate. Hills and lakes could be good hunting grounds as they allow for trapping the prey but mountains and trees provide shelter. Also, some wolves will be intrinsically faster runners; some will have more appetite than others and so on. A rabbit population with more fast-running hares is overall more difficult to catch. Cute, small, brown, fuzzy rabbits are more appetizing. A single wolf's appetite might vary every day depending on the wolves' pack success the prior day. All these are examples of *random effects*, which are likely to introduce *systematic variation*.

All these systematic variations appear at different levels. If the model does not incorporate their effect, they will solely be accounted for as *averaged effects* and will misleadingly inflate the variability of the random error component of the model (see 1.1). A high variability requires more data, and so not accounting for these random effects will ultimately underpower statistical tests of significance.

4.2 Mixed models

Mixed models are a sound way to capture these systematic variations and to make sure they will be kept separate from the error variance. The idea is to assume that the specifically studied individual wolves are *a sample of a larger population* of wolves with an overall average appetite, experience and speed. Each wolf's appetite, experience and speed can

then be seen as a slight departure from that average. For explanatory reasons, we will use appetite as an example.

We can now turn the problem of accounting for the effect of each wolf's appetite into the problem of accounting for an *averaged fixed effect* of appetite plus a *random component* of which variability describes the departure of the effect of each wolf's appetite to the average. In this case, we say that appetite (and speed, experience, others) can be viewed as *random effects*.

4.3 Hierarchy (not the one in the wolf pack), repeated measures

Similarly, the mixed model can be built in a multilevel fashion, meaning there is a hierarchical order to the data. The units analyzed (capture rate) are typically at lower level (wolf, rabbit), but the data is nested in higher-level contextual data (landscape).

In our example, we can think of the type of landscape as a random effect. The landscape can be viewed as having (a) an averaged fixed effect on the capture rate and (b) a random component with no additional effect on average. The random component though, has a variability that accounts for the difference between each landscape effect on the capture rate and the averaged fixed effect of landscape.

Repeated measures, obtained from the same wolves, can additionally be used to incorporate another intrasubject level. This again can be split up as (a) an averaged fixed effect of appetite, plus (b) a random component which variability captures the difference in appetite of that wolf *followed over several days*. This way, rather than being a limitation of the data, repeated measures can actually be used to reduce the variability of the random error component, and improve the fit of the model.

Part C. References, further reading

1. Wood SN. Generalized Additive Models (Chapman & Hall/CRC Texts in Statistical Science). Kindle edition: Chapman and Hall/CRC, 2011.
2. Peters JM, Sahin M, Vogel-Farley VK, et al. Loss of white matter microstructural integrity is associated with adverse neurological outcome in tuberous sclerosis complex. Acad Radiol 2012; 19:17-25.
3. McQuarrie A, Shumway R, Tsai C. The model selection criteria AICu. Statistics and Probability Letters 1997;34:285-292.
4. Hothorn T, Bretz F, Westfall P. Simultaneous inference in general parametric models. Biometric Journal Biometrische Zeitschrift 2008;50:346-363.
5. Hastie T, Tibshirani R. Generalized additive models for medical research. Stat Methods Med Res 1995;4:187-196
6. Wood SN, Augustin NH. GAMs with integrated model selection using penalized regression splines and applications to environmental modelling. Ecological Modelling 2002; 157:157-177.

SUPPLEMENTARY FIGURES

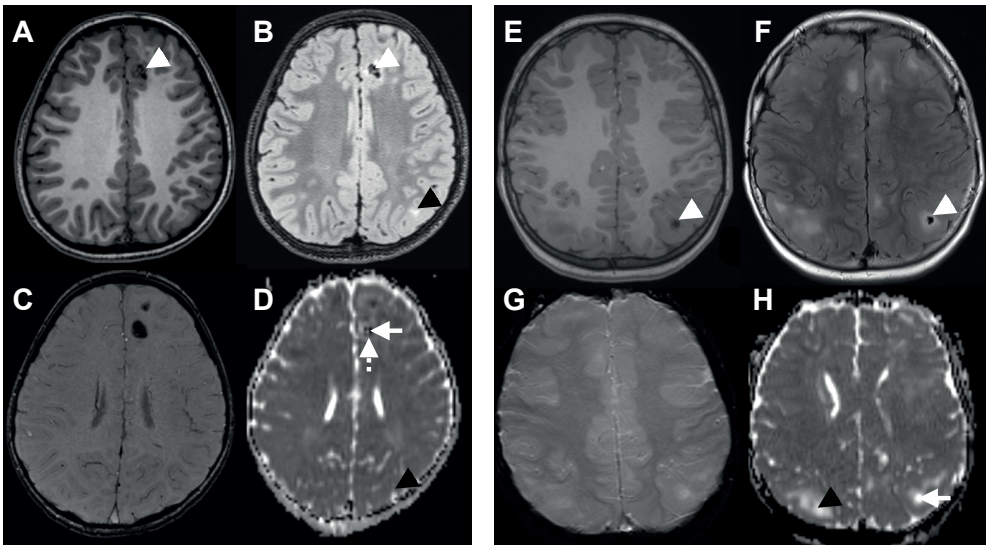

Supplementary Figure e-1: Challenges in diffusion imaging and cyst-like tubers

(A-D) Calcified tuber
(A) Axial T1-weighted image reveals a hypointense area in a mesial frontal calcified tuber (white arrowhead), which is also dark on T2-weighted FLAIR imaging (B). The calcium deposits induce a phase inconsistency, appreciated on susceptibility weighted imaging (SWI)(C). This phase difference will correspond to a signal loss in the DWI image (D). In addition, there is a "blossoming effect", which means the area of diffusion signal loss is greater than the voxels containing calcium, noted on the T1- and T2-weighted images. The blossoming effect is evident in the SWI image(C), where a large hypo intensity can be appreciated. In (D), FA values of calcified tuber 0.00 (white arrow), directly adjacent 0.08 (white dotted arrow), remote noncalcified tuber 0.20 (black arrowhead).

(E-H) Cyst-like tuber
(E) Axial T1-weighted image reveals a hypointense area in a left parietal tuber (white arrowhead), which is also dark on T2-weighted FLAIR imaging (F). The water in the cyst demonstrates no fase inconsistency on SWI (G), and has isotropic, unhindered diffusion on DWI (H). In (H), FA values of cyst-like tuber 0.06 (white arrow), remote non-cyst-like tuber 0.22 (black arrowhead).

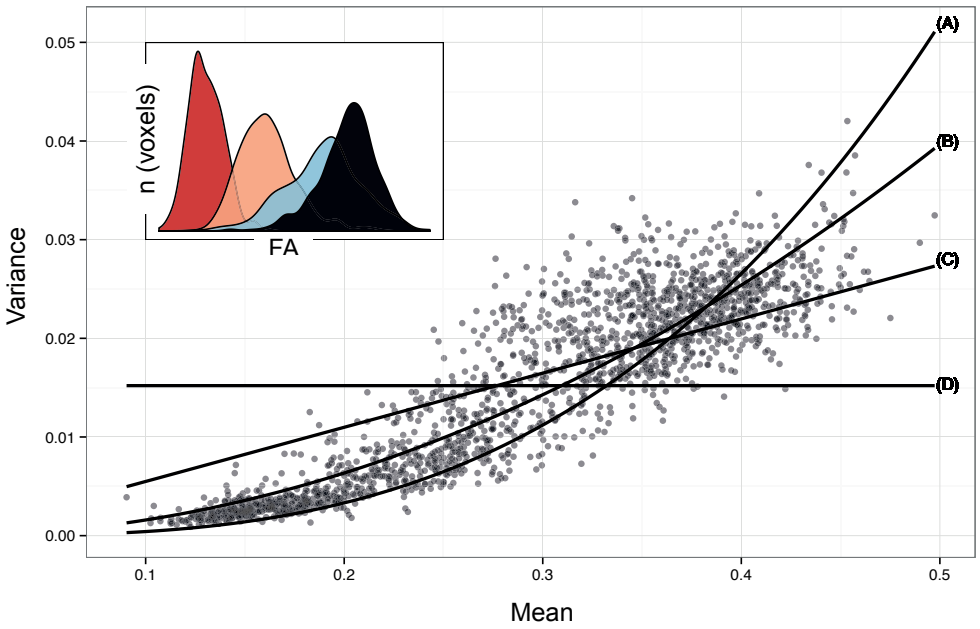

Supplementary Figure e-2: Distribution of mean and variance of FA values

The choice of the outcome distribution for our model is dependent on the relation between mean, and variance. The fits of 4 distributions are displayed for illustration. The FA variance varies more linearly with the squared mean (B) than with the cubic mean (A), thus a gamma-distribution was used. (C) illustrates a linear relation between mean and variance, (D) illustrates a variance that does not depend on the mean at all. In the top left, an illustration of an average distribution histogram is inserted, demonstrating the non-Gaussian of tuber (red), perituber (salmon), normal appearing white matter (light blue), and control white matter (black) tissue types.

Note that in this particular example case, in this lobe, there is incomplete overlap between normal appearing white matter and the white matter of a control subject, suggesting a lower mean FA of the NAWM in this example.

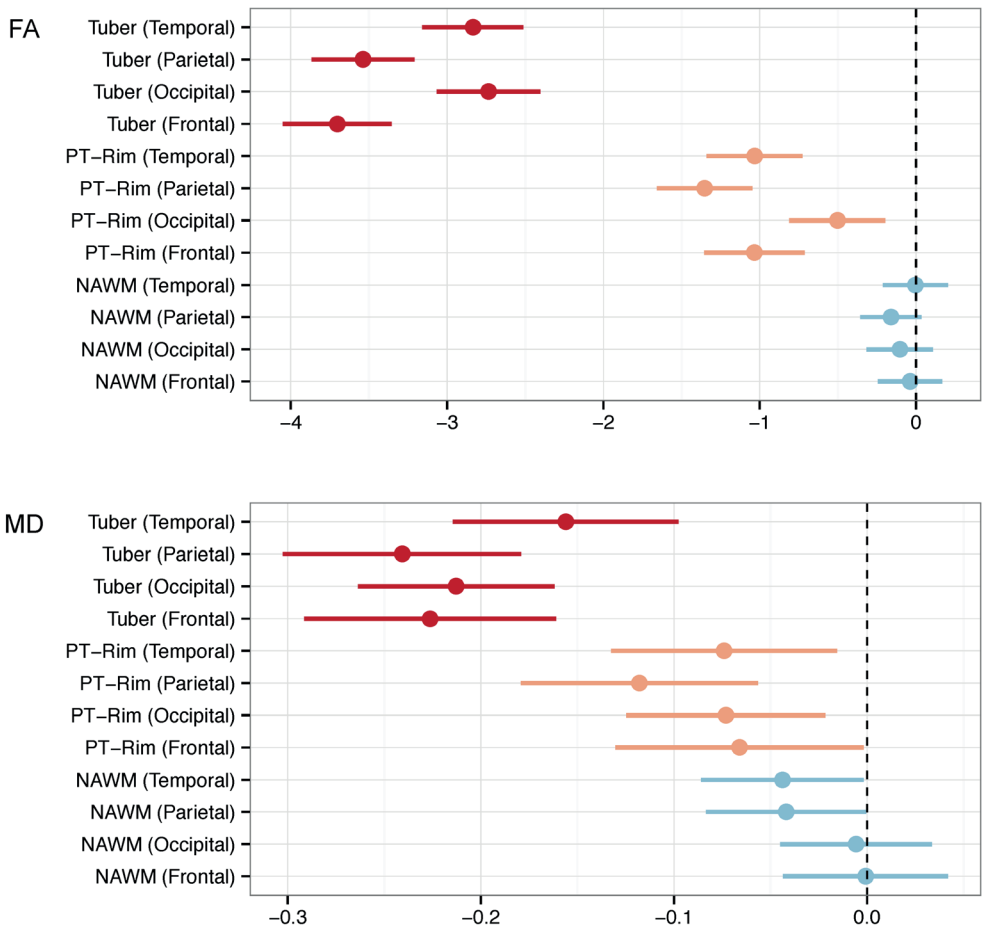

Supplementary Figure e-3: Comparison of tissue type evolution to control white matter, per lobe
For fractional anisotopy (A) and mean diffusivity (B), tuber (red), perituber (salmon), and normal appearing white matter (light blue) tissue types are compared to the white matter of controls, per lobe, using Dunnett's multiple-to-one multiple comparison procedure. The x-axis displays coefficients, and the confidence intervals crossing zero indicate no significant difference.

Supplemental table 1. Comparison of tissue type evolution to control white matter, independent of lobe

	FA	CI (lower, upper)	MD	CI (lower, upper)
NAWM	−0.309	(−0.851, 0.233)	−0.092	(−0.198, 0.014)
Perituber	−3.924	(−4.666, −3.182)	−0.331	(−0.468, −0.195)
Tuber	−12.810	(−13.579, −12.042)	−0.836	(−0.973, −0.699)

Coefficients from Dunnett's many-to-one multiple comparison procedure. CI = confidence interval; FA = Fractional Anisotropy; NAWM = Normal Appearing White Matter; MD = Mean Diffusivity.

Chapter 7

Clinical Electroencephalographic Biomarker for Impending Epilepsy in Asymptomatic Tuberous Sclerosis Complex Infants

Joyce Y. Wu[1], Jurriaan M. Peters[2], Monisha Goyal[3], Darcy Krueger[4], Mustafa Sahin[2], Hope Northrup[5], Kit Sing Au[5], Gary Cutter PhD[3], E. Martina Bebin[3].

1. Division of Pediatric Neurology, Mattel Children's Hospital at UCLA, Los Angeles, CA
2. Department of Neurology, Boston Children's Hospital, Boston, MA
3. Department of Neurology, University of Alabama Birmingham, Birmingham, AL
4. Division of Neurology, Department of Pediatrics, Cincinnati Children's Hospital Medical Center, Cincinnati, OH
5. Division of Medical Genetics, Department of Pediatrics, University of Texas Medical School at Houston, Houston, TX

ABSTRACT

Background: We assessed the clinical utility of routine electroencephalography (EEG) in the prediction of epilepsy onset in asymptomatic infants with tuberous sclerosis complex.

Methods: This multicenter prospective observational study recruited infants younger than 7 months, seizure-free and on no antiepileptic drugs at enrollment, who all underwent serial physical examinations and video EEGs throughout the study. Parental education on seizure recognition was completed at the time of initial enrollment. Once seizure onset occurred, standard of care was applied, and subjects were followed up until 24 months.

Results: Forty patients were enrolled, 28 older than 12 months with completed EEG evaluation at the time of this interim analysis. Of those, 19 (67.8%) developed seizures. Epileptic spasms occurred in 10 (52.6%), focal seizures in five (26.3%), generalized tonic-clonic seizure in one (5.3%), and a combination of epileptic spasms and focal seizures in three (15.7%). Fourteen infants (73.6%) had the first emergence of epileptiform abnormalities on EEG at an average age 4.2 months, preceding seizure onset by a median of 1.9 months. Hypsarrhythmia or modified hypsarrhythmia was not found in any infant before onset of epileptic spasms. All children with epileptiform discharges subsequently developed epilepsy (100% positive predictive value), and the negative predictive value for not developing epilepsy after a normal EEG was 64%.

Conclusions: Serial routine EEGs in infants with tuberous sclerosis complex is a feasible strategy to identify individuals at high risk for epilepsy. The most frequent clinical presentation was epileptic spasms followed by focal seizures, and then a combination of both seizure types.

INTRODUCTION

Tuberous sclerosis complex (TSC) is an autosomal dominant disease that affects approximately one in 6000 people, represents one of the most common genetic causes of epilepsy[1-3], and is caused by TSC1 or TSC2 mutation. The neurological manifestations in TSC are common and in children represent the most disabling problems of the disease, including epilepsy, intellectual disabilities, psychiatric problems, and autism. Epilepsy is particularly prevalent, affecting about 80% of individuals with TSC[4-6] with over 60% having seizures that are severe and refractory[4,7,8]. Almost half of infants with TSC develop epileptic spasms, which is associated with poor neurological prognosis[4].

Increasingly TSC is diagnosed at a young age before the onset of epilepsy from non-neurological findings, such as cardiac rhabdomyomas[9]. The earlier diagnosis of TSC provides a unique opportunity to identify and validate a biomarker for epilepsy. A predictive biomarker would allow earlier intervention that may alter or curtail epileptogenesis and its adverse effects. A recent open-label study suggests that treating patients with TSC with an abnormal electroencephalography (EEG) before onset of epileptic spasms with vigabatrin may improve neurological outcome[10]. An earlier retrospective study reported similar benefit with early treatment[11]. Nonetheless, the use of clinical EEG as a reliable biomarker of epilepsy has not been rigorously validated and has been limited to retrospective analyses subject to referral, recording, and recall biases[4,12]. Our prospective study provides a unique opportunity to document the evolution of epileptogenesis, development of clinical seizures, and the utility of EEG as an early biomarker for epilepsy in TSC.

METHODS

Subject recruitment

Infants with TSC in this multicenter prospective observation study were enrolled from the neonatal nursery, pediatric cardiology, general pediatrics, genetics, pediatric neurology, and obstetrics/perinatology/ maternal-fetal medicine clinics. TSC diagnosis was based on clinical features (i.e., cardiac rhabdomyomas, intracranial tubers or subependymal nodules or giant cell astrocytomas, characteristic skin findings, and/or other evidence on prenatal or perinatal cardiac echocardiography, neuroimaging, and skin examinations) or genetic diagnosis[13].

Each infant with TSC enrolled met all the following inclusion criteria: (1) age <7 months, (2) seizure-free at enrollment, and (3) the genetic or clinical diagnosis for TSC[13]. Infants were excluded if any one of the following criteria was present: (1) age 27 months, (2) history of

seizures of any type, or (3) current or past treatment with vigabatrin or inhibitors of the mammalian target of rapamycin, before study enrollment. Prematurely born infants with TSC as young as 32 weeks' gestation could participate only if there were no medical complications from prematurity, involving the brain or other major organs, such as hypoxic-ischemic encephalopathy, any intracranial hemorrhage, necrotizing enterocolitis, any respiratory diagnoses requiring ventilator support, or cardiovascular compromise. The earliest time of enrollment for these premature infants was when they reached term (37 weeks' gestation).

Infants with TSC were recruited from the TSC centers at each of the five sites (University of Alabama at Birmingham, University of California at Los Angeles, Boston Children's Hospital, Cincinnati Children's Hospital Medical Center, and University of Texas Medical School at Houston).

Study design

This study was approved by the institutional review boards of all five institutions. Parental consent was obtained for all subjects. At designated time points following enrollment (1.5, 3, 4.5, 6, 9, 12, 18, and 24 months chronological age), physical and neurological examination and a 1-hour research video EEG (to include both sleep and wakefulness) were performed. The 1 hour duration of the video EEG was chosen to maximize capturing both wakefulness and sleep during the same study, yet sufficiently brief to use in and extend to the clinical setting, as well as taking into consideration families' time commitment and staying within funding constraints.

Subjects referred for initial screening and enrollment were seen within 2 weeks. Initial evaluation included physical and neurological examination and baseline video EEG (1 hour wakefulness and sleep). As part of our research protocol, a seizure recognition educational video was shown to the parents or caregivers at the time of enrollment. Enrolled subjects were followed up until age 2 years.

If the infant or child at any point in the study developed seizures, history and additional clinical video EEG(s) of varying duration were completed to confirm epilepsy onset, and antiepileptic drug (AED) treatment was initiated at the managing neurologist's discretion as dictated by individual clinical scenarios, but this clinical information was recorded, as were all medical therapies throughout the duration of the study. The research video EEGs continued at the designated time points stated above, even after clinical seizure onset.

In addition to the scheduled serial research 1-hour video-EEG studies to monitor for the development and evolution of EEG abnormalities, the parent or caregiver maintained a seizure

log throughout the study. Once a diagnosis of seizures was made, the subject continued in the study to monitor developmental progress, seizure control, and response to AEDs.

Video-EEG acquisition and interpretation

Video EEGs were uniformly acquired across all five TSC centers, with standard 23 electrodes placed according to the 10-20 international placement system. All video-EEG studies were recorded for 1 hour, incorporating both sleep and wakefulness, at a high sampling rate of 2000 Hz, with a high-frequency and low-pass filter of 500 Hz. All video EEGs from all five sites were anonymized, then uploaded to a secure central server and located and maintained at the University of California at Los Angeles. To view the video EEGs from all five sites, which collectively used three different video-EEG vendors, video-EEG analysis was viewed digitally with Persyst software (San Diego, CA), in the standard timescale of 30 mm/sec and standard filter settings of 1-Hz low-frequency filter (high pass) and 70 Hz high frequency (low pass), along with a 60-Hz notched filter.

To render a more balanced interpretation, each video-EEG study was reviewed by two independent central EEG reviewers (JMP, MG), who are both board-certified pediatric electroencephalographers and blinded to all clinical information except the age of the subject necessary for the EEG interpretation. Differences in the EEG interpretation, when present, were adjudicated by a third, blinded board-certified pediatric electroencephalographer (JYW).

The EEG results were classified based on age-appropriate norms, as either normal or abnormal. EEG abnormalities were evaluated in terms of the presence or absence of background abnormalities, such as generalized or focal slowing, epileptiform discharges (focal, regional, bilateral, or generalized spike or spike and wave discharges), (modified) hypsarrhythmia, voltage attenuation, as well as clinical and/or electrographic seizures, in accordance with the National Institutes of Neurologic Disorders and Stroke Common Data Element Tools for Epilepsy.

Statistical analysis

The study design made the following assumptions for statistical sample size. In a population of patients with TSC the study assumed the incidence of epilepsy to be 85% and that the overall frequency of epileptiform discharges is 50%. Based on the statistical analysis of the preliminary data from the University of Alabama Birmingham and the University of California Los Angeles, enrolling 30 patients results in >80% power at a nondirectional alpha of 0.05 assuming that the ratio of patients with normal EEG versus EEG with epileptiform discharges will vary from 0.2 to 0.5. The association between epileptiform discharges and epilepsy was analyzed by multiple methods, performed by a statistician at the University of Alabama Birmingham (GC): (1) time-to-event survival analysis to determine the temporal relationship between epileptiform discharges and seizure onset, (2) multivariable Cox pro-

portional hazard analysis, to assess the contribution of multiple variables to development of epilepsy, and (3) logistical regression analysis to determine the strength of association between epileptiform discharges and epilepsy at the end of the 24-month follow-up period.

RESULTS

Cohort and clinical characteristics

A total of 40 subjects were prospectively enrolled into the study (Table 1). At the time of 2/1/15 data cut-off for this interim analysis, 28 infants were older than 1 year and were included in the current analysis (Figure 1). Three additional subjects older than 12 months were excluded since most recent EEG analysis by the blinded reviewers was not completed at the time of cut-off. Of the remaining subjects, three had either electrographic seizures or epileptiform discharges on EEG and were excluded because they were treated with AEDs before the onset of clinical seizures. These subjects could not be included in the statistical calculation for positive and negative predictive values because they had received a therapeutic intervention. The remaining six subjects were excluded from this interim analysis because they were still younger than 12 months and therefore needed longer follow-up time.

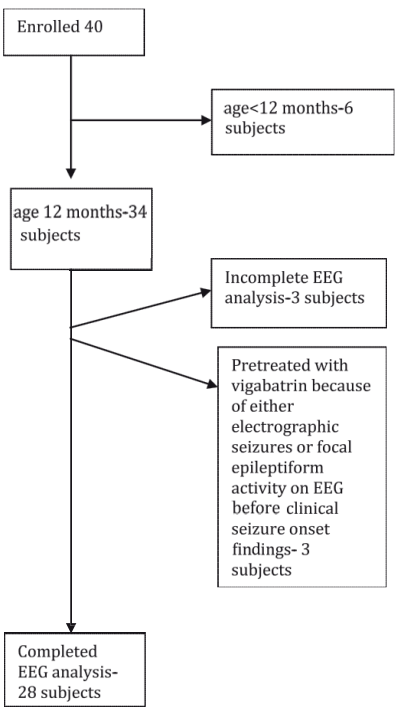

Figure 1: Cohort of study participants with tuberous sclerosis complex. EEG, electroencephalography.

Gender was distributed evenly among the 28 infants included for the interim analysis, and the average age at time of enrollment was 2.7 ± 2.0 months. Of the 28 subjects enrolled, 26 underwent TSC genetic testing, 20 (76.9%) had a pathologic mutation in TSC2. Mutations in TSC1 were identified in five (19.2%). In 1 (3.8%), no mutation in either TSC1 or TSC2 was found.

Table 1. Summary of infants with TSC over age 12 months

Subject	Race	Gender	TSC1/2	Age enrolled (months)	Age EEG abnormal (months)	EEG abnormality	Age clinical seizure onset (months)	Clinical seizure type(s)	Age at data cut-off (months)
1	C	M	Normal	5.4					16
2	C	M	Not tested	3.8					15
3	C	F	Not tested	2.1					22
4	C	F	TSC2	1.4					18
5	C	F	TSC1	7.2					20
6	C	M	TSC2	2.1					25
7	C	M	TSC2	1.5					24
8	C	F	TSC1	7					27
9	C	M	TSC1	4.4					26
10	C	F	TSC2	2.3			6	ES	13
11	C	F	TSC1	2.6			5.5	GTC	15
12	C	F	TSC2	1.5			2	Focal	14
13	AA	F	TSC2	0.4			11	Focal	14
14	C	F	TSC2	1.6			3.5	ES	20
15	C	M	TSC2	0.7	4.2	Focal spikes	6	Focal & ES	15
16	C	F	TSC1	3.3	3.4	Regional spikes	4	ES	12
17	C	F	TSC2	6.5	6.5	Regional spikes	8	ES	17
18	C	M	TSC2	6	9	Regional spikes	12.5	ES	16
19	C	M	TSC2	1.1	4	Regional spikes	7	ES	17
20	C	F	TSC2	4	4	Bilateral spikes	5.5	ES	15
21	C	M	TSC2	3.9	4	Regional spikes	5	ES	18
22	C	M	TSC2	1.1	6	Bilateral spikes	6.2	ES	22
23	A	M	TSC2	1.4	1.5	Focal spikes	3.5	Focal	21
24	C	F	TSC2	2.5	4	Bilateral spikes	6	Focal & ES	20
25	AI	M	TSC2	1.5	1.6	Bilateral spikes	3.5	Focal	20
26	H	F	TSC2	6	6	Focal spikes	20	Focal	29
27	C	M	TSC2	4.2	4.2	Bilateral spikes	6	ES	28
28	C	M	TSC2	1.1	1.2	Bilateral spikes	6	ES & Focal	25

AA, African American; AI American Indian; C Caucasian, EEG electroencephalogram; ES epileptic spasms; F Female; GTC Generalized tonic clonic seizure; H Hispanic; M Male; TSC Tuberous Sclerosis Complex

In this cohort of 28 infants older than 12 months, 19 (67.9%) developed clinical seizures during the observation period. The average age at time of seizure onset was 6.7 ± 4.1 months, the youngest within age 2.0 months and the oldest at age 20 months. Epileptic spasms were the most common seizure type and occurred in 10 infants (52.6%). Focal seizures occurred either as the sole seizure type (five subjects, 26.3%) or with epileptic spasms (three subjects, 15.8%). In contrast, seizures with generalized onset were rare, with generalized tonic-clonic seizures occurring only in one (5.3%) subject, and no other clinical seizure types were reported (Table 2).

Of these EEG interictal and ictal findings, the presence of epileptiform discharges preceded the onset of first clinical seizure in 14 of 19 infants (73.7%), which occurred between ages 1.2 and 9.0 months (Table 2). The interval between the first EEG with epileptiform discharges and the first clinical seizure was an average of 2.8 ± 3.4 months, median of 1.9 months (interquartile range 1.5, 3.0 months). No epileptiform discharges were detected with any of the video EEGs in five subjects (26.3%) before the onset of clinical seizures. Seizure type in this latter group included focal seizures, epileptic spasms, and generalized tonic-clonic seizure (Figure 2).

Table 2. Clinical seizure semiology and EEG characteristics

Seizure characteristics in 19 subjects who have had a clinical seizure since enrollment, by group:

Seizure Type	Epileptiform discharges (n=14)	Normal EEG (n=5)
Focal seizures	3	2
Epileptic spasms	8	2
Focal seizures & epileptic spasms	3	0
Generalized seizures	0	1

EEG characteristics in 19 subjects who have had a clinical seizure since enrollment:

- Fourteen of 19 (73.6%) had epileptiform activity detected on EEG before the onset of clinical seizures

	Average (months)	Median (months)
Age at time of first epileptiform discharges	4.2 (S.D. = 2.1)	4.0
Age at time of first clinical seizure	6.7 (S.D. = 4.1)	6.0
Time interval between epileptiform discharges and seizure	2.8 (S.D.= 3.4)	1.9

- Five of 19 (26.3%) had no epileptiform activity detected on EEG before the onset of clinical seizures

Subject ID	Last normal EEG (months)	Clinical seizure onset (months)
10	4	6
11	4	5.5
12	1.5	2
13	9	11
14	1.5	3.5

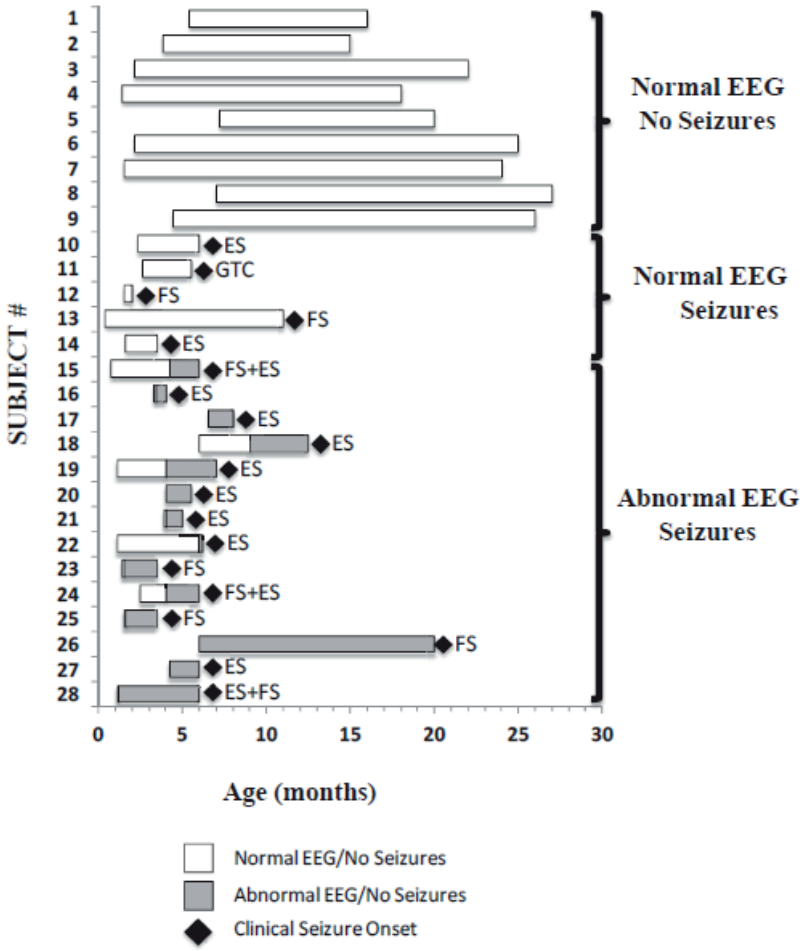

Figure 2: Summary of electroencephalography (EEG) in relation to clinical seizure onset. ES, epileptic spasms; FS, focal seizures.

The remaining nine infants of the cohort of 28 have remained seizure-free, on no AED, at the time of this interval analysis, and all nine infants have had normal video EEGs, without the presence of epileptiform discharges on any of the video EEGs (Table 3).

The positive predictive value (PPV), or how often the presence of a biomarker can correctly predict the disease in a population, can be determined from the ratio of true positives (those subjects with both abnormal EEG and subsequent seizures) to the sum of true positives and false positives (those with abnormal EEG and no subsequent seizures). The corresponding PPV (Table 3) for the presence of epileptiform activity on an EEG preceding the development of clinical seizure onset in infants with TSC is then 14/(14 + 0), or 100% CI (76.8%, 100.0%).

Similarly, the negative predictive value (NPV), or how often the absence of a biomarker can correctly predict the nondisease state in a population, is determined from the ratio of true negatives (subjects with both normal EEG and no seizures) to the sum of true negatives and false negatives (subjects with normal EEG but subsequently developing seizures). The corresponding NPV (Table 3) of the absence of epileptiform activity on the EEG and no subsequent epilepsy in infants with TSC is then 9/(9 + 5), or 64.3% CI (35.1%, 87.2%).

The other EEG findings of focal or generalized slowing, attenuation, hypsarrhythmia or modified hypsarrhythmia, and ictal events did not consistently precede the onset of clinical seizures, and none reached statistical significance.

Table 3. Statistical analysis summary

		Clinical seizure	**No clinical seizure**
Epileptiform discharges		14	0
Normal EEG / no epileptiform discharges		5	9
Sensitivity (%)	**Specificity (%)**	**Positive predictive value (%)**	**Negative predictive value (%)**
73.7	100	100	64

DISCUSSION

This prospective multicenter observational study provides unique insight into the development of epilepsy in TSC and the clinical utility of serial EEGs in the identification of patients at high risk for impending seizure onset. This preliminary report is driven by compelling strength of interim analysis and provides early supportive data for risk stratification in planned prospective research on effects of pre-emptive antiepileptic treatment in TSC.

The risk for epilepsy in TSC has been previously estimated to be 80%, based on retrospective studies in patients of all ages, including older children and adults[4,14,15]. Determining prevalence in infants is more difficult as not all the studies separated their analyses into younger cohorts. Jozwiak et al.[14] reported seizures present by age 2 years in 83%, whereas Chu-Shore et al.[4] reported 63% by age 1 year and 82% by age 3 years. Using an observational study design in which infants were enrolled before seizure onset, and followed up prospectively, we calculated in this study the incidence of infants with TSC developing clinical seizures before age 2 years as 67.8 %. Although our approach overcomes recall and reporting bias inherent to retrospective studies, the estimate in this prospective study may yet underestimate the true incidence, as not all subjects have been observed past age 24 months. Continuing to follow our present cohort prospectively will allow more definitive calculation of annual and cumulative incidence of epilepsy for infants with TSC, by age, throughout infancy and childhood.

Only one prior published study has evaluated EEG findings in infants with TSC before the onset of seizures, consisting of five subjects[16]. Patients were enrolled from age 9 days to 9 weeks and had serial EEGs at 4-week intervals. EEG abnormalities were detected in four subjects between ages 0.5 and 5.0 months, all of whom (100%) subsequently developed seizures within 1-8 days of the first abnormal EEG. The remaining subject with a normal EEG never developed clinical seizures. In this study, we found a similar high correlation between epileptiform discharges and subsequent seizures, with the average age when epileptiform discharges were first detected as 4.2 months. However, sensitivity was notably lower (73.7%) and with a much longer time interval between epileptiform discharges and clinical seizure onset that averaged 2.8 months and median of 1.9 months. Our study involved multiple centers, a larger cohort than previous studies, and multiple blinded EEG readers, adding additional patient diversity, power, and scientific rigor to the calculated lower limit of sensitivity. An unresolved variable that could contribute to the differences observed is the frequency of surveillance EEGs in the asymptomatic cohort. The every 6 weeks EEG at earlier time points in our study was chosen to balance study sensitivity with clinical feasibility for participating families. This longer time interval between scheduled EEGs, especially at later time points when expanded to 3-6 month intervals, may also explain the relatively high false-negative rate observed (and corresponding calculated NPV) in our study. The longer interval between scheduled EEGs increases the likelihood that newly emerging epileptiform abnormalities before the onset of clinical seizures may have gone undetected in the interim. However, the calculated time between epileptiform activity and seizures was an average 2.8 months, median 1.9 months. We suspect that with more frequent sampling, the interval time, here measured only in monthly increments, would likely be shorter with the possibility of showing higher sensitivity and lower NPV. A sizeable window between epileptiform discharges and clinical seizure onset is key, as such a window provides a unique and feasible opportunity to design and implement antiepileptogenic treatment strategies that may delay or prevent clinical seizure onset.

In our study infants with TSC are as likely to present with focal seizures, epileptic spasms, or focal seizures mixed with epileptic spasms (either concurrently or subsequently to onset of focal seizures). Furthermore, similar to results of the Domanska-Pakiela et al. study[16], classic or modified hypsarrhythmia was not found in any infant before the onset of focal seizures or epileptic spasms. This would suggest that classic or modified hypsarrhythmia, reported to occur in up to 71% of patients with TSC and clinical epileptic spasms[17], occurs after seizure onset and corresponds to later events in the epileptogenesis process. These observations on the evolution of epilepsy onset in infants with TSC have an important impact on clinical management, as treatment delay may adversely affect long-term epilepsy and developmental outcome[11,17]. First, parents and clinicians should know that either focal-onset seizures or epileptic spasms may be an initial seizure manifestation in infants with TSC. Second, because hypsarrhythmia

may follow epileptic spasms, clinicians should not wait for hypsarrhythmia, either in the classic or modified form, to appear on EEG before initiating appropriate treatment for epileptic spasms. Finally, the earliest signs of seizures, whether focal seizures, epileptic spasms, or a mix thereof, may be very subtle and could go unrecognized or misdiagnosed without a high index of clinical suspicion on the part of parents and clinicians. We found it very useful to show videos of multiple clinical seizure types, both classic and subtle forms, to parents to increase their likelihood of recognizing and reporting to clinicians the earliest clinical events of concern. We also encouraged parents and caregivers to send video files obtained with mobile phones for clinician review and confirmation.

Although an EEG is currently recommended at the time of initial TSC diagnosis[11,13,18] the results of this study not only support the importance of that initial EEG but also the importance of subsequent EEGs in monitoring the development of seizures and epileptiform discharges. This recommendation is consistent with the European recommendation, which suggested close EEG monitoring in the first few months of life and consideration of preventative treatment in the presence of EEG ictal discharges[19].

In conclusion, this study is the first multicenter prospective study to evaluate serial EEGs as a biomarker for subsequent epilepsy in the infant population with TSC. Our study demonstrates the feasibility and importance of close EEG surveillance in infants with TSC, with high PPV of epileptiform discharges for predicting those who subsequently develop epilepsy. This interim analysis highlights the value of early diagnosis of infants with TSC and the value of serial EEG beginning at the time of diagnosis. Importantly, our study suggests there is a critical window of time between emergence of epileptiform discharges and clinical seizure onset, which provides a unique opportunity to investigate potentially disease-modifying antiepileptogenic treatment strategies in this population.

ACKNOWLEDGEMENTS

Supported by the National Institute of Neurological Diseases and Stroke of the National Institutes of Health (U01-NS082320, P20-NS080199) and the Tuberous Sclerosis Alliance. JYW also supported by the NIH (R01-NS082649), the Department of Defense (W81X-WH-11-1-0365) Congressionally Directed Medical Research Program, and the Today's and Tomorrow's Children Fund from Mattel Children's Hospital at the University of California, Los Angeles. MS was supported by the Senior Investigator award from Boston Children's Translational Research Program. This study also utilized clinical research facilities and resources supported by the National Center for Advancing Translational Sciences (NCATS) of the National Institutes of Health Grant (8UL1TR000077 and UL1RR033176).

REFERENCES

1. Sparagana SP, Roach ES. Tuberous sclerosis complex. Curr Opin Neurol. 2000;13:115-119.
2. Kwiatkowski DJ. Rhebbing up mTOR: new insights on TSC1 and TSC2, and the pathogenesis of tuberous sclerosis. Cancer Biol Ther. 2003;2:471-476.
3. Crino PB, Nathanson KL, Henske EP. The tuberous sclerosis complex. N Engl J Med. 2006;355:1345-1356.
4. Chu-Shore CJ, Major P, Camposano S, Muzykewicz D, Thiele EA. The natural history of epilepsy in tuberous sclerosis complex. Epilepsia. 2010;51:1236-1241.
5. Webb DW, Fryer AE, Osborne JP. On the incidence of fits and mental retardation in tuberous sclerosis. J Med Genet. 1991;28:395-397.
6. Sparagana SP, Delgado MR, Batchelor LL, Roach ES. Seizure remission and antiepileptic drug discontinuation in children with tuberous sclerosis complex. Arch Neurol. 2003;60:1286-1289.
7. Curatolo P. Mechanistic target of rapamycin (mTOR) in tuberous sclerosis complex-associated epilepsy. Pediatr Neurol. 2015;52:281-289.
8. Aboian MS, Wong-Kisiel LC, Rank M, Wetjen NM, Wirrell EC, Witte RJ. SISCOM in children with tuberous sclerosis complexrelated epilepsy. Pediatr Neurol. 2011;45:83-88.
9. Datta AN, Hahn CD, Sahin M. Clinical presentation and diagnosis of tuberous sclerosis complex in infancy. J Child Neurol. 2008;23:268-273.
10. Jozwiak S, Kotulska K, Domanska-Pakiela D, et al. Antiepileptic treatment before the onset of seizures reduces epilepsy severity and risk of mental retardation in infants with tuberous sclerosis complex. Eur J Paediatr Neurol. 2011;15:424-431.
11. Bombardieri R, Pinci M, Moavero R, Cerminara C, Curatolo P. Early control of seizures improves long-term outcome in children with tuberous sclerosis complex. Eur J Paediatr Neurol. 2010;14:146-149.
12. Jozwiak S, Goodman M, Lamm SH. Poor mental development in patients with tuberous sclerosis complex: clinical risk factors. Arch Neurol. 1998;55:379-384.
13. Northrup H, Krueger D, International Tuberous Sclerosis Complex Consensus Group. Tuberous sclerosis complex diagnostic criteria update: recommendations of the 2012 International Tuberous Sclerosis Complex Consensus Conference. Pediatr Neurol. 2013;49:243-254.
14. Jozwiak S, Schwartz RA, Janniger CK, Bielicka-Cymerman J. Usefulness of diagnostic criteria of tuberous sclerosis complex in pediatric patients. J Child Neurol. 2000;15:652-659.
15. Devlin LA, Shepherd CH, Crawford H, Morrison PJ. Tuberous sclerosis complex: clinical features, diagnosis, and prevalence within Northern Ireland. Dev Med Child Neurol. 2006;48:495-499.
16. Domanska-Pakiela D, Kaczorowska M, Jurkiewicz E, Kotulska K, Dunin-Wasowicz D, Józwiak S. EEG abnormalities preceding the epilepsy onset in tuberous sclerosis complex patients a prospective study in 5 patients. Eur J Paediatr Neurol. 2014;18:456-468.
17. Muzykewicz DA, Costello DJ, Halpern EF, Thiele EA. Infantile spasms in tuberous sclerosis complex: prognostic utility of EEG. Epilepsia. 2009;50:290-296.
18. Krueger D, Northrup H, on behalf of the International Tuberous Sclerosis Complex Consensus Group. Tuberous sclerosis complex surveillance and management: recommendations of the 2012 International Tuberous Sclerosis Complex Consensus Conference.Pediatr Neurol. 2013;49:255-265.
19. Curatolo P, Jó'zwiak S, Nabbout R, TSC Consensus Meeting for SEGA and Epilepsy Management. Management of epilepsy associated with tuberous sclerosis complex (TSC): clinical recommendations. Eur J Paediatr Neurol. 2012;16:582-586.

Chapter 8

Brain functional networks in syndromic and non-syndromic autism: a graph theoretical study of EEG connectivity

Jurriaan M. Peters[1,2†*], Maxime Taquet[1,3†*], Clemente Vega [2], Shafali S. Jeste[4], Iván Sánchez Fernández[2,5], Jacqueline Tan[6], Charles A. Nelson, III[7], Mustafa Sahin[2], Simon K. Warfield[1]

1. Computational Radiology Laboratory, Department of Radiology, Boston Children's Hospital, 300 Longwood Ave – Main 2, Boston, MA 02115, USA2. Division of Epilepsy and Clinical Neurophysiology, Department of Neurology, Boston Children's Hospital, 300 Longwood Ave – Fegan 9, Boston, MA 02115, USA

3. ICTEAM Institute, Université Catholique de Louvain, Euler Building, Avenue Georges Lemaître, 4 - bte L4.05.01, 1348 Louvain-la-Neuve, Belgium

4. Center for Autism Research and Treatment, Semel Institute 68-237, University of California, 760 Westwood Plaza, Los Angeles, CA 90095, USA

5. Hospital Sant Joan de Déu, Department of Child Neurology, Universidad de Barcelona, 2 Passeig Sant Joan de Déu, Esplugues de Llobregat, Barcelona, Spain

6. VU University Medical Center, de Boelelaan 1117, 1081 HV Amsterdam, the Netherlands

7. Laboratories of Cognitive Neuroscience, Department of Developmental Medicine, Boston Children's Hospital, 1 Autumn Street, Boston, MA 02215, USA

ABSTRACT

Background: Graph theory has been recently introduced to characterize complex brain networks, making it highly suitable to investigate altered connectivity in neurologic disorders. A current model proposes autism spectrum disorder (ASD) as a developmental disconnection syndrome, supported by converging evidence in both nonsyndromic and syndromic ASD. However, the effects of abnormal connectivity on network properties have not been well studied, particularly in syndromic ASD. To close this gap, brain functional networks of electroencephalographic (EEG) connectivity were studied through graph measures in patients with Tuberous Sclerosis Complex (TSC), a disorder with a high prevalence of ASD, as well as in patients with non-syndromic ASD.

Methods: EEG data were collected from TSC patients with ASD (n = 14) and without ASD (n = 29), from patients with non-syndromic ASD (n = 16), and from controls (n = 46). First, EEG connectivity was characterized by the mean coherence, the ratio of inter- over intra-hemispheric coherence and the ratio of long- over short-range coherence. Next, graph measures of the functional networks were computed and a resilience analysis was conducted. To distinguish effects related to ASD from those related to TSC, a two-way analysis of covariance (ANCOVA) was applied, using age as a covariate.

Results: Analysis of network properties revealed differences specific to TSC and ASD, and these differences were very consistent across subgroups. In TSC, both with and without a concurrent diagnosis of ASD, mean coherence, global efficiency, and clustering coefficient were decreased and the average path length was increased. These findings indicate an altered network topology. In ASD, both with and without a concurrent diagnosis of TSC, decreased long- over short-range coherence and markedly increased network resilience were found.

Conclusions: The altered network topology in TSC represents a functional correlate of structural abnormalities and may play a role in the pathogenesis of neurological deficits. The increased resilience in ASD may reflect an excessively degenerate network with local overconnection and decreased functional specialization. This joint study of TSC and ASD networks provides a unique window to common neurobiological mechanisms in autism.

BACKGROUND

Tuberous Sclerosis Complex (TSC) is a genetic neurocutaneous disorder, with highly variable, unpredictable and potentially devastating neurological outcome [1], and approximately 40% of these patients develop autism spectrum disorders (ASD) [2]. No conventional magnetic resonance imaging (MRI) biomarker can reliably predict intractable epilepsy, cognitive impairment or autism in this population [3]. Research has conventionally focused on non-syndromic ASD, but now consensus is emerging that single gene disorders with high penetrance of ASD (e.g. TSC, Fragile X syndrome, Rett syndrome) can be used to better understand the cellular and circuitry bases of ASD [4-6]. Moreover, to advance the understanding of common neurobiological mechanisms in ASD, these should be present in subjects with ASD regardless of an underlying neurogenetic abnormality. For example, using diffusion tensor imaging (DTI), we have recently demonstrated abnormalities in structural connectivity of the corpus callosum of children with TSC and a co-morbid diagnosis of ASD, adding to a growing body of evidence of callosal microstructural deficits in subjects with ASD alone [3, 7-10].

Although such structural data from DTI provide insight into the architecture of interregional connections, to understand how neurophysiological function is supported by this architecture, functional networks should be analyzed as well [11]. Functional networks are implicated in cognitive functioning [12], and may form the physiological basis of information processing and mental representations [11]. They are made up by brief states of coordinated activity between physiological signals from neuronal aggregates in spatially distributed and specialized brain regions [13-16]. Functional connections form the building blocks of a functional network, and can be studied with neurophysiological techniques (e.g. electroencephalography, EEG) and by neuroimaging (e.g., functional MRI, fMRI).

Compared to fMRI, EEG has poor spatial resolution and is subject to volume conduction. However, it has a better signal-to-noise ratio, and a significantly better temporal resolution. Moreover, EEG connectivity is directly related to neural activity, whereas fMRI is derived from the cerebral hemodynamic response to an increased metabolic demand [17], with a lag of 1 to 2 seconds from the neuronal activation. Recently, intermittent motion of the head during fMRI acquisition was shown to generate an artifactual reduction in long range connectivity and increase in short range connectivity. This artifact may mask alterations in functional connectivity associated with autism, and complicate appropriate interpretation of functional connectivity MRI studies [18]. The best way to compensate for this artifact after the acquisition is completed remains unclear and the acquisition of MRI scans of children with autism without motion is a challenging task. On the contrary, artifact assessment is

part of routine EEG interpretation by the clinical neurophysiologist, and common post-processing techniques allow for motion rejection or correction.

Thus, the main advantage of electroencephalography is the high temporal resolution, allowing for direct characterization of higher frequency coordinated activity [19]. Recently, two data-driven analyses of EEG signals allowed for robust classification of subjects with (or at high risk for) autism and controls [20, 21]. Although these EEG studies reflect functional connectivity, they do not measure the complex network properties.

To characterize these complex networks with quantitative measures, graph analysis can be applied [11]. Graph theory has been recently introduced to characterize biological systems, in the brain in particular. Graph analysis of fMRI, magnetoencephalography (MEG) and EEG signals has revealed fundamental insights into the large-scale functional organization of the human brain in health and disease. Using EEG and MEG, syndrome-specific patterns of abnormal functional networks have been described in epilepsy [22], Alzheimer's disease [14] and in adult subjects with ASD [23-25].

For ASD, graph theoretical measures of brain networks are particularly well suited as ASD is, like Alzheimer's disease, considered a disconnection syndrome [26-30]. In disconnection syndromes, functional impairment is theoretically related to the disruption or abnormal integration of spatially distributed brain regions that would normally constitute a large-scale network subserving function [11, 28]. In ASD specifically, the developmental disconnection theory proposes a decreased long-range integration accompanied by increased local connectivity [7]. To synthesize the apparent inconsistencies of various long-range deficits or local surfeits in physical (DTI) and functional (fMRI) connectivity reported in ASD, a network approach may also be used [26, 27, 31-33].

We studied connectivity in ASD, and the effects of abnormal connectivity on network properties. As the study of a homogeneous group of cooperative, high-functioning (young) adults precludes generalization of findings to the entire autism spectrum, a two-way study population was chosen: patients with and without TSC, and patients with and without ASD. To include the early developmental period of accelerated brain growth, during which autism symptoms become apparent [7] and secondary, maladaptive developmental changes have not yet occurred [34], a wide age-range was included in our study.

We hypothesized that (micro-) structural deficits in connection in TSC and ASD affect functional network properties, quantifiable by neurobiologically meaningful graph measures [35] of conventional EEG coherence. In particular, we hypothesized a widespread disconnectivity in TSC based on structural imaging findings, and decreased long-range

and increased short-range connectivity in ASD, in agreement with the current model of developmental disconnection.

METHODS

Subjects

TSC patients were identified through the Boston Children's Hospital Multidisciplinary Tuberous Sclerosis Program, and were diagnosed with definite TSC based on clinical criteria described by the Tuberous Sclerosis Consensus Conference [36]. All patients with TSC were neurologically examined, and clinical data were obtained during office visits and from review of medical records. Genetic confirmatory testing included TSC1 and TSC2 gene sequencing and micro-deletion analysis at Athena Diagnostics (Worcester, MA) or Boston University School of Medicine Center for Human Genetics (Boston, MA). The ASD diagnoses were based on the clinical assessment by a board-certified pediatric neurologist (MS and SSJ) using the Diagnostic and Statistical Manual DSM-IV-TR, supplemented in most with the Autism Diagnostic Observation Schedule (ADOS) [37] by clinical- or research-ADOS certified specialists.

Autistic subjects without TSC (non-syndromic ASD group) were recruited from the Early Childhood Partial Hospitalization Program (ECPHP), an intensive, multidisciplinary, and highly specialized intervention program for children with ASD ages 2-5, via the Center for Autism Research and Treatment, Semel Institute, University of California, Los Angeles, Los Angeles, CA. ASD diagnoses were made as described for the TSC population.

Controls were selected from the general neurology clinic at Boston Children's Hospital in 2010, and were considered when they would have an EEG prompted by single clinical event of moderate-to-low suspicion for epilepsy (e.g. syncope, tics, behavioral outbursts, headache, and prominent startle). Included were only those subjects with a normal neurological development for age, a normal physical examination, a normal EEG both during wakefulness and sleep and a clinical follow-up of at least 1 month to confirm the trivial nature of the EEG referral. 15 controls had a normal imaging study, others were not imaged. Subject recruitment, data collection, retrieval and analysis were conducted with informed consent for the participation of children in the study by the parents when appropriate (e.g. waived for use of retrospective EEG data), using protocols approved by the Institutional Review Boards from Boston Children's Hospital and the Semel Institute, University of California, Los Angeles.

The study populations are represented in (Figure 1 A). Previous literature has implicated an important role of the corpus callosum in ASD [8-10]. For illustrative purposes, and to ensure our functional connectivity measure was representative of callosal integrity, the effects of an absent or severely malformed corpus callosum (ACC) on coherence were assessed. These subjects were retrieved through a search of radiological reports and confirmed by review of the images and electronic medical records.

EEG recording and artifact rejection

In Boston, through review of electronic medical records, digital EEG data was identified and retrieved from the archives. Both routine electroencephalographic data and inpatient data from long-term monitoring with video-EEG was used, utilizing the 10-20 International System of electrode placement (Figure 1 B). If multiple recordings were present, a single record was chosen based on proximity to the acquisition of imaging data, for future correlation of imaging and EEG findings. If data were of insufficient quality, the next closest EEG was chosen. EEGs were recorded on Biologic recording systems, 256 – 512 Hz sampling rate, 1-100 Hz bandpass, or on a Natus Neuroworks® EEG system, 200 Hz sampling rate, 0.1-100 Hz bandpass. Data in Los Angeles were collected using a 128 Hydrocel Geodesic Sensor Net System (EGI®, Inc). Data were collected and recorded using NetAmps Amplifiers and NetStation software, sampled at 250 Hz, and digitized with a National Instruments Board (12 bit).

All raw data was imported, pruned, notch filtered at 60 Hz, and if needed spatially downsampled to the standard clinical 19 electrodes (Fig 1B). An average reference was created using the BESA® Research 3.5 software package. Next, data was imported into EEGlab for band-pass filtering (FIR filter, 1-70 Hz), rejection of artifact-ridden epochs and selection of awake task-free data, with a minimum of 2 minutes. Epochs with evidence of muscle artifact were, where possible, rejected. ICA was used for semi-automated artifact rejection of eye blinks and lateral eye movements, according to previously described methods [38]. The average reference was used for calculation of connectivity. After artifact removal, for each subject several segments of continuous EEG signal

were available for analysis. While these segments varied in their number and length, no group difference was observed in the mean, minimum and maximum length of these segments ($p > 0.15$ for both TSC and ASD conditions). The total duration of EEG data analyzed was higher in TSC subjects ($p < 0.01$) with an average time of 646 seconds compared to 439 seconds for non-TSC subjects. No difference related to ASD was observed in the total duration of EEG data analyzed. This difference in total length was accounted for in our definition of the connectivity measure.

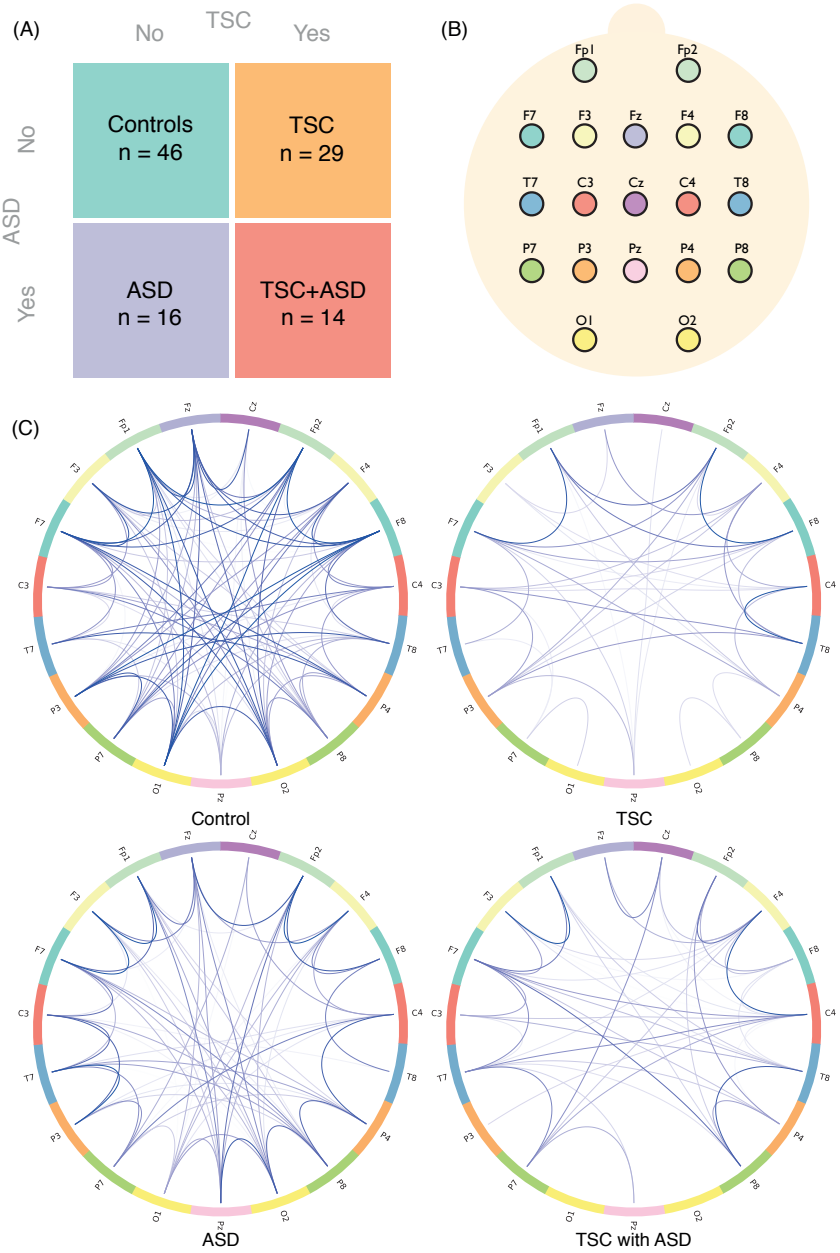

Figure 1. Group structure and functional networks.
(A) In the two-way representation of our population, group status is defined by the subject being diagnosed with Tuberous Sclerosis Complex (TSC) or not, and with Autism Spectrum Disorder (ASD) or not. This structure allows to independently attribute effects specific to TSC and ASD. (B) Electrode locations from the international 10-20 system of electrode placement are used as nodes in the network. (C) Illustrations of the functional networks of a control subject, a TSC patient, a non-syndromic autistic patient, and TSC patient diagnosed with autism. Colors on the connection terminations correspond to the colors in (B).

Connectivity measure

The connections between brain regions that make up functional networks are measures of linear or non-linear statistical interdependence between two time-series [39, 40]. Coherence is a measure of the stability of phase correlation over time, and is sensitive to both changes in power and phase relationships, although the former is typically negligible [17]. High coherence values between two signals are taken as a measure of strong connectivity between the responsible brain regions [41, 42]. Advantages of this measure include ample experience across the literature, the intuitive intelligibility by clinician-scientists and the description of statistically consistent, recurrent connections over a longer period of time. Drawbacks include the neglect of shorter interactions in the time domain and of non-linear relations, the assumption of stationarity of the signal, and sensitivity to volume conductance through skull, scalp and cerebrospinal fluid [14, 17, 42].

Combining the data from the different segments of continuous EEG recording by concatenation would span transitions which translate into artifactual high frequency content of the power spectrum. Thus, coherence was calculated for each segment individually. Our connectivity measure was obtained by computing the average of these coherences weighted by segment length. This method weighs longer segments more, and gives negligible weight to short segments. Specifically, let $Si(t)$ be the signal in the i-th segment, Li be its length, N be the number of segments, $Coh(S,f)$ be the coherence of signal S at frequency f and φ be the frequency band of interest, the connectivity measure reads:

$$C = \int_{\Phi} \frac{\sum_{i=1}^{N} L_i \, Coh(S_i, f)}{\sum_{i=1}^{N} L_i} df.$$

Group comparison of coherences

To illustrate the validity of pre-processing methods and coherence calculations, data were analyzed on a sample of 16 patients with an absent or severely underdeveloped corpus callosum. The corpus callosum is the largest interhemispheric white matter pathway, critical to direct long-range information transfer between homotopic cortical regions and is implicated in autism [3, 8-10]. We calculated the ratio of the mean coherence of all corresponding interhemispheric electrode pairs over all non-midline intrahemispheric electrode pairs. As anticipated [43, 44], decreased interhemispheric coherence was found in the group with an abnormal or absent corpus callosum (one-tailed two-sample t-test: $p<.006$ in all three bands).

For comparison of long- versus short-range coherences, neighboring electrode pairs were ignored because of excessive volume conductance [42, 45]. Short-distance mean coherence was calculated from all intra- and interhemispheric electrode pairs not immediately adjacent, i.e. with a Euclidean distance of 2. Long-distance pairs were defined as a Euclidean distance of 3 or more on the grid (Figure 1 B), i.e. 75% or more of the maximum distance between aligned electrodes. For analysis of TSC and ASD populations, we controlled for baseline coherences and volume conduction by comparison to healthy subjects and for maturational changes by including age as a covariate into the regression model.

The theta band (4-8 Hz) and the lower- and upper alpha bands (8-10 and 10-12 Hz, respectively) were chosen on the basis of previous findings in disconnection syndromes (e.g. Alzheimer's disease [14] and autism (e.g. [45, 46]), the higher power and signal-to-noise ratio in these bands and the increased susceptibility of beta- and gamma-bands to contamination by muscle artifact in routine clinical EEG. This also allowed for limiting the number of statistical analyses.

In addition, graph analysis allows to avoid the multiple comparisons typically needed for group analyses at the connection level (19 electrodes have 171 possible connections in each subject). The actual correction for the comparisons of the few graph measures used would require knowing the correlation between these measures.

Graph analysis

Mathematically, networks are represented by graphs, which consist of nodes connected by edges. A graph based on a connection measure without directionality (e.g. coherence) is referred to as undirected. Graphs can also be weighted or unweighted. In an unweighted graph, edges represent the presence or absence of a connection between two nodes regardless of its strength. By contrast, weighted graphs also encode the strength of the connections within the edges. For this study, an undirected weighted graph was built using the 19 electrodes as nodes and inter-electrode coherence values as edges (Figure 1 B-C). Edge strength can be mapped to a functional distance by applying a function f to it [35]. We choose f to be the negative logarithm as it will associate a functional distance of 0 to times series in perfect synchronization (coherence equal to 1) and an infinite functional distance to incoherent time series (coherence equal to 0). Functional distances then allow the definition of functional path lengths being the sum of the functional distances along a particular path [35].

Graphs can be characterized by various global measures. It is not yet established which measures are most appropriate for the analysis of brain networks [11]. Three important ones

are the characteristic path length, clustering coefficient, and global efficiency [14, 35]. The characteristic path length is the average length of the shortest paths that must be traversed to go from one node to another. The clustering coefficient indicates the likelihood that two nodes strongly connected to a third node are also strongly connected to each other, forming a strongly connected triangular cluster [11]. As such, the clustering coefficient is a measure of the network *segregation*. The global efficiency is the average of the inverse path lengths. As a result, the global efficiency is primarily driven by shorter paths (stronger connections) while characteristic path length is primarily driven by longer paths (weaker connections). In particular, the characteristic path length of a disconnected network is infinite while its global efficiency is finite. Both characteristic path lengths and global efficiency are measures of network *integration*. A high clustering coefficient and a low average path length form a network with 'small-world' characteristics. Small-world architecture suggests a network with connections that are neither regular nor random, and is found ubiquitously in natural and technological systems [11, 35].

Additional file 1 provides an accessible introduction to graph theory and our network measures used, as well as examples of brain and airline networks.

Another interesting property of networks is its resilience to the removal of random or highly connected nodes, known as *Random Failure* and *Targeted Attack*, respectively [43,47]. In technological networks, the resilience is typically enforced by structurally replicating the nodes, inducing a *redundancy* in the network. In biological systems (and in the brain in particular), nodes typically cannot be replicated and resilience may indicate that structurally different components can perform similar functions, known as functional *degeneracy*. Thus, while a resilient functional network may reflect the ability to preserve system function in neuropathological conditions [14, 43, 47], an excess of degeneracy indicates a decreased functional specialization [48-50]. To measure resilience, attacks and failures are simulated by removing nodes and their connections from the graph. The global efficiency is computed for the resulting damaged network and compared to its initial value. Global efficiency is chosen to investigate resilience, as suggested in [35].

Additional file 2 contains an entry-level description of network resilience, and the main methods of assessing resilience through the two modes of network attack. Again examples are provided for airline networks and brain networks.

All graph measures were computed using the NetworkX toolbox in Python [51] except for the global efficiency which was developed in-house.

Statistical analysis

To distinguish the influence of autism spectrum disorders from that of tuberous sclerosis, a two-way ANCOVA was applied. This statistical model can assess effects specific to TSC and specific to ASD, and allows the inclusion of age as a covariate. However, it cannot account for differences in the group that are not additive. For example, if some measure is larger in both ASD and TSC group but the effects do not add up in the TSC with ASD subgroup, then the group differences may not be shown by the model. Conversely, it cannot account for situations in which a group difference is attributable to a single subgroup.

Our unique two-way study population structure is somewhat akin to a repeated analysis, since, for each hypothesis tested, we have two subgroups to study. If the hypothesis is consistent for both subgroups (i.e. both ASD with and without TSC, or both TSC with and without ASD), the finding is more intrinsic to ASD (or TSC).

The subject's age was used as a covariate, given the maturational changes in both EEG coherence [52, 53] and in graph measures of brain networks [54, 55]. The corresponding generalized linear model for each of the measures y is as follows:

$$y = \bar{y} + \beta_{ASD}\, ASD + \beta_{TSC}\, TSC + \beta_{age}\, age$$

where ȳ is the baseline value, ASD and TSC are binary group variables indicating the presence or absence of autism spectrum disorders and tuberous sclerosis complex respectively, and age is the subject's age in years. The two-way ANCOVA then allows us to assess whether βASD and/or βTSC is significantly different from zero, indicating the influence of ASD and/or TSC on the measured properties.

Statistical and graph analyses were done with in-house developed software and standard issue toolbox on a MatLab platform (2009a, MatLab Inc., Natick, MA).

RESULTS

All results of statistical tests are displayed in Table 1.

Demographic data

43 subjects with TSC were included (27 male, mean age 6.9 years, range 0.7 - 25.6), and 46 age-matched control subjects (19 male, mean age 7.1 years, range 0.08 - 17.4). 14 TSC subjects were diagnosed with ASD (9 male, mean age 9.3 years, range 1.0 - 25.6), and 29 were not (17 male, mean age 6.0 years, range 0.7 - 23.4). 16 subjects with non-syndromic autism

Table 1. p-values of the differences associated with autism spectrum disorder (ASD) and tuberous sclerosis complex (TSC).

	ASD			TSC		
Property	**Theta**	**Lower Alpha**	**Upper Alpha**	**Theta**	**Lower Alpha**	**Upper Alpha**
Mean Coherence	0.68	0.5	0.1	0.31	**0.0044(**)**	0.089
Inter-Intra ratio	**0.022(*)**	0.26	0.47	0.14	0.78	0.58
Long-Short ratio	**0.0004(***)**	**0.00012(***)**	**0.00033(***)**	0.083	0.082	0.67
Clustering Coefficient	0.8	0.66	0.6	0.23	**0.001(**)**	**0.016(*)**
Average Path Length	0.5	0.57	0.085	0.33	**0.0076(**)**	0.17
Global Efficiency	0.71	0.31	0.2	0.37	**0.0087(**)**	0.11
Resilience:						
1 node removed	**0.0019(**)**	**0.0049(**)**	**0.001(**)**	0.097	0.74	0.39
2 nodes removed	**0.0073(**)**	0.06	**0.0049(**)**	0.19	0.53	0.45
3 nodes removed	**0.003(**)**	**0.016(*)**	0.12	0.11	0.58	0.92
4 nodes removed	**0.0013(**)**	**0.018(*)**	0.089	0.085	0.6	0.86
5 nodes removed	**0.0008(***)**	**0.042(*)**	0.094	0.1	0.74	0.88

Numbers in bold indicate significant differences between groups, asterisks are defined as follows* <0.05, ** <0.01, *** <0.001)

were included (12 male, mean age 4.1 years, range 2.2 - 5.5). Using Fisher's exact test (binary variables) and student t-test (continuous variables), no group differences were found in gender and age between all TSC subjects and controls (p = 0.45, and 0.06, respectively). Age of TSC subjects with and without autism did not differ from controls (p =0.48 and 0.16, respectively). No age difference was found between all ASD subjects and controls (p = 0.29), but there was a slight male predominance (p = 0.02). Non-syndromic ASD subjects were younger than controls (mean 4.1 years +/- 1.1 vs. 7.9 years +/- 5.6). Age differences were controlled for all four groups in all subsequent analyses, through the incorporation of age as a covariate into the ANCOVA model.

ASD was not associated with TSC1 or TSC2 mutations (p = 1.0). In all patients, there was no association between significant cognitive impairment (clinical assessment or, if available, full scale intelligence quotient < 70) and ASD (p = 0.15). There was no difference in the prevalence of significant cognitive impairment between patients with ASD alone and patients with ASD and TSC (p = 1.0). In TSC patients, there was no association between ASD and epilepsy, or ASD and infantile spasms (p = 1.0 and 0.19, respectively), perhaps reflecting an inclusion bias of those patients who underwent EEG recordings.

Coherence measures

The age-related increase in mean coherence (data not shown) result from developmental changes in brain maturation [52, 53]. On a network level, it represents increasing integration

and decreasing segregation of structural and functional network hubs found by DTI and functional MRI (fMRI) studies [54-56].

In the TSC group, *mean coherence* between all electrode pairs was significantly decreased in the lower alpha band. This decreased indicates a significant global underconnectivity specific to TSC, corrected for age and regardless of the presence of ASD. In the ASD group, no difference in mean coherence was observed (Figure 2 A). However, note that the mean coherence does reflect the distribution of long- and short-range connections (Figure 2 C).

For TSC, despite our prior report on microstructural deficits of the corpus callosum [3], there was no difference in the *ratio of inter-hemispheric over intra-hemispheric coherence* (Figure 2 B).

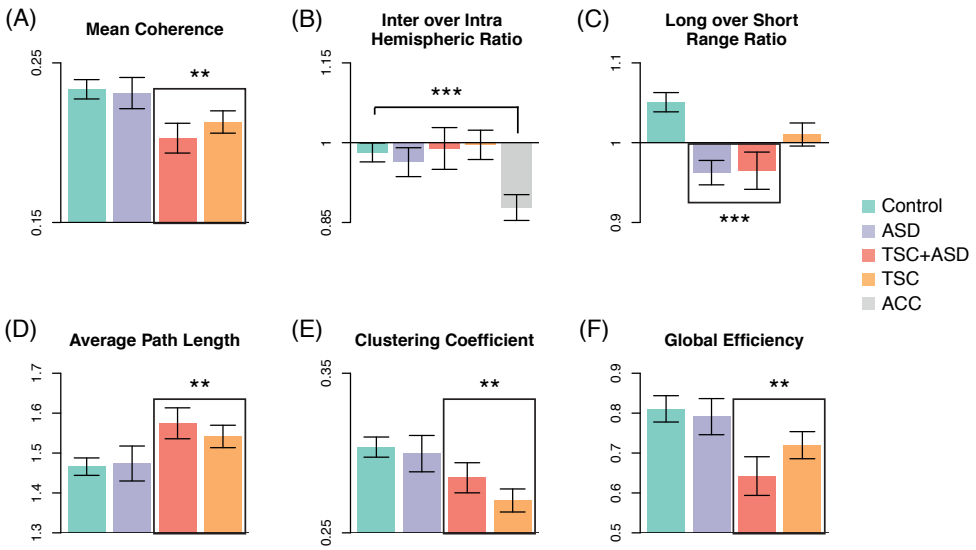

Figure 2. Connectivity by measures of conventional coherence and network topology.
(A - C) Conventional coherence measures: (A) Mean coherence over all pairs of electrodes shows a significantly global under-connectivity for the Tuberous Sclerosis Complex (TSC) group regardless of the presence of Autism Spectrum Disorder (ASD). (B) Inter- versus intrahemispheric coherence ratio. The significantly smaller value for patients with an absent corpus callosum (ACC) illustrates the validity of coherence as a connectivity measure. (C) Long- over short-range connectivity ratio is significantly smaller in the ASD group. As the mean coherence in (A) is not altered, this indicates a short-range overconnectivity and long-range underconnectivity in patients with ASD, evident in both subgroups (in ASD related to TSC and in ASD alone). (D - F) Network topology measures: TSC is characterized by a higher average path length (D) and lower clustering coefficient (E) and global efficiency (F). This departure from the small-world network topology results in a less functionally integrated and segregated network. No ASD group effect was found for these network topology measures. Only the lower alpha band is shown, see Table 1 for details.
All measures are corrected for age. * $p<0.05$, ** $p<0.01$, *** $p<0.001$.

For ASD, with the exception of a group effect in the theta band, this ratio was unchanged as well. To illustrate coherence as a measure of connectivity, this ratio indeed showed a reduction of interhemispheric connections in the group with an absent corpus callosum [43, 44].

In the TSC group, the *ratio of long- over short-distance coherence* trended lower but did not reach significance (Figure 2 C).

In the ASD group, this ratio was significantly and consistently decreased over all examined frequency bands. As the mean coherence (Figure 2 A) was not altered, the decreased ratio indicates a local overconnectivity accompanied by a proportional long-range underconnectivity in patients with ASD. This pattern was evident in both subgroups, i.e. in both ASD with and without TSC.

Graph measures

In patients with TSC, we found both a longer average path length (weak, long connections are weaker) and a decreased global efficiency (strong, short connections are weaker), indicating less integration through both short and long network paths (Figure 2 D-F). The clustering coefficient was decreased, indicating a decreased local connectedness in the graph. Together, the increased path length and the decreased clustering coefficient represent a network that departs from small-world topology in TSC, independent of a comorbid diagnosis of ASD.

In patients with ASD, regardless of the presence of TSC, no significant group difference was found for the three topological measures. Since in ASD the ratio of long- over short-range connectivity is significantly lower, the absence of topological differences in this population suggests that functional networks are altered while maintaining an unaltered distribution of connection strengths (Figure 3).

Resilience measures

For TSC, there was no group effect for either the targeted attack or the random failure in all three spectral bands. The decreased mean coherence in TSC (Figure 2 A) does not affect resilience measures, as these measures reflect a percentage change relative to the baseline global efficiency of a network.

For ASD, with the targeted attack, a significantly decreased decline of the global efficiency was found. This group effect was not present with the random failure. In ASD, regardless of the presence of TSC, this significantly increased resilience to targeted attack was found in all frequency bands (Figure 4). As increased resilience could be related to an altered organization of *hubs* (highly connected nodes) in the network, we calculated the connection degree

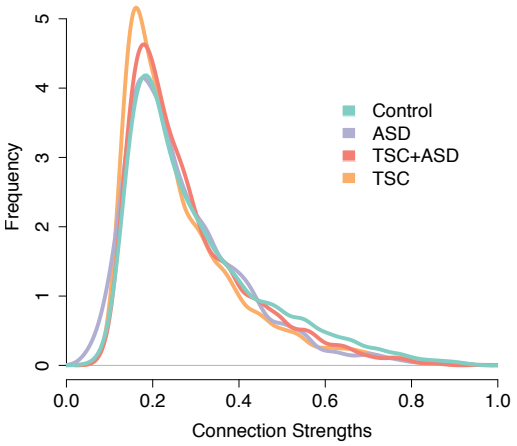

Figure 3. Distribution of all connection strengths (coherences between electrode pairs).
In Tuberous Sclerosis Complex (TSC), the distribution is left-skewed from a relative increase of lower coherence values. In Autism Spectrum Disorder (ASD, the distribution of connection strengths is similar to controls. This indicates the alteration of the functional network in ASD stems from the allocation of similar connection strengths in a different electrode pairing scheme. Only the lower alpha band is shown.

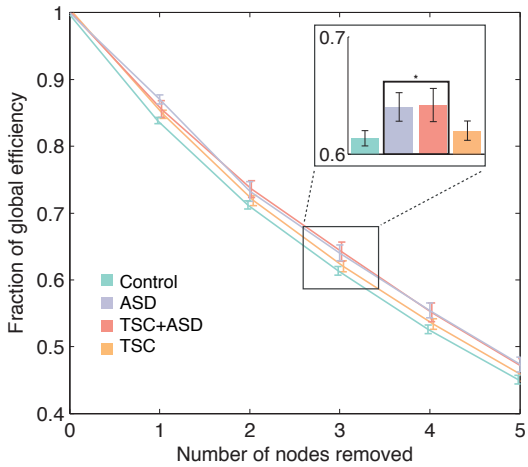

Figure 4. Resilience to targeted attacks.
Autism Spectrum Disorder (ASD) is characterized by significantly higher network resilience to targeted attacks, indicating a higher degree of functional degeneracy (see discussion for details). This difference is consistent in both ASD subgroups (with and without TSC). Only the lower alpha band is shown. A sample bar plot of the global efficiency of the network after removal of 3 nodes is inserted (top right).

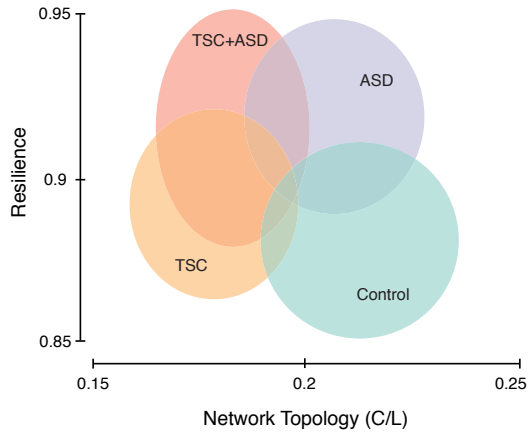

Figure 5. Summary of network analysis.
In summary, functional networks in Autism Spectrum Disorder (ASD) are characterized by a high resilience to targeted attacks, and this is consistent for both ASD alone and ASD related to Tuberous Sclerosis Complex (TSC). Functional networks in the TSC group have an altered topology with a decreased clustering coefficient and increased average path length, regardless of a co-morbid diagnosis of ASD. The consistency of our findings is highlighted by the alignment of the data-cloud on the Y-axis (increased resilience for ASD) and on the X-axis (altered network topology for TSC). Groups are displayed with a span of one standard deviation.

of the three highest connected nodes, compared to the sum of the degree of all nodes. In ASD, this *normalized degree* was significantly decreased across all bands ($p < 0.005$ for the first hub; $p < 0.001$ for second hub except in the upper alpha band; $p < 0.01$ for the third hub except in the upper alpha band).

Subgroup analysis

Results in Figures 2, 3, 4 and 5 and Table 1 suggest that the observed differences are specific to a condition (TSC or ASD) rather than a subgroup. To validate this observation, we performed post-hoc t-tests on the differences between the subgroups. The contributions of TSC with and without ASD to the findings related to TSC (mean coherence and graph measures) were not significantly different. Similarly, the contributions of ASD with and without TSC to the findings related to ASD (long- over short-range connectivity and resilience to targeted attack) were not significantly different across all bands (except in the theta band for 1 and 2 nodes removed, $p=0.02$ and 0.04 respectively). The difference in subgroup age between idiopathic ASD and controls did not in turn lead to the identification of a subgroup difference on these measures. There were no differences in the findings between the groups and the subgroups on these measures.

For clarity, the findings characterizing TSC by an altered network topology and ASD by an increased resilience are summarized in Figure 5.

DISCUSSION

We analyzed functional connectivity through EEG coherence in a large sample of children with TSC with and without ASD. Incorporating subjects with ASD alone allowed us to study connectivity abnormalities common to autism, regardless of etiology. In TSC, a pattern of global underconnectivity and altered network topology was found. ASD was characterized by a decreased long- over short range connectivity, and a markedly increased resilience to targeted attack.

Coherence measures

In TSC, mean coherence was significantly lower, suggesting a global connection deficit. On a structural level, diffuse deficits in connectivity have also been described in TSC. First, animal models of TSC have demonstrated aberrant structural connectivity on a neural level, stemming from abnormalities in myelination, guidance and specification of the axon [57-59]. Second, in human subjects, DTI studies have revealed widespread decreased white matter microstructural integrity (for a brief overview, see [3]). This study is the first to demonstrate a functional correlate of structurally aberrant connectivity in TSC.

In ASD as well as in TSC, the *ratio of inter- over intrahemispheric connectivity* did not reflect abnormalities of the corpus callosum, evident from volumetric, microstructural and functional imaging studies [3, 7-9, 60]. This either suggests a more subtle decrease in interhemispheric functional connectivity or more widespread distribution of altered connectivity in these disorders.

In ASD, a consistent and significant decreased *ratio of long- over short-range coherence*, in the setting of an unaltered mean coherence, is in support of the current model of autism as a developmental disconnection syndrome. A comprehensive synthesis of prior findings in EEG and MEG coherence studies of ASD is challenging due to methodological differences [21, 27]. Nonetheless, patterns of regional underconnectivity and local overconnectivity were found in several studies. 18 autistic adults were found to have locally increased frontal and temporal resting state theta coherence, and decreased coherence between frontal lobe and all other regions in the lower alpha band [45]. In 20 children with ASD, decreased intrahemispheric and interhemispheric delta and theta coherences were reported [46]. Similar to our findings, Mathewson and colleagues found no significant difference of coherence at rest in the alpha band in adults with autism compared to controls [61]. Barttfeld *et al*. studied EEGs of 10 autistic adults with a measure of synchronization, and reported a prominent deficit in long-range and an increase of short-range connectivity [25]. Our data for the first time demonstrate similar findings in both ASD associated with TSC, and in ASD alone, in support of a common mechanism.

Graph measures

In TSC, despite extensive neurological involvement, functional connectivity has not been studied before. In ASD, the classic autistic cognitive profile of superior simple information processing and impaired higher order information processing stresses the importance to examine functional network *as a whole*, and not only *specific* connections between specific regions [10]. To investigate properties of the entire functional network both in TSC and in ASD, we applied graph theoretical analysis.

In TSC, the widespread deficits in local and regional connectivity in TSC are reflected both in conventional and graph measures of coherence. The aberrant network topology results in a decreased efficiency of information processing. The miswiring of axonal connections may contribute to the pathogenesis of neurological deficits in TSC [3, 62, 63], and our EEG study demonstrates the functional implications of these structural abnormalities on a network level.

The comparison of TSC to other disorders is complicated by the developmental rather than neurodegenerative nature of the disconnection. Using MEG, a recent study on connectivity

and demyelination from multiple sclerosis reported an increased path length and clustering coefficient, suggesting a more regular network topology [64]. A similar MEG study of connectivity in Alzheimer's disease, considered a disconnection syndrome, found a decreased path length and clustering coefficient, indicating a more random network [14]. Both studies found associations between neuropsychological performance measures and graph connectivity measures, underscoring the neurobiological relevance of network analysis.

In patients with ASD, no significant differences in network topology measures were found. In the model of autism as a developmental disconnection syndrome, decreased small-worldness could be anticipated, as demonstrated in a MEG study using the synchronization likelihood in young adults with high-functioning autism [25]. Decreased small-worldness may then represent a decrease in local specialization (lower clustering coefficient) and regional integration (longer average path length) [65]. Our data may not have shown this due to the young age of the study-population, where such refinement has

not taken place yet [56]. Also, the absence of a higher clustering coefficient and of a longer path length for ASD despite the decrease in long-over-short range coherence demonstrates that nodes are *spatially* more clustered (conventional analysis) but not *functionally* more clustered (network analysis). This discrepancy is based on the conceptual difference between "physical distance" and "network distance".

Resilience

In the ASD group, a key finding of significantly increased resilience to targeted attack was found. Different explanations to this observation can be posited, each reflecting different aspects of proposed neurobiological mechanisms of ASD.

First, increased resilience in the networks of autistic subjects could be related to redundant connectivity patterns. An abundance of connections makes a network highly resilient to attacks. However, connections in the brain are formed at a high physical cost [11,66] and the brain constantly negotiates the trade-off between wiring costs and topological efficiency [67]. In particular, normal early developmental overconnectivity is followed by a pruning of connections in the maturing brain [55], suggesting network refinement [56].

Physiologically, in autism, the redundancy of connections could be explained by an impaired pruning of connections in the aforementioned dynamic process. The remaining overconnected network operates at different scales, from the neuronal level to the system level, and is consistent with studies of early cerebral overgrowth in autism (for a summary, see [7, 26]).

Cognitively, overconnectivity can result in a poor signal-to-noise ratio where the system is flooded with noise and swamps the signal [34]. With a poor signal-to-noise ratio, the output of a network may not be sufficiently distinct to achieve the necessary information processing [30]. Thus, overconnectivity can create abnormally undifferentiated response to any stimulus. This excess of information gets equal rather than selective attention, creating an overstimulated, inefficient and delayed processing bottleneck [34].

Second, increased resilience could imply decreased functional specialization of brain regions. In technological systems, resilience refers to *redundancy*, as the same function is performed by identical elements. In biological networks, however, it refers to *degeneracy*, as structurally different elements can perform the same function [48, 50]. A degenerate system implies less specialization as the same output can be generated by different elements. Therefore, the increased resilience found in ASD could indicate an excessively degenerate system, where the removal of targeted nodes does not much affect the global properties of the network. Their presence is apparently less critical to the network, providing evidence of decreased functional specialization of these nodes. Our finding of a decreased level of connectivity of the main three hubs in the ASD population adds support to this interpretation.

In summary, the integration of primary order perceptions into higher order concepts is altered in ASD, but whether this is a top-down deficit (developmental disconnection syndrome) or due to heightened primary processing remains unclear [28]. A study using local coherence measures has argued decreased responsiveness of autistic subjects to external stimuli may stem from a signal reduction through excess dampening [21]. Our network approach, however, suggests it rather comes from an excess of information processed in an overconnected, less specialized network [7, 31].

Future directions

Nodes should best represent brain regions with coherent patterns of extrinsic anatomical or functional connections which is problematic with EEG [35]. Specifically, node definition with only 19 electrodes is problematic as the locations do not match well defined functional regions. Higher density EEG with 128 or 256 channels in an experimental setting can overcome this problem in part, although inherent to the technique only superficial aspects of the brain network can be modeled. In addition, electrode positions relative to underlying anatomical structures and functional areas are subject to variability, to changes related to growth and maturation and to methods of electrode placement used (e.g. high density electrode cap or net). Thus, the level of anatomic accuracy of current study does not allow for examining in detail the relation between functional and structural connectivity. Volume conduction will result in lattice-like graphs with highly clustered connections between neighboring electrodes, potentially confounding analysis of network properties [66]. Other

measures of connectivity are less sensitive to this problem such as the phase lag index, synchronization likelihood [14, 68, 69], and partial directed coherence [17]. Nevertheless, it is encouraging that many 'headline' results seem to be robust to methodological details at several steps of network generation [70].

Frequency bands clearly have different associations with different aspects of cognitive activity, with different roles in pathology and with different biophysical mechanisms, reviewed in [71] and [72]. Also, connectivity levels between regions are different for each frequency band [73]. Some authors have proposed that long distance communication may be mainly reflected by synchronization in low frequency bands (alpha and theta range) while shorter distance local communication is supported by synchronization in beta and gamma frequency bands [74]. As a result, it is imperative that any study should try to be as complete as possible in investigating connectivity in the different bands. However, to limit the number of comparisons, but more importantly because of potential muscle artifact (interference with beta and gamma bands) and potential residual motion artifact interference with the delta band) in the EEG data of this challenging population, our study was restricted to the theta, upper and lower alpha bands.

Bands not studied include the delta band and the beta and gamma bands. Slower brain oscillations in the delta and sub-delta range appear to have a physiological role in sensory processing and cognition, even in the absence of environmental stimulation (e.g., the default mode network in resting EEG and fMRI studies) [75]. In autistic patients, Coben and colleagues found the most significant coherence changes in autistic patients in the delta and theta bands compared to controls [46]. Gamma frequency oscillatory activity has been implicated in local cognitive processes, and in the development of distributed cortical networks through both resting-state and task-related neural synchrony in this band [76].

Unfortunately, while analysis of these bands would be no additional challenge to execute, with the current limitations of the clinically acquired data, findings would not be meaningful.

Finally, the heterogeneity of the study population should be emphasized. First, the use of clinical EEG data as controls could have introduced a bias from subtle EEG abnormalities that have escaped routine interpretation by the clinical neurophysiologist, and controls were recruited from a population with neurological complaints. Second, autism is a spectrum disorder with a wide range of severity, not well reflected by a binary variable

(presence or absence of ASD). In future studies continuous variables could be used, such as the calibrated severity score of the Autism Diagnostic Observation Schedule [77], or the Social Responsiveness Score (SRS), which was recently used in another cross-disorder approach of autism [78]. Third, patients with TSC have wide variability in their phenotypical

presentation. We did not incorporate anti-epileptic or psychoactive medication, and epilepsy severity variables into the model, while in TSC up to 90% experiences seizures in their lifetime [1]. With this high co-occurrence of epilepsy, cognitive impairment and autism in TSC [1] differences found may represent more global neurocognitive and behavioral dysfunction in TSC [78] – although in our patients we did not find an association between severe cognitive impairment and autism. While EEG segments with epileptic discharges were excluded from analysis, it remains possible epilepsy impacted the network analysis, in particular of the TSC population. However, interictal functional networks of patients with epilepsy are characterized by increased connectivity (especially in the theta band) and topological changes including increased regularity and hub-like organization [79-82] – which we did not find.

In summary, several limitations of our study including the retrospective nature, the sources of EEG data and the possibility of different cognitive states of subjects [27] can largely be addressed by a prospective study design. The burden associated with an EEG procedure is especially prominent in the young, low-functioning autistic population, and may only be justified by clinical indication [21] - warranting the exploratory use of already collected data. Still, a large, prospective, multicenter endeavor for determination of advanced neuroimaging and EEG correlates of autism in TSC has been launched. In addition, graph theoretical analysis of resting state fMRI connectivity in our population could validate our findings with much higher spatial resolution.

CONCLUSIONS

Connectivity analysis can provide fundamental insights into temporal functional coupling of spatially separate, specialized brain regions. Our EEG coherence study demonstrates decreased functional connectivity related to tuberous sclerosis complex (TSC) in a global manner, and to autism spectrum disorder (ASD) in a more complex pattern.

In TSC, this study is the first to demonstrate altered functional connectivity, both through direct measurement of EEG coherence and on a network level. These results may represent a functional correlate of structural connectivity abnormalities in TSC, and contribute to the neurological pathogenesis in TSC.

In ASD, a decreased long-over short-range coherence and markedly increased resilience to targeted attack renders an excessively degenerate network with local overconnection and decreased functional specialization.

ACKNOWLEDGEMENTS

This work was supported in part by the National Institutes of Health [grant numbers R01 RR021885, R01 LM010033, R03 EB008680, UL1 RR025758 to S.K.W., P20 RFA-NS-12-006, 1U01NS082320-01 to M.S. and J.M.P.], the National Institute of Mental Health [grant number K23MH094517 to S.S.J.], the National Institute on Deafness and Other Communication Disorders [grant number DC 10290 to C.A.N.], and the Department of Defense [grant number W81XWH-11-1-0365 to C.A.N.] In addition, JMP is supported by a Faculty Development Fellowship from the "Eleanor and Miles Shore 50th Anniversary Fellowship Program for Scholars in Medicine", Boston Children's Hospital, Department of Neurology, 2012–2013 and performs video-EEG long-term monitoring, EEGs, and other electrophysiological studies at Boston Children's Hospital and bills for these procedures. MT is supported by the Fonds de la Recherche Scientifique - FNRS, and the Belgian American Educational Foundation. CAN supported by the Simons Foundation. MS is supported by the John Merck Fund and a Junior Investigator Award from the Boston Children's Hospital Translational Research Program. The authors thank the EEG technologists of BCH for their high quality data collection in this challenging population, Tina Shimizu and Amanda Noroña
for their assistance with the Los Angeles data, and Caterina Stamoulis, PhD, for her help with questions related to coherence. We are mostly indebted to the patients and their families for their support and time contributed.

REFERENCES

1. Crino PB, Nathanson KL, Henske EP: The tuberous sclerosis complex. N Engl J Med 2006, 355:1345-1356.
2. Jeste SS, Sahin M, Bolton P, Ploubidis GB, Humphrey A: Characterization of autism in young children with tuberous sclerosis complex. J Child Neurol 2008, 23:520-525.
3. Peters JM, Sahin M, Vogel-Farley VK, Jeste SS, Nelson CA, 3rd, Gregas MC, Prabhu SP, Scherrer B, Warfield SK: Loss of white matter microstructural integrity is associated with adverse neurological outcome in tuberous sclerosis complex. Acad Radiol 2012, 19:17-25.
4. Khwaja OS, Sahin M: Translational research: Rett syndrome and tuberous sclerosis complex. Curr Opin Pediatr 2011, 23:633-639.
5. Sahin M: Targeted treatment trials for tuberous sclerosis and autism: no longer a dream. Curr Opin Neurobiol 2012.
6. Hampson DR, Gholizadeh S, Pacey LK: Pathways to drug development for autism spectrum disorders. Clin Pharmacol Ther 2012, 91:189-200.
7. Courchesne E, Pierce K, Schumann CM, Redcay E, Buckwalter JA, Kennedy DP, Morgan J: Mapping early brain development in autism. Neuron 2007, 56:399-413.
8. Keller TA, Kana RK, Just MA: A developmental study of the structural integrity of white matter in autism. Neuroreport 2007, 18:23-27.
9. Alexander AL, Lee JE, Lazar M, Boudos R, DuBray MB, Oakes TR, Miller JN, Lu J, Jeong EK, McMahon WM, Bigler ED, Lainhart JE: Diffusion tensor imaging of the corpus callosum in Autism. Neuroimage 2007, 34:61-73.
10. Travers BG, Adluru N, Ennis C, Tromp DP, Destiche D, Doran S, Bigler ED, Lange N, Lainhart JE, Alexander AL: Diffusion Tensor Imaging in Autism Spectrum Disorder: A Review. Autism Res 2012.
11. Bullmore E, Sporns O: Complex brain networks: graph theoretical analysis of structural and functional systems. Nat Rev Neurosci 2009, 10:186-198.
12. Varela F, Lachaux JP, Rodriguez E, Martinerie J: The brainweb: phase synchronization and large-scale integration. Nat Rev Neurosci 2001, 2:229-239.
13. Raichle ME, MacLeod AM, Snyder AZ, Powers WJ, Gusnard DA, Shulman GL: A default mode of brain function. Proc Natl Acad Sci U S A 2001, 98:676-682.
14. Stam CJ, de Haan W, Daffertshofer A, Jones BF, Manshanden I, van Cappellen van Walsum AM, Montez T, Verbunt JP, de Munck JC, van Dijk BW, Berendse HW, Scheltens P: Graph theoretical analysis of magnetoencephalographic functional connectivity in Alzheimer's disease. Brain 2009, 132:213-224.
15. Truccolo W, Donoghue JA, Hochberg LR, Eskandar EN, Madsen JR, Anderson WS, Brown EN, Halgren E, Cash SS: Single-neuron dynamics in human focal epilepsy. Nat Neurosci 2011, 14:635-641.
16. van Putten MJ: Proposed link rates in the human brain. J Neurosci Methods 2003, 127:1-10.
17. Sakkalis V: Review of advanced techniques for the estimation of brain connectivity measured with EEG/MEG. Comput Biol Med 2011, 41:1110-1117.
18. Deen B, Pelphrey K: Perspective: Brain scans need a rethink. Nature 2012, 491:S20.
19. Van de Ville D, Britz J, Michel CM: EEG microstate sequences in healthy humans at rest reveal scale-free dynamics. Proc Natl Acad Sci U S A 2010, 107:18179-18184.
20. Bosl W, Tierney A, Tager-Flusberg H, Nelson C: EEG complexity as a biomarkerfor autism spectrum disorder risk. BMC Med 2011, 9:18.
21. Duffy FH, Als H: A stable pattern of EEG spectral coherence distinguishes children with autism from neurotypical controls - a large case control study. BMC Med 2012, 10:64.

22. van Dellen E, Douw L, Baayen JC, Heimans JJ, Ponten SC, Vandertop WP, Velis DN, Stam CJ, Reijneveld JC: Long-term effects of temporal lobe epilepsy on local neural networks: a graph theoretical analysis of corticography recordings. PLoS One 2009, 4:e8081.
23. Tsiaras V, Simos PG, Rezaie R, Sheth BR, Garyfallidis E, Castillo EM, Papanicolaou AC: Extracting biomarkers of autism from MEG resting-state functional connectivity networks. Comput Biol Med 2011, 41:1166-1177.
24. Pollonini L, Patidar U, Situ N, Rezaie R, Papanicolaou AC, Zouridakis G: Functional connectivity networks in the autistic and healthy brain assessed using Granger causality. Conf Proc IEEE Eng Med Biol Soc 2010, 2010:1730-1733.
25. Barttfeld P, Wicker B, Cukier S, Navarta S, Lew S, Sigman M: A big-world network in ASD: dynamical connectivity analysis reflects a deficit in long-range connections and an excess of short-range connections. Neuropsychologia 2011, 49:254-263.
26. Belmonte MK, Allen G, Beckel-Mitchener A, Boulanger LM, Carper RA, Webb SJ:Autism and abnormal development of brain connectivity. J Neurosci 2004, 24:9228-9231.
27. Vissers ME, Cohen MX, Geurts HM: Brain connectivity and high functioning autism: a promising path of research that needs refined models, methodological convergence, and stronger behavioral links. Neurosci Biobehav Rev 2012, 36:604-625.
28. Geschwind DH, Levitt P: Autism spectrum disorders: developmental disconnection syndromes. Curr Opin Neurobiol 2007, 17:103-111.
29. Minshew NJ, Williams DL: The new neurobiology of autism: cortex, connectivity, and neuronal organization. Arch Neurol 2007, 64:945-950.
30. Rippon G, Brock J, Brown C, Boucher J: Disordered connectivity in the autistic brain: challenges for the "new psychophysiology". Int J Psychophysiol 2007,63:164-172.
31. Rubenstein JL, Merzenich MM: Model of autism: increased ratio of excitation/inhibition in key neural systems. Genes Brain Behav 2003, 2:255-267.
32. Anderson JS, Druzgal TJ, Froehlich A, DuBray MB, Lange N, Alexander AL, Abildskov T, Nielsen JA, Cariello AN, Cooperrider JR, Bigler ED, Lainhart JE: Decreased interhemispheric functional connectivity in autism. Cereb Cortex 2011, 21:1134-1146.
33. Dinstein I, Pierce K, Eyler L, Solso S, Malach R, Behrmann M, Courchesne E: Disrupted neural synchronization in toddlers with autism. Neuron 2011, 70:1218-1225.
34. Belmonte MK, Cook EH, Jr., Anderson GM, Rubenstein JL, Greenough WT, Beckel- Mitchener A, Courchesne E, Boulanger LM, Powell SB, Levitt PR, Perry EK, Jiang YH, DeLorey TM, Tierney E: Autism as a disorder of neural information processing: directions for research and targets for therapy. Mol Psychiatry 2004,9:646-663.
35. Rubinov M, Sporns O: Complex network measures of brain connectivity: uses and interpretations. Neuroimage 2010, 52:1059-1069.
36. Roach ES, Gomez MR, Northrup H: Tuberous sclerosis complex consensus conference: revised clinical diagnostic criteria. J Child Neurol 1998, 13:624-628.
37. Lord C, Risi S, Lambrecht L, Cook EH, Jr., Leventhal BL, DiLavore PC, Pickles A, Rutter M: The autism diagnostic observation schedule-generic: a standard measure of social and communication deficits associated with the spectrum of autism. J Autism Dev Disord 2000, 30:205-223.
38. Jung TP, Makeig S, Humphries C, Lee TW, McKeown MJ, Iragui V, Sejnowski TJ: Removing electroencephalographic artifacts by blind source separation. Psychophysiology 2000, 37:163-178.
39. Friston KJ, Tononi G, Reeke GN, Jr., Sporns O, Edelman GM: Value-dependent selection in the brain: simulation in a synthetic neural model. Neuroscience 1994, 59:229-243.
40. Fingelkurts AA, Kahkonen S: Functional connectivity in the brain--is it an elusive concept? Neurosci Biobehav Rev 2005, 28:827-836.

41. van Drongelen W: Signal Processing for Neuroscientists: An Introduction to the Analysis of Physiological Signals. Burlington, MA: Academic Press; 2006.
42. Srinivasan R, Winter WR, Ding J, Nunez PL: EEG and MEG coherence: measures of functional connectivity at distinct spatial scales of neocortical dynamics. J Neurosci Methods 2007, 166:41-52.
43. Alstott J, Breakspear M, Hagmann P, Cammoun L, Sporns O: Modeling the impact of lesions in the human brain. PLoS Comput Biol 2009, 5:e1000408.
44. Nielsen T, Montplaisir J, Lassonde M: Decreased interhemispheric EEG coherence during sleep in agenesis of the corpus callosum. Eur Neurol 1993, 33:173-176.
45. Murias M, Webb SJ, Greenson J, Dawson G: Resting state cortical connectivity reflected in EEG coherence in individuals with autism. Biol Psychiatry 2007, 62:270-273.
46. Coben R, Clarke AR, Hudspeth W, Barry RJ: EEG power and coherence in autistic spectrum disorder. Clin Neurophysiol 2008, 119:1002-1009.
47. Achard S, Salvador R, Whitcher B, Suckling J, Bullmore E: A resilient, lowfrequency, small-world human brain functional network with highly connected association cortical hubs. J Neurosci 2006, 26:63-72.
48. Price CJ, Friston KJ: Degeneracy and cognitive anatomy. Trends Cogn Sci 2002, 6:416-421.
49. Sole RV, Ferrer Cancho R, Montoya JM, Valverde S: Selection, tinkering, and emergence in complex networks. Complexity 2003, 8:20-33.
50. Tononi G, Sporns O, Edelman GM: Measures of degeneracy and redundancy in biological networks. Proc Natl Acad Sci U S A 1999, 96:3257-3262.
51. Hagberg AA, Schult DA, Swart PJ: Exploring network structure, dynamics, and function using NetworkX. In: 7th Python in Science Conference (SciPy 2008): Aug 2008 2008; Pasadena, CA; 2008: 11-15.
52. Tarokh L, Carskadon MA, Achermann P: Developmental changes in brain connectivity assessed using the sleep EEG. Neuroscience 2010, 171:622-634.
53. Thatcher RW, Walker RA, Giudice S: Human cerebral hemispheres develop at different rates and ages. Science 1987, 236:1110-1113.
54. Micheloyannis S, Vourkas M, Tsirka V, Karakonstantaki E, Kanatsouli K, Stam CJ: The influence of ageing on complex brain networks: a graph theoretical analysis. Hum Brain Mapp 2009, 30:200-208.
55. Supekar K, Musen M, Menon V: Development of large-scale functional brain networks in children. PLoS Biol 2009, 7:e1000157.
56. Hagmann P, Sporns O, Madan N, Cammoun L, Pienaar R, Wedeen VJ, Meuli R, Thiran JP, Grant PE: White matter maturation reshapes structural connectivity in the late developing human brain. Proc Natl Acad Sci U S A 2010, 107:19067-19072.
57. Choi YJ, Di Nardo A, Kramvis I, Meikle L, Kwiatkowski DJ, Sahin M, He X: Tuberous sclerosis complex proteins control axon formation. Genes Dev 2008, 22:2485-2495.
58. Meikle L, Talos DM, Onda H, Pollizzi K, Rotenberg A, Sahin M, Jensen FE,Kwiatkowski DJ: A mouse model of tuberous sclerosis: neuronal loss of Tsc1 causes dysplastic and ectopic neurons, reduced myelination, seizure activity, and limited survival. J Neurosci 2007, 27:5546-5558.
59. Nie D, Di Nardo A, Han JM, Baharanyi H, Kramvis I, Huynh T, Dabora S, Codeluppi S, Pandolfi PP, Pasquale EB, Sahin M: Tsc2-Rheb signaling regulates EphAmediated axon guidance. Nat Neurosci 2010, 13:163-172.
60. Just MA, Cherkassky VL, Keller TA, Kana RK, Minshew NJ: Functional and anatomical cortical underconnectivity in autism: evidence from an FMRI study of an executive function task and corpus callosum morphometry. Cereb Cortex 2007, 17:951-961.
61. Mathewson KJ, Jetha MK, Drmic IE, Bryson SE, Goldberg JO, Schmidt LA: Regional EEG alpha power, coherence, and behavioral symptomatology in autism spectrum disorder. Clin Neurophysiol, 123:1798-1809.
62. Tsai P, Sahin M: Mechanisms of neurocognitive dysfunction and therapeutic considerations in tuberous sclerosis complex. Curr Opin Neurol 2011, 24:106-113.

63. Lewis WW, Sahin M, Scherrer B, Peters JM, Suarez RO, Vogel-Farley VK, Jeste SS, Gregas MC, Prabhu SP, Nelson CA, 3rd, Warfield SK: Impaired Language Pathways in Tuberous Sclerosis Complex Patients with Autism Spectrum Disorders. Cereb Cortex 2012; ePub ahead of print.
64. Schoonheim MM, Geurts JJ, Landi D, Douw L, van der Meer ML, Vrenken H, Polman CH, Barkhof F, Stam CJ: Functional connectivity changes in multiple sclerosis patients: A graph analytical study of MEG resting state data. Hum Brain Mapp 2011.
65. Sporns O, Zwi JD: The small world of the cerebral cortex. Neuroinformatics 2004, 2:145-162.
66. Bullmore E, Bassett DS: Brain graphs: graphical models of the human brain connectome. Annu Rev Clin Psychol 2011, 7:113-140.
67. Bullmore E, Sporns O: The economy of brain network organization. Nat Rev Neurosci 2012, 13:336-349.
68. Stam CJ, Nolte G, Daffertshofer A: Phase lag index: assessment of functional connectivity from multi channel EEG and MEG with diminished bias from common sources. Hum Brain Mapp 2007, 28:1178-1193.
69. Stam CJ, van Straaten EC: Go with the flow: Use of a directed phase lag index (dPLI) to characterize patterns of phase relations in a large-scale model of brain dynamics. Neuroimage 2012, 62:1415-1428.
70. Bassett DS, Bullmore ET: Human brain networks in health and disease. Curr Opin Neurol 2009, 22:340-347.
71. Basar E, Basar-Eroglu C, Karakas S, Schurmann M: Gamma, alpha, delta, and theta oscillations govern cognitive processes. Int J Psychophysiol 2001, 39:241-248.
72. Knyazev GG: Motivation, emotion, and their inhibitory control mirrored in brain oscillations. Neurosci Biobehav Rev 2007, 31:377-395.
73. Stam CJ, van Straaten EC: The organization of physiological brain networks.Clin Neurophysiol 2012, 123:1067-1087.
74. von Stein A, Sarnthein J: Different frequencies for different scales of cortical integration: from local gamma to long range alpha/theta synchronization. Int J Psychophysiol 2000, 38:301-313.
75. Van Someren EJ, Van Der Werf YD, Roelfsema PR, Mansvelder HD, da Silva FH: Slow brain oscillations of sleep, resting state, and vigilance. Prog Brain Res 2011, 193:3-15.
76. Uhlhaas PJ, Roux F, Rodriguez E, Rotarska-Jagiela A, Singer W: Neural synchrony and the development of cortical networks. Trends Cogn Sci, 14:72-80.
77. Gotham K, Pickles A, Lord C: Standardizing ADOS scores for a measure of severity in autism spectrum disorders. J Autism Dev Disord 2009, 39:693-705.
78. van Eeghen AM, Pulsifer MB, Merker VL, Neumeyer AM, van Eeghen EE, Thibert RL, Cole AJ, Leigh FA, Plotkin SR, Thiele EA: Understanding relationships between autism, intelligence, and epilepsy: a cross-disorder approach. Dev Med Child Neurol 2012 - ePub ahead of print.
79. Chavez M, Valencia M, Navarro V, Latora V, Martinerie J: Functional modularity of background activities in normal and epileptic brain networks. Phys Rev Lett 2010, 104:118701.
80. Douw L, van Dellen E, de Groot M, Heimans JJ, Klein M, Stam CJ, Reijneveld JC: Epilepsy is related to theta band brain connectivity and network topology in brain tumor patients. BMC Neurosci 2010, 11:103.
81. Horstmann MT, Bialonski S, Noennig N, Mai H, Prusseit J, Wellmer J, Hinrichs H, Lehnertz K: State dependent properties of epileptic brain networks: comparative graph-theoretical analyses of simultaneously recorded EEG and MEG. Clin Neurophysiol 2010, 121:172-185.
82. Wilke C, Worrell G, He B: Graph analysis of epileptogenic networks in human partial epilepsy. Epilepsia 2010, 52:84-93.

APPENDIX

Box 1 Graph Analysis: An introduction

Graphs are mathematical representations of networks in which nodes are connected by edges (see figure below). In the case of an airline network, for example, the nodes are the airports and the edges are the flights connecting them. In the case of brain networks, nodes correspond to brain regions (e.g. electrodes in EEG) and edges represent the connections between them. Graphs can be weighted or unweighted. In weighted graphs, edges are weighted by the strength of the connection. In the figure, the strength is represented by the darkness of the edges. The strength can then be used to define a network distance, which increases when the strength decreases. In the airline network, the duration of the flight can be used as a temporal distance between airports. In the brain network, edges can be weighted by the coherence between times series. A functional distance can be computed by applying a function f to the coherence. Once the graph is constructed, different measures can be computed to investigate different properties of the network.

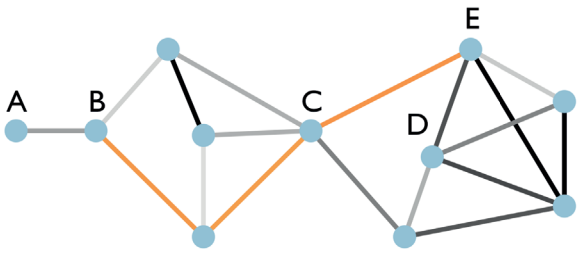

Average path length

Description: Different paths may connect one node to another (path from B to E). The *shortest path length* is the total distance of the shortest path. Averaging these shortest path lengths for all pairs of nodes yields the *average path length*. This graph measure reflects the integration of the network, i.e. how well connected distributed regions are.

Airline networks: The average path length is the average time needed to go from any airport to any other. The average path length is high if there are poorly connected airports (node A). To decrease it, airline companies would need to make sure no small airport is isolated.

Brain networks: The average path length is the average functional distance between any two brain regions. It is a measure of how rapidly information from different specialized regions can be combined.

Clustering coefficient

Description: The clustering coefficient indicates the likelihood that two nodes strongly connected to a third node are also strongly connected to each other, forming a strongly connected triangle in the graph (ref Rubinov and Sporns). In the figure, the clustering coefficient is higher in the right part of the graph than in the left part. The clustering coefficient is considered a measure of the network *segregation*. Networks that are both integrated and segregated are commonly called *small world networks*.

Airline networks: The clustering coefficient is high if regional airports (e.g. Long Beach, CA, and Monterey, CA) have direct connections to each other and not just to major hubs (e.g. New York JFK). Thanks to small-world properties, one could fly from Long Beach, CA to Bordeaux, France, with only two transfers in major hubs.

Brain networks: In the brain, a high clustering coefficient indicates the presence of local cliques forming specialized functional units. Brain networks are small-worlds in which different functional units can work independently but are connected to each other through hubs.

Global efficiency

Description: The global efficiency is another measure of network integration. It is defined as the average of the inverse path lengths. In contrast to the average path length that is very affected by long path with isolated nodes, the global efficiency is mostly driven by short paths between hubs. The graph in the figure would have a larger efficiency if nodes C and D were directly connected.

Airline networks: The global efficiency is high when fast direct flights exist. To increase it, airline companies can introduce fast planes to connect hubs (like the Concorde that used to connect Paris, London and New-York).

Brain networks: In brain networks, a high global efficiency indicates that functional units are well integrated. It is primarily influenced by strong direct connections, which, in EEG analysis, are more physiologically meaningful than long paths between nodes.

Box 2 Graph Analysis: Resilience

The resilience of a network to the removal of nodes provides insight into the presence of spare connections. Spare connections allow for alternative paths to be crossed in the network when the shortest path can no longer be taken due to missing nodes. Resilience is typically measured by simulation of node removal in the network, either as a random failure or a targeted attack. Resilience of the airline network would allow one to get to its destination even if one airport is closed due to weather conditions. In brain networks, resilience may indicate degeneracy, where a path through functionally different nodes yields the same output.

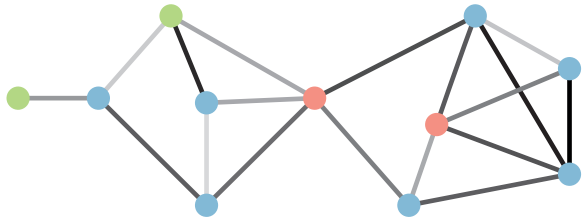

Random failure

Description: With each next random omission of nodes (green nodes in the figure), the decline in the graph performance is measured (typically global efficiency, see Box 1).

Airline networks: Due to progressively worsening international strikes of ground-workers, more and more random airports are temporarily closed, leading to inefficient travel.

Brain networks: Multifocal head trauma could be viewed as an injury to randomly distributed regions. With scattered small injuries, large neurological deficits may be limited, indicating resilience to random failure.

Targeted attacks

Description: Hubs with a high degree centrality are removed first (red nodes in the figure).

Airline networks: A global terrorist group executes a coordinated sequential bomb-attack against the control towers of major international airports. International travel and travel between major metropolitan areas become impossible.

Brain networks: A targeted attack may better mimic preferential neurodegeneration of highly connected hubs (ref Stam). Physiologically, such attacks may be more plausible, as highly connected nodes tend to be more metabolically active, rendering them more vulnerable for neurodegenerative disease (ref Alstott). Excessive resilience could indicate that removal of such active hubs is less critical to network function, suggesting decreased specialization.

Chapter 9

Summary and Discussion

Tuberous Sclerosis Complex (TSC) is a severe multisystem genetic disorder, with a highly variable and unpredictable outcome. While there is increasing insight into basic molecular and cellular mechanism of the disease, and there are promising targeted therapies under investigation, the factors contributing to neurological outcome are only partially understood. Clinical and genetic indicators may reflect the initial burden of the disease, but readily available, biologically relevant, robust, repeated, non-invasive and objective measures are needed to increase our understanding of mechanisms of epilepsy and neurocognitive morbidity, to characterize the disorder longitudinally, and to facilitate interventional trials via the use of validated biomarkers of neurological outcome in TSC.

This thesis describes the use of advanced neuroimaging and neurophysiologic methods in the assessment of phenotypic variation in tuberous sclerosis complex, to serve a dual purpose: To improve the understanding of the pathophysiology, and to evaluate the application as a disease marker.

Below, the work is placed in the context of current developments in the field. Next, it is discussed with regards to strengths and weaknesses, and its potential clinical implications in the diagnosis and management of TSC and neurological co-morbidity.

In the last section, an outline of future work describes the need for further elucidation of TSC pathophysiology, and for research in the development of optimal early treatment and prevention strategies.

THE WORK IN CURRENT CONTEXT

Density-weighted statistics in DTI

A technical contribution in **Chapter 4** is the application of density-weighted statistics (DWS) in the calculation of a weighted average of DTI parameters. In this chapter, we describe a novel solution for the problem of partial volume averaging in region-of-interest (ROI) analysis with DTI tractography. When voxels associated with a fiber tract are identified, the proportion of the voxel associated with the fiber tract is important. A common strategy to select a tract-based ROI has been to threshold the streamline density to identify voxels associated with a particular white matter tract. Average DTI parameters of the region are then assessed by computing the mean value by summing the parameter over all the voxels above the threshold and dividing by the number of voxels in the region. However, partial volume effects confound the analysis[1], and the total number of voxels associated with tracts may actually exceed the total number of voxels[2].

In **Chapter 4**, we describe the use of streamline density to enable an appropriate weighted average of diffusion tensor parameters. In our analysis, the diffusion tensor parameters of a region are calculated on the basis of equal weighting of each of the trajectories, rather than equal weighting of each voxel. This approach has two effects: First, the average DTI measures are calculated per streamline, rather than an average of the values of voxels. Second, voxels with a dense fiber anatomy (e.g. in the center of corpus callosum) count proportionally more towards the average, while spurious tracts are largely ignored. With some adjustment, the method can be applied to multifascicle models, too.

Phenotypical variability

Chapter 4 does not address co-morbidity, and the phenotype characterization was limited. While this is inherent to retrospective studies, there are additional challenges in the characterization of this complex disorder (*what's in a name?*).

First and foremost, there is a marked phenotypical variability, ranging from an incidental diagnosis in a college student to ADL dependence with profound intellectual disability, refractory seizures and overt ASD in another patient.

Second, as TSC is a genetic multisystem disorder with prominent imaging abnormality in most, patients have a multitude of genetic, clinical, and neuroimaging (and neurophysiology) features, each with the potential of being a key determinant in the neurological outcome. Moreover, as these features change with development, sophisticated statistical models and longitudinal data are needed.

As a consequence, because TSC is rare, it is a challenge for any study to cover the full spectrum of neurological and cognitive function. To prospectively collect imaging and neurophysiology variables in a systematic and consistent manner, well-organized collaboration between specialized centers is required.

Third, there is considerable co-variation of neurological and neurodevelopmental co-morbidity. While there are evident exceptional cases of severe epilepsy and no autism (or vice versa), this is not the rule. Therefore, a peer scientific reviewer's demand to "correct for" intelligence quotient (IQ) or epilepsy-related variables may be unreasonable. This was seen in **Chapter 5**, where, for example, there was more severe epilepsy in patients with both TSC and ASD. Statistically, if one regresses for all covariates, the effects of the variable of interest can be lost. The creation of subgroups like in **Chapter 5** can be one potential alternative approach.

Another approach is described in **Chapter 5** and **Chapter 8**, where the utility of a cross-disorder approach is demonstrated. This concept was in part inspired by another study, in which the clinical phenotype of autism spectrum disorder across 3 disorders (TSC, neurofibromatosis 1 (NF-1), and childhood-onset epilepsy) was investigated. Regardless of etiology, what the 3 disorders had in common was that intelligence and epilepsy-related variables were inextricably linked to the phenotype of ASD symptoms[3]. Thus, findings common to a diagnosis (ASD) across several disorders, provides insight in the contribution from epilepsy and impaired cognition to the autistic phenotype.

A changing view of tubers

In **Chapter 6**, tubers, the peritubers rim and the adjacent NAWM are described as a continuum of abnormality, with the tuber being the most abnormal, and the most evidently visible on conventional imaging. In addition, tuber tissue is not static, as the diffusion properties evolve over time. This dynamic nature of tubers is easy to understand in a context of widespread tuber-like pathology found adjacent to tubers, and in the white matter more remotely from tubers. There is a variable amount of pathology intermixed with more normal tissue, and the degree of diffusion evolution over time corresponds to the amount of microscopic pathology. The concept of tuberous sclerosis as "rocky road ice cream", where the tubers are the chunks and the ice cream represents healthy normal white matter (personal communication with Peter Crino) has been abandoned. Instead, tuber pathology evident on the MRI can now be viewed as the "tip of the iceberg".

The poorly delineated and dynamic nature of tubers can explain several apparent controversies in the literature. First, there is ongoing debate whether electrophysiologically, seizures arise from within the tuber[4,5] or from the peritubers rim[6,7]. Electrodes that appear perilesional on imaging may in fact be touching upon "microtubers", small satellite lesions of tuber-like pathology in the vicinity of tubers. A second controversy is whether TSC is a disorder with ubiquitous and diffuse pathology, or rather one of multifocal areas of abnormality in a context of otherwise healthy tissue. For example, one study arguing the latter, examined diffusion metrics of the NAWM in only those lobes without lesions evident on conventional MRI. There were no statistical differences found between TSC NAWM and the white matter of controls[8]. **Chapter 6**, however, suggests the presence of a continuum of pathological abnormality, large portions of which may be below MRI (or DTI) resolution. Notably, even rare patients with well-defined TSC but without identified tubers on conventional MRI can have refractory epilepsy, likely reflecting subtle tuber-like pathology resulting in increased synaptic excitation[9]. Third, using serial conventional imaging, both increases and decreases of tuber volume over time have been reported, even within the same patient. In the context of poorly delineated pathology as outlined in **Chapter 6**, such volume changes could be

due to alterations in acquisition parameters, and to myelination and other maturational changes affecting tissue contrast.

DTI and EEG biomarkers

In **Chapter 4 and 5**, DTI measures of the NAWM white matter of the corpus callosum are studied with regards to outcome. In **Chapter 4**, a pilot study demonstrates that a low FA and high MD are associated with ASD in TSC. In **Chapter 5**, this work is expanded and the specificity of the marker is investigated. Rather than ASD alone, the DTI measures appear to mark a broad neurodevelopmental and neurological outcome. This is not surprising, given the complex co-morbidity of epilepsy, cognition and ASD in TSC.

A true biomarker not only is robust to subtle changes in image acquisition and post-processing, it should reflect the underlying neurobiology, and change in parallel to changes in the clinical phenotype. DTI is a neuroimaging technique that meets these criteria. Multiple independent groups have reported DTI associations with neurological outcome, using similar but not the same imaging tools[10-14]. DTI reflects the microstructure of large white matter pathways and is anatomically well-validated[15-18], but the specific neuropathological change underlying DTI abnormality in TSC needs to be elucidated. Finally, in a trial of the treatment of SEGA with mTOR-inhibitors, patients underwent baseline and repeat diffusion imaging. Improvement in hydrocephalus and in secondary clinical improvements in epilepsy and behavior were associated with improvement of DTI measures of the NAWM.

In summary, DTI holds strong promise as a biomarker of neurological outcome in TSC. It can be applied repeatedly, is non-invasive, and readily available in most institutions. It should be incorporated in the clinical acquisition protocol as it contains actionable, clinically relevant data with regards to localization of the epileptogenic zone[19-21].

The limitation of DTI as a marker for neurological outcome in TSC is evident from **Chapter 5,** which revealed a considerable overlap of the FA-values of the subgroups early on. Aside from more imaging samples at a young age, prospective and longitudinal data is needed to enable an early diagnosis of specific neurological comorbidity in TSC with DTI.

In **Chapter 7**, serial EEG is applied to predict seizure onset. The detrimental effects of early epilepsy, whether infantile spasms or focal seizures, on the development of epilepsy, have been recognized to an extent where in 2012 a consensus meeting of TSC specialists have already recommended monthly EEG monitoring in the first 6 months of life, and every 6-8 weeks thereafter[22]. This practice has not been adopted worldwide, although the study of **Chapter 7** is set up with similar goals of early and aggressive treatment of epilepsy with

potential beneficial effect on outcome. Potential clinical implications of EEG and MRI biomarkers are discussed below.

While the positive predictive value was high, of the 19 children who developed clinical seizures, however, 5 had a normal EEG prior to onset, so the negative predictive value was 64%. A normal EEG does not rule out epilepsy, and epilepsy remains a clinical diagnosis. Now, one can add that it also does not rule out future epilepsy.

One clinically relevant finding was that none of the patients with infantile spasms (IS) had hypsarrhythmia on the EEG. This constitutes an important message that recognition of infantile spasms can be done early, through parental vigilance and (video) education on the appearance of IS, and through similar awareness of the clinician. If infantile spasms go on longer, the full spectrum of West Syndrome may develop: IS, developmental plateauing or regression, and hypsarrhythmia. Another clinical finding was that focal seizures could appear before, with or after IS. Focal seizures may not respond as dramatic to vigabatrin, and may need a second antiepileptic drug. This is a phenomenon that warrants further study as IS are increasingly recognized as a rapidly generalizing focal process.

The study interim analysis was performed early in the process, and of the 40 patients included, only 28 could be analyzed. The final analysis will provide more valuable data in the prediction of impending epilepsy in TSC.

In **Chapter 8**, functional connectivity was studied, and graph theoretical network measures were applied to the EEG data of patients with TSC and/or ASD. This study adds to a growing body of connectivity studies, in a wide spectrum of patients with ASD, with variation in the methodological detail, too[23-28]. The EEG signal, with a low signal-to-noise ratio, and ample data points, lends itself well to an array of statistical and physical approaches to analysis, and the risk of overfitting data is high. This risk may be higher in studies where no formal hypothesis is tested, but claim to rather be data-driven instead. In such studies, multiple iterations of methodological refinement inevitably lead to significant findings for the "generation of hypotheses"[23]. Potential solutions include making both the data and the code available for reproduction of studies by others, and encouraging more rigid data acquisition and post-processing standards[27].

Chapter 8 attempts to avoid this pitfall by formulating a hypothesis prior to embarking on testing, and by executing only a limited number of statistical tests, obviating the need for correcting for multiple comparisons. Only relevant frequency bands based on previous literature were investigated, and the delta and beta bands were omitted to avoid excessive

noise. One weakness of the use of frequency bands in the study, however, is that these may represent different neurophysiological processes in different age groups.

In the **Chapter 8** study, EEG data was obtained from clinical studies, with low spatial resolution and no electrode registration. Another limitation was the coherence measure chosen, as it is subject to skull conductance more than novel measures such as partially directed coherence or (directed) phase-lag index[29]. One could wonder what the relevance is of sophisticated graph network measures in low spatial resolution data, as the interpretation and biological relevance of graph theory is challenging enough in high quality imaging data[30]. The work **of Chapter 8** has not been reproduced by others, but a prospective validation study in a large sample of patients with TSC undergoing serial EEG monitoring is in progress.

LIMITATIONS AND METHODOLOGICAL CONSIDERATIONS

Limitations of the DTI model

When fascicles cross, kiss, or fan, an artificially low fractional anisotropy (FA) is found when the single tensor model is applied[31]. This is due to the different main directions of two or more fascicles (partially) cancelling each other out. It is not a trivial problem, given that an estimated 60-90% of voxels contain more than one main fiber tract. In addition, DTI cannot probe freely diffusion water, for example in glial cells or stemming from edema[32]. While essentially a resolution problem, with the implementation of a novel acquisition scheme referred to as CUbe and SPhere (CUSP) imaging, multiple non-zero B-values can be obtained in a clinically acceptable time frame, and this data can inform a multifascicle model[33]. With this same scheme, inferences can be made about the non-anisotropic fraction of the diffusion, providing insight in different compartments of the voxel[34]. Both for TSC and for other disorders, it will be important to learn whether the application of diffusion compartment imaging (DCI) will provide localizing information in the presurgical workup of patients with refractory epilepsy.

Limitations of the cross-disorder approach

Finding commonality across disorders does not necessarily elucidate the disease mechanism. For example in our work, while the corpus callosum structure may have a role in the pathophysiology of ASD, there is considerable variation in the literature on which subsection may be relevant[35]. In **Chapter 5** we describe only a subtle difference between the corpus callosum of healthy controls and of subjects with isolated ASD, and once corrected for an estimate of overall cognitive function, no difference is evident. It appears the corpus callosum does not function as a marker of ASD, but rather of overall developmental outcome.

A second but related limitation is that the callosal white matter microstructural integrity may be only a generic marker of disease severity in TSC. While we also demonstrated a similar DTI abnormality in the language tracts of patients with TSC and ASD[12], the findings basically replicated the earlier work in the corpus callosum[11]. The integrity of these white matter pathways is not specifically related to the clinical phenotype, and the cognitive functions they subserve may not be specifically reflected by DTI measures. Thus, as the corpus callosum and components of the arcuate fasciculus were similarly affected, the average of the region-of-interest (ROI) analysis with DTI tractography may ultimately be "yet another measure of total disease burden", akin to counting tubers[2], estimating the tuber-brain-proportion[36], or quantifying radial migration lines[8].

Improvements in the atlas-based registration of diffusion data should enable the study of specific tracts and the relation to the phenotypic variation in multiple subjects[32]. Examination of tracts involved in ASD-specific deficits in language, stimulus reward systems, and social cognition may yield more specific markers[37-39]. Only a large, longitudinal, prospective imaging study with (a) detailed documentation of the clinical phenotype including epilepsy, treatment, and full neuropsychological profile and (b) an appropriate and consistent MRI acquisition scheme can solve the question of tract-specific neurological deficits in TSC.

Challenges in the diagnosis of autism

The studies in **Chapters 4, 5 and 8** relied on retrospective data. The diagnosis was made clinically, by a pediatric neurologist or developmental medicine specialist, supplemented by formal neuropsychological ADOS testing in most[40]. In these chapters, the presence of an ASD was treated as a binary variable, where in practice the spectrum is wide. Prospective studies allow for proper phenotypical characterization, and for instance the use of calibrated ADOS score to indicate the severity of the autistic features as a continuous variable[41].

In addition, ASD have been subject to blanket theories, with a lack in specificity allowing for scientific speculation as many findings can be placed in such a broad context. These theories include that of developmental disconnection[42,43] and, more recently, an inhibition-excitation imbalance[44]. There is a diverse range of etiologies of ASD, and a very wide spectrum of clinical phenotypes from low-functioning patients with associated intellectual impairment to intelligent people with a subtle deficit in social skills. As a consequence, the expanding spectrum has led to a rapid increase in diagnosis, and patients may be given an empiric or temporary label to obtain more supportive services. Media attention and a related publication bias have muddied the water further, hampering scientific progress. Already, researchers have argued that, akin to historically broad labels like cerebral palsy, autism must be taken apart[45].

Chapter 8 was hypothesis-driven, and a limited amount of statistical testing was done to avoid spurious findings. Still, the challenge of this work lies in the extrapolation from EEG signals to the understanding of a subtle neurobehavioral phenotype, that is, autism. It is hard to know what the neurobehavioral implications are of increased resilience to targeted attack in patients with ASD.

In summary, interpolation of imaging and neurophysiologic data into the behavioral and social domain deserves close scrutiny. This increased rigor is the responsibility of the scientific community, not the lay press.

EEG intervals in the prediction of epilepsy onset

Of the 19 patients who developed clinical seizures in **Chapter 7**, five had a normal EEG prior to onset (negative predictive value 64%). One patient had a normal EEG at age 1.5 months and had seizure onset at 2 months, and another had a normal EEG at age 9 months and seizure onset by age 11 months, highlighting the challenges of choosing an appropriate and feasible EEG monitoring interval. With the development of EEG recording equipment small enough to strap to the upper arm, the possibility of home application of dry EEG electrodes, and current innovations in telemedicine and health monitoring, TSC seems a suitable candidate disorder to study home EEG monitoring. Daily monitoring is neither feasible nor desirable, but a 1 or 2 week interval could be achievable. Spike and seizure detection software could reduce the work burden by marking areas for expert review with sufficient reliability.

CLINICAL IMPLICATIONS

Prevention of epileptic encephalopathy

More than a decade ago, it was first reported that treatment may improve but not reverse cognitive impairment[46]. Since then, a retrospective series of 10 patients with early successful treatment of infantile spasms had better neurological outcome than historical controls from the same center[47]. Conversely, late treatment may negatively affect outcome[48]. Moreover, 5 patients with TSC treated before the onset of infantile spasms based on abnormal electroencephalograms (EEGs), had improved outcomes compared to historical controls[49]. Even though that open-label study was small, and neither blinded nor randomized, it highlights the current direction of the field towards early and possibly preemptive treatment of infantile spams, to reduce or prevent detrimental effects of an epileptic encephalopathy on an already fragile brain.

To put this in perspective, a recent review article poses genetically determined encephalopathy where early onset seizures contribute to the outcome as opposed to an early epileptic encephalopathy. This distinction is not trivial, and indeed effects of early seizure control or prevention may be limited. Moreover, evidence from human trials and animal studies document ample neurodevelopmental, behavioral and psychiatric co-morbidity in TSC in the absence of an active seizure disorder[50]. There is consensus, however, that an early seizure onset contributes to a poor outcome, and that seizure control is critical in the reduction of those detrimental effects.

An early anti-epileptic intervention is possible due to the efficacy of vigabatrin (VGB) for infantile spasms in TSC. Vigabatrin is an irreversible blocker of gamma-aminobutyric acid (GABA)-transaminase, preventing breakdown of synaptic GABA and increasing GABA levels in the cerebrospinal fluid several hundred-fold[51]. In patients with infantile spasms, a high response rate in patients with TSC has been reported repeatedly, and another prospective trial in the treatment of IS found vigabatrin more effective than adrenocorticotropic hormone (ACTH) in cases with cortical malformations or with TSC[52,53]. Indeed, when TSC patients with IS were studied specifically, there was a clear superiority of vigabatrin over steroids[54]. A review of the literature estimated this response rate to be consistently as high as 90-95%[55]. Currently, the International Tuberous Sclerosis Consensus Group, the American Academy and the Child Neurology Society recommend vigabatrin as first-line treatment for IS in patients with TSC[56,57].

The uniquely high response rate of IS in TSC to vigabatrin is offset by important risks of side-effects, preventing ubiquitous use[55]. Most important is a cumulative and irreversible retinal toxicity, associated clinically with a progressive peripheral visual field constriction[55]. Clinical monitoring of visual function in a young, non-compliant patient with TSC is technically very challenging[58], but reliable. Abnormalities on electroretinogram (ERG), the standard of care for monitoring retinal health in the US, do no consistently correlate with clinical symptoms[59].

Given these side-effects, patients at high risk for adverse neurological outcome should be identified. Such stratification can justify the use of potentially hazardous medication. Both the European multi-nation EPISTOP trial (NCT02098759) and the US multi-center Tuberous sclerosis complex Autism Center of Excellence Research Network (TACERN, NCT02461459) study are applying a variety of approaches to identify early markers of neurological outcome. These include genetic association studies, blood biomarkers, neuropsychological features, EEG and neuroimaging markers.

The study **in Chapter 7** raises the possibility of the use of serial EEG in the detection of early epileptiform abnormality. **Chapters 4 and 5** demonstrate a promise for white matter

DTI for marking neurological co-morbidity in TSC, although the abnormalities in the corpus callosum are not specific and may be too subtle to be detected in early stages.

(Early) determination of the epileptogenic tuber

An increasing body of research has demonstrated increased diffusivity in tubers, perituber tissue and in the normal appearing white matter (NAWM), summarized in **Chapters 3 and 4**. Three studies have shown that epileptogenic tubers have increased diffusion compared to non-epileptogenic tubers[19-21]. **Chapter 6** uses serial DTI imaging to demonstrate that locally increased diffusion of tuber and perituber areas evolves longitudinally, establishing these tissues as dynamic over time[60]. Others have reported cyst-like degeneration of tubers over time, suggesting that that epileptogenic tubers may evolve different from non-epileptogenic areas[61].

Thus, a sensible next step would be to apply the methods from **Chapter 6** in the determination of the epileptogenic zone. Using a novel approach in atlas-based registration of diffusion data, outliers in diffusion dynamics can be detected[32]. Preliminary data shows that the epileptogenic zone can be identified by a larger focal increase in mean diffusion over time as compared to the decreased diffusion in non-epileptogenic areas. Comparison with EEG, electrical source imaging (ESI), and other modalities (MEG, AMT-PET, others) will be needed to validate these findings. The clinical utility of serial diffusion imaging in the detection of the epileptogenic zone will ultimately depend on comparison to both ESI and the surgical cavity in the context of surgical outcome in pediatric patients with TSC.

The use of longitudinal data and normative data raises the possibility of prediction which tuber area may become epileptogenic. Such a prediction could guide a potential focal early intervention in the infant or young toddler, like surgery, rather than needing sustained systemic therapy. In patients with malformations of cortical development (MCD), early surgery may prevent or mitigate catastrophic epilepsy[62], but data in TSC are lacking. Technically, there is an additional challenge in lesion segmentation given the unmyelinated neonatal brain. Logistically, patients may not undergo a sufficient number scans prior to the clinical onset of seizures, but normative data within and between patients may suffice to inform the model. Ethically, the focal intervention would have to be appropriately safe, non-invasive and potentially reversible (e.g. transcranial magnetic stimulation), although surgery still is the only curative intervention at this point.

In summary, the methods described in **Chapter 6** should be applied to track DTI properties of individual tubers and the perituber rim longitudinally. Clinically, the method could identify epileptogenic tubers by their different trajectories over time, in the context of epilepsy surgery.

Below, in the final section, the implications of the work in this thesis for future research are described. These include improving the understanding of TSC pathophysiology, and strategies in the design of optimal early treatment and prevention trials.

FUTURE DIRECTIONS

Understanding the underlying neuropathology of DTI abnormality

The neuropathology underlying the diffusion changes in tuber, perituber tissue, and NAWM has not been elucidated. Based on animal models, increases in axonal diameter, defects in myelination, increased heterotopic cells including gliosis, decreased density of axonal packing are possible explanations[63-67]. From human post-mortem studies, small pockets of pathology referred to as "microtubers" and isolated heterotopic neurons referred to as "sentinel cells" have been described beyond tuber borders evident on conventional MRI[68]. In post-surgical resection specimens, abundant tuber-like pathology is present adjacent to tubers[69]. Thus, a widely distributed microscopic tuber-like pathology is a potential good explanation for abnormal diffusion. But if these are not sufficiently abundant, but rather spread sporadically as described[68], is a predominance of scattered heterotopic cells a more suitable explanation?

Astrocytes are abundantly present in tubers and perituber tissue, and could contribute to diffusion abnormality beyond the tubers too, in the NAWM[70]. Studies in both human resection specimen and in animal models increasingly recognize that cellular and molecular abnormalities of glial cells both inside and outside of the tuber contribute to epileptogenesis[70-72]. Moreover, epileptogenesis in TSC is hallmarked by focal progressive astrogliosis noted on pathology, but whether astrogliosis or another feature in the TSC brain causes the diffusion changes is not known.

To study the nature of tissue abnormality underlying abnormal diffusion in TSC, a potential approach is the examination of pediatric epilepsy surgery resection specimens. High-resolution ex-vivo structural and diffusion MRI of this tissue can be followed by registration with quantitative neuropathology[73].

This approach poses several formidable technical challenges. First, ex-vivo studies generally rely on the fixation of specimen to inhibit tissue decay which starts as soon as tissue is deprived from its blood supply. In addition, ex-vivo DW-MRI requires particular care when packaging the specimen because the presence of microscopic air bubbles gives rise to geometric and intensity image distortion. Unfortunately, fixation of tissues substantially alters tissue diffusivity profiles[74]. In addition, ex-vivo DW-MRI requires particular care when

packaging the specimen because the presence of microscopic air bubbles gives rise to geometric and intensity image distortion. With well-designed optimized acquisition methods for ex-vivo brain diffusion-weighted imaging, however, one should be able to address the specific requirements of post-mortem and resection specimen imaging using a clinical 3T scanner[74].

Second, methods for alignment of microscopy data and feature-based registration with MRI structural need refinement to be applied to such tissue specimen[75,76]. Comparison with pre-operative MRI for specimen orientation is also possible.

Based on preliminary data from non-rigid registration of 2D microscopy slices with ex-vivo MRI, the next step would be to compare local diffusion metrics (fractional anisotropy, mean diffusivity) in perituber white matter to optical density measures of glutamine synthetase (GS) negative and glial fibrillary acidic protein (GFAP) positive astrocytes, and with neuronal or myelin markers (Figure 1).

Rational design of early interventional trials

With regards to early preemptive treatment of epilepsy in TSC, several questions can be asked:

When does an intervention amount to a "disease modifying" therapy?

Is changing the long-term outcome sufficient, through amelioration of seizures? Or do effects need to be sustained, even in the context of eventual drug withdrawal? For TSC specifically, vigabatrin has not yet proven to primarily prevent seizures, and may rather provide (long-term) symptom suppression therapy[49,50].

Which agent is mechanism-based and should be tried first?

Since there is no evidence that vigabatrin is antiepileptogenic, and the preliminary data in human is limited, why opt for vigabatrin as an early therapy? The initial open label[49] and retrospective data[47] supporting pre-emptive vigabatrin use were promising, but the benefits of early vigabatrin may be more limited than anticipated. In the TACERN observational study, of which preliminary results are provided in **Chapter 7**, so far of the 5 patients treated pre-emptively with vigabatrin, 4 went on to have infantile spasms, focal seizures, or both, and only 1 remained seizure free at 2 years follow-up[77].

Another avenue of possible intervention is the use of mTOR inhibitors. To reiterate, the TSC1 and TSC2 proteins, hamartin and tuberin, respectively, form a heterodimer and inhibit the mTOR pathway, responsible for protein synthesis and cell-growth[78]. Defects in the Tsc1 or Tsc2 gene lead to loss of this inhibitory function. With rapamycin and everolimus, and other

mTOR inhibitors currently under investigation, the effects of a disinhibited mTOR cascade can be reduced mere steps downstream from the defective proteins. Such a targeted therapeutic intervention, almost addressing the primary molecular defect, may be referred to as precision medicine[79].

The use of everolimus is currently FDA approved for the treatment of subependymal giant cell astrocytomas (SEGAs), central brain tumors that arise in the lining of the ventricles and carry potential for obstructing CSF flow and causing hydrocephalus. During these trials, beneficial effects on seizures and behavior were also reported, although data was limited to parental report with limited formal assessments[80,81]. The effects of mTOR inhibitors on epilepsy and on neurodevelopment in TSC are currently under more thorough investigation in prospective, randomized controlled trials[82].

In whom, and when?

Preliminary data and secondary outcome measures from the SEGA trial suggest seizures do not universally respond to mTOR inhibitors, and the same applies to neurobehavioral symptoms. There may be a window of opportunity for optimal timing of effective treatment, for example during stages of rapid brain development[60,83]. The mTOR pathway has an important role in normal growth and development[78], however, and rodent models of TSC develop severe congenital anomalies when exposed to mTOR inhibitors in utero[84]. While long-term use for SEGA appears safe[80], and the federal drug administration (FDA) approval has been extended for use in the neonatal with SEGA, there may be limits to very early use and it probably cannot be universally administered to all patients with TSC.

To conclude, a study with rapamycin or everolimus would be a true mechanism-based anti-epileptogenic treatment trial in the prevention of detrimental neurodevelopmental effects in TSC. There is a paucity of literature on vigabatrin in animal models of TSC, while virtually all animal models of TSC have been treated with mTOR inhibitors[85,86]. Safety data for everolimus has already been obtained through the treatment of neonates with SEGA. Prolonged treatment with mTOR-inhibitors using a periodic pulse regimen could improve safety and tolerability, but has not been tried in humans yet[87]. Feasibility of preemptive treatment is good given the presence of an EEG biomarker for risk stratification, and the high but not ubiquitous rate of seizures. Ideally, mTOR-inhibitors should be studied both separately and concurrently with antiepileptic drugs (Figure 2).

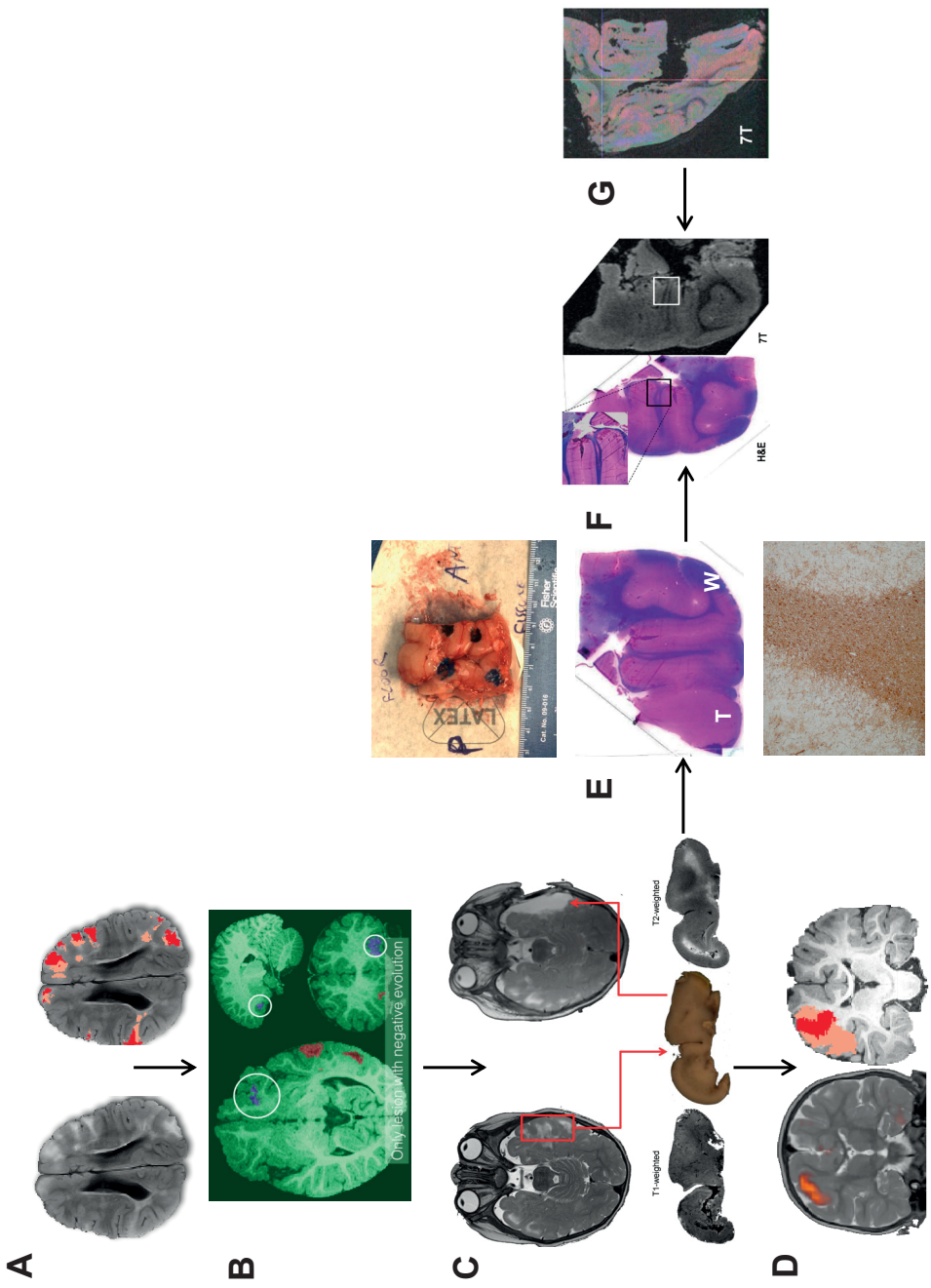
A
B
Only lesion with negative evolution
C
T2-weighted
T1-weighted
D
E
T
W
F
7T
H&E
G
7T

Figure 1: Ex-vivo high-resolution MRI to study neuropathology of DTI abnormality in TSC.
(A) Axial FLAIR images, with tubers visible as subcortical areas of T2-prolongation (white, left image) and after automated segmentation of tuber and perituber tissue (red and salmon, right image).
(B) Via the alignment of serial MRIs, the longitudinal diffusion changes of tuber regions-of-interest (ROIs) are displayed in red (typical evolution) and a single region has an increased FA over time (blue). The regions of diffusion over time are superimposed on a T1-weighted structural scan.
(C) Surgery with intraoperative stereotactic orientation of the specimen. Preoperative (left) and postop (right) T2-weighted axial MRI of a 1-year old patient with TSC. At the bottom, the left lateral temporal lobe resection specimen (center), and T1-weighted (left) and T2-weighted (right) ex-vivo MRI.
(D) Validation of the longitudinal DTI tuber identification technique. On the left, coronal pre-operative T2-weighted MRI with the distributed electrical source imaging (ESI) solution superimposed. On the right, the post-operative resection cavity (salmon, manually segmented) and tuber area (red) are projected onto an axial pre-operative T1-weighted MRI.
(E) Resection specimen (top); macroscopic pathology of resected occipital lobe (middle); and microscopic pathology (bottom). The white matter (W) remote from the epileptogenic tuber (T) shows extensive GFAP positivity (brown stain).
(F) Registration of a pathology specimen (H&E stain, on the left) to ex-vivo 7T structural MRI (on the right). The square highlights a microscopic pocket of tuber pathology known as a "microtuber".
(G) Ex-vivo 7T DTI with color-coded FA-map (red: left - right; blue: rostral - caudal; green: anterior - posterior) from a resection specimen from the occipital lobe of 6-y.o. girl with TSC. Note that the gradient direction encoding needs to be corrected, and this is a different specimen than (F).

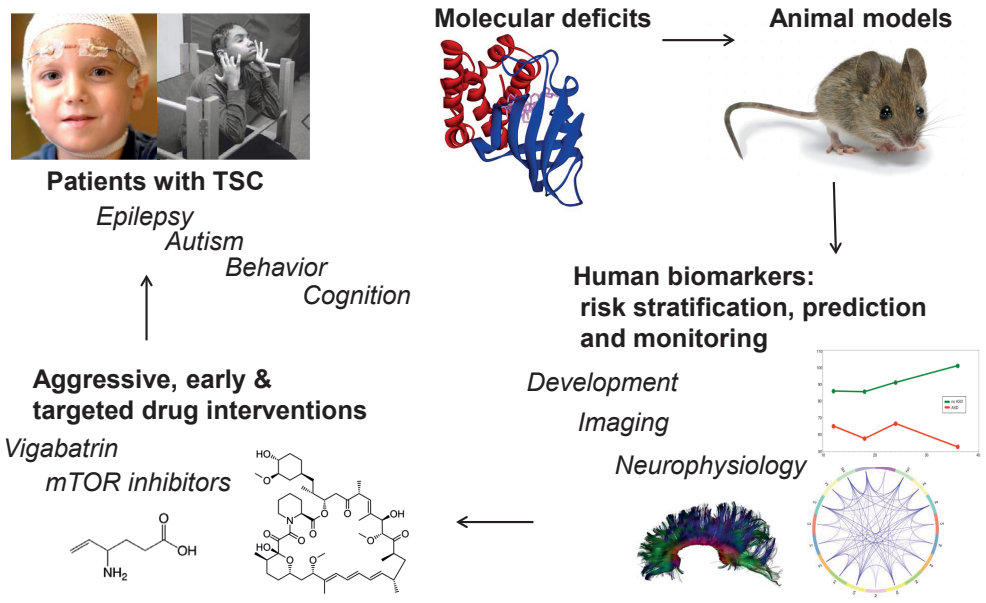

Figure 2: Pathway to disease modification in TSC.
Well-characterized molecular and cellular deficits can be modeled in rodent models. Through translation of basic neuroscience, human markers of neurological co-morbidity in TSC can be studied. Early developmental red flags, serial EEG, and DTI are potential candidates in the early identification of those at high risk for adverse neurological outcome. Early mechanism-based interventions may reduce detrimental effects from early onset seizures on neurodevelopment.

CONCLUSION

TSC is a unique disorder in which fundamental insights into epileptogenesis and neurodevelopment can both benefit patients and be directly applied to related disorders. The early diagnosis, the clinical indications for frequent monitoring with EEG and MRI, the presence of mechanism-based medications, and the coordination of research across multiple facilities provides a unique opportunity to modify disease outcome in this population through early targeted intervention.

REFERENCES

1. Vos SB, Jones DK, Viergever MA, Leemans A. Partial volume effect as a hidden covariate in DTI analyses. Neuroimage 2011;55:1566-76.
2. Chou IJ, Lin KL, Wong AM, et al. Neuroimaging correlation with neurological severity in tuberous sclerosis complex. Eur J Paediatr Neurol 2008;12:108-12.
3. van Eeghen AM, Pulsifer MB, Merker VL, et al. Understanding relationships between autism, intelligence, and epilepsy: a cross-disorder approach. Dev Med Child Neurol 2013;55:146-53.
4. Koh S, Jayakar P, Dunoyer C, et al. Epilepsy surgery in children with tuberous sclerosis complex: presurgical evaluation and outcome. Epilepsia 2000;41:1206-13.
5. Mohamed AR, Bailey CA, Freeman JL, Maixner W, Jackson GD, Harvey AS. Intrinsic epileptogenicity of cortical tubers revealed by intracranial EEG monitoring. Neurology 2012;79:2249-57.
6. Major P, Rakowski S, Simon MV, et al. Are cortical tubers epileptogenic? Evidence from electrocorticography. Epilepsia 2009;50:147-54.
7. Ma TS, Elliott RE, Ruppe V, et al. Electrocorticographic evidence of perituberal cortex epileptogenicity in tuberous sclerosis complex. J Neurosurg Pediatr 2012;10:376-82.
8. van Eeghen AM, Ortiz-Teran L, Johnson J, Pulsifer MB, Thiele EA, Caruso P. The neuroanatomical phenotype of tuberous sclerosis complex: focus on radial migration lines. Neuroradiology 2013;55:1007-14.
9. Wang Y, Greenwood JS, Calcagnotto ME, Kirsch HE, Barbaro NM, Baraban SC. Neocortical hyperexcitability in a human case of tuberous sclerosis complex and mice lacking neuronal expression of TSC1. Ann Neurol 2007;61:139-52.
10. Wong V, Khong PL. Tuberous sclerosis complex: correlation of magnetic resonance imaging (MRI) findings with comorbidities. J Child Neurol 2006;21:99-105.
11. Peters JM, Sahin M, Vogel-Farley VK, et al. Loss of white matter microstructural integrity is associated with adverse neurological outcome in tuberous sclerosis complex. Acad Radiol 2012;19:17-25.
12. Lewis WW, Sahin M, Scherrer B, et al. Impaired language pathways in tuberous sclerosis complex patients with autism spectrum disorders. Cereb Cortex 2013;23:1526-32.
13. Baumer FM, Song JW, Mitchell PD, et al. Longitudinal changes in diffusion properties in white matter pathways of children with tuberous sclerosis complex. Pediatr Neurol 2015;52:615-23.
14. Wong AM, Wang HS, Schwartz ES, et al. Cerebral diffusion tensor MR tractography in tuberous sclerosis complex: correlation with neurologic severity and tract-based spatial statistical analysis. AJNR Am J Neuroradiol 2013;34:1829-35.
15. Mori S, Crain BJ, Chacko VP, van Zijl PC. Three-dimensional tracking of axonal projections in the brain by magnetic resonance imaging. Ann Neurol 1999;45:265-9.
16. Mori S, Kaufmann WE, Pearlson GD, et al. In vivo visualization of human neural pathways by magnetic resonance imaging. Ann Neurol 2000;47:412-4.
17. Basser PJ, Pajevic S, Pierpaoli C, Duda J, Aldroubi A. In vivo fiber tractography using DT-MRI data. Magn Reson Med 2000;44:625-32.
18. Conturo TE, Lori NF, Cull TS, et al. Tracking neuronal fiber pathways in the living human brain. Proc Natl Acad Sci U S A 1999;96:10422-7.
19. Yogi A, Hirata Y, Karavaeva E, et al. DTI of tuber and perituberal tissue can predict epileptogenicity in tuberous sclerosis complex. Neurology 2015;85:2011-5.
20. Jansen FE, Braun KP, van Nieuwenhuizen O, et al. Diffusion-weighted magnetic resonance imaging and identification of the epileptogenic tuber in patients with tuberous sclerosis. Arch Neurol 2003;60:1580-4.

21. Chandra PS, Salamon N, Huang J, et al. FDG-PET/MRI coregistration and diffusion-tensor imaging distinguish epileptogenic tubers and cortex in patients with tuberous sclerosis complex: a preliminary report. Epilepsia 2006;47:1543-9.
22. Curatolo P, Jozwiak S, Nabbout R, SEGA TSCCMf, Epilepsy M. Management of epilepsy associated with tuberous sclerosis complex (TSC): clinical recommendations. Eur J Paediatr Neurol 2012;16:582-6.
23. Duffy FH, Als H. A stable pattern of EEG spectral coherence distinguishes children with autism from neurotypical controls - a large case control study. BMC Med 2012;10:64.
24. Lazar AS, Lazar ZI, Biro A, et al. Reduced fronto-cortical brain connectivity during NREM sleep in Asperger syndrome: an EEG spectral and phase coherence study. Clin Neurophysiol 2010;121:1844-54.
25. Murias M, Webb SJ, Greenson J, Dawson G. Resting state cortical connectivity reflected in EEG coherence in individuals with autism. Biol Psychiatry 2007;62:270-3.
26. Rippon G, Brock J, Brown C, Boucher J. Disordered connectivity in the autistic brain: challenges for the "new psychophysiology". Int J Psychophysiol 2007;63:164-72.
27. Vissers ME, Cohen MX, Geurts HM. Brain connectivity and high functioning autism: a promising path of research that needs refined models, methodological convergence, and stronger behavioral links. Neurosci Biobehav Rev 2012;36:604-25.
28. Wass S. Distortions and disconnections: disrupted brain connectivity in autism. Brain Cogn 2011;75:18-28.
29. Stam CJ, Nolte G, Daffertshofer A. Phase lag index: assessment of functional connectivity from multi channel EEG and MEG with diminished bias from common sources. Hum Brain Mapp 2007;28:1178-93.
30. Bullmore E, Sporns O. Complex brain networks: graph theoretical analysis of structural and functional systems. Nat Rev Neurosci 2009;10:186-98.
31. Vos SB, Jones DK, Jeurissen B, Viergever MA, Leemans A. The influence of complex white matter architecture on the mean diffusivity in diffusion tensor MRI of the human brain. Neuroimage 2011;59:2208-16.
32. Taquet M, Scherrer B, Commowick O, et al. A mathematical framework for the registration and analysis of multi-fascicle models for population studies of the brain microstructure. IEEE Trans Med Imaging 2014;33:504-17.
33. Scherrer B, Warfield SK. Parametric representation of multiple white matter fascicles from cube and sphere diffusion MRI. PLoS One 2012;7:e48232.
34. Scherrer B, Schwartzman A, Taquet M, et al. Characterizing the distribution of anisotropic micro-structural environments with diffusion-weighted imaging (DIAMOND). Med Image Comput Comput Assist Interv 2013;16:518-26.
35. Travers BG, Adluru N, Ennis C, et al. Diffusion Tensor Imaging in Autism Spectrum Disorder: A Review. Autism Res 2012.
36. Jansen FE, Vincken KL, Algra A, et al. Cognitive impairment in tuberous sclerosis complex is a multifactorial condition. Neurology 2008;70:916-23.
37. Abrams DA, Lynch CJ, Cheng KM, et al. Underconnectivity between voice-selective cortex and reward circuitry in children with autism. Proc Natl Acad Sci U S A 2013;110:12060-5.
38. Fletcher PT, Whitaker RT, Tao R, et al. Microstructural connectivity of the arcuate fasciculus in adolescents with high-functioning autism. Neuroimage 2010;51:1117-25.
39. Von Der Heide RJ, Skipper LM, Klobusicky E, Olson IR. Dissecting the uncinate fasciculus: disorders, controversies and a hypothesis. Brain 2013;136:1692-707.
40. Lord C, Risi S, Lambrecht L, et al. The autism diagnostic observation schedule-generic: a standard measure of social and communication deficits associated with the spectrum of autism. J Autism Dev Disord 2000;30:205-23.
41. Gotham K, Pickles A, Lord C. Standardizing ADOS scores for a measure of severity in autism spectrum disorders. J Autism Dev Disord 2009;39:693-705.

42. Geschwind DH, Levitt P. Autism spectrum disorders: developmental disconnection syndromes. Curr Opin Neurobiol 2007;17:103-11.
43. Minshew NJ, Williams DL. The new neurobiology of autism: cortex, connectivity, and neuronal organization. Arch Neurol 2007;64:945-50.
44. Uzunova G, Pallanti S, Hollander E. Excitatory/inhibitory imbalance in autism spectrum disorders: Implications for interventions and therapeutics. World J Biol Psychiatry 2015:1-13.
45. Waterhouse L, Gillberg C. Why autism must be taken apart. J Autism Dev Disord 2014;44:1788-92.
46. Jambaque I, Chiron C, Dumas C, Mumford J, Dulac O. Mental and behavioural outcome of infantile epilepsy treated by vigabatrin in tuberous sclerosis patients. Epilepsy Res 2000;38:151-60.
47. Bombardieri R, Pinci M, Moavero R, Cerminara C, Curatolo P. Early control of seizures improves long-term outcome in children with tuberous sclerosis complex. Eur J Paediatr Neurol 2010;14:146-9.
48. Muzykewicz DA, Costello DJ, Halpern EF, Thiele EA. Infantile spasms in tuberous sclerosis complex: prognostic utility of EEG. Epilepsia 2009;50:290-6.
49. Jozwiak S, Kotulska K, Domanska-Pakiela D, et al. Antiepileptic treatment before the onset of seizures reduces epilepsy severity and risk of mental retardation in infants with tuberous sclerosis complex. Eur J Paediatr Neurol 2011;15:424-31.
50. Curatolo P, Aronica E, Jansen A, et al. Early onset encephalopathy or genetically determined encephalopahy with early onset epilepsy? Lessons learned from TSC. Eur J Paediatr Neurol 2016;*in press*.
51. Ben-Menachem E. Mechanism of action of vigabatrin: correcting misperceptions. Acta Neurol Scand Suppl 2011:5-15.
52. Elterman RD, Shields WD, Mansfield KA, Nakagawa J, Group USISVS. Randomized trial of vigabatrin in patients with infantile spasms. Neurology 2001;57:1416-21.
53. Vigevano F, Cilio MR. Vigabatrin versus ACTH as first-line treatment for infantile spasms: a randomized, prospective study. Epilepsia 1997;38:1270-4.
54. Chiron C, Dumas C, Jambaque I, Mumford J, Dulac O. Randomized trial comparing vigabatrin and hydrocortisone in infantile spasms due to tuberous sclerosis. Epilepsy Res 1997;26:389-95.
55. Willmore LJ, Abelson MB, Ben-Menachem E, Pellock JM, Shields WD. Vigabatrin: 2008 update. Epilepsia 2009;50:163-73.
56. Go CY, Mackay MT, Weiss SK, et al. Evidence-based guideline update: medical treatment of infantile spasms. Report of the Guideline Development Subcommittee of the American Academy of Neurology and the Practice Committee of the Child Neurology Society. Neurology 2012;78:1974-80.
57. Krueger DA, Northrup H, International Tuberous Sclerosis Complex Consensus G. Tuberous sclerosis complex surveillance and management: recommendations of the 2012 International Tuberous Sclerosis Complex Consensus Conference. Pediatr Neurol 2013;49:255-65.
58. Koenraads Y, Braun KP, van der Linden DC, Imhof SM, Porro GL. Perimetry in young and neurologically impaired children: the Behavioral Visual Field (BEFIE) Screening Test revisited. JAMA Ophthalmol 2015;133:319-25.
59. Akula JD. Vigabatrin retinal toxicity in children with infantile spasms: An observational cohort study. Neurology 2015;85:655-6.
60. Peters JM, Prohl AK, Tomas-Fernandez XK, et al. Tubers are neither static nor discrete: Evidence from serial diffusion tensor imaging. Neurology 2015;85:1536-45.
61. Chu-Shore CJ, Frosch MP, Grant PE, Thiele EA. Progressive multifocal cystlike cortical tubers in tuberous sclerosis complex: Clinical and neuropathologic findings. Epilepsia 2009.
62. Holthausen H, Pieper T, Kudernatsch M. Towards early diagnosis and treatment to save children from catastrophic epilepsy -- focus on epilepsy surgery. Brain Dev 2013;35:730-41.

63. Budde MD, Xie M, Cross AH, Song SK. Axial diffusivity is the primary correlate of axonal injury in the experimental autoimmune encephalomyelitis spinal cord: a quantitative pixelwise analysis. J Neurosci 2009;29:2805-13.
64. Song SK, Sun SW, Ramsbottom MJ, Chang C, Russell J, Cross AH. Dysmyelination revealed through MRI as increased radial (but unchanged axial) diffusion of water. Neuroimage 2002;17:1429-36.
65. Song SK, Yoshino J, Le TQ, et al. Demyelination increases radial diffusivity in corpus callosum of mouse brain. Neuroimage 2005;26:132-40.
66. Beaulieu C, Allen PS. Determinants of anisotropic water diffusion in nerves. Magn Reson Med 1994;31:394-400.
67. Gulani V, Webb AG, Duncan ID, Lauterbur PC. Apparent diffusion tensor measurements in myelin-deficient rat spinal cords. Magn Reson Med 2001;45:191-5.
68. Marcotte L, Aronica E, Baybis M, Crino PB. Cytoarchitectural alterations are widespread in cerebral cortex in tuberous sclerosis complex. Acta Neuropathol 2012;123:685-93.
69. Ruppe V, Dilsiz P, Reiss CS, et al. Developmental brain abnormalities in tuberous sclerosis complex: a comparative tissue analysis of cortical tubers and perituberal cortex. Epilepsia 2014;55:539-50.
70. Sosunov AA, Wu X, Weiner HL, et al. Tuberous sclerosis: a primary pathology of astrocytes? Epilepsia 2008;49 Suppl 2:53-62.
71. Sosunov AA, McGovern RA, Mikell CB, et al. Epileptogenic but MRI-normal perituberal tissue in Tuberous Sclerosis Complex contains tuber-specific abnormalities. Acta neuropathologica communications 2015;3:17.
72. Wong M, Crino PB. Tuberous sclerosis and epilepsy: role of astrocytes. Glia 2012;60:1244-50.
73. Parekh MB, Rutt BK, Purcell R, Chen Y, Zeineh MM. Ultra-high resolution in-vivo 7.0T structural imaging of the human hippocampus reveals the endfolial pathway. Neuroimage 2015;112:1-6.
74. Scherrer B, Afacan O, Stamm A, Singh JM, Warfield SK. Optimized magnetic resonance diffusion protocol for ex-vivo whole human brain imaging with a clinical scanner. In: Hoeschen C, Kontos D, Flohr TG, editors. Proc SPIE Medical Imaging 2015: Physics of Medical Imaging; 2015; Orlando, Florida, United States.
75. Gholipour A, Estroff JA, Warfield SK. Robust super-resolution volume reconstruction from slice acquisitions: application to fetal brain MRI. IEEE Trans Med Imaging 2010;29:1739-58.
76. Gholipour A, Akhondi-Asl A, Estroff JA, Warfield SK. Multi-atlas multi-shape segmentation of fetal brain MRI for volumetric and morphometric analysis of ventriculomegaly. Neuroimage 2012;60:1819-31.
77. Wu JY, Peters JM, Goyal M, et al. Clinical EEG Biomarker for Seizures in Asymptomatic Tuberous Sclerosis Complex (TSC) Infants. Pediatr Neurol 2015:*in press*.
78. Lipton JO, Sahin M. The Neurology of mTOR. Neuron 2014;84:275-91.
79. Davis P, Peters JM, Krueger DA, Sahin M. Tuberous Sclerosis: A new frontier in targeted treatment of autism. Neurotherapeutics 2015:in press.
80. Krueger DA, Care MM, Agricola K, Tudor C, Mays M, Franz DN. Everolimus long-term safety and efficacy in subependymal giant cell astrocytoma. Neurology 2013;80:574-80.
81. Krueger DA, Care MM, Holland K, et al. Everolimus for subependymal giant-cell astrocytomas in tuberous sclerosis. N Engl J Med 2010;363:1801-11.
82. Krueger DA, Wilfong AA, Holland-Bouley K, et al. Everolimus treatment of refractory epilepsy in tuberous sclerosis complex. Ann Neurol 2013;74:679-87.
83. Ess KC, Chugani HT. Dynamic tubers in tuberous sclerosis complex: A window for intervention? Neurology 2015;85:1530-1.
84. Murakami M, Ichisaka T, Maeda M, et al. mTOR is essential for growth and proliferation in early mouse embryos and embryonic stem cells. Molecular and cellular biology 2004;24:6710-8.

85. Davis PE, Peters JM, Krueger DA, Sahin M. Tuberous Sclerosis: A New Frontier in Targeted Treatment of Autism. Neurotherapeutics 2015;12:572-83.
86. Tsai P, Sahin M. Mechanisms of neurocognitive dysfunction and therapeutic considerations in tuberous sclerosis complex. Curr Opin Neurol 2011;24:106-13.
87. Rensing N, Han L, Wong M. Intermittent dosing of rapamycin maintains antiepileptogenic effects in a mouse model of tuberous sclerosis complex. Epilepsia 2015;56:1088-97.

Addendum

SUMMARY

TSC and Autism Spectrum Disorder

Chapter 2 reviews the progress made in understanding the pathogenesis of TSC, and the promise these insights bare for possible mechanism-based treatment of associated neurobehavioral and cognitive morbidity. On a cellular level, the loss of hamartin or tuberin results in the upregulation of the mechanistic target of rapamycin (mTOR) pathway. At the circuitry level, TSC and mTOR play crucial roles in axonal, dendritic, and synaptic development and function. As such, molecular changes result in aberrant neural connectivity at multiple levels in the central nervous system, and **Chapter 2** reviews how these can lead to the autism spectrum disorder (ASD) phenotype. In addition, early results and advances in mechanism-based treatments of TSC are reviewed.

Diffusion Tensor Imaging in TSC

Chapter 3 provides an introduction to DWI and DTI, reviews current developments, and discusses limitations of the single tensor model. *Conventional MRI* demonstrates various abnormalities in TSC; the most prominent are tuber lesions, radial migration lines, subependymal nodules and subependymal giant cell astrocytomas. Quantification of any of these lesions can provide an estimate of the overall lesion burden, which is correlated with overall neurological outcome. For specific outcomes, including epilepsy, ASD, and intellectual impairment, conventional neuroimaging is insufficiently predictive, and may not change over time to reflect clinical changes in the phenotype.

Diffusion-weighted imaging (DWI) can non-invasively probe the microstructure of the brain[1]. Diffusion Tensor Imaging (DTI) is a method for modeling and quantifying this water diffusion in various brain tissues. The physical principles of DWI and the essentials of the DTI model are discussed in detail in **Chapter 3**. The limitations of the single tensor model are reviewed.

In TSC, DTI differentiates well-known macroscopic pathology from its environment (e.g. tubers, radial migration lines), and can assist with detecting the epileptogenic tuber[2-4]. Moreover, white matter deemed previously normal on structural MRI, demonstrates abnormalities with diffusion imaging. In TSC, such areas are now referred to as normal appearing white matter (NAWM)[5-7]. DTI abnormalities of the white matter are associated with neurocognitive morbidity including autism spectrum disorder[8,9].

Chapter 4 describes decreased fractional anisotropy (FA) and increased mean diffusivity (MD), corrected for age, in patients with both TSC and autism spectrum disorder (ASD). Structural and diffusion magnetic resonance imaging was carried out in 40 children

and young adults with TSC, 12 of whom also had ASD, and in 29 age-matched controls. Tractography of the corpus callosum was used to define a three-dimensional volume of interest. Regional averages of diffusion scalar parameters of the callosal projections were calculated for each subject. As a group, subjects with TSC had significantly lower average FA and higher average MD values compared to controls. Next, subjects were grouped as TSC alone, or as having both TSC and ASD. The presence of TSC with ASD was associated with significantly lower average FA values compared to those without ASD and compared to controls. Subjects with TSC alone had similar average FA values as controls.

This was the first DTI study sufficiently large for an assessment of imaging – phenotype correlations in TSC, and raised the possibility of the use of DTI of the NAWM as a marker of adverse neurological outcome. **Chapter 4** does not address co-occurrence of intellectual disability (ID), epilepsy, and ASD; thus, the findings are unlikely to be specific for ASD.

Chapter 5 partly addresses this problem, by further exploring the use of callosal white matter diffusion as a marker for *more specific* neurological outcomes in TSC. Specifically, DTI data was collected of a larger sample of subjects with TSC with and without ASD, of epilepsy variables, and of patients with ASD but no TSC. This way, the study described in **Chapter 5** aimed to distinguish effects attributable to autism spectrum disorder (ASD), intellectual disability (ID) and epilepsy.

186 children underwent 3T MRI with 35 direction DTI: 32 with TSC alone, 19 with both TSC and ASD, 46 with ASD but no TSC, and 89 healthy controls (HC). Comparable to **Chapter 4**, density-weighted DTI metrics were obtained from DTI tractography of the corpus callosum. Logistic regression of the age-adjusted FA function was done, correcting for volume and volume-age interactions. Again, TSC with ASD was associated with a significantly lower FA than TSC alone, ASD alone and HC.

TSC patients demonstrated significantly lower FA (higher MD) values than those with ASD, and ASD patients had a lower FA than HC. Intellectual disability, epilepsy and the presence of ASD were associated with lower FA values in both the TSC and ASD populations. The co-morbid presence of TSC, ASD, ID or epilepsy demonstrated additive effects, but some subgroups were too small for reliable data fitting.

In summary, using a cross-disorder approach, **Chapter 5** demonstrates cumulative effects of TSC, ASD, ID and epilepsy-related variables on callosal white matter diffusion metrics. In TSC, ASD was inextricably linked to ID and epilepsy, and the DTI measures reflect the total neurological disease burden rather than ASD specifically.

In **Chapter 6**, DTI of various MRI-identified tissue types is described longitudinally. Twenty-five patients underwent two to six 3T structural MRI and 35 direction DTI scans each. The total of 70 scans was compared to those of 73 healthy controls. Using a previously established parcellation, and an automatic segmentation based on a combined global-local intensity mixture model, three regions were defined: tuber tissue, an equal volume peritube rim, and the remaining NAWM. For each patient, scan, lobe, and tissue type, the averages of MD and FA were analyzed in a generalized additive mixed model. FA values were lowest, and MD values were highest in tubers, next in peritube tissue, then in NAWM. Longitudinal analysis showed a positive (FA) and negative (MD) correlation with age in tubers, peritube tissue, and NAWM. All 3 tissue types followed a biphasic developmental trajectory, similar to the white matter of controls. An additional qualitative analysis showed a gradual transition of diffusion values across the tissue type boundaries.

This data showed that tuber and peritube tissues in tuberous sclerosis complex underwent microstructural evolution with age, comparable to the maturational changes of the NAWM. The extent of diffusion abnormality decreased with distance to the tuber, in line with known extension of histologic, immunohistochemical, and molecular abnormalities beyond tuber pathology. In summary, tubers are no longer seen as inert, isolated islands of abnormality, but rather as dynamic and poorly delineated lesions.

Neurophysiology in TSC

In **Chapter 7**, preliminary results from serial monitoring of infants with TSC are discussed in the context of the development of epilepsy. It describes a multi-center observational study in which EEGs were carried out with 6 week intervals before age 6 months, then every 3 months until age 1 year, and every 6 months thereafter. Goals were three-fold: (1) To determine whether repeated EEGs during infancy are a reliable biomarker for identifying TSC infants who will develop epilepsy in the near future; (2) to gain insight in early changes in brain EEG patterns prior to the onset of epilepsy; and (3) to identify the time interval between EEG changes and the onset of clinical seizures.

40 infants with TSC younger than 7 months, seizure-free and on no antiepileptic drugs were enrolled. Parental education at time of enrollment in the study was done to increase vigilance for the early recognition of potential seizures. This education was aimed at facilitating an early diagnosis and treatment, and at improving the accuracy of the estimated age of seizure onset. Once seizure onset occurred, standard of care was applied, and subjects were followed up until 24 months.

Of the 40 patients enrolled at time of the interim analysis, 28 were 12 months old with completed EEG evaluations. Of those, 19 had developed seizures. Epileptic spasms occurred in

10, focal seizures in five, and a combination of epileptic spasms and focal seizures in three. Fourteen infants had the first emergence of epileptiform abnormalities on EEG at an average age of 4.2 months, preceding seizure onset by a median of 1.9 months. Hypsarrhythmia or modified hypsarrhythmia was not found in *any* infant before onset of epileptic spasms.

Thus, the positive predictive value of an EEG with epileptiform abnormality for the development of epilepsy was 100%. **Chapter 7** provides early evidence for serial EEG monitoring as a feasible strategy in the prediction of impending epilepsy in TSC, perhaps paving the road for an interventional trial.

Chapter 8 covers a study of functional connectivity based on EEG coherence during the resting state (or more accurately: non task-related EEG). The study was motivated by the prior work of DTI in patients with TSC and ASD (**Chapter 4**). If decreased FA of the callosal white matter implied *decreased structural connectivity* between the hemispheres, such a difference should be present on a *functional connectivity* level, too. Next, based on unifying models of autism current at that time[10,11], we examined whether there was increased short-range connectivity, and decreased long-range connectivity. Finally, the study applied a graph-theoretical approach to network modeling.

EEG data were collected from TSC patients with ASD (n = 14) and without ASD (n = 29), from patients with non-syndromic ASD (n = 16), and from controls (n = 46). The data showed an overall decreased connectivity in patients with TSC. There were no differences in any of the groups in the ratio of *inter*hemispheric over *intra*hemispheric connectivity, counter to what was hypothesized. A "field test" of the interhemispheric over intrahemispheric ratio measure on the EEGs of 16 patients with an absent corpus callosum was done. Indeed, a significant decrease in EEG functional connectivity reflected the (near-)absence of commissural white matter in this group.

Like **Chapter 5**, in **Chapter 8**, the inclusion of subjects with ASD but without TSC allowed for a cross-disorder approach, and attribute findings specifically to ASD. For patients with ASD, regardless of the presence of TSC or not, a decreased ratio of long-range over short-range connectivity was found. The graph theoretical measures, once corrected for overall connection strength, were essentially negative. When the resilience of the networks was tested by a targeted attack of network nodes, the patients with ASD appeared to be more resilient.

REFERENCES

1. Le Bihan D, Breton E, Lallemand D, Grenier P, Cabanis E, Laval-Jeantet M. MR imaging of intravoxel incoherent motions: application to diffusion and perfusion in neurologic disorders. Radiology 1986;161:401-7.
2. Yogi A, Hirata Y, Karavaeva E, et al. DTI of tuber and perituberal tissue can predict epileptogenicity in tuberous sclerosis complex. Neurology 2015;85:2011-5.
3. Jansen FE, Braun KP, van Nieuwenhuizen O, et al. Diffusion-weighted magnetic resonance imaging and identification of the epileptogenic tuber in patients with tuberous sclerosis. Arch Neurol 2003;60:1580-4.
4. Chandra PS, Salamon N, Huang J, et al. FDG-PET/MRI coregistration and diffusion-tensor imaging distinguish epileptogenic tubers and cortex in patients with tuberous sclerosis complex: a preliminary report. Epilepsia 2006;47:1543-9.
5. Makki MI, Chugani DC, Janisse J, Chugani HT. Characteristics of abnormal diffusivity in normal-appearing white matter investigated with diffusion tensor MR imaging in tuberous sclerosis complex. AJNR Am J Neuroradiol 2007;28:1662-7.
6. Arulrajah S, Ertan G, Jordan L, et al. Magnetic resonance imaging and diffusion-weighted imaging of normal-appearing white matter in children and young adults with tuberous sclerosis complex. Neuroradiology 2009;51:781-6.
7. Simao G, Raybaud C, Chuang S, Go C, Snead OC, Widjaja E. Diffusion tensor imaging of commissural and projection white matter in tuberous sclerosis complex and correlation with tuber load. AJNR Am J Neuroradiol 2010;31:1273-7.
8. Peters JM, Sahin M, Vogel-Farley VK, et al. Loss of white matter microstructural integrity is associated with adverse neurological outcome in tuberous sclerosis complex. Acad Radiol 2012;19:17-25.
9. Lewis WW, Sahin M, Scherrer B, et al. Impaired language pathways in tuberous sclerosis complex patients with autism spectrum disorders. Cereb Cortex 2013;23:1526-32.
10. Geschwind DH, Levitt P. Autism spectrum disorders: developmental disconnection syndromes. Curr Opin Neurobiol 2007;17:103-11.
11. Minshew NJ, Williams DL. The new neurobiology of autism: cortex, connectivity, and neuronal organization. Arch Neurol 2007;64:945-50.

SAMENVATTING

TSC en het autisme spectrum

Hoofdstuk 2 bespreekt de nieuwe ontwikkelingen in het begrip van de pathogenese van TSC, en de mogelijkheden deze inzichten bieden in behandelingen van neurologische sequelae die gericht zijn op onderliggende mechanismen. Op een cellulair niveau leidt het verlies van de hamartin of tuberin eiwitten tot overstimulatie van de *mechanistic target of rapamycin (mTOR)* cascade. Op een netwerk niveau spelen TSC en mTOR een kritische rol in de ontwikkeling en functie van axonen, dendrieten, en synapsen. Op deze wijze leiden de moleculaire veranderingen tot afwijkingen in de verbindingen op verschillende niveaus in het centraal zenuwstelsel, en **Hoofdstuk 2** bespreekt hoe dergelijke veranderingen tot autisme zouden kunnen leiden. Voorlopige resultaten en nieuwe behandelmethoden gericht op de onderliggende moleculaire biologie komen ook aan bod.

Diffusie Tensor Imaging in TSC

Hoofdstuk 3 bevat een introductie tot DWI en DTI, bespreekt nieuwe ontwikkelingen, en de beperkingen van het enkelvoudig tensor model. Met conventionele MRI kunnen verschillende afwijkigen worden waargenomen; de meest voorkomende zijn tubers, radiale migratie lijnen, en SEGAs. De mate van deze afwijkingen is proportioneel met de totale ziektelast. Maar, voor specifieke neurologische problemen inclusief epilepsie, autisme, en cognitieve ontwikkeling biedt conventionele MRI onvolvoende prognostiek.

Diffusie-gewogen imaging (DWI) can non-invasief de microstructuur van het brein onderzoeken[1]. Diffusie Tensor Imaging (DTI) is een modelerings methode die water diffusie kwantificeert. De fysische beginselen van DWI en de kern begrippen van het DTI model worden besproken in **Hoofdstuk 3**. De beperkingen van het enkelvoudig tensor model worden ook samengevat.

DTI kan macroscopische neuropathologie (tubers, radiale migratie lijnen) identificeren, en kan een bijdrage leveren aan het identificeren van de epileptogene tuber[2-4]. Witte stof afwijken die niet zichtbaar zijn met conventionele, structurele MRI, zijn wel te detecteren met diffusie beeldvorming. Dergelijke witte stof wordt nu de *Normal Appearing White Matter* (NAWM) genoemd[5-7]. De mate van witte stof diffusie afwijkingen is gecorreleerd met neurologische en cognitive prognose inclusief autisme[8,9].

In **Hoofdstuk 4** worden een afgenomen fractionele anisotropie (FA) en toegenomen gemiddelde diffusiviteit (MD) in patienten met zowel TSC als autisme besproken. 40 kinderen en jong volwassenen met TSC, waarvan 12 met autisme, ondergingen structurele en diffusie MRI. Een 3-dimensionale tractografie van het corpus callosum (de hersenbalk)

werd gebruikt om de gemiddelde diffusie maten te berekenen (FA, MD, en anderen). Op groepsniveau hadden patienten met TSC een lagere FA en hogere MD vergeleken met gezonde controle patienten. Patienen met zowel TSC en autisme had een nog lagere FA en nog hogere MD, terwijl de waarden van de subgroep zonder autisme dicht in de buurt van de gezonde controles kwam.

Deze studie was uniek omdat het aantal patienten groot genoeg was om verbanden te onderzoeken tussen diffusie imaging en de klinisch neurologische presentatie van TSC. Een dergelijk verband zou tot het gebruik van DTI als biologische merker van neurologische uitkomst kunnen leiden. In het werk besproken in **Hoofdstuk 4** kwamen de andere neurologische symptomen van TSC (ontwikkelingsachterstand, epilepsie) nauwelijks aan bod, en dus correspondeerden de witte stoff DTI afwijkingen niet specifiek met autisme.

In Hoofdstuk 5 wordt een poging ondernomen om dit probleem te ondervangen. DTI data van een veel grotere patienten populatie werd verzameld, samen met meer specifieke gegevens wat betreft intelligentie, autisme, epilepsie. Er werder ook patienten met autisme maar zonder TSC geincludeerd. Op deze wijze poogt **Hoofdstuk 5** de efffecten te onderscheiden die kunnen worden toegeschreven aan autisme, cognitie, en epilepsie

186 kinderen ondergingen 3T MRI en 35 richtingen DTI, inclusief 89 controle patienten. Net als in **Hoofdstuk 4** werd er een correctie gemaakt voor de densiteit van het aantal banen per voxel in het corpus callosum. In deze studie werd het duidelijk dat er een cumulatief effect is van epilepsie, autisme en intellectueel functioneren op de witte stof. (De term "effect" wordt hier in statistisch en niet in causaal verband gebruikt.) Opnieuw bleek dat een ontwikkelings achterstand, ernstige epilepsie en autisme vaak samen voorkomen.

In **Hoofdstuk 6** worden 3 regios geïdentifeerd op conventionele (structurele) MRI: de tuber, de perituber en de NAWM. Deze worden vervolgens geprojecteerd op een longitudinale serie van diffusie scans, vergaard gedurende meerdere jaren in dezelfde patienten. Met behulp van statistisch modeleren bleek dat tuber en perituber regios minder diffusie maturatie ondergingen dan de witte stof, maar op een gelijkaardige wijze. Met andere woorden, tubers zijn niet statisch, maar dynamisch. Vervolgens werd in een aantal patienten stapsgewijs van de tuber, via de perituber, naar de diepe witte stof een lijn getrokken. Hiermee werd aangetoond dat tubers niet goed afgelijnd zijn, en dat de neuropathologie zich buiten de grenzen van de tuber op de MRI bevindt. Dit was reeds gesuggereerd in de neuropathologie, en in de neurofysiologie, maar werd nu ook duidelijk op imaging gebied.

Neurophysiology in TSC

In Hoofdstuk 7 komen de voorlopige resultaten aan bod van een studie waarbij kinderen met TSC prospectief werden gemonitord met seriele EEG. De eerste 6 maanden kregen de kinderen elke 6 weken een EEG, daarna elke 3 maanden, en van 1 jaar tot en met 3 yaar elke 6 maande. Het doel van de studie was 3-voudig: Om de onderzoeken of het EEG bruikbaar was om patienten die epilepsie zouden ontwikkelingen vroegtijdig te detecteren; (2) om inzicht te krijgen in EEG patronen voor de eerste klinische epilepsie aanval en (3) om de tijdsduur tussen EEG afwijkingen en eerste aanval te bestuderen.

Veertig babies met TSC werden geincludeerd. De ouders kregen specifieke instructie en een informatie video, zodat aanvallen vroeg konden worden herkend. Op het moment van deze interim studie, waren slechts 28 patienten oud genoeg voor analyze van het eerste jaar. Negentien kinderen hadden tegen die tijd nepilepsie ontwikkeld, waarvan 10 met infantiele spasmen, focale aanvallen in 5, en 3 met beide. Veertien van de 19 hadden een afwijkend EEG in gemiddeld 2 maanden voorafgaand aan de eerste waargenomen aanval. Alle kinderen met een afwijkend EEG kregen epilepsie, dus de positief predictieve waarde was 100% voor deze voorlopige studie. Het lijkt erop dat serieel EEG monitoring een geode mogelijkheid biedt voor het vroegtijdig identificeren van patienten met een hoog risico op aanvallen.

In **Hoofdstuk 8** wordt een studie over de functionele connectiviteit van het brein besproken, gebaseerd op een coherentie maat. We wilden onderzoeken of de structurele afwijkingen in de witte stof van de hersenbalk (Hoofdstuk 4) ook implicaties hadden voor de functionele connectiviteit. De hersenbalk verbindt de twee hemisferen, dus we onderzochten of inter-hemisferische connectiviteit anders was dan de intra-hemisferische connectiviteit. Korte en lange afstand connectiviteit zou, volgens een toen gangbare theorie voor autisme, ook afwijkend moeten zijn[10,11].

EEG data van TSC patienten met autisme (n = 14) en zonder autisme (n = 29) werd gebruikt, alsmede EEG data van 16 patienten met idiopathische (of niet syndromale) autisme. Patienten met TSC hadden een globale afname van connectiviteit. Er waren geen verschillen tussen inter- en intrahemisferische connectiviteit, in tegenstelling tot de hypothese.

Zoals ook in **Hoofstuk 5**, in **Hoofstuk 8** werden er opnieuw patienten met autisme maar zonder TSC geincludeerd. Patienten met autisme, los van de aanwezig van TSC of niet, hadden een afgenomen ratio van lange-afstand connecties in verhouding tot korte afstand connecties. Een aantal netwerk maten, gebaseerd op graf-theoretische modellen, werden geexploreerd maar waren negatief. Wel bleek dat het EEG netwerk van patienten met autisme beter bestand waren tegen het verwijderen van netwerk knopen.

REFERENTIES

1. Le Bihan D, Breton E, Lallemand D, Grenier P, Cabanis E, Laval-Jeantet M. MR imaging of intravoxel incoherent motions: application to diffusion and perfusion in neurologic disorders. Radiology 1986;161:401-7.
2. Yogi A, Hirata Y, Karavaeva E, et al. DTI of tuber and perituberal tissue can predict epileptogenicity in tuberous sclerosis complex. Neurology 2015;85:2011-5.
3. Jansen FE, Braun KP, van Nieuwenhuizen O, et al. Diffusion-weighted magnetic resonance imaging and identification of the epileptogenic tuber in patients with tuberous sclerosis. Arch Neurol 2003;60:1580-4.
4. Chandra PS, Salamon N, Huang J, et al. FDG-PET/MRI coregistration and diffusion-tensor imaging distinguish epileptogenic tubers and cortex in patients with tuberous sclerosis complex: a preliminary report. Epilepsia 2006;47:1543-9.
5. Makki MI, Chugani DC, Janisse J, Chugani HT. Characteristics of abnormal diffusivity in normal-appearing white matter investigated with diffusion tensor MR imaging in tuberous sclerosis complex. AJNR Am J Neuroradiol 2007;28:1662-7.
6. Arulrajah S, Ertan G, Jordan L, et al. Magnetic resonance imaging and diffusion-weighted imaging of normal-appearing white matter in children and young adults with tuberous sclerosis complex. Neuroradiology 2009;51:781-6.
7. Simao G, Raybaud C, Chuang S, Go C, Snead OC, Widjaja E. Diffusion tensor imaging of commissural and projection white matter in tuberous sclerosis complex and correlation with tuber load. AJNR Am J Neuroradiol 2010;31:1273-7.
8. Peters JM, Sahin M, Vogel-Farley VK, et al. Loss of white matter microstructural integrity is associated with adverse neurological outcome in tuberous sclerosis complex. Acad Radiol 2012;19:17-25.
9. Lewis WW, Sahin M, Scherrer B, et al. Impaired language pathways in tuberous sclerosis complex patients with autism spectrum disorders. Cereb Cortex 2013;23:1526-32.
10. Geschwind DH, Levitt P. Autism spectrum disorders: developmental disconnection syndromes. Curr Opin Neurobiol 2007;17:103-11.
11. Minshew NJ, Williams DL. The new neurobiology of autism: cortex, connectivity, and neuronal organization. Arch Neurol 2007;64:945-50.

PUBLICATIONS

1. Peters JM, Camfield CS, Camfield PR. Population study of benign rolandic epilepsy: is treatment needed? Neurology 2001; 57(3):537-9.
2. Peters JM, Waber DP, McAnulty GB, Duffy FH. Event-related correlations in learning impaired children during A hybrid go/no-go choice reaction visual-motor task. Clin Electroencephalogr. 2003; 34(3):99-109.
3. Peters JM, Vriens EM, Stam CJ. Continue EEG-monitoring op de intensive care. Tijdschr Neurol Neurochir. 2003; 104(5):276-282.
4. van Putten MJ, Peters JM, Mulder SM, de Haas JA, Bruijninckx CM, Tavy DL. A brain symmetry index (BSI) for online EEG monitoring in carotid endarterectomy. Clin Neurophysiol. 2004; 115(5):1189-94.
5. Peters JM, Padberg M, Nederveen PJ, Tavy DL, van Putten MJAM. Tijdschr Neurol Neurochir. Neuromonitoring met on-line qEEG tijdens carotisendarteriectomie: ervaringen met de Brain Symmetry Index. Tijdschr Neurol Neurochir. 2005; 106(4):143-150.
6. Kingma R, Peters JM, Coene LN. Intracranial penetration of a halo pin causing an epileptic seizure. J Bone Joint Surg Br. 2006; 88(12):1654-5.
7. Sánchez Fernández I, Peters JM. Picture of the month--quiz case. Moyamoya disease. Arch Pediatr Adolesc Med. 2009; 163(2):179-80.
8. Depositario-Cabacar DT, Peters JM, Pong AW, Roth J, Rotenberg A, Riviello JJ, Takeoka M. High-dose intravenous levetiracetam for acute seizure exacerbation in children with intractable epilepsy. Epilepsia. 2010; 51(7):1319-22.
9. Peters JM, McLean AV, Young GS. Rapid resolution of diffusion-weighted MRI abnormality in a patient with a stuttering stroke. BMJ Case Reports 2010; doi:10.1136/bcr.07.2009.2063
10. Pier DB, Hallbergson A, Peters JM. Guillain-Barré syndrome in a child with pain: lessons learned from a late diagnosis. Acta Paediatr. 2010; 99(10):1589-91.
11. Loddenkemper T, Fernández IS, Peters JM. Continuous spike and waves during sleep and electrical status epilepticus in sleep. J Clin Neurophysiol. 2011; 28(2):154-64.
12. Peters JM, Sahin M, Vogel-Farley V, Jeste SS, Nelson CA, Gregas MC, Prabhu SP, Scherrer B, Warfield SK. Loss of White Matter Microstructural Integrity Is Associated with Adverse Neurological Outcome in Tuberous Sclerosis Complex. Acad Radiol. 2012; 19(1):17-25.
13. Peters JM, Tomas Fernandez M, van Putten MJAM, Loddenkemper TL. Behavioral measures and EEG monitoring using the Brain Symmetry Index during the Wada test in children. Epilepsy and Behavior 2012; 23:247-253.
14. Sánchez Fernández I, Takeoka M, Tas E, Peters JM, Prabhu S, Stannard K, Gregas M, Eksioglu Y, Rotenberg A, Riviello JJ, Kothare SV, Loddenkemper. Early thalamic lesions in patients with sleep potentiated epileptiform activity. Neurology. 2012;78(22):1721-7.
15. Sánchez Fernández I, Eksioglu Y, Peters JM, Takeoka M, Tas E, Abdelmoumen I, Rotenberg A, Riviello JJ, Kothare SV, Loddenkemper T. Short-term response of sleep potentiated spiking to high-dose diazepam in electrical status epilepticus in sleep. Pediatr Neurol. 2012;46(5):312-8.
16. Kelly TG, Madhavan VL, Peters JM, Kazacos KR, Silvera VM. Spinal cord involvement in a child with raccoon roundworm (Baylisascaris procyonis) meningoencephalitis. Pediatr Radiol. 2012;42(3):369-73.
17. Peters JM, Madhavan V, Husson R, Kazacos K, Soul JS. Early Empiric Treatment of Neural Larva Migrans Due to Baylisascaris procyonis Associated With Good Outcome. Pediatrics 2012; 129(3):e806-811.
18. Sánchez Fernández I, Loddenkemper T, Peters JM, Kothare SV. Electrical status epilepticus in sleep: clinical presentation and pathophysiology. Pediatr Neurol. 2012; 47(6):390-410.

19. Peters JM*, Sánchez Fernández I*, Hadjiloizou S, Prabhu SP, Zarowski M, Stannard KM, Takeoka M, Rotenberg A, Kothare SV, Loddenkemper T. Clinical staging and electroencephalographic evolution of continuous spikes and waves during sleep. Epilepsia. 2012; 53(7):1185-95 *shared first authorship
20. Sánchez Fernández I, Takeoka M, Tas E, Peters JM, Prabhu S, Stannard K, Gregas M, Eksioglu Y, Rotenberg A, Riviello JJ, Kothare SV, Loddenkemper. Early thalamic lesions in patients with sleep potentiated epileptiform activity. Neurology 2012; 78(22):1721-7.
21. Sánchez Fernández I, Eksioglu Y, Peters JM, Takeoka M, Tas E, Abdelmoumen I, Rotenberg A, Riviello JJ, Kothare SV, Loddenkemper T. Short-term response of sleep potentiated spiking to high-dose diazepam in electrical status epilepticus in sleep. Pediatr Neurol. 2012; 46(5):312-8.
22. Akhondi-Asl A, Hans A, Scherrer B, Peters JM, Warfield SK. Whole Brain Group Network Analysis Using Network Bias and Variance Parameters, ISBI 2012: Proc IEEE Int Symp Biom Imaging, Barcelona, Spain, 2012 (1511-1514).
23. Lewis WW, Sahin M, Scherrer B, Peters JM, Suarez R, Vogel-Farley VK, Jeste SS, Gregas MC, Prabhu SP, Nelson CA, Warfield SK. Impaired language pathways in tuberous sclerosis complex patients with autism spectrum disorders.Cereb Cortex. 2013; 23(7):1526-32.
24. Taquet M, Scherrer B, Commowick O, Peters JM, Sahin M, Macq B, Warfield SK. Registration and analysis of white matter group differences with a multi-fiber model. Med Image Comput Comput Assist Interv. 2012; 15(Pt 3):313-20.
25. Sánchez Fernández I, Chapman KE, Peters JM, Kothare SV, Nordli DR Jr, Jensen FE, Berg AT, Loddenkemper T. The tower of Babel: survey on concepts and terminology in Electrical Status Epilepticus in Sleep (ESES) and Continuous Spikes and Waves during Sleep (CSWS) in North America. Epilepsia. 2013; 54(4):741-750.
26. Sánchez Fernández I, Peters JM, Takeoka M, Rotenberg A, Gregas M, Kothare SV, Loddenkemper T. Patients with electrical status epilepticus in sleep share similar clinical features regardless of their focal or generalized sleep potentiation of epileptiform activity. J Child Neurol. 2013; 28(1):83-9.
27. Weisenfeld NI, Peters JM, Tsai P, Sahin M, Warfield SK. Cerebellar Volume Loss in Tuberous Sclerosis Complex: A Magnetic Resonance Imaging Study. Pediatr Neurol. 2013; 48(2):105-10.
28. Chavakula V, Sánchez Fernández I, Peters JM, Popli G, Bosl W, Rakhade S, Rotenberg A, Loddenkemper T. Automated quantification of spikes. Epilepsy Behav. 2013; 26(2):143-52.
29. Sánchez Fernández I, Peters JM, An S, Bergin AM, Takeoka M, Rotenberg A, Kothare SV, Riviello JJ Jr, Loddenkemper T. Long-term response to high-dose diazepam treatment in continuous spikes and waves during sleep. Pediatr Neurol. 2013; 49(3):163-170.
30. Taimouri V, Alireza Akhondi-Asla A, Tomas-Fernandez X, Peters JM, Prabhu SP, Poduri A, Takeoka M, Loddenkemper T, Bergin AM, Harini C, Madsen JR, Warfield SK. Electrode Localization for Planning Pediatric Epilepsy Surgery. Int J Comput Assist Radiol Surg. 2014; 9(1):91-105.
31. Peters JM, Taquet M, Vega C, Jeste SS, Sánchez Fernández I, Tan J, Nelson III CA, Sahin M and Warfield SK. Brain Functional Networks in Syndromic and Non-syndromic Autism: a Graph Theoretical Study of EEG Connectivity. BMC Medicine 2013; 11(1):54.
32. Peters JM, Taquet M, Prohl AK, Scherrer B, van Eeghen AM, Sahin M, Warfield SK. Diffusion Tensor Imaging and related techniques in Tuberous Sclerosis Complex: Review and future directions. Future Neurology 2013; 8(5):583-597.
33. Sánchez Fernández I, Chapman KE, Peters JM, Harini C, Rotenberg A, Loddenkemper T. Continuous spikes and waves during sleep: electro-clinical presentation and suggestions for management. Epilepsy Res Treat. 2013; 2013:583531.
34. Taquet M, Peters JM. Le réseau cérébral fonctionnel des enfants atteints d'autisme : redondance et déconnexion [The brain functional network of children with autism: redundancy and disconnection]. Article in French. Med Sci (Paris) 2013; 29(6-7)567-9.

35. Taquet M, Scherrer B, Commowick O, Peters JM, Sahin M, Macq B, Warfield SK. A Mathematical Framework for the Registration and Analysis of Multi-Fascicle Models for Population Studies of the Brain Microstructure. IEEE Trans Med Imaging. 2014; 33(2):504-17.
36. Pinto AL, Sánchez Fernández I, Peters JM, Manganaro S, Singer JM, Vendrame M, Prabhu SP, Loddenkemper TL, Kothare SV. Localization of sleep spindles, K-complexes, and vertex waves with subdural electrodes in children. J Clin Neurophys 2014; 31(4):367-74.
37. Peters JM, Sánchez Fernández I. Insult to injury: transient encephalopathy in a brain-injured adolescent. J Paediatr Child Health. 2014; 50(5):411-4. PMID:24372698.
38. O'Rourke DJ, Bergin A, Rotenberg A, Peters JM, Gorman M, Poduri A, Cryan J, Lidov H, Madsen J, Harini C. Rasmussen's encephalitis presenting as focal cortical dysplasia. Epilepsy and Behavior Case Reports. 2014;2:86-89.
39. Tanaka N, Peters JM, Prohl AK, Takaya S, Madsen JR, Bourgeois BF, Dworetsky BA, Hämäläinen MS, Stufflebeam SM. Clinical value of magnetoencephalographic spike propagation represented by spatiotemporal source analysis: Correlation with surgical outcome. Epilepsy Res. 2014; 108(2):280-8.
40. Klehm J, Thome-Souza S, Sánchez Fernández I, Bergin, AM, Bolton J, Harini C, Kadish NE, Libenson MH, Peters JM, Poduri A, Rotenberg A, Takeoka M, Bourgeois BF, Loddenkemper T. Clobazam: effect on frequency of seizures and safety profile in different subgroups of children with epilepsy. Pediatr Neurol. 2014; 51(1):60-6.
41. Thome-Souza S, Kadish NE, Ramgopal S, Sánchez Fernández I, Bergin AM, Bolton J, Harini C, Libenson M, Olson H, Peters JM, Poduri A, Rotenberg A, Takeoka M, Kothare SV, Kapur K, Bourgeois BF, Loddenkemper T. Safety and retention rate of rufinamide in 300 patients: A single pediatric epilepsy center experience. 2014;55(8):1235-44.
42. Peters JM, Taquet M, Scherrer B, Singh J, Prohl AK, Prabhu SP, Sahin M, Warfield SK. Insights in tuberous sclerosis complex from novel diffusion-weighted imaging models. Siemens MAGNETOM Flash. 2014;2:24-31.
43. Sánchez Fernández I, Chapman K, Peters JM, Klehm J, Jackson MC, Berg AT, Loddenkemper T. Treatment for Continuous Spikes and Waves during Sleep (CSWS): Survey on treatment choices in North America. Epilepsia. 2014; 55(7):1099-108.
44. Taquet M, Scherrer B, Peters JM, Prabhu SP, Warfield SK. A fully bayesian inference framework for population studies of the brain microstructure. Med Image Comput Comput Assist Interv. 2014; 17(Pt 1):25-32.
45. Erem B, Hyde DE, Peters JM, Duffy FH, Brooks DH, Warfield SK. Combined delay and graph embedding of epileptic discharges in EEG reveals complex and recurrent non-linear dynamics. Proc IEEE Int Symp Biomed Imaging. 2015:347-350.
46. Davis PE, Peters JM, Krueger DA, Sahin M. Tuberous Sclerosis: A new frontier in targeted treatment of autism. Neurotherapeutics 2015;12(3):572-83
47. Walsh, B, Baumer F, Bernson-Leung M, Lerou P, Peters JM. Nonepileptic Myoclonus in a Neonate Following Severe Hypoxic-Ischemic Injury. Neurology 2015;84:e90.
48. Baumer F, Peters JM, Al-Achkar C, Pearl PL. SCN2A Related Early Onset Epileptic Encephalopathy Responsive to Phenobarbital. J Ped Epilepsy 2015: in press.
49. Im K, Ahtam B, Haehn D, Peters JM, Warfield SK, Sahin M, Grant PE. Altered structural brain networks in tuberous sclerosis complex. Cereb Cortex 2015 Mar 5. pii: bhv026. [Epub ahead of print].
50. Peters JM, Prohl AK, Tomas-Fernandez X, Taquet M, Scherrer B, Prabhu SP, Lidov HG, Singh JS, Jansen FE, Braun KP, Sahin M, Warfield SK, Stamm A. Tubers are neither static nor discrete: Evidence from serial diffusion tensor imaging. Neurology 2015;85(18):1536-45.

51. Wu JY, Peters JM, Goyal M, Krueger D, Sahin M, Northrup H, Sing Au K, Cutter G, Bebin EM. Clinical EEG Biomarker for Seizures in Asymptomatic Tuberous Sclerosis Complex (TSC) Infants. Pediatric Neurology 2015: in press.
52. Taquet M, Scherrer B, Boumal N, Peters JM, Macq B, Warfield SK. Improved Fidelity of Brain Microstructure Mapping from Single-Shell Diffusion MRI. Med Image Anal 2015;26(1):268-286.

CURRICULUM VITAE

Jurriaan Peters was born on December 16, 1974, in Leiden, the Netherlands. After completing his high school (VWO) he spent a year at Delft University of Technology (not) doing (much) mechanical engineering. In 1994 he left for Belgium, to study medicine at the Faculty of Medicine, at the Catholic University of Leuven. He suspended his medical school training from 1999-2000 to spend a year abroad, in Halifax, Nova Scotia, Canada, and in Boston, Massachusetts, USA, studying Rolandic epilepsy, and cognitive event-related potentials, respectively. After completing his medical school in Belgium, he started in 2002 as a resident-not-in-training in Neurology at the VU University Medical Center in Amsterdam, and then worked as a resident in Neurology from 2003-2006 at the Leyenburg Hospital, now HagaZiekenhuis, in The Hague. He completed an Epilepsy and Clinical Neurophysiology fellowship at Boston Children's Hospital and Harvard Medical School in 2007; fell in love (in no particular order) with the hospital and with his wife Farida, and re-entered residency in Boston from 2007-2010, this time to pursue Child Neurology. After completing an internship in pediatrics in 2011, he finished his palindromic training in 2012 with a fellowship in pediatric neuroimaging. He now is an Assistant Professor of Neurology at Harvard Medical School, and works as a staff epileptologist and clinical neurophysiologist at Boston Children's Hospital in the Division of Epilepsy and Clinical Neurophysiology, Department of Neurology. Jurriaan Peters and his wife have two daughters and a son.

ACKNOWLEDGEMENTS

I would like to express my profound gratitude to many people have contributed significantly to this thesis, and ask forgiveness of those who I have erroneously omitted.

First and foremost, Simon Warfield. Dear Simon, it has been a privilege and an honor to work with you. Your quick mind and your unwillingness to acknowledge an impossibility ("we ought to be able to …") continue to be a source of inspiration. I sincerely hope we have many more fruitful years to come.

My promotor, Kees Braun. Dear Kees, it has been a whirlwind and an exceptionally efficient collaboration. Thank you for your trust in me and for your support of the generation of this thesis. Your astute thinking and setting of a clear agenda have been instrumental. I very much look forward to expanding our research endeavors.

My copromotor, Mustafa Sahin. Dear Mustafa, we connected first during my residency, then I joined Simon's lab and worked with you in the TSC. Your unrelenting support and career development guidance has provided me with a mentorship one could only wish for. I am proud to be your clinical epilepsy side-kick in the TSC world.

My copromotor, Floor Jansen. Dear Floor, I can completely imagine why you form such a good tag-team with Kees. The two of you are both complimentary and alike. For me, your keen mind and rapid turnaround of manuscripts, proposals, and abstracts have hopefully set the stage for more work together. I am massively impressed by your persona, your drive and your career; it is no wonder my resumé almost appears as if it's modeled after yours.

I would like to thank the members of the promotion committee, Prof. dr. R.M. Dijkhuizen, Prof. dr. J. Hendrikse, Prof. dr. G.J. Biessels, Prof. dr. L. Lagae en Prof. dr. M.J.A.M. van Putten for their time, preparation and participation in the committee.

My paranimphs, Maxime and Ties, I am grateful for yor friendship and presence here. Maxime, I will continue to find you as a friend and collaborator no matter how many miles you try to move away. Ties, ouwe rups, without you Marblehead would be a different, less colorful place.

I have had many mentors and supporters over the years. In order of appearance, I would like to thank Lieven Lagae for introducing me to clinical neurophysiology (and for putting me to work on sawing a computer desk), Frank Duffy for taking me on as a research assistant, Michel van Putten for being both a long-time friend and a research mentor. Blaise Bour-

geois, I miss your presence, your humor and your ability to make complex matters seem straightforward. I was honored to be your protégé. Rest assured that Phil Pearl is furthering your division by setting example in hard work, but also by mentoring, career guidance, and by providing us with a rich and supportive environment. Phil, I am thrilled to have such a creative and fast-paced division head, more to come!

On that note, Scott Pomeroy, Neurologist-in-Chief at Boston Children's Hospital, has always been similarly encouraging and supportive, for which I consider myself blessed. I am indebted to all my colleagues from the Division of Epilepsy and Clinical Neurophysiology, and the nursing, EEG and administrative staff. Iván, keep up the amazing pace and please don't ask inappropriate questions in a bar when you need a greencard. Jack, we've come a long way.

Two more informal mentors, Darcy Krueger and Kevin Ess, should be mentioned. With Darcy I tend to have quick meetings in taxi-cabs, in his minivan, or during conferences, but perhaps unknowingly he has provided valuable advice on research projects. I promise you to deliver the long-term imaging data! Kevin, I seem to check in with you on a yearly basis on our runs together during AES or CNS, and your comments – even if they may seem casual to you – have been formative in my path.

From the Computational Radiology Laboratory and beyond, I have too many collaborators to mention all. Anna Prohl (star in the making, running mate and crazy early bird), Maxime (see earlier), Aymeric (Triple Karmeliet), Clemente Vega (runner and personal therapist), Peter Davis (squatter), Koen Dreijerink (please come back to the East coast), Robbert Struyven (who I plan to recruit), Chris Benjamin (at last in the same timezone again), Agnies van Eeghen (our kids throw up on each other's driveways), and Fiona (who reminds me to be PC) are some highlights of this group.

The Multidisciplinary TSC Clinic, led by Mustafa, has become a cornerstone of my clinical activities, and our program continues to attract more national and international patients. This growth is no surprise given the composition of the team. Jen McCrave single-handedly keeps the medical aspects in line – and I just love working with her. Kira, Maggie, Rajna, Molly, Meghan, Rachel, Allison, you are a great team.

My dear pals from the Mechelse Leuven gang, please behave at least during the thesis defense, I realize that afterwards all bets are off. Bart, Roland, Roderik, Edgar en Sjoefke – wish you were closer to here, may our friendships continue indefinitely.

Bas, Larry and Alex are my loyal Dutch pals in the greater Boston area. In Marblehead I have been warmly received, despite my foreignness, by the Corbetts and all members of the Strem-Ruys clan. The get-togethers with Jurriaan and Arielle range from pricelessly silly to moments of profound reflection. I am also grateful to be part of the extended Abbadi family now.

To my brothers: Dear Derek, it appears we are more alike than at first glance. I am deeply moved by how close we have become over the years. Dear Daniel, best buddy, your unconditional friendship and justness has provided me with much needed stability in life. I salute you, brothers!

Dear Mom and Dad, you have gone through a rough transition, but now is the time to heal. Each of you has uniquely contributed to our upbringing, for which I am ever grateful. Dad, the pleasure you had in your work as a child neurologist has since long motivated my aspirations as a clinician-scientist. Mom, your creativity and social drive has formed all of us. Both, please look forward, and be generous.

Linaatje, Douniaatje and Simootje – you are too young to partake but one day I will tell you about this day. Dear Farida, my lovely wife, your strength and unrelenting dedication provide me with the best possible support and love I could ever wish for. Infinitsy timez tsu.